ÇANKAYA UNIVERSITY

THE GRADUATE SCHOOL OF NATURAL AND APPLIED SCIENCES

MASTER THESIS

STRESS ANALYSIS IN SINGLE LAP JOINTS OF COMPOSITE PLATES UNDER DIFFERENT LOADING CONDITIONS

Samer Kadhim KAREEM

SEPTEMBER 2018

ÇANKAYA UNIVERSITY

THE GRADUATE SCHOOL OF NATURAL AND APPLIED

SCIENCES

MASTER THESIS

STRESS ANALYSIS IN SINGLE LAP JOINTS OF COMPOSITE PLATES
UNDER DIFFERENT LOADING CONDITIONS

A THESIS SUBMITTED TO

MECHANICAL ENGINEERING DEPARTMENT
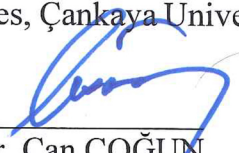
ÇANKAYA UNIVERSITY

BY

Samer Kadhim KAREEM

IN PARTIAL FULFILLMENT OF THE REQUIREMENTS FOR

THE DEGREE OF MASTER OF SCIENCE IN

MECHANICAL ENGINEERING

SEPTEMBER 2018

Title of the Thesis: **Stress Analysis In Single Lap Joints Of Composite Plates Under Different Loading Conditions**

Submitted by **Samer Kadhim KAREEM**

Approval of the Graduate School of Natural and Applied Sciences, Çankaya University
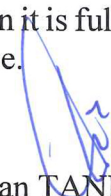
_____

Prof. Dr. Can ÇOĞUN
Director

I certify that this thesis satisfies all the requirements as a thesis for the degree of Master of Science.

_____

Prof. Dr. Haşmet TÜRKOĞLU
Head of Department

This is to certify that we have read this thesis and that in our opinion it is fully adequate, in scope and quality, as a thesis for the degree of Master of Science.

_____

Assist. Prof. Dr. Hakan TANRIOVER
Supervisor

Examination Date   :   26.09.2018

Examining Committee Members (first name belongs to the chairperson of the jury and the second name belongs to supervisor)

Assist. Prof. Dr. Özgün SELVİ	Çankaya Univ.	_____
Assoc. Prof. Dr. Caner koç	Ankara Univ.	_____
Assist. Prof. Dr. Hakan TANRIÖVER	Çankaya Univ.	_____

STATEMENT OF NON-PLAGIARISM

I hereby declare that all information in this document has been obtained and presented in accordance with academic rules and ethical conduct. I also declare that, as required by these rules and conduct, I have fully cited and referenced all material and results that are not original to this work.

Name, Last Name : Samer Kadhim KAREEM

Signature : _Samer Kareem_

Date : 03.10.2018

ABSTRACT

**STRESS ANALYSIS IN SINGLE LAP JOINTS OF COMPOSITE PLATES
UNDER DİFFERENT LOADING CONDITIONS**

Samer Kadhim Kareem

Graduate Thesis, Faculty of Mechanical Engineering Department

Thesis Supervisor: Assist. Prof. Dr. Hakan Tanriover

September-2018, 168 pages

In the recent four decades, the demand of the different industries about the light but strong materials which can be used massively, caused a big progress in producing the composite materials. According to the proposed requirement, the necessity of researching about composite materials and the structures which can be constructed based on them is obvious. In this thesis, firstly a brief introduction about the composite materials and their applications are presented. Then, the analyses of three different structured of single-lap single-bolt composite joints are presented. The aforementioned analysis are done because to corroborate the process of simulation which we have done for our design and find features which can be compared together. The analyses are based on stress and deformation. According to the proposed analyses, the T800 carbon epoxy composite material has better performance in terms of deformation under 0-5KN force. Based on the results which are obtained from the aforementioned analyses, using two supportive plates are used to reduce the effect of load effect on the composite plates. Based on the analyses which are done in chapter 3, a new design is presented in chapter four. According to the results which are done in ANSYS in term of deformation, the performance of our design can be used as an alternative design to replace with the three ones, which are presented in chapter three. Finally, some suggestions as ongoing and future works are presented in chapter five, like, doing experimental test on our design structure.

Key Words: Composite material, finite element method, displacement analysis, stress analysis.

ÖZ

DEĞİŞİK YÜKLEME ALTINDAKİ TEK BİNDİRME BAĞLANTILI KOMPOZİT PLAKLARIN GERİLME ANALİZİ

Samer Kadhim Kareem

Yükseklisans, Makine Mühendisliği Anabilim Dalı

Tez Yöneticisi: Assist. Prof. Dr. Hakan Tanrıöver

Eylül 2018, 168 sayfa

Son kırk yılda, değişik endüstriler tarafından kitlesel olarak kullanılabilen hafif ama güçlü malzemelerin talep edilmesi, kompozit malzemelerin üretiminde büyük bir ilerlemeye neden oldu.

Önerilen şartlara göre, kompozit materyaller ve bunlar temel alınarak oluşturulabilecek yapılar hakkında araştırmaların yapılmasının gerekçesi açıktır.

Bu tezde, öncelikle kompozit materyaller ve uygulamaları hakkında kısa bir tanıtım sunulmaktadır. Daha sonra, üç farklı yapıya sahip tek bindirmeli ve tek cıvatalı kompozit bağlantıların analizleri sunuldu. Söz konusu analizler, tasarımımız için yaptığımız simülasyon sürecini desteklemek ve birlikte karşılaştırılabilecek özellikler bulmak için yapılmıştır. Analizler, gerilme ve şekil değiştirmeye dayanmaktadır. Önerilen analize göre, T800 karbon epoksi kompozit malzemenin 0-5KN gücü altında deformasyon açısından daha iyi bir performansı vardır.

Yukarıda bahsedilen analizden elde edilen sonuçlara dayanarak, kompozit plakalar üzerinde etkili olan yükün etkisini azaltmak için iki destekleyici levha kullanılmıştır. Bölüm 3'te yapılan analize dayanarak, dördüncü bölümde yeni bir tasarım sunulmuştur. ANSYS'te deformasyon anlamında yapılan sonuçlara göre tasarımımızın performansı, üçüncü bölümde sunulan üçlü ile değiştirilecek alternatif bir tasarım olarak kullanılabilir. Son olarak, halen yürütülmekte olan ve deneysel çalışmalar gibi gelecekte yürütülebilecek işler belirtilmiştir.

Anahtar Kelimeler: Kompozit malzeme, sonlu elemanlar metodu, yer değiştirme analizi, gerilme analizi

ACKNOWLEDGMENTS

Foremost, I would like to express my sincere gratitude to my supervisor Assist. Prof. Dr. Hakan Tanriover for the continuous support of my MSc thesis. Besides, I would like to thank the rest of my thesis committee, for their encouragement and insightful comments.

Finally, I would like to express special thanks to my family for their patience, motivation and endless supports.

TABLE OF CONTENTS

LIST OF TABLES

LIST OF FIGURES

CHAPTER 1

A GENERAL OVERVIEW OF COMPOSITE MATERIALS AND THEIR APPLICATIONS

1.1. Introduction

In this section a short bibliography of the composite materials and the different structures and stacking which can be used for it are presented. Moreover, the generality of constructing the composite materials and the applications of them in various industries are presented.

1.2 Basic Concepts of Composite Materials

One of the short definition which is used for describing the composite material is, a material consisting of two or more parts, which is formed by combining two or more different components in a macroscopic manner along an interface [1].

The first main progress of composite materials happened in 1930's in America, in that time the availability of glass fiber cause to product the modern composite laminate, which causes glass fiber reinforced composite materials took its place in the world market [2]. Composite materials can be seen as relatively new and advanced technology materials, when they are evaluated in terms of material science. One of the most important features of composite material can be considered as its homogeneity at micro level. Figure 1.1 illustrates the global glass market volume share.
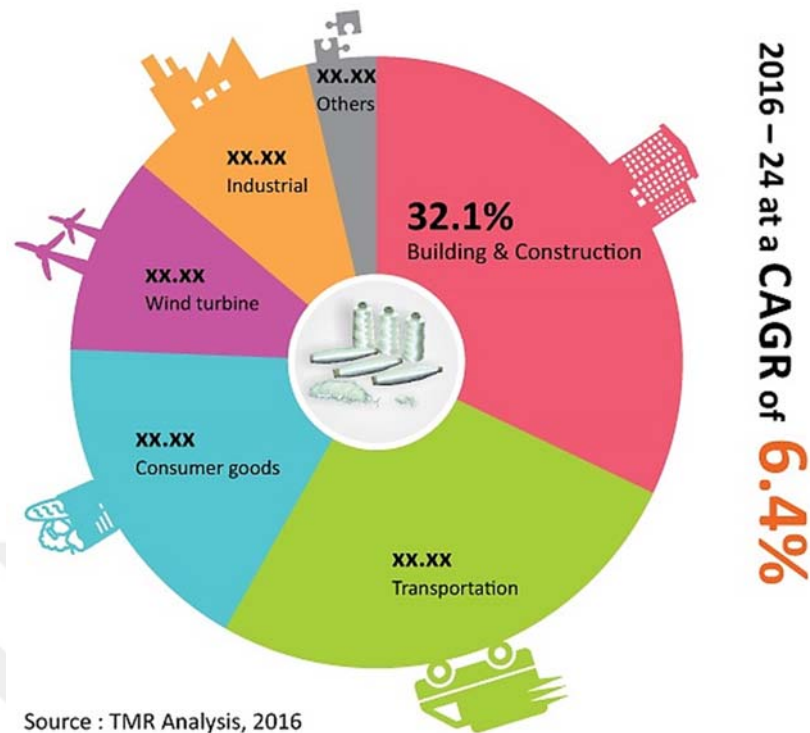
Figure 1.1: The global glass market volume share [3].

1.2.1 Fibers

The main reason that the using of fibers are widespread in the recent three decades significantly can be considered as their ability to obtain the maximum tensile energy and stiffness of a material [4]. Fibers are normally vain as structural materials except they are held collectively in a structural unit with a binder or matrix material and except some transverse reinforcement is provided [5]. The want for fiber placement in distinctive directions in accordance to the precise utility has led to a range of types of composites [6]. Figure 1.2 depicts the progress of using carbon-fiber composites since 2013 and the prediction about using it.

CFRP Market will Grow to $35 Billion in 2020
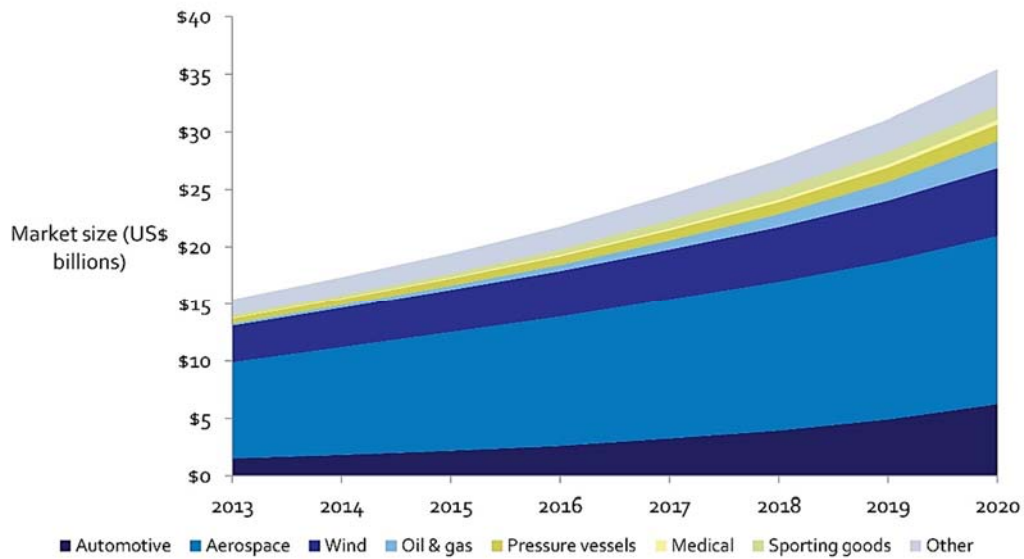
Figure 1.2: The progress of using carbon-fiber composites since 2013 and the prediction about using it [7].

The woven fiber composites do now not have extremely good lamina and are now no longer prone to delamination, however, electricity and stiffness are sacrificed due to the fact the fibers are not as straight as in the non-stop fiber laminate. Chopped fiber composites are used appreciably in high-volume purposes due to their low manufacturing cost [8].

1.2.1.1 Glass Fiber

Fiberglass or glass fiber is a fabric made from extraordinarily best fibers of glass. The ensuing composite material, exact regarded as fiber-reinforced polymers (FRP), is known as "fiberglass" in popular usage. Fiberglass is used for mats, insulation, reinforcement for quite a number polymer products, and industrial fabric that are heat-resistant, corrosion-resistant, and excessive in energy [9].

The wide range applications of the Fiberglass in different industries like aircraft panels producing, rocket engines, helicopter rotor propellers, pressure vessels and sports equipment because of its medium cost, mechanical, chemical and electrical properties makes it under a significant attention [10].

As a sum up, the main characteristics of the Fiberglass which make it more applicable can be regarded as [11]:

- ❖ High Tensile Strength
- ❖ Dimensional Stability
- ❖ High Heat Resistance
- ❖ Fire Resistance
- ❖ Good Thermal Conductivity
- ❖ Durability
- ❖ Economical

In the other hand the Fiberglass has so disadvantages like, high elongation, relatively low strength and moderate strength and weight.

1.2.1.2 Carbon Fibers

One of the high performance composite which are usually used as reinforcement elements in constructions is Carbon fibers [12]. The aforementioned material usually makes from artificial silk and polyacrylonitrile (PAN). The main distinguish features of Carbon fibers compare to the glass fibers can be regarded as, their highly strength and stiffness of them. The aforementioned material is used in different industries like, airplanes and turbine blades manufacturing. Figure 3, depicts the end-use markets for Carbon fibers.
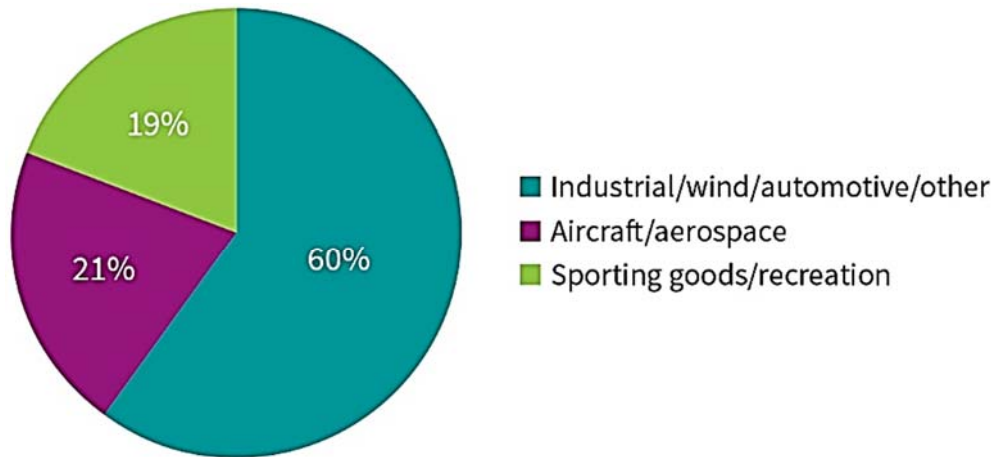
Figure 1.3: Major global end-use markets for Carbon fibers [13].

1.2.1.3 Aramid Fibers

One of the other material that is used as composite material is Aramid. The main feature of the aforementioned material is, its high strength. However, some of the weakness point of Aramid fibers like, the ability to hold the poor adhesion of the matrix have been limited the usage of it [14].

1.2.1.4 Boron Fibers

Boron fiber is five times stronger than steel. The chemical vapor deposition process to deposit boron vapors on fine tungsten or carbon filaments carries it out [15]. Boron provides strength, congested and light weight, and possesses excellent property Newton buckling resistance. The Boron uses for, golf club skiing, and biking are worn out tires, space applications such as aircraft empennage variety leather member gear ready for the repair and maintenance of aircraft.

Table 1.1: A comparison between Boron and Silicon carbide laminate [16].

	Boron	Silicon Carbide
Density (g/cc)	2.40-2.59	2.98-3.20
Tensile Strength (GPa)	3.60	3.90
Tensile Modulus (GPa)	441	400
Elongation (%)	0.9	N/A
CTE (10^{-6} cm/cm/^{o}C)	2.5	N/A

1.2.1.5 Silicon Fiber

In the textile industries, must not be used at all stages of the process, on the fiber during the production of the fabric and/or directly to manufactured goods. Should be applied to different systems to provide different benefits, easing control or toluene diisocyanate foam and paint. We should not also be used to achieve a reduction inspired by the friction between the fibers itself. Table 1 presents a comparison between Born and Silicon carbide laminate. Generally, Silanol silicon posts, reaction, through the linker to the condensation catalyst in the paint to encapsulate the fiber. These fibers high thermal treatment will lead to immunize textiles fiberfill filling the material contained in the regulations and duvets or wearing life jackets. Clean up should only be used during the sometimes fiber production [17]. Silicon lubricant to reduce this and put polyether higher hydrophobicity and easier to clean. Fiber can be addressed should not legitimize the initial softness to textile fibers made of them. It must not be limited to the fiber processing or termination. Used in various applications of the coating extends fashion wear socks, such as women in the technically demanding air bags [18].

1.2.2 Matrices

Fiber reinforced composite (FRC), a high-performance composite material is consisting of three elements. The matrix is essentially homogeneous, coherent rom composite materials fiber optic network. It continues. The edges provide average

bound and reinforcements in the case of the lighting. It provides protection from environmental damage, reinforcements to help the transfer of cargo, and offers end properties color durability and functionality [19].

1.3 Classification of Composite Materials

As a classification for the composite material, they can be categorized in three classes which are, particles and fiber supported, supported and structural composites [20].

In order to the strengthening of the particles and the dispersion of the synthetic drugs are supported sub-classifications of molecules composite materials. A broad term to indicate that the interactions between the particle bitmap can be the treatment of atomic or molecular level, but uses the continuum mechanics. Most of these synthetic materials, the particle is the most difficult stage of the matrix [21]. The goals of the design synthetic fibers supported include high often force and/or congested in the basis weight. These characteristics in specific terms of modulus the parameters that are consistent respectively attributed the most serious specific Infinity modulus of elasticity to specific gravity. Figure 1.4 illustrates a classification of composite materials.
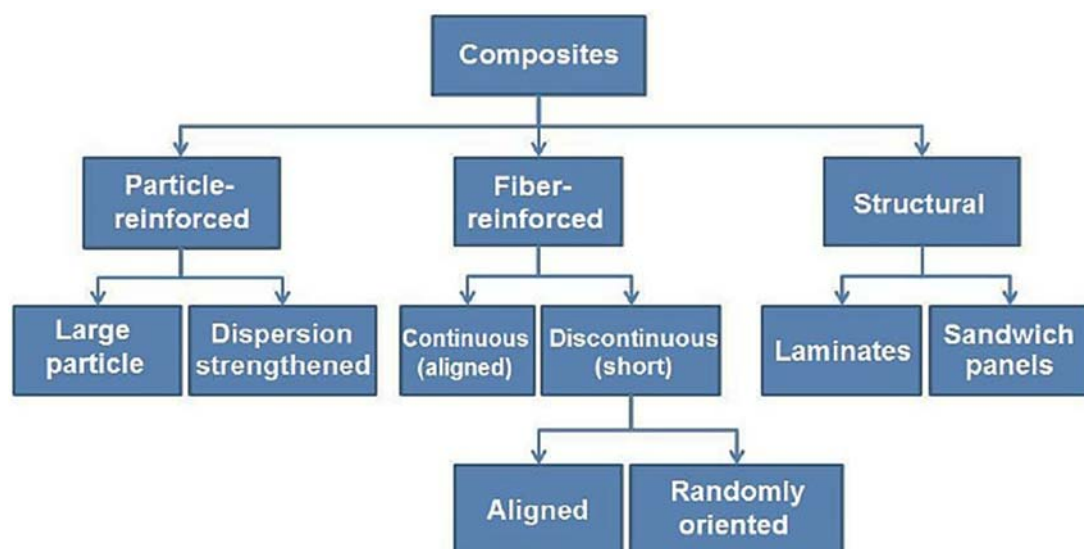
Figure 1.4: A classification of composite materials [22].

Synthetic fiber supported with the strengths and weaknesses of the exceptionally high specific module and use fiber optic dot density materials. Usually composed of composite structural composite materials and homogeneous property that does not depend on the characteristics of the materials, but also on the geometric design of the various. The structural elements, the sandwich plates laminar are and vehicles are the most common structural composites [23].

1.3.1 Fibrous Composite Materials

The fibrous composites are materials which consist of lightweight, high modulus fibers imbedded in a surrounding material called the matrix [24]. Their notable appeal lies in the fact that, frequently, something greater is gained. The longevity is an example. If a crack virtually ran via a GFRP composite, one would possibly (at first sight) count on the durability to be an easily weighted average of that of glass and epoxy; and both are low. But that is now not what happens. The sturdy fibers pull out of the epoxy. In pulling out, work is completed and this work contributes to the toughness of the composite. The longevity is larger – regularly an awful lot larger than the linear combination [9].

1.3.1.1 Whiskers

Particles have no favored orientation and provide minimal upgrades in mechanical properties. Whiskers are single crystals that are extraordinarily sturdy however are challenging to disperse uniformly in the matrix. They are small in each size and diameter in contrast to fibers. Fibers have a very lengthy axis in contrast to particles and whiskers used to give a boost to metal and ceramic matrices [9]. Whiskers are quite small and, in contrast to the bulk material, have very high electricity and stiffness in the lengthwise course the properties of microscopic whiskers can be very close to the perfect houses of a single unit [25]. Whiskers used for reinforcement generally have a random orientation within the material, and so the strengthened cloth nonetheless has isotropic properties [25].

1.3.2 Laminated Composite Materials

Laminated composite materials are notably used in aerospace, defense, marine, automobile, and many other industries. They are normally lighter and stiffer than other structural materials. A laminated composite fabric consists of quite a few layers of a composite mixture consisting of matrix and fibers. Each layer might also have comparable or distinct fabric residences with one of a kind fiber orientations below various stacking sequence. Because, composite substances are produced in many combinations and forms, the layout engineer have to think about many design alternatives. It is integral to know the dynamic and buckling characteristics of such buildings subjected to dynamic masses in complex environmental conditions [26, 27].

1.3.2.1 Fibrous Laminated Composite Materials

The use of fibrous composite substances for structural purposes grew to become quite frequent as the twentieth century got here to a close. The self-belief in and ability to format and manufacturer with these materials was once exemplified by the twenty-first-century application of carbon fiber composite as the major load-bearing structural material in the Boeing 787 industrial aircraft. The benefits of fibrous composites include high stiffness, excessive strength, mild weight, non-corrosive, zero or near-zero thermal expansion, incredible fatigue life, high have an effect on resistance, reduced manufacturing fees due to reduced parts depend and reduced preservation costs [28]. Figure 1.5, depicts a schematic of laminated composite material.

1.3.2.1.1 Laminae

A lamina is a level (or from time to time bent) course of action of unidirectional (or woven) strands suspended in a network material. A lamina is, for the most part, thought to be orthotropic, and its thickness relies upon the material from which it is made [29]. A cover is a pile of a lamina, which is arranged in a one of a kind way to harvest a favored outcome. The singular lamina is reinforced together with the guide

of a curing procedure that relies upon the material gadget utilized. The mechanical reaction of a cover is uncommon from that of the character lamina that structures it. The cover's reaction relies upon the properties of each lamina, as appropriately as the request in which the lamina is stacked [30].
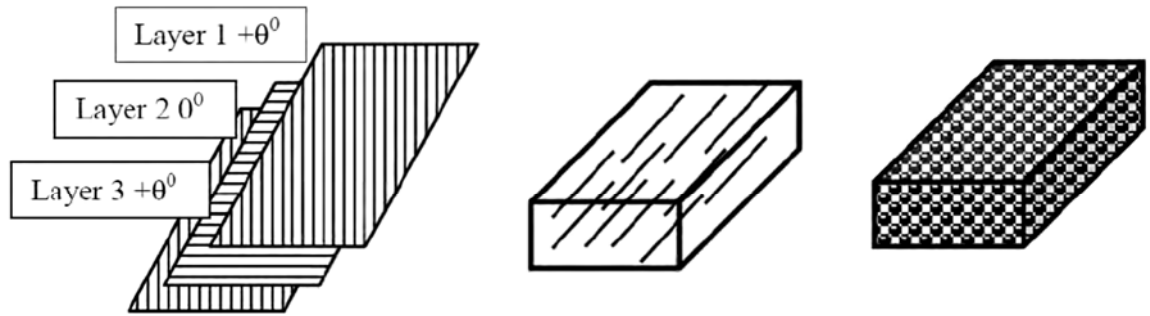
(a) Laminated Composite   (b) Discontinuous Fiber Composite (c) Particulate Composite

Figure 1.5: A schematic of laminated composite material [31].

The male or female layers comprise of high-modulus, high-quality strands implanted in a polymeric, metallic, or artistic grid material. Strands right now being used comprise of carbon, glass, aramid, boron, and silicon carbide. Lattice materials that are being used comprise of thermoplastic and thermoset saps, fired, and metallic. Figure 1.6 depicts examples of the topologies of a variety of cellular lattices configured as the cores of sandwich panel structures. Layers of particular materials may also be utilized[6], bringing about a mixture overlay. The man or lady layers of a cover, for the most part, are orthotropic (key homes in orthogonal bearings) or transversely (isotropic homes in a transverse plane of the layer). Covers may likewise flaunt anisotropic (variable course of vital properties), orthotropic, or semi isotropic properties. Semi isotropic covers flaunt isotropic (free of heading) in plane reaction, however, do never again show isotropic out-of-plane (bowing) reaction [6].
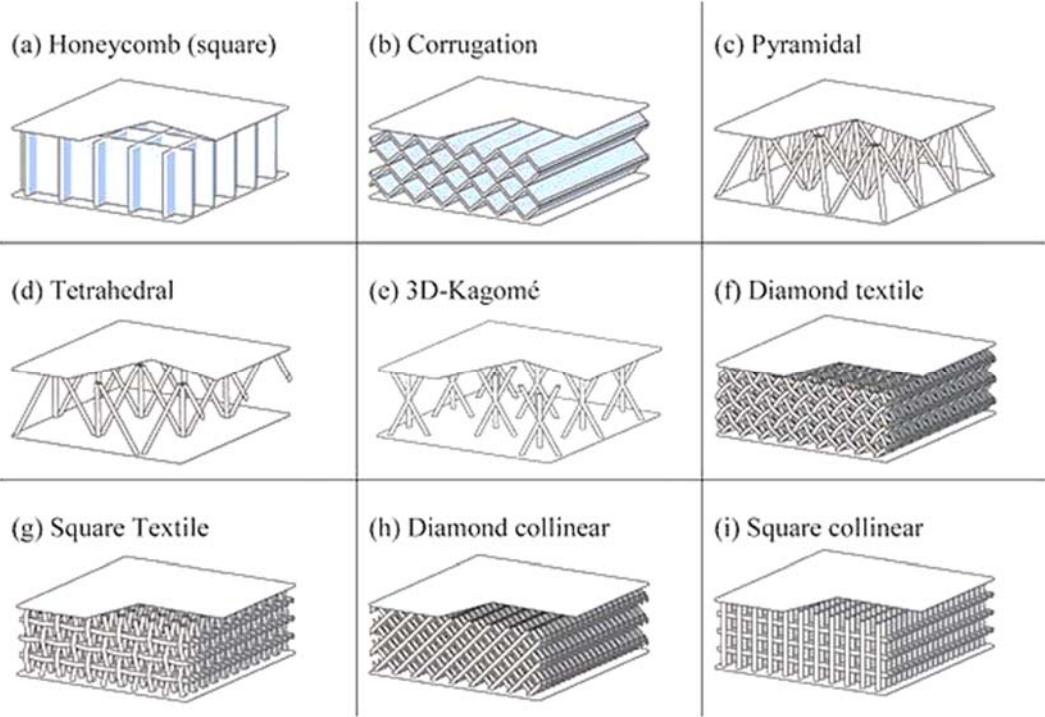
Figure 1.6: Some of the topologies of a variety of cellular lattices configured as the cores of sandwich panel structures [32].

1.3.3 Particulate Composite Materials

Particulate composites are made by means of mixing silica flour, glass beads, even sand into a polymer at some stage in processing. Particulate composites are an awful lot much less environment-friendly in the way the filler contributes to the strength. There is a small obtain in stiffness, and every so often in strength and toughness [33], but it is some distance less than in a fibrous composite. Their enchantment lies extra in their low cost and in the correct put on resistance that a challenging filler can supply [34].

1.3.4 Combinations of Composite Materials

Composite are mixtures of two resources in which one of the materials, referred to as the reinforcing phase, is in the shape of fibers, sheets, or particles, and are

embedded in the different substances called the matrix phase. The reinforcing fabric and the matrix cloth can be metal, ceramic, or polymer. Typically, reinforcing substances are sturdy with low densities whilst the matrix is commonly a ductile, or tough, material. The draw lower back is that such composites are often increased excessive priced than traditional materials. Examples of some current day software of composites include the diesel piston[35], brake-shoes and pads, tires and the Beech craft aircraft in which one hundred percent of the structural aspects are composites [36].

1.4 Major Composite Classes

Consisting of two or a lot of distinct phases, secure along. Solid materials will be divided into four categories: polymers, metals, ceramics, and carbon, that we tend to think about as a separate category attributable to its distinctive characteristics. The kinds of fabric combos currently in use. Composites square measure sometimes classified by the sort of fabric used for the matrix. The four primary classes of composites square measure chemical compound matrix composites (PMCs), metal matrix composites (MMCs), ceramic matrix composites (CMCs), and carbon/carbon composites (CCCs). At this point, PMCs square measure the foremost wide used category of composites. However, there square measure vital applications of the opposite varieties, that square measure indicative of their nice potential in applied science applications [37]. The most sorts of reinforcements employed in composite materials: aligned continuous fibers, discontinuous fibers, whiskers (elongated single crystals)[38], particles, and diverse kinds of fibrous architectures created by textile technology, like materials and braids. More and more, designers' square measure mistreatment hybrid composites that mix differing kinds of reinforcements to realize a lot of potencies and to cut back price [39].

1.4.1 Polymer-Matrix Composites

Polymer-matrix composites (PMCs) carries with it a compound organic compound because the matrix, with fibers as the reinforcement medium. These

materials are employed in the best diversity of composite applications, furthermore as within the largest quantities, in lightweight of their room-temperature properties[40], simple fabrication, and value [41].

1.4.2 Metal-Matrix Composites

As the name implies, the matrix is a metal for metal matrix composites. Moreover, strengthening can increase specific hardness, specific strength, corrosion resistance, creep resistance, thermal conductivity and dimensional stability. Some of the advantages of these materials over polymer matrix compounds are high operating temperatures, resistance to inhibition of inflammation and degradation of organic liquids. Metal matrix compounds are much more expensive than small and medium size vehicles, so the use of mc is somewhat limited. Aluminum, magnesium, titanium, and copper alloys are used as matrix materials as well as super alloys. The reinforcement may be in the form of continuous or interspersed fibers or particles in the form of bristles; the concentrations typically vary between 10% and 60%. The materials include continuous carbon fiber, silicon carbide, boron, aluminum oxide and thermal minerals[42]. Intermittent reinforcements, on the other hand, are mainly composed of silicon carbide yarns, fibers cut from aluminum and carbon oxides, silicon carbide particles and aluminum oxide [43].

1.4.3 Ceramic-Metal Composites

Composite technology is rapidly evolving to accommodate a wide variety of industrial sectors such as aviation, automotive and electricity. New fibers, new matrices, new composite structures and innovative production processes continue to offer exciting opportunities for performance and discounts. It is necessary to protect the competitive power in the globalizing world markets. The prediction of compound behavior continues to improve with advanced scientific understanding and modeling capabilities that allow for more efficient and reliable use of these complex materials. Industrial stage and key design drivers and material requirements are discussed in detail in this section. The manufacturers around the world are obliged to increase

productivity in order to comply with increasingly stringent emission laws. Over the years, various methods have been used to realize these productivity gains. However, increasing the temperature at which the engine is operating has caused the most significant increase in gas turbine efficiency [44].

1.4.4 Carbon-Carbon Composites

Carbon carbon-based materials (CCM) are a conventional type of classes comparable to the graphite/epoxide household of polymer matrix compounds. These substances can be produced in a huge range of substances using monolithic, unidimensional, one-way boxes, ribbons or fabrics. Thanks to its versatility, its mechanical residences can be without problems adjusted. Carbon-based substances have excessive strength, hardness potential, and high thermal and chemical stability in inert environments. The carbon compounds consist of a fibrous carbon sub layer in a carbon matrix. Although both factors are identical, the compound does not facilitate complex behavior. Because the nation of each issue may additionally be distinct from carbon dioxide. Crystallized carbon, namely graphite, is intently associated with susceptible Van der Waal forces of hexagonal carbon binding plates [45].

1.4.5 Hybrid Composites

An especially new fiber bolstered composite is a hybrid bought by means of the usage of two or more exclusive fiber patterns in a single matrix; Hybrids have a better mixture of homes than composites containing a single fiber type. Various mixtures of fibers and matrix substances are used, but in the most frequent system, the carbon and glass fibers are incorporated into a polymeric resin. The carbon fibers are solid and quite challenging and supply low-density reinforcement; however, this is expensive. Glass fibers are cheaper and do now not exhibit carbon stiffness. The glass-carbon hybrid is stronger and harder, has greater affect electricity and can be produced at a decrease fee than same carbon or glass plastics. The two distinctive fibers can be mixed with quite a number of approaches to eventually influence their average properties. When hybrid composites are stressed, failure is typically no longer

14

catastrophic. The important applications for hybrid composites are lightweight, structural elements of water and air transport, carrying items and lightweight orthopedic surgeons' components [46, 47].

1.5 Current Applications

Composite materials have played an important role in weight reduction and today there is three main use is that fiber, Aramid reinforcement glass, and epoxy. There are others, such as toughening of boron (compound, which had a tungsten core). Since 1987, the use of space, composites have doubled every five years, will become the new compounds is always visible. Having been raised about the ability of components de descriptions and applications, versatile, and space vehicles using warm, and hot air balloon gondolas gliders travelers to employees, customers, and the battle space shuttles. The applications developer from all poultry and other animals, helicopter rotor blades, propellers, bodies of seats and a tool [48].

1.5.1 Aircraft Brakes

Carbon brakes had been in the beginning used in excessive performance navy aircraft applications. The lower weight and higher electricity absorption capability of carbon brakes justified their cost, which historically used to be higher than the fee of steel brakes. These value concerns frequently resulted in the use of metal brakes on smaller, short-haul industrial airplanes and carbon brakes on larger, long-haul commercial airplanes. In the past, the higher fee of carbon brakes may want to greater without difficulty be justified for larger airplanes due to the fact of the cost savings related to reduced weight and longer service life. However, current upgrades in carbon brake manufacturing and overhaul. Carbon brakes are a realistic choice to metal brakes. Advances in engineering and manufacturing suggest that retrofitting carbon brakes onto existing airplanes can minimize gasoline costs for certain models. This article affords historic history about carbon brakes and outlines their operational advantages, such as their wonderful environmental impact. It is essential to be aware that this article does no longer address total fee of possession subjects such as usage

and overhaul costs. Operators should weigh the decisions on brake type based totally on countless considerations, together with specific model usage, route utilization, and price shape [49].

1.5.2 Automotive

The cutting-edge materials used in car industry each category of metals and composites are reviewed. Also, the most current topics of research on improvement of new compositions, manufacturing, and characterizations of these materials for the specific cause of use in automotive is presented. Polymer composite substances have been used for purposes with low production volumes, because of their shortened lead times and lower funding charges relative to traditional metal fabrication. Important drivers of the boom of polymer composites have been the reduced weight and parts consolidation opportunities the cloth offers, as well as graph flexibility, corrosion resistance, fabric anisotropy, and mechanical properties. The price of composite substances is generally a lot higher (up to 10 instances greater when the usage of carbon fibers) than those of traditional metals. The essential targets for future development have to be the use of hybrid composites (low-cost fibers to be used the place viable and aramid and carbon fibers to be used only where they are required for damage tolerance or stiffness reasons), the contrast of particularly automated and speedy manufacturing strategies which include the utility of intelligent performs or half-finished goods, and the full use of the achievable of composites for components integration. The glass-reinforced thermo set composites are the most generally used composite in car functions today, however with the development of very excessive [50].

1.5.3 Other Commercial Applications

The renewed hobby in wind generators has been induced through the use of composites in the fabrication of the blades. One can mention additionally the composite propeller blades for the cooling blowers, which borrow the science of the aircraft propellers, which have a velocity of rotation larger than for the wind turbines.

As it is shown in Fig. 1.7, fifty percent of Boeing 787 have been constructed with composites material.
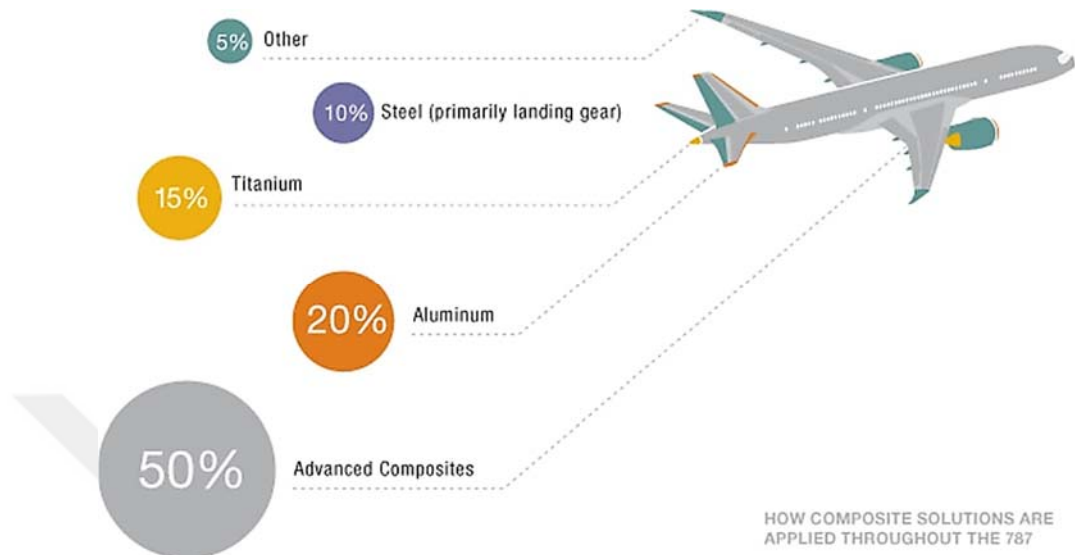
Figure 1.7: Fifty percent of Boeing 787 have been constructed from carbon fiber [51].

Some of other vehicles that are used composite materials in them can be regarded as, bicycles and sail boats like "multishells". Compressed fuel bottles are made the usage of filament-wound glass epoxy or Kevlar epoxy. Tubes for off-shore installations made of glass/carbon/resin, which are three to four instances lighter than tubes made of steel. Biomechanics the carbon/carbon composites have the rare properties of now not upsetting fibrous outgrowth when in contact with the blood stream; they are so called Thrombo resistant. Telepherique cabin the use of composites on the classical answer for the telepherique motors made of metals gives, at equal mass, an excellent augmentation of the beneficial payload [52].

1.6 Conclusion

      In this section a brief bibliography about the composite material and the different kinds of fibers, which have been used in the process of constructing the different kinds of laminates were presented. Furthermore, some of the laminate joints were presented and the pro and cons of using composite material for laminate joints were described. Moreover, some of the applications of composite materials in industries were presented. According to this section it is obvious that the progress of using the composite material is so fast and doing research about them is valuable.

CHAPTER 2

DESCRIBING THREE MATHEMATICAL MODEL FOR LAMINATE JOINTS

2.1 Introduction

In this section three composite modeling methods are presented. The proposed models are based on three journal papers that are simulated in chapter 3. In the proposed models the effect of different parameters which can change the characteristics of the composite material like friction force are considered. Moreover, the models are obtained based on different mechanical structures.

2.2 Laminate Joints

One of the most important application of the composite material is using to make a highly efficient structure like joints. Some of the reasons which have been convinced the engineers to use this kind of material in different application as the joint can be regarded as, highly strength, low weight and robust to vibration.

Based on the points about the composite material, it is obvious that doing research in this field can help to improve the safety of the structures so significantly. The two main classes for the laminate joints can be considered as, bonded joints and bolted joints. Figures 2.1 and 2.2 illustrates the bonded joints of composite structures [53].
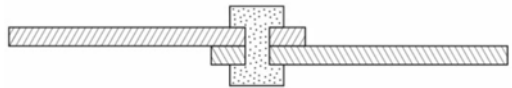
Figure 2.1: Established joining technique.
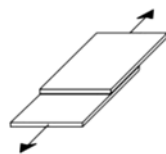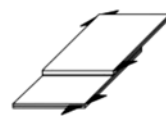
Figure 2.2: Various joint design options.

Based on the adhesive technology which is supported with the bonded joints the structures with the different mechanical properties can join, like the composite and metal parts. The main concern in bonded joints design is the bond area in shear, which

should carry the load through the joint. According to the mechanical fasteners, which usually require for joining composite structural components, like bolted composite joints, some failure modes of bolted joints have been happed like, bearing failure of the materials, tension failure, shear-out or cleavage failure. Figure 2.3 represents bolted joint failures.
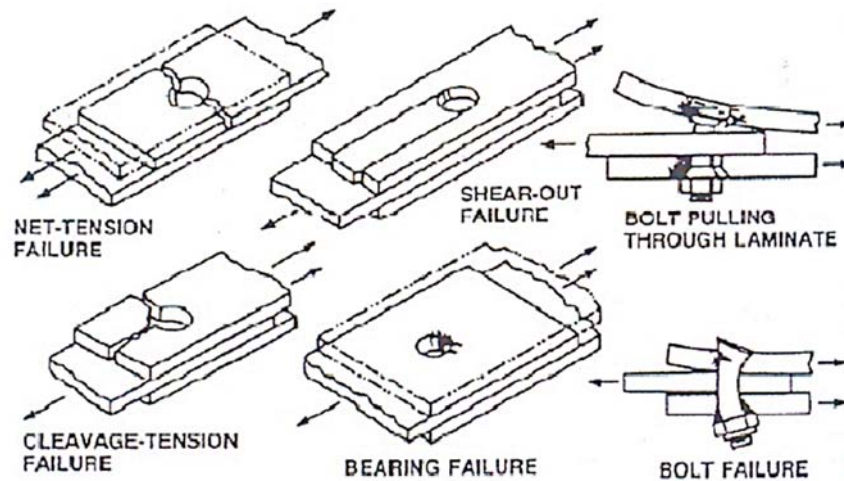
Figure 2.3: bolted joint failures [54].

2.3 First Model

According to [47], in the first level, before the clearance was eliminated, the external applied force F considered as a very small value, and assumed that the secondary bending did not occur in the joint [55]. The F variable is defined as the external tensile force which is transferred from the upper laminate to the lower laminate through the friction force, which is defined as f_{l-n} and effect between the laminate and nut. Figure 2.4 illustrates schematic diagrams of the bolt-load carrying mechanism in a single-lap. The friction force between the two laminates is defined as f_{l-l} [56].
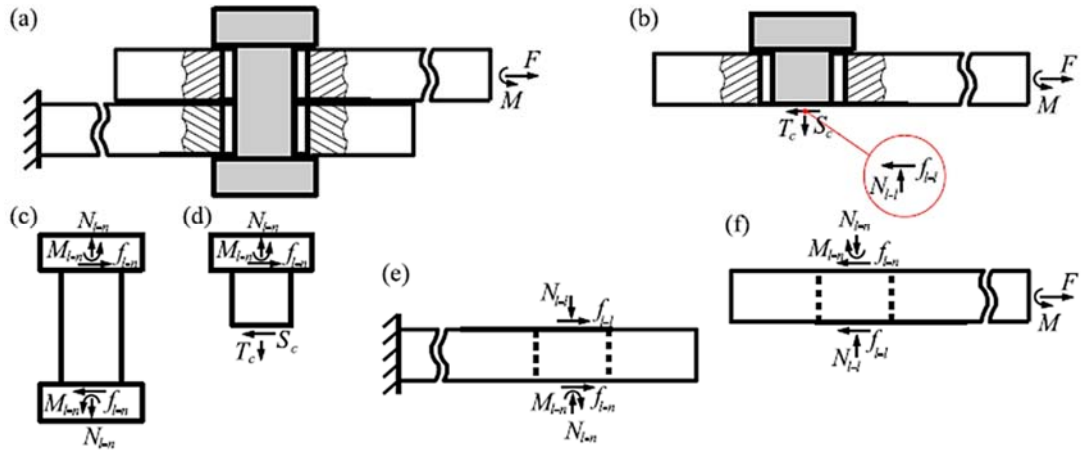
Figure 2.4: Schematic diagrams of the bolt-load carrying mechanism in a single-lap.

In Eq. 1 the friction force between the lower laminate and nut which is defined with f_{l-n} cause to the friction force between the upper laminate and nut was balanced during the load transfer, Fig. 2.1(c). The friction force resulted in the bolt being subjected to a shear load S_c, Fig. 2.4. According to Fig. 2.4,

$$F = f_{l-n} + f_{l-l} \tag{1}$$

$$f_{l-n} = S_c \tag{2}$$

$$f_{l-l} = F - S_c \tag{3}$$

It is assumed that the rotation angle of the bolt is equal to the laminates, θ, because the deformation can be negligible. In addition, the bolt bearing load and friction force developed on the contact surface are denoted by N_o and f_o, respectively. Based on Fig. 2.5.

$$F \cos \theta = f_{l-n} + f_{l-l} + N_o \tag{4}$$

$$F \sin \theta = f_o + N_{l-n} - N_{l-l} = T_c - N_{l-l} \tag{5}$$
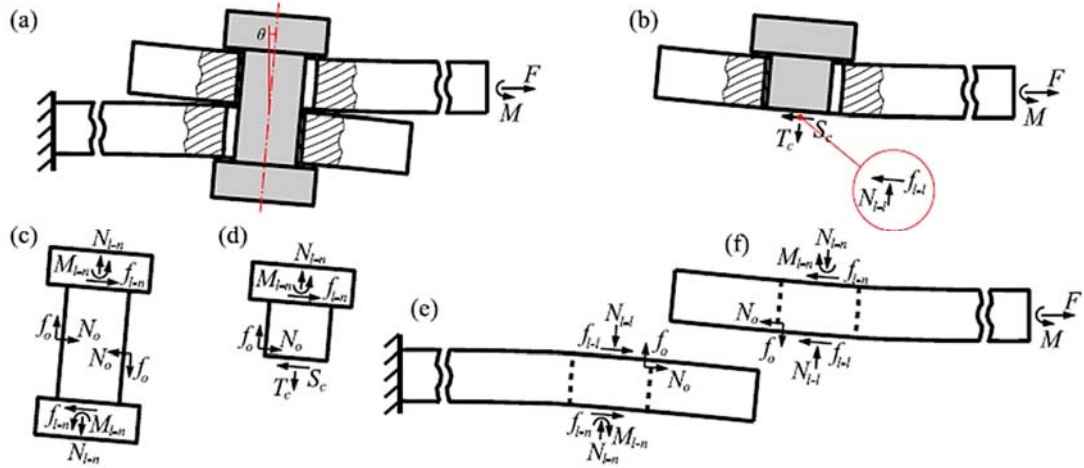
Figure 2.5: Schematic diagrams of the bolt bearing mechanism.

According to Fig. 2,5, it is found that the bolt shear load is obtained from the friction force between the upper laminate and nut as well as the bolt bearing load N_o. Based on the proposed point, S_c obtained as follow,

$$S_c = N_o + f_{l-n} \qquad (6)$$

2.4 Second Model

In this section an analytical model is presented as an extension of the model proposed by McCarthy and Gray [57]. Figure 2.6 presents the configuration of the under study single-lap single-bolt composite joint.
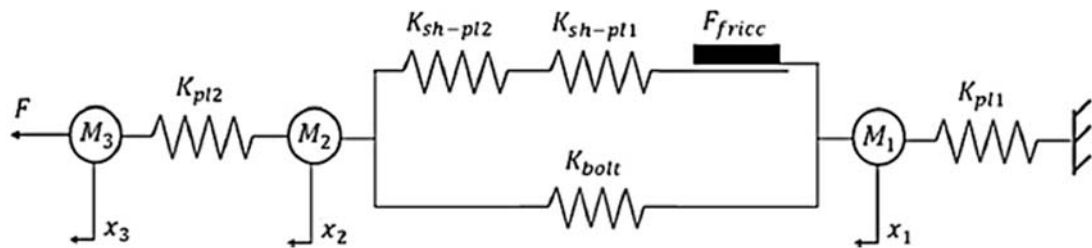
Figure 2.6: Mass-spring model of a single-lap composite bolted-joint.

Based on the [48], the masses are free to move in the x-direction only. According to the Fig. 2.6 linear equations of the system can be form as follows,

$$[M]\{\ddot{x}\} + [K]\{x\} = \{F\} \tag{7}$$

The accelerations can be neglected for the quasi-static loading, which leads to,

$$[K]\{x\} = \{F\} \tag{8}$$

where [K] is the value of stiffness matrix and c is the clearance between bolt diameter and hole, and u_f is the maximum displacement reached during the first region.

$$\begin{bmatrix} K_{pl1} + K_{shear} & -K_{shear} & 0 \\ -K_{shear} & K_{shear} + K_{pl2} & -K_{pl2} \\ 0 & -K_{pl2} & K_{pl2} \end{bmatrix} \begin{bmatrix} x_1 \\ x_2 \\ x_3 \end{bmatrix} = \begin{bmatrix} 0 \\ 0 \\ F \end{bmatrix} \tag{9}$$

$$\begin{bmatrix} K_{pl1} + K_{bolt} & -K_{bolt} & 0 \\ -K_{bolt} & K_{bolt} + K_{pl2} & -K_{pl2} \\ 0 & -K_{pl2} & K_{pl2} \end{bmatrix} \begin{bmatrix} x_1 \\ x_2 \\ x_3 \end{bmatrix} = \begin{bmatrix} -K_{bolt}.c - K_{bolt}.u_f + F_{fricc} \\ K_{bolt}.c + K_{bolt}.u_f - F_{fricc} \\ F \end{bmatrix} \tag{10}$$

By considering E_{Lci} as elasticity modulus in longitudinal direction, and W_{ci} and t_{ci} as the width and thickness of the composite plate respectively, the Eq. 11 is obtained as follows,

$$K_{pli} = \frac{E_{Lci}.W_{ci}.t_{ci}}{P_{ci} - D/2} \tag{11}$$

where P_{ci} is defined as the distance between the hole center and the plate free end where load is applied, and D is the hole diameter. The shear stiffness K_{shear} is obtained as follows, two composite plates in series.

$$K_{shear} = \left[\frac{1}{K_{sh-pl1}} + \frac{1}{K_{sh-pl2}} \right]^{-1} \tag{12}$$

Where K_{sh-pl1} and K_{sh-pl2} are the stiffness under shear load of composite plates 1 and 2. By considering G_{xzi}, A_{Wpli}, and t_{ci} as the interlaminar stiffness of the laminate, the washer area in contact with the composite plate and the plate thickness, respectively, Eq. 13 obtained as follows,

$$K_{sh-pli} = \frac{A_{Wpli}.G_{xzi}}{t_{ci}} \tag{13}$$

24

By considering F_{fricc} as the maximum friction forces value that the joint can transmit and μ and F_{torque} as the friction coefficient and the normal force produced by the bolt torque, Eq. 14 can be defined as follows,

$$F_{fricc} = \mu . F_{torque} \tag{14}$$

$$F_{torque} = \frac{\tau}{K.D} \tag{15}$$

where τ and k are defined as, the bolt torque and the torque coefficient which usually taken as 0.2, respectively [48]. By considering K_{sh-b}, K_{bend-b}, K_{be-pli} and β as the bolt shear stiffness, K_{sh-b}, the bolt bending stiffness, the bearing stiffnesses of plates 1 and 2, K_{be-pli}, and an experimental coefficient, β, the secondary bending effect is obtained as follows,

$$K_{bolt} = \left[\frac{1}{K_{sh-b}} + \left[\frac{1}{K_{bend-b}} + \frac{1}{K_{be-pl1}} + \frac{1}{K_{be-pl2}} \right] (1 + 3\beta) \right]^{-1} \tag{16}$$
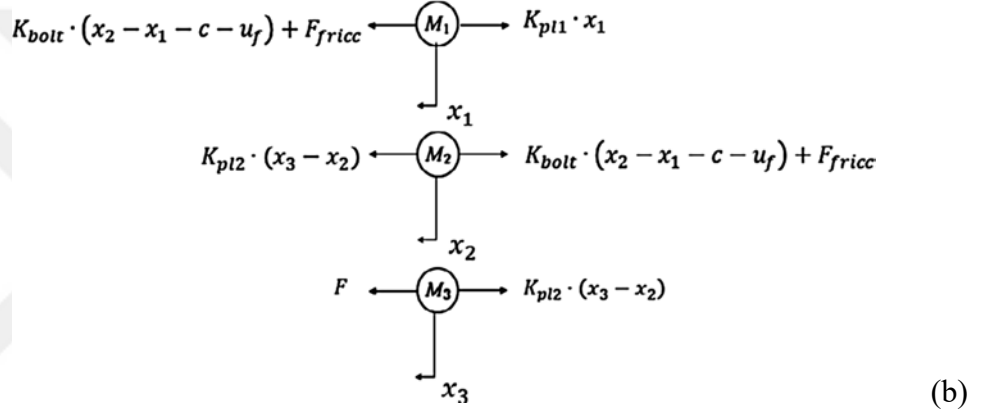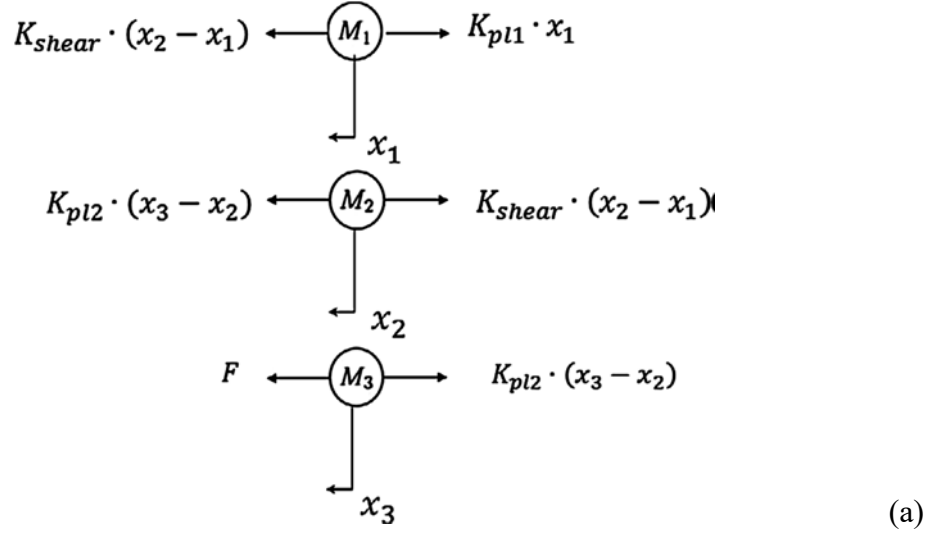
Figure 2.7: Free body diagrams for each mass during the first and second regions.

Moreover, by considering the G_b as the bolt shear modulus, and A_b as the bolt transverse section area the stiffnesses included in K_{bolt} can be achieved as follows:

$$K_{sh-b} = \frac{3G_b A_b}{2(t_{c1}+t_{c2})} \tag{17}$$

$$K_{bend-b} = \frac{E_b t_{c1} t_{c2}}{2(t_{c1}+t_{c2})} \tag{18}$$

In Eq. 18, E_b is defined as the bolt Young modulus. Moreover, E_{Tci} is defined as the elasticity modulus of composite plate in transverse direction which is calculated by using the laminate theory.

$$K_{be-pl1} = t_{c1}\sqrt{E_{Lc1}E_{Tc1}}$$ (19)

$$K_{be-pl2} = t_{c2}\sqrt{E_{Lc2}E_{Tc2}}$$ (20)

According to the main contribution of this work, which is estimating the secondary bending stiffness, two springs are included in the model, $K_{\varphi 1}$ and $K_{\varphi 2}$, and the effect of the secondary bending coefficientβ, can be avoided.

$$K_{bolt} = \left[\frac{1}{K_{sh-b}} + \frac{1}{K_{bend-b}} + \frac{1}{K_{be-pl1}} + \frac{1}{K_{\varphi 1}} + \frac{1}{K_{be-pl2}} + \frac{1}{K_{\varphi 2}}\right]^{-1}$$ (21)
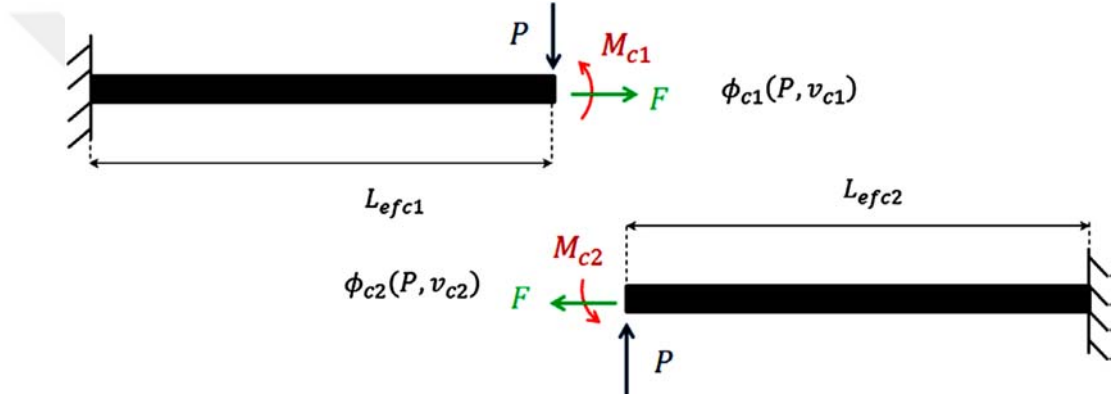
Figure 2.8: Loading conditions applied to composite plates to estimate the secondary bending stiffness [48].

By considering t_m as the load path eccentricity, the Eq.22 can be obtained as follows,

$$M_{c1} + M_{c2} = F.t_m$$ (22)

Equations 23 and 24 present the compatibility equations of rotations and transverse displacement, respectively. By considering, L_{efci}, E_{FCi} and I_{Ci} as the distance between the hole surface and the plate free end, the composite plate flexural modulus which are obtained with the laminate theory and the composite plate's moment of inertia, Eqs. 23 and 24 are obtained.

$$\varphi_{c1} = \varphi_{c2} =$$

$$\frac{F t_m L_{efc1} L_{efc2} (L^3_{efc2} E_{FC1} I_{C1} + L^3_{efc1} E_{FC2} I_{C2})}{L^4_{efc2} E^2_{FC1} I^2_{C1} + 2 L_{efc1} L_{efc2} E_{FC1} E_{FC2} I_{C1} I_{C2} (2 L^2_{efc1} + 3 L_{efc1} L_{efc2} + 2 L^2_{efc2}) + L^4_{efc1} E^2_{FC2} I^2_{C2}}$$

(23)

$$v_{c1} = v_{c2} =$$

$$\frac{F t_m L_{efc1} L_{efc2} (L^2_{efc2} E_{FC1} I_{C1} + L^2_{efc1} E_{FC2} I_{C2})}{2 L^4_{efc2} E^2_{FC1} I^2_{C1} + 4 L_{efc1} L_{efc2} E_{FC1} E_{FC2} I_{C1} I_{C2} (2 L^2_{efc1} + 3 L_{efc1} L_{efc2} + 2 L^2_{efc2}) + 2 L^4_{efc1} E^2_{FC2} I^2_{C2}}$$

(24)

By considering φ_{ci} and t_{ci} as a function of the rotations and plate thickness the longitudinal displacements can be obtained as follows,

$$u_{ci} = \varphi_{ci} \cdot \frac{t_{ci}}{2}$$

(25)

$$K_{\varphi i} = \frac{F}{u_{ci}}$$

(26)

Equations 27 and 28 are presented the secondary bending stiffness for each composite plate yields.

$$K_{\varphi 1} = \frac{2 \left[L^4_{efc2} E^2_{FC1} I^2_{C1} + 2 L_{efc1} L_{efc2} E_{FC1} E_{FC2} I_{C1} I_{C2} (2 L^2_{efc1} + 3 L_{efc1} L_{efc2} + 2 L^2_{efc2}) + L^4_{efc1} E^2_{FC2} I^2_{C2} \right]}{t_{c1} t_m L_{efc1} L_{efc2} (L^3_{efc2} E_{FC1} I_{C1} + L^3_{efc1} E_{FC2} I_{C2})}$$

(27)

$$K_{\varphi 2} =$$

$$\frac{2 \left[L^4_{efc2} E^2_{FC1} I^2_{C1} + 2 L_{efc1} L_{efc2} E_{FC1} E_{FC2} I_{C1} I_{C2} (2 L^2_{efc1} + 3 L_{efc1} L_{efc2} + 2 L^2_{efc2}) + L^4_{efc1} E^2_{FC2} I^2_{C2} \right]}{t_{c2} t_m L_{efc1} L_{efc2} (L^3_{efc2} E_{FC1} I_{C1} + L^3_{efc1} E_{FC2} I_{C2})}$$

(28)

2.5 Third Model

In this model which is presented in [58], the failure criteria which are based on an extension of Chang–Lessard criteria considering as a three-dimensional stress field. Hahn and Tsai by using high-order elasticity theory formulated the non-linear shear

stress–strain relationship. By considering G_{12}, G_{13} and G_{23} are shear modulus, τ_{12}, τ_{13} and τ_{23} are shear stress, α is a constant parameter which is determined experimentally. Based on the proposed variables shear strain, γ_{12} , γ_{13} and γ_{23} are obtained as follows,

$$\gamma_{12} = \frac{1}{G_{12}}\tau_{12} + \alpha\tau^2{}_{12} \tag{29}$$

$$\gamma_{13} = \frac{1}{G_{13}}\tau_{13} + \alpha\tau^2{}_{13} \tag{30}$$

$$\gamma_{23} = \frac{1}{G_{23}}\tau_{23} + \alpha\tau^2{}_{23} \tag{31}$$

Chang–Lessard criteria consider four failure modes which can be regarded as, matrix crushing, matrix cracking, fiber–matrix shearing failure, and fiber failure. In the following each one of them will be presented.

2.5.1 Matrix Crushing

The Eq. 32 presents the compressive transverse stress and in-plane stress, which is based on Chang–Lessard criteria matrix crushing failure ($\sigma_2 < 0$). Moreover, in Eq. 33 the failure criterion includes the out-of plane shear stress contribution is calculated. By considering, σ_2 , Y_c , and γ_{12}^M and γ_{23}^M as the normal stress in transverse direction, the transverse compressive strength, and the ultimate shear strains, the Eqs. 32 and 33 are obtained as follows,

$$\left(\frac{\sigma_2}{Y_c}\right)^2 + \frac{\int_0^{\gamma_{12}} \tau_{12}d\gamma_{12}}{\int_0^{\gamma_{12}^M} \tau_{12}d\gamma_{12}} = e^2{}_{mc2} \tag{32}$$

$$\left(\frac{\sigma_2}{Y_c}\right)^2 + \frac{\int_0^{\gamma_{12}} \tau_{12}d\gamma_{12}}{\int_0^{\gamma_{12}^M} \tau_{12}d\gamma_{12}} + \frac{\int_0^{\gamma_{23}} \tau_{23}d\gamma_{23}}{\int_0^{\gamma_{23}^M} \tau_{23}d\gamma_{23}} = e^2{}_{mc2} \tag{33}$$

where $e_{mc} > 1$. By defining S_{12} and S_{23} as the in-plane and out-of-plane shear strengths, the Eq. 34 can be calculated as follows,

$$\left(\frac{\sigma_2}{Y_c}\right)^2 + \frac{\frac{\tau_{12}^2}{2G_{12}}+\frac{3}{4}\alpha\tau_{12}^4}{\frac{S_{12}^2}{2G_{12}}+\frac{3}{4}\alpha S_{12}^4} + \frac{\frac{\tau_{23}^2}{2G_{23}}+\frac{3}{4}\alpha\tau_{23}^4}{\frac{S_{23}^2}{2G_{23}}+\frac{3}{4}\alpha S_{23}^4} = e^2_{mc2} \tag{34}$$

If the in Eq. 34 the composite material is considered as composite with linear elastic behavior, then the $\alpha = 0$ and the Eq. 34 can be rewrite to:

$$\left(\frac{\sigma_2}{Y_c}\right)^2 + \left(\frac{\tau_{12}}{S_{12}}\right)^2 + \left(\frac{\tau_{23}}{S_{23}}\right)^2 = e^2_{mc2} \tag{35}$$

Equation. 8 presents the failure criterion which can take into account the damage produced by tightening torque.

$$\left(\frac{\sigma_3}{Z_c}\right)^2 + \frac{\frac{\tau_{13}^2}{2G_{13}}+\frac{3}{4}\alpha\tau_{13}^4}{\frac{S_{13}^2}{2G_{13}}+\frac{3}{4}\alpha S_{13}^4} + \frac{\frac{\tau_{23}^2}{2G_{23}}+\frac{3}{4}\alpha\tau_{23}^4}{\frac{S_{23}^2}{2G_{23}}+\frac{3}{4}\alpha S_{23}^4} = e^2_{mc3} \tag{36}$$

The variables σ_3 and Z_C in Eq. 36 are, the out-of-plane normal stress, and the out-of-plane compressive strength, respectively. Moreover, S_{13} is the out-of-plane shear strength. For linear elastic composites that α is equal to zero in them Eq. 36 can be rewrite as,

$$\left(\frac{\sigma_3}{Z_c}\right)^2 + \left(\frac{\tau_{13}}{S_{13}}\right)^2 + \left(\frac{\tau_{23}}{S_{23}}\right)^2 = e^2_{mc3} \tag{37}$$

2.5.2 Matrix Cracking

Based on the Chang–Lessard criterion for in-plane tensile matrix cracking failure ($\sigma_2 > 0$) the contribution of out of- plane shear stress is also considered, Eq. 38.

$$\left(\frac{\sigma_2}{Y_T}\right)^2 + \frac{\int_0^{\gamma_{12}} \tau_{12}d\gamma_{12}}{\int_0^{\gamma_{12}^M} \tau_{12}d\gamma_{12}} + \frac{\int_0^{\gamma_{23}} \tau_{23}d\gamma_{23}}{\int_0^{\gamma_{23}^M} \tau_{23}d\gamma_{23}} = e^2_{mt2} \tag{38}$$

In Eq. 38, Y_T is defined as the transverse tensile strength. One of the main points in this stage is, when the criterion is satisfied ($e_{mt} > 1$) the composite fails by matrix cracking.

$$\left(\frac{\sigma_2}{Y_T}\right)^2 + + \frac{\frac{\tau_{12}^2}{2G_{12}}+\frac{3}{4}\alpha\tau_{12}^4}{\frac{S_{12}^2}{2G_{12}}+\frac{3}{4}\alpha S_{12}^4} + \frac{\frac{\tau_{23}^2}{2G_{23}}+\frac{3}{4}\alpha\tau_{23}^4}{\frac{S_{23}^2}{2G_{23}}+\frac{3}{4}\alpha S_{23}^4} = e^2{}_{mt2} \tag{39}$$

For linear elastic composites Eq. 39 can be rewrite as,

$$\left(\frac{\sigma_2}{Y_T}\right)^2 + \left(\frac{\tau_{12}}{S_{12}}\right)^2 + \left(\frac{\tau_{23}}{S_{23}}\right)^2 = e^2{}_{mt2} \tag{40}$$

Furthermore, a matrix cracking failure criterion can be used to predict delamination onset,

$$\left(\frac{\sigma_3}{Y_T}\right)^2 + + \frac{\frac{\tau_{13}^2}{2G_{13}}+\frac{3}{4}\alpha\tau_{13}^4}{\frac{S_{13}^2}{2G_{13}}+\frac{3}{4}\alpha S_{13}^4} + \frac{\frac{\tau_{23}^2}{2G_{23}}+\frac{3}{4}\alpha\tau_{23}^4}{\frac{S_{23}^2}{2G_{23}}+\frac{3}{4}\alpha S_{23}^4} = e^2{}_{mt3} \tag{41}$$

In Eq. 41, Z_T is defined as the out-of-plane tensile strength. Equation 41 can rewrite for the linear elastic composites as follows:

$$\left(\frac{\sigma_3}{Z_T}\right)^2 + \left(\frac{\tau_{13}}{S_{13}}\right)^2 + \left(\frac{\tau_{23}}{S_{23}}\right)^2 = e^2{}_{mt3} \tag{42}$$

2.5.3 Fiber–Matrix Shearing Failure

In Eq. 43 the present failure criterion, which includes the of out-of-plane shear stresses' contribution is presents as follows,

$$\left(\frac{\sigma_1}{X_c}\right)^2 + \frac{\int_0^{\gamma_{12}} \tau_{12}d\gamma_{12}}{\int_0^{\gamma_{12}^M} \tau_{12}d\gamma_{12}} + \frac{\int_0^{\gamma_{13}} \tau_{13}d\gamma_{13}}{\int_0^{\gamma_{13}^M} \tau_{13}d\gamma_{13}} = e^2{}_s \tag{43}$$

In Eq. 43, σ_1 and X_c are, the normal stress in fiber direction and the fiber compressive strength.

$$\left(\frac{\sigma_1}{X_c}\right)^2 + + \frac{\frac{\tau_{12}^2}{2G_{12}} + \frac{3}{4}\alpha\tau_{12}^4}{\frac{S_{12}^2}{2G_{12}} + \frac{3}{4}\alpha S_{12}^4} + \frac{\frac{\tau_{13}^2}{2G_{13}} + \frac{3}{4}\alpha\tau_{13}^4}{\frac{S_{13}^2}{2G_{13}} + \frac{3}{4}\alpha S_{13}^4} = e^2{}_s \tag{44}$$

$$\left(\frac{\sigma_1}{X_c}\right)^2 + \left(\frac{\tau_{12}}{S_{12}}\right)^2 + \left(\frac{\tau_{12}}{S_{12}}\right)^2 = e^2{}_s \tag{45}$$

2.5.4 Fiber failure

In order to consider the possibility of tensile loads, the present model includes a tensile fiber failure criterion based on Chang–Chang failure criteria,

$$\frac{\sigma_1}{X_c} = e^2{}_{fc} \tag{46}$$

$$\left(\frac{\sigma_1}{X_T}\right)^2 + \frac{\int_0^{\gamma_{12}} \tau_{12} d\gamma_{12}}{\int_0^{\gamma_{12}^M} \tau_{12} d\gamma_{12}} + \frac{\int_0^{\gamma_{13}} \tau_{13} d\gamma_{13}}{\int_0^{\gamma_{13}^M} \tau_{13} d\gamma_{13}} = e^2{}_{ft} \tag{47}$$

where X_T is the fiber tensile strength. Moreover, the tensile fiber failure criterion yields:

$$\left(\frac{\sigma_1}{X_T}\right)^2 + + \frac{\frac{\tau_{12}^2}{2G_{12}} + \frac{3}{4}\alpha\tau_{12}^4}{\frac{S_{12}^2}{2G_{12}} + \frac{3}{4}\alpha S_{12}^4} + \frac{\frac{\tau_{13}^2}{2G_{13}} + \frac{3}{4}\alpha\tau_{13}^4}{\frac{S_{13}^2}{2G_{13}} + \frac{3}{4}\alpha S_{13}^4} = e^2{}_{ft} \tag{48}$$

For composites with linear elastic behavior,

$$\left(\frac{\sigma_1}{X_T}\right)^2 + \left(\frac{\tau_{12}}{S_{12}}\right)^2 + \left(\frac{\tau_{13}}{S_{13}}\right)^2 = e^2{}_{ft} \tag{49}$$

2.6 Conclusion

In this section three different models which were used for the composite materials were presented. According to the proposed models, considering the parameters like friction force can improve the accuracy of the model, but it has direct effect in the calculating time.

CHAPTER 3

ANALYZING DIFFERENT CASES FOR THE SINGLE COMPOSITE LAP-JOINTS

3.1 Introduction

In this chapter some of the main parameters which effect on the single composite lap-joint's deformation and stress are analyzed. Firstly, some of the designs and the composite materials which are used in the other papers are described and the effect of thickness and the clearance on the under study system are assessed. Then, three design are considered to simulate in ANSYS software to achieve the best design based on the materials which are applied for them. Finally, a comparison between the proposed simulated systems are done and some suggestions are presented to ameliorate the effect of load on the single lap joint of composite plates in terms of, decreasing the deformation and stress value. Moreover, the boundary conditions of all case studies are considered like the first case study.

3.2 The Importance of Analysis the Effect of Thickness and Clearance

The thickness and clearance can be considered as the factors which have direct effect on the single composite lap-joint's deformation and stress condition. In the following the proposed factors will be analyzed.

Analyzing the effect of load sharing composite joints is one of the main points which can give us a good view about designing and constructing the high performance composite plate in terms of reduce the deformation and stress that is happened based on the effect of the load. According to [49], the IM7/MTM-45-1 carbon/epoxy

composite material is used for the plates and the bolt and nut are constructed based on 6Al–4V titanium alloy. Figure 1 illustrates the general geometry of the aforementioned single-bolt, single-lap joint.
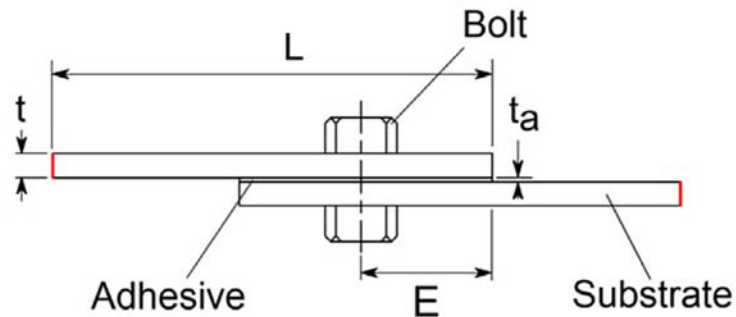
Figure 3.1: The general geometry of the single-bolt, single-lap joint [49].

Based on the proposed analysis, the friction force that the joint can transmit based on the applying the maximum load. Furthermore, when the values of plate length be increased, it leads to a lower joint stiffness. On the contrary, when the values of plate width be increased, it leads to a higher joint stiffness. Based on the aforementioned analysis, if the bolt diameter is reduced, the joint stiffness increases only in the first region, if the bolt diameter is reduced. Figure 3.2 represents the effect of clearance on bolt load transfer.
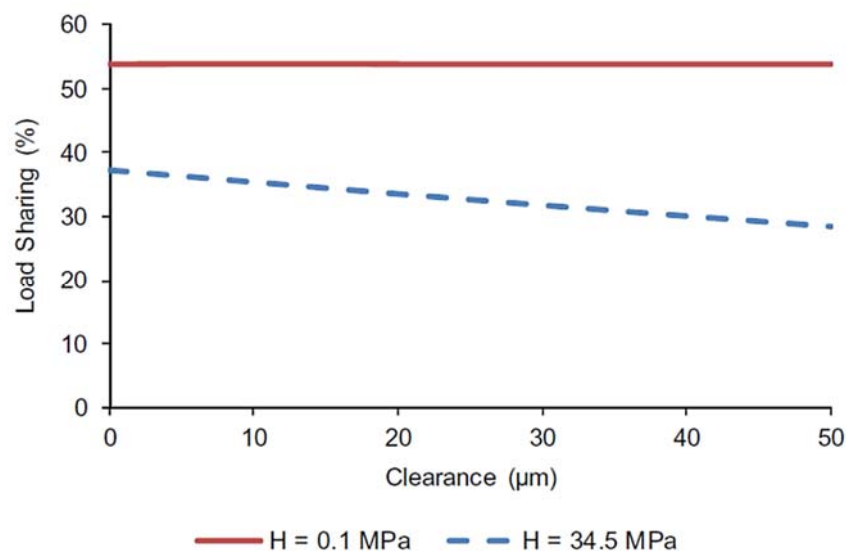
Figure 3.2: the effect of clearance on bolt load transfer [59].

The other paper analysis based on [60], are presented that thin joints experience

higher degrees of out-of-plane displacement and the taper type has a significant effect on secondary bending and hence the final mode of failure in the joint. Figure 3.3 depicts different kinds of tappers, which are analyzed in the proposed research.
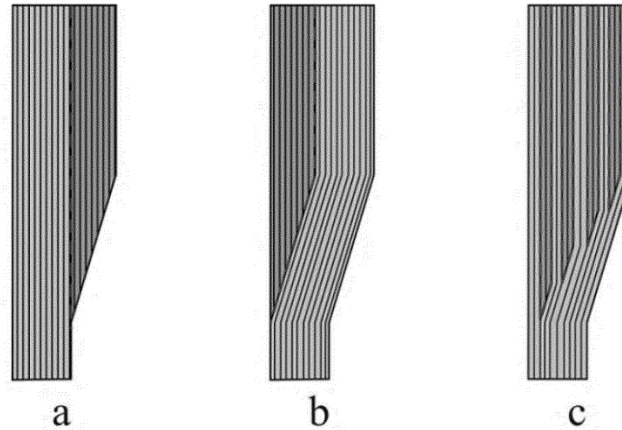
Figure 3.3: Different kinds of tappers, which are analyzed in [60].

Moreover, in terms of increasing joint thickness, out-of-plane displacement is less severe in thick joints.

The main purpose of the analysis like the ones which are explained in this section, is finding a model or method to predict the bolted single-lap composite joints. In [59] a method for predicting a composite single shear lap joints strength is presented. Moreover, under tensile loading, the contact area between the fasteners and the hole edges' secondary bending increased, which increased the bearing strength and reduced the bearing stresses.

As mentioned at the beginning of this section, clearance is one of the main factors of important features of a composite bolted single-lap joint. In the following some of the researches, which have focused on the proposed factor are represented.

According to [61], the effects of bolt-hole clearance on Bearing strength of carbon fiber-epoxy laminates is considered. Based on the proposed research, significant reduction in bearing strength at 4% hole deformation was obtained for the pin-loaded and clamped laminates, according to the bolt-hole clearance, which verified the significant effect of bolt-hole clearance with regard to the design bearing strength

of mechanically fastened joints. Moreover, the magnitude and distribution of stress at the hole was found to be significantly dependent on the level of clearance. Figures 3.4 and 3.5 represent the bolt–hole clearance effect on the static bearing strength of pin loaded and clamped, respectively.

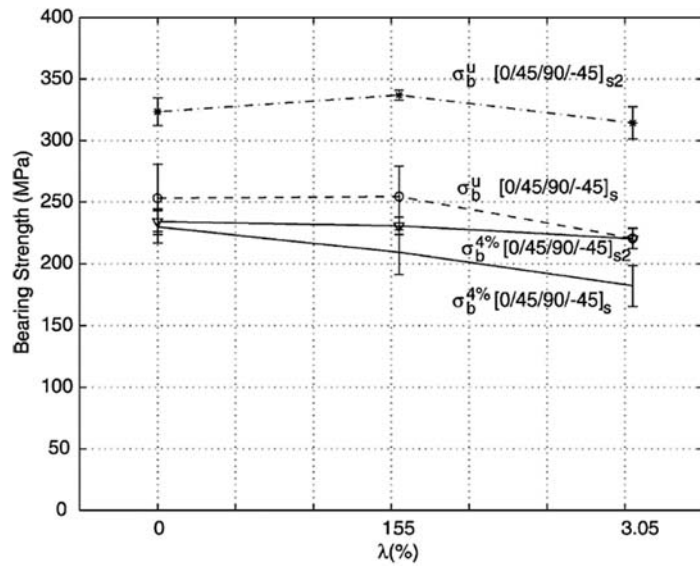**Figure 3.4:** Effect of bolt-hole clearance on the static bearing strength of pin loaded [0/45/90/-45]s and [0/45/90/-45]s2 laminates [61].
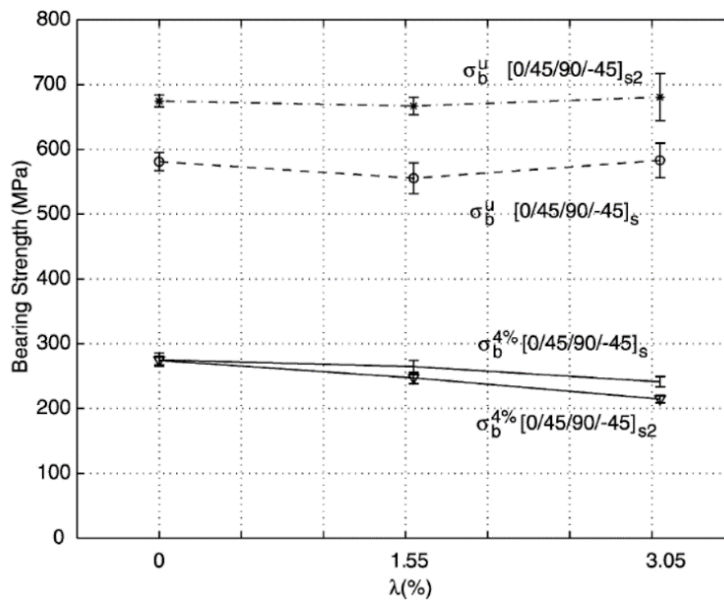
Figure 3.5: Effect of bolt-hole clearance on the static bearing strength of clamped [0/45/90/-45] s and [0/45/90/-45] s2 laminates [61].

Furthermore, the damage in the bearing plane was found to be more extensive

36

for laminates with larger bolt-hole clearance.

One of the other researches which has concentrated on effect of clearance is done by C.T. McCarthy 1, M.A. McCarthy [62]. Based on the proposed research, when the clearance be increased, it leads to increased bolt rotation, decreased bolt-hole contact area, and decreased joint stiffness. Moreover, increasing clearance should result in reduced load capacity for the joint; however only a few papers have included an analysis of failure, or experimental evidence to support this claim. Furthermore, a reduction in slope (stiffness) due to increasing clearance is clearly visible. The peak radial stress increases with increasing clearance (due to the load being distributed over a smaller contact area). Table 3.1 represents the clearances in the proposed research.

Table 3.1: Clearances in present in [62].

Clearance code	Nominal clearance (μm)
C1	0
C2	80
C3	160
C4	240

Figure 3.6 illustrates the experimental joint bearing stiffness variations with increasing applied bearing stress, together with model predictions of first fiber failure.
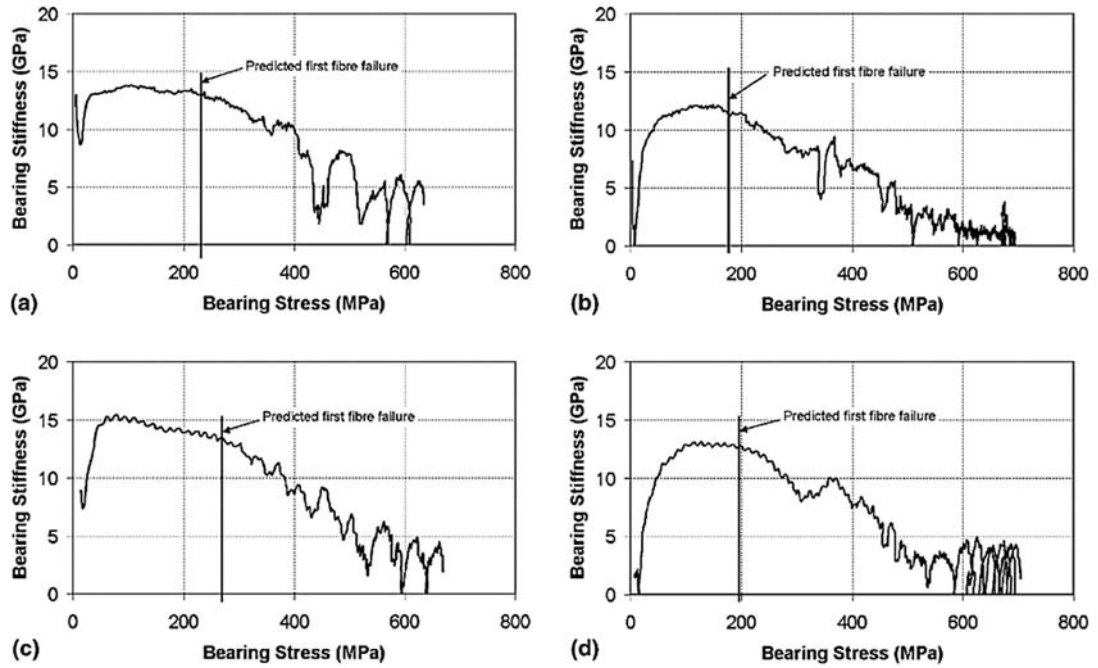
Figure 3.6: Experimental joint bearing stiffness variations with increasing applied bearing stress [62].

3.3 Simulation Case Study

In this section three single composite lap-joint, which are different in terms of design and material are simulated in ANSYS software and the obtained results are compared with each other. The proposed single composite lap-joints are based on three research papers, which are represented briefly in the following.

3.3.1 The First Case Study

The first case study is based on the research of Fengrui Liu [56]. The structure of the composite single-lap bolted joint depicts in Fig. 3.7.
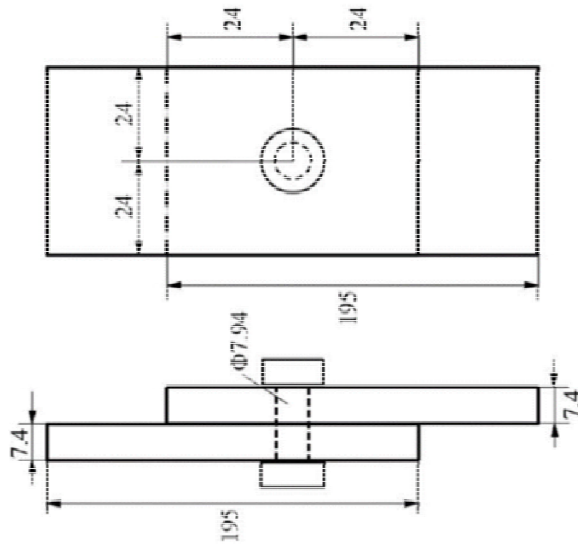
Figure 3.7: The structure of the composite single-lap bolted [56].

The two laminate plates have been made of T800 carbon epoxy composites with lay-ups of [45/0/-45/0/90/0/45/0/-45/0]$_{s2}$. The surface to- surface contact technique was used. Moreover, hexahedral meshes on the outer layer of the bolt shank is implemented. Figure 3.8 represents the FE model of the single-lap, single-bolt joint, which is applied in the first case study.
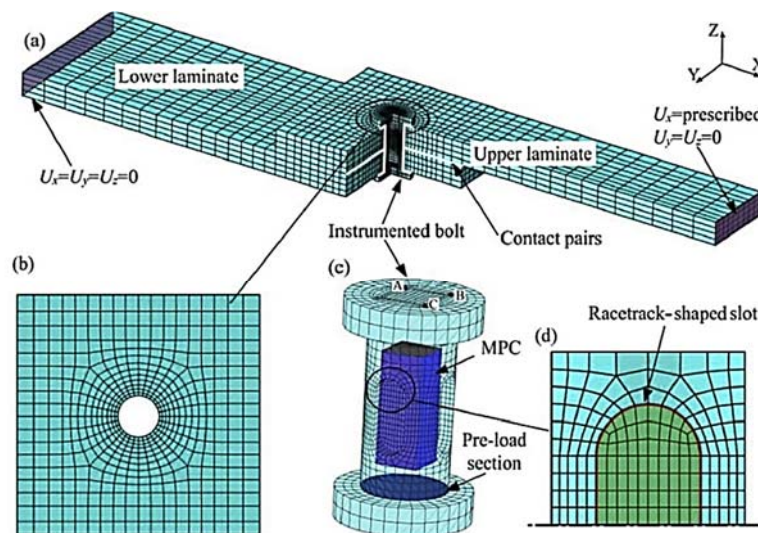
Figure 3.8: FE model of the single-lap, single-bolt joint: (a) mesh and boundary conditions (b) refined FE mesh around the bolt hole (c) internal cube and surrounding parts (d) refined meshes on the bolt shank surface [56].
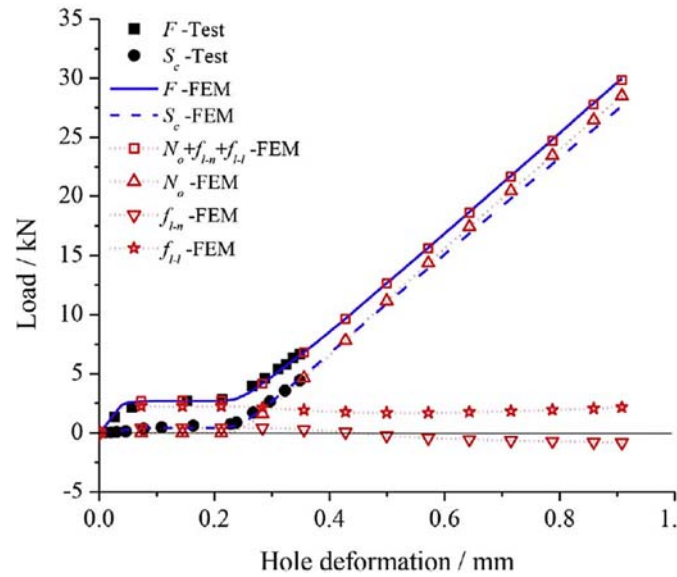
Figure 3.9: Experimental and numerical load vs. hole-deformation curves for the single-bolt joint [56].

Figure 3.9 represents the experimental and numerical load and hole-deformation curves for the single-bolt joint.

3.3.1.1 Simulation of the First Case Study in ANSYS

Based on the aforementioned research, the structure of the single-lap, single-bolt joint is designed in SOLIDWORKS software. In the next step the proposed designed structure is imported to the ANSYS software. Figure 3.10 illustrates the designed the single-lap, single-bolt joint in ANSYS software.
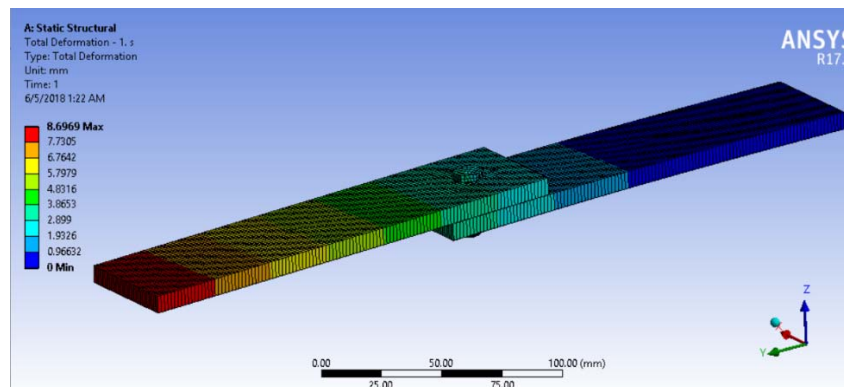
Figure 3.10: The designed single-lap, single-bolt joint which is imported in ANSYS software.

Based on the first case study the structure of single-lap, single-bolt joint which is designed in SOLIDWORKS software is imported in ANSYS software and based on the characteristics of the first case study, the parameters are set on the system. Table 3.2 represents some of the characteristics of the system which is analyzed in ANSYS. In all results in this chapter the forces are implemented on the system from zero to 5 KN for a one second period [63].

The parameters which are analyzed in this section can be regarded as, the total deformation of the composite plates, bolt and the hole of each plates. Moreover, the directional deformation of composite plates, bolt and the hole of each plates are calculated in X, Y and Z directions, which is mentioned in Fig. 3.10. The down and upside laminate plates was modeled with 2515 elements and the aluminum plates with 30710 elements. The boundary conditions for the proposed simulation is the same as given in Fig. 3.8. The parameters TH, DH are upper plate hole and bottom plate hole, respectively. According to the paper the bolt was subdivided into an internal cube and surrounding part and the Tie Constraint technique was used to connect these two components. Furthermore, the meshes far from the hole boundary were not as refined as those near the hole. Table 3.3 represents the minimum and maximum total and directional deformation values.

Table 3.2: Characteristics of the designed single-lap, single-bolt joint, which is analyzed in ANSYS.

	Material		
Assignment	40CrNiMoA alloy	T800 Carbon Epoxy	40CrNiMoA alloy
Nonlinear Effects		Yes	
Thermal Strain Effects		Yes	
Bounding Box			
Length X	12.973 mm	48. mm	12.888 mm
Length Y	11.24 mm	195. mm	11.411 mm
Length Z	4. mm	0. mm	3.4694e-015 mm	28. mm
Properties			
Volume	230.52 mm³	68898 mm³	1369.6 mm³
Mass	1.8096e-003 kg	0.10266 kg	1.0752e-002 kg
Centroid X	5.9399e-003 mm	1.1986e-015 mm	-1.1378e-015 mm	-2.9815e-004 mm
Centroid Y	2.727e-003 mm	-73.887 mm	73.887 mm	7.3222e-003 mm
Centroid Z	-33.619 mm	-24.227 mm	-16.827 mm	-26.437 mm
Moment of Inertia Ip1	2.5896e-002 kg·mm²	343.9 kg·mm²	0.89207 kg·mm²
Moment of Inertia Ip2	2.5879e-002 kg·mm²	19.813 kg·mm²	0.89213 kg·mm²
Moment of Inertia Ip3	4.6927e-002 kg·mm²	324.09 kg·mm²	0.10259 kg·mm²
Surface Area(approx.)		9310.5 mm²	

Table 3.3: The minimum and maximum total and directional deformation values.

Object Name	Total Deformation - 1. s	Total Deformation - TH - 1. s	Total Deformation - DH - 1. s	X Axis - Directional Deformation - Up - End Time	X Axis - Directional Deformation - Down - End Time	X Axis - Directional Deformation - Bolt - End Time	X Axis - Directional Deformation - TH - End Time	X Axis - Directional Deformation - DH - End Time	Y Axis - Directional Deformation - Up - End Time	Y Axis - Directional Deformation - Down - End Time	Y Axis - Directional Deformation - Bolt - End Time
Minimum	0. mm	2.6874 mm	2.6558 mm	-3.7785e-002 mm	-2.1254e-002 mm	-4.1175e-002 mm	-3.3839e-002 mm	-1.5191e-002 mm	0.31237 mm	0. mm	-0.44315 mm
Maximum	8.6969 mm	2.9547 mm	2.9257 mm	-2.0042e-002 mm	4.0724e-003 mm	2.9519e-002 mm	-3.273e-002 mm	-1.4587e-002 mm	0.43479 mm	0.16848 mm	0.51788 mm
Minimum Occurs On	Down	Up	Down	Up	Down	Bolt	Up	Down	Up	Down	Bolt
Maximum Occurs On	Up		Down	Up	Down	Bolt	Up	Down	Up	Down	Bolt

Figures 3.11 and 3.12 depict the total deformation of the hole in upper and bottom plates, respectively. Moreover, Figs. 3.13, 3.14, 3.15, 3.16 and 3.17 illustrate the X- directional deformation of upper and bottom laminate plates and the bolt, the hole in the upper and bottom laminate plates, respectively.
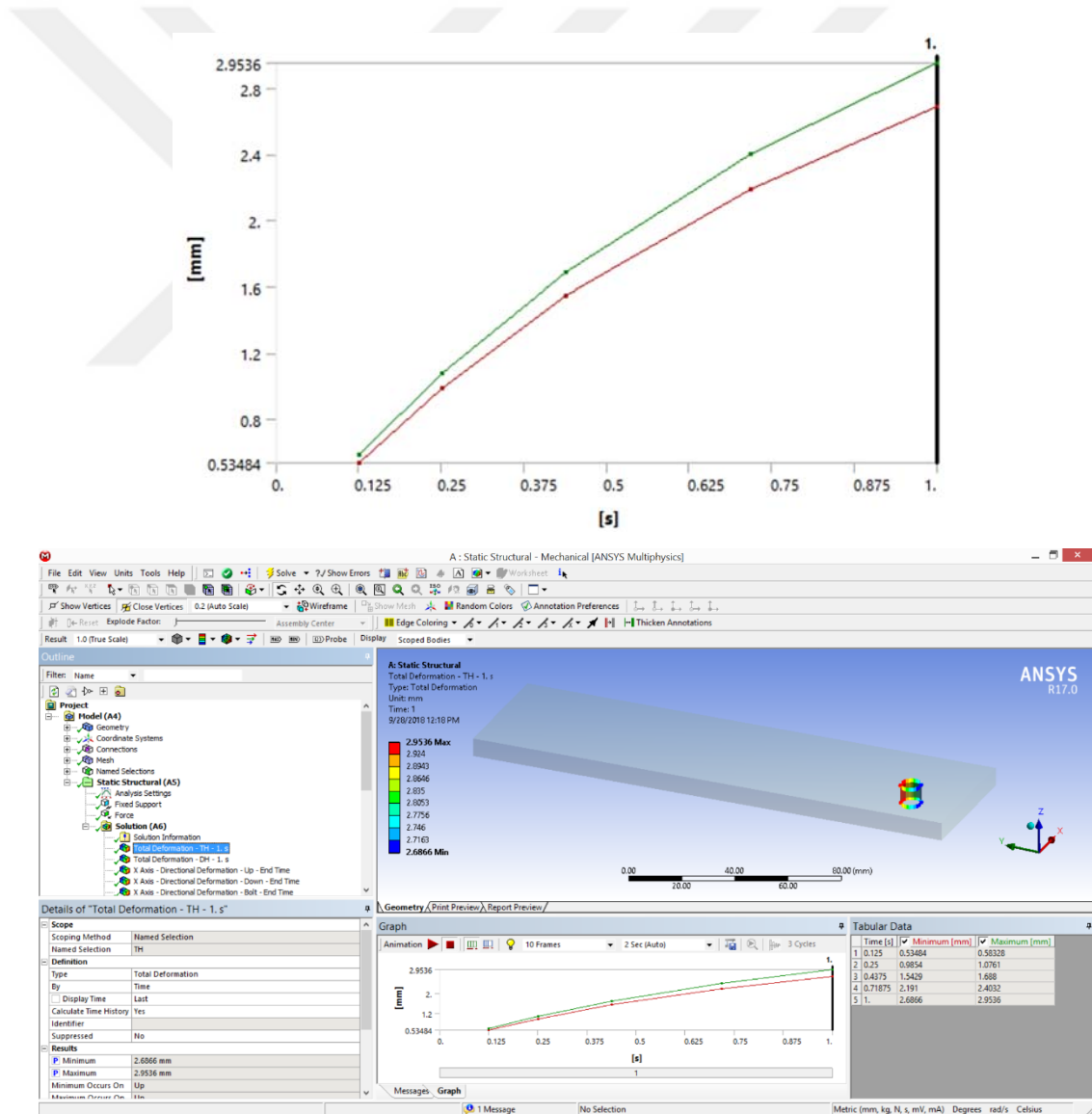

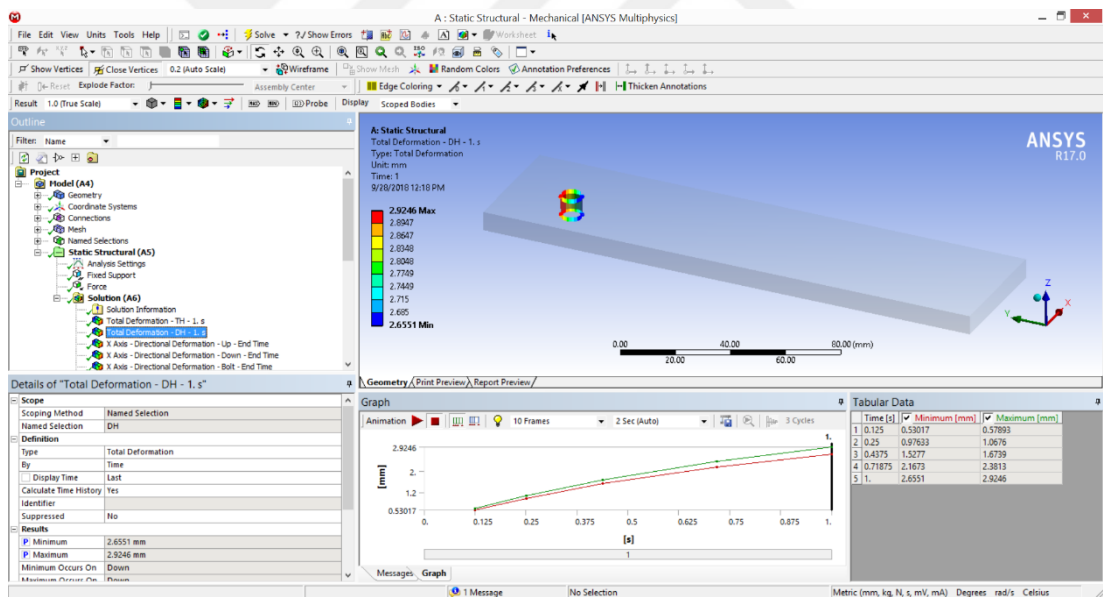**Figure 3.11:** Total deformation of the hole in upper laminate plate.
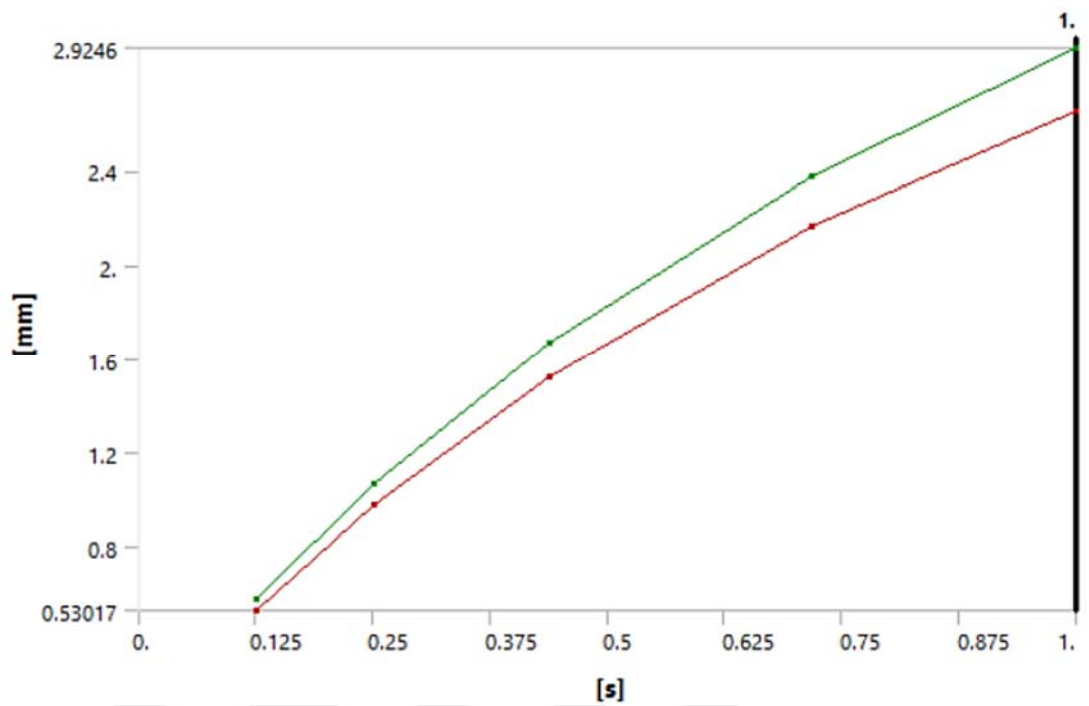
Figure 3.12: Total deformation of the hole in bottom laminate plate.

Figure 3.13: X Axis - Directional deformation of upper laminate plate.

Figure 3.14: X Axis - Directional deformation of bottom laminate plate.

Figure 3.15: X Axis - Directional deformation of the bolt.

Figure 3.16: X Axis - Directional deformation of the hole in the upper laminate plate.

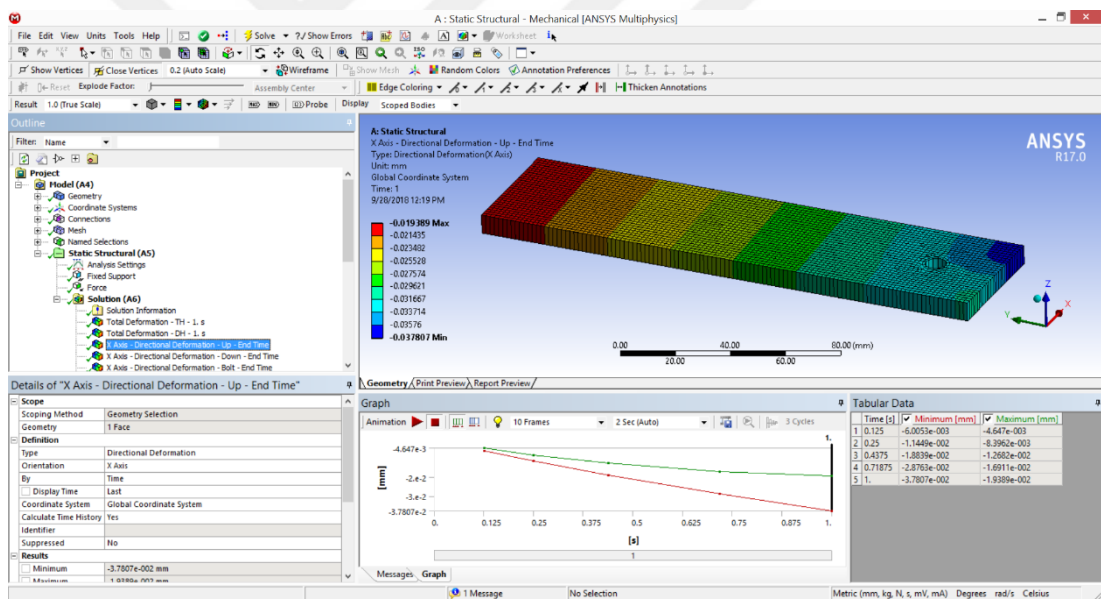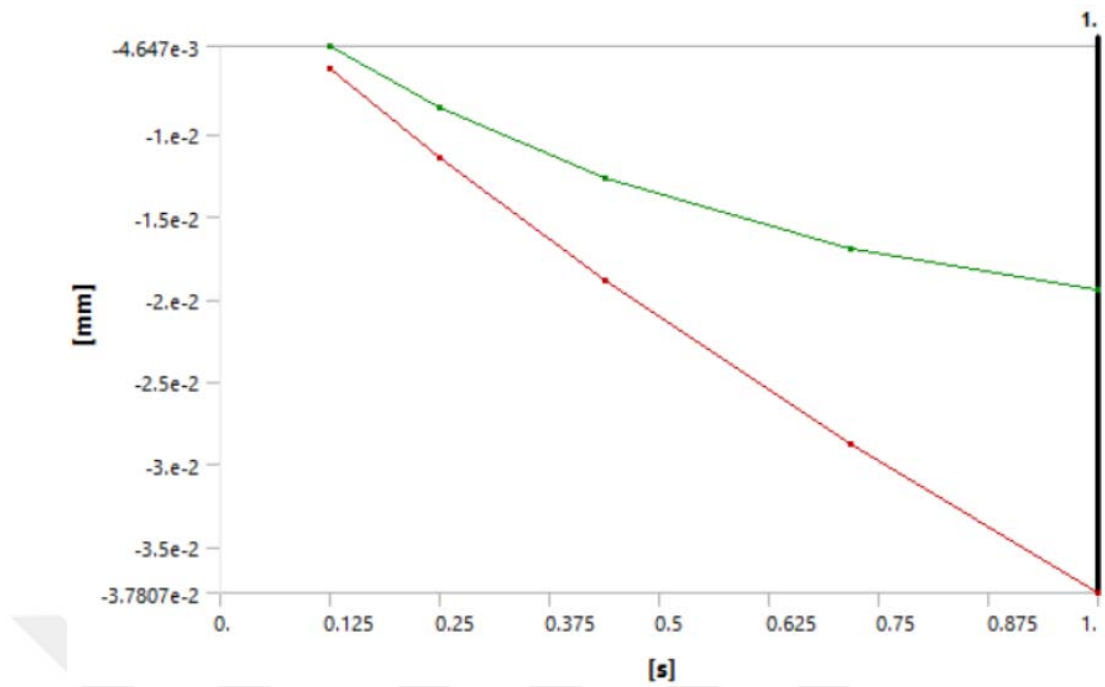**Figure 3.17:** X Axis - Directional deformation of the hole in the bottom laminate plate.

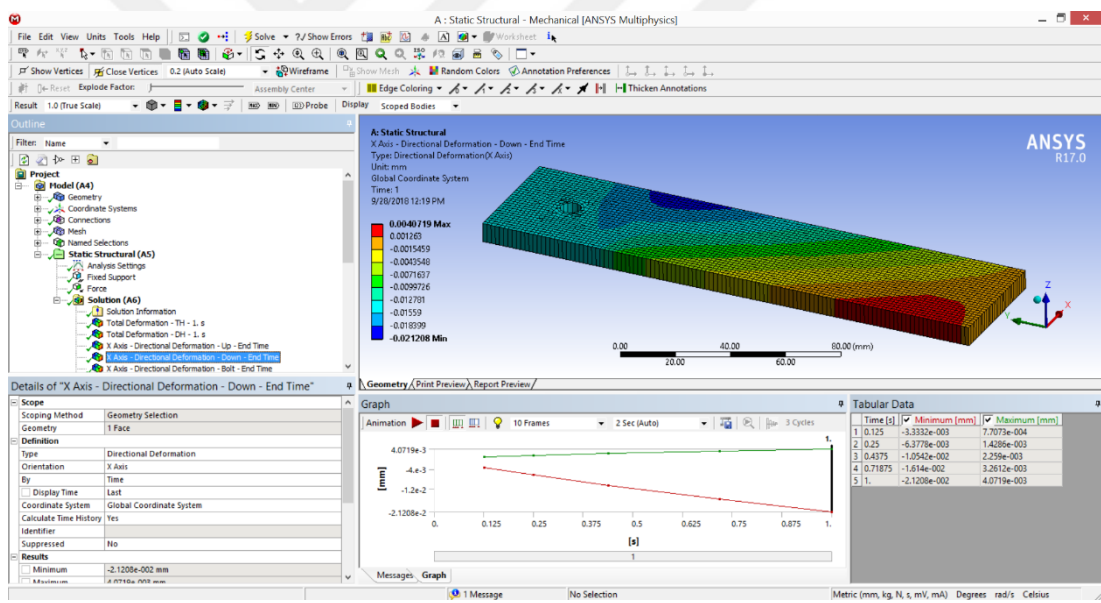**Figure 3.18:** Y Axis - Directional deformation of upper laminate plate.
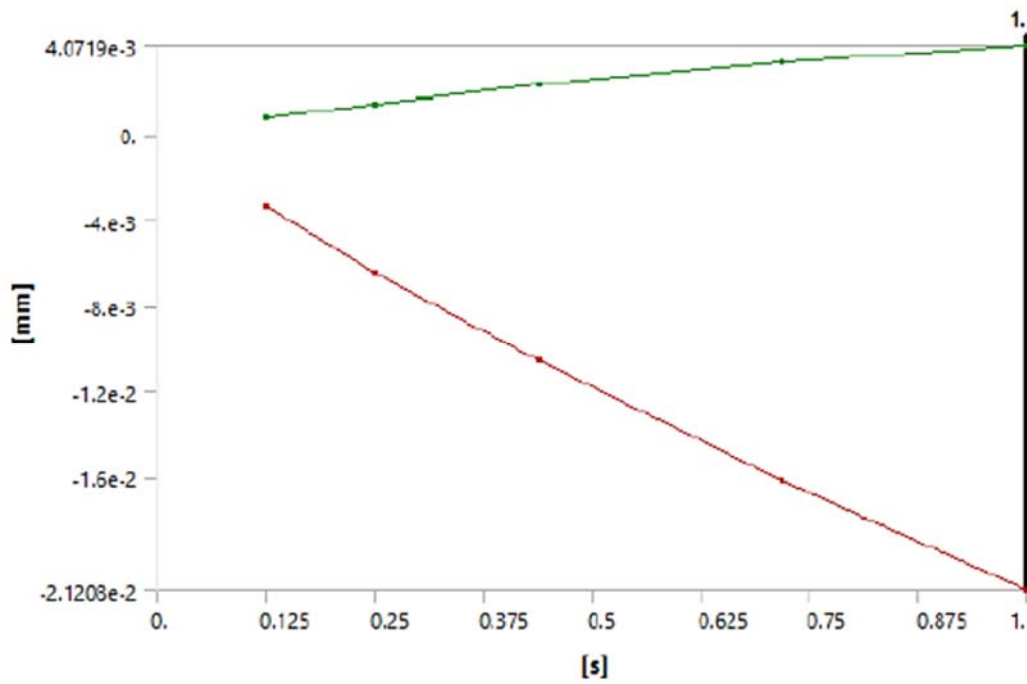
Figure 3.19: Y Axis - Directional deformation of bottom laminate plate.

Figures 3.18, 3.19 and 3.20 represent the Y-directional deformation of upper laminate plate bottom laminate plate and the bolt. Furthermore, Table 3.4 represents the minimum and maximum directional deformation values.
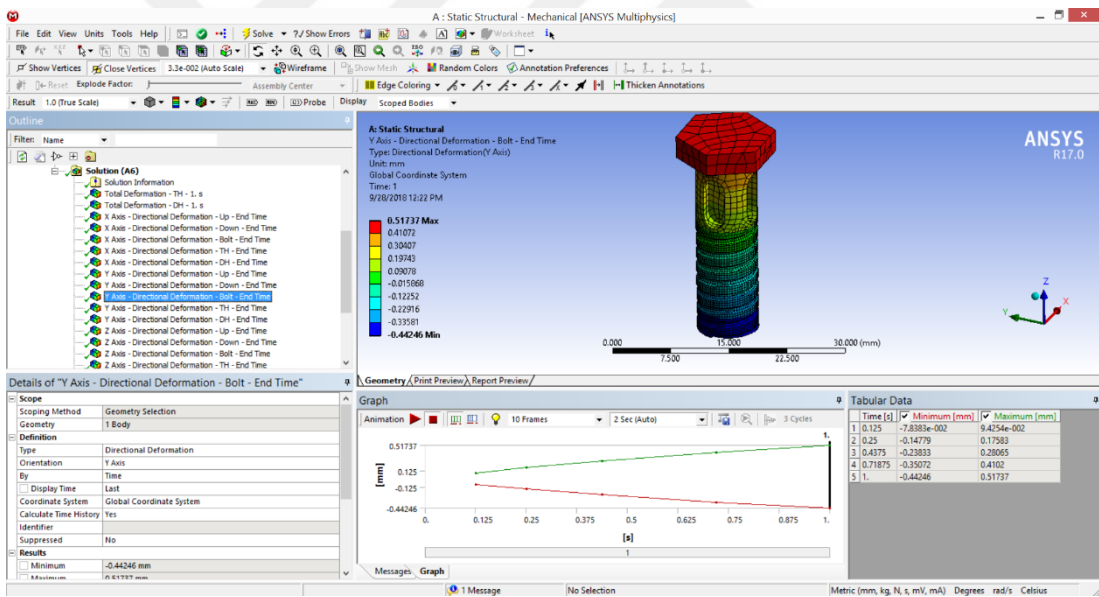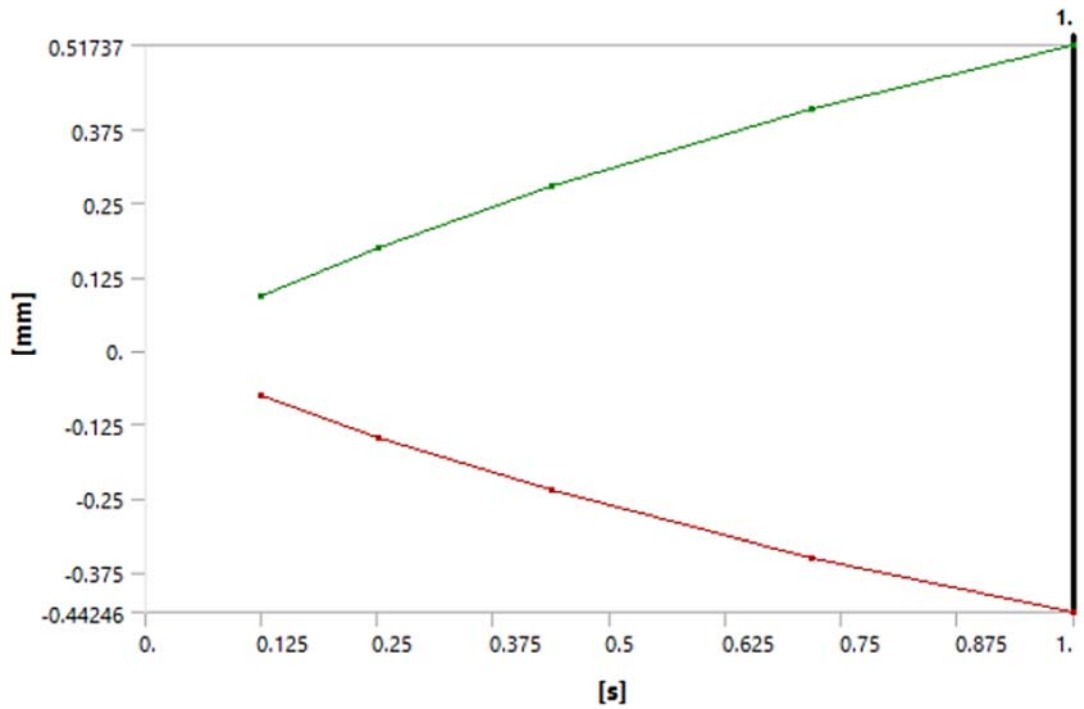
Figure 3.20: Y Axis - Directional deformation of the bolt.

Table 3.4: The minimum and maximum directional deformation values.

Object Name	Y Axis - Directional Deformation - TH - End Time	Y Axis - Directional Deformation - DH - End Time	Z Axis - Directional Deformation - Up - End Time	Z Axis - Directional Deformation - Down - End Time	Z Axis - Directional Deformation - Bolt - End Time	Z Axis - Directional Deformation - TH - End Time	Z Axis - Directional Deformation - DH - End Time
Minimum	0.4099 mm	0.15699 mm	-8.6912 mm	-3.6657 mm	-2.987 mm	-2.926 mm	-2.9214 mm
Maximum	0.41449 mm	0.16128 mm	-1.9068 mm	1.189e-003 mm	-2.5957 mm	-2.655 mm	-2.6509 mm
Minimum Occurs On	Up	Down	Up	Down	Bolt	Up	Down
Maximum Occurs On	Up	Down	Up	Down	Bolt	Up	Down

51

Figures 3.21 and 3.22 illustrate the Y- Axis directional deformation of upper and bottom laminate plates in YZ plane. Moreover, Figs. 3.23, 3.24, 3.25, 3.26 and 3.27 depict Z Axis directional deformation of upper and bottom laminate plates, the bolt, the hole in upper and bottom laminate plates.
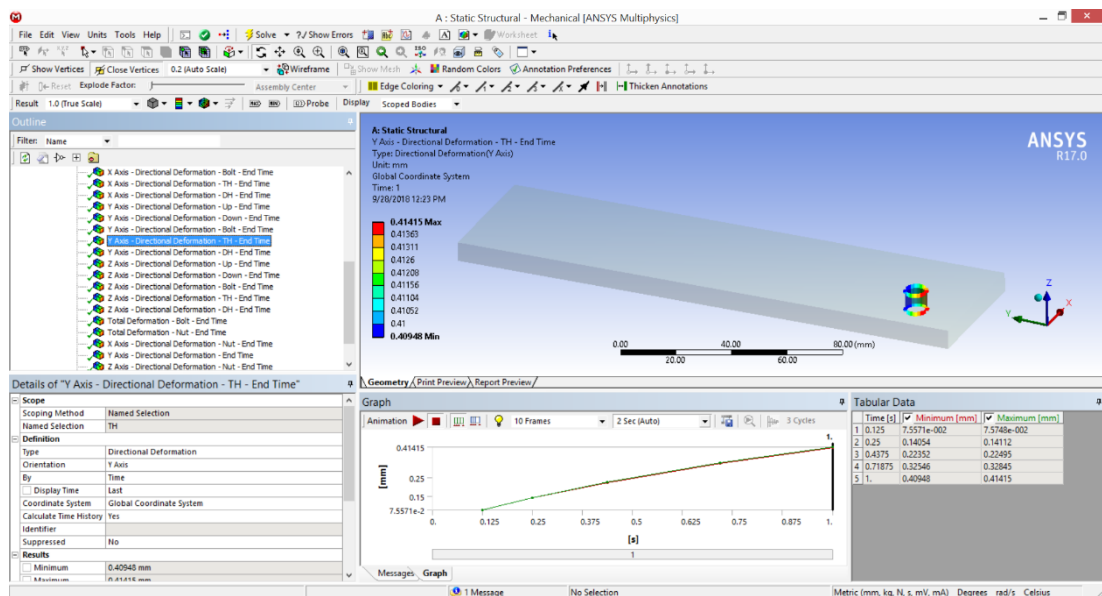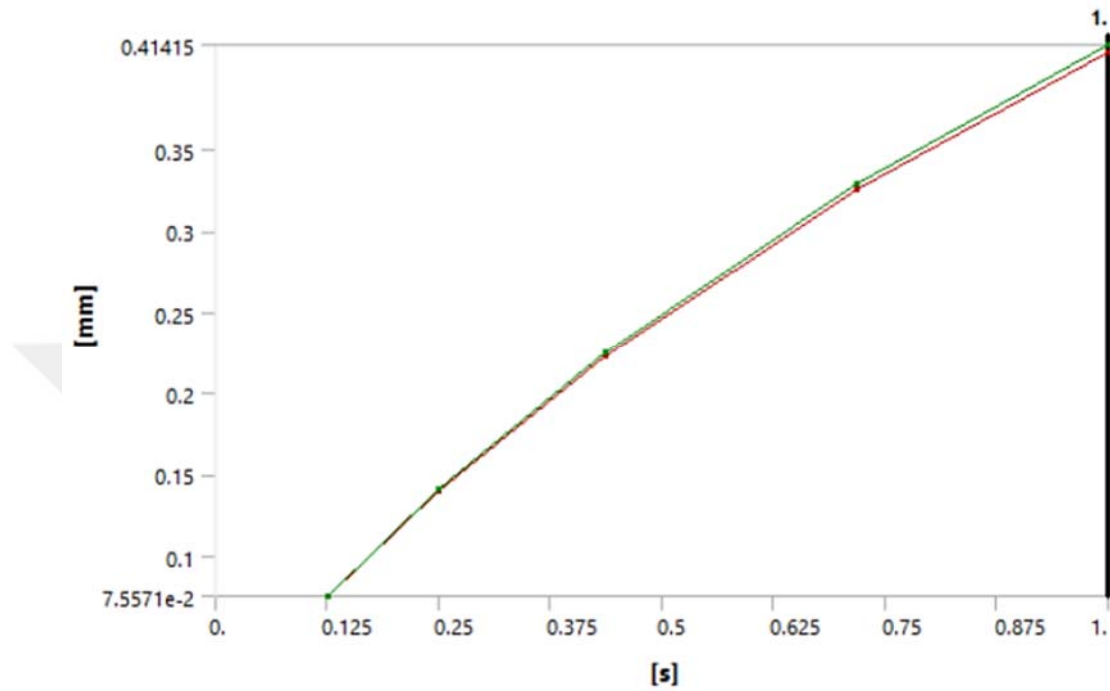
Figure 3.21: Y Axis - Directional deformation of upper laminate plate.
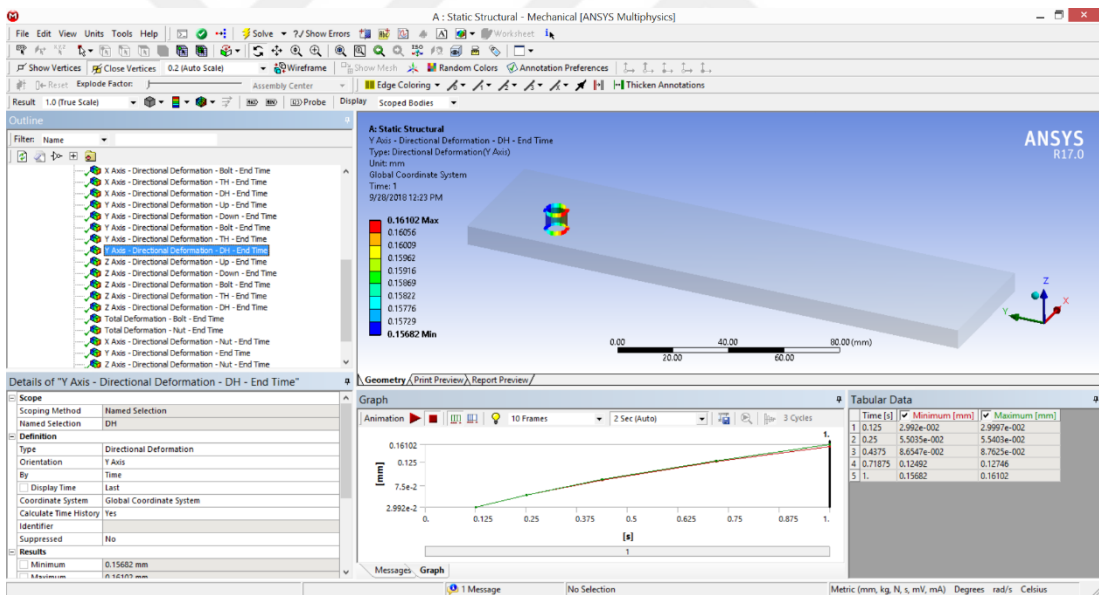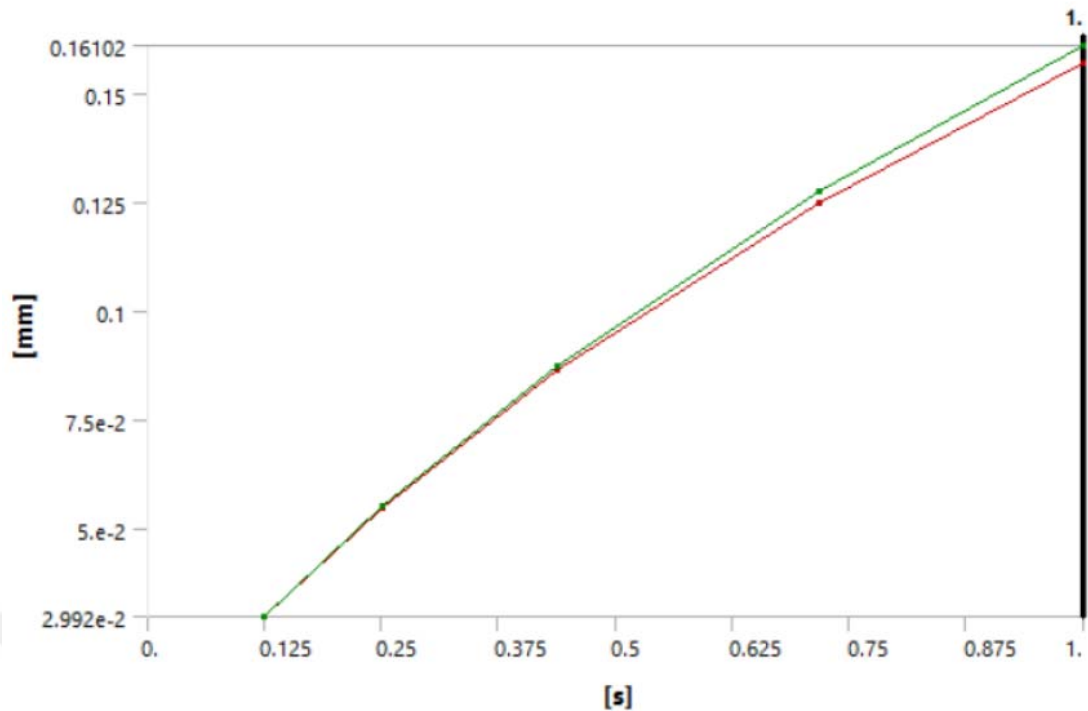
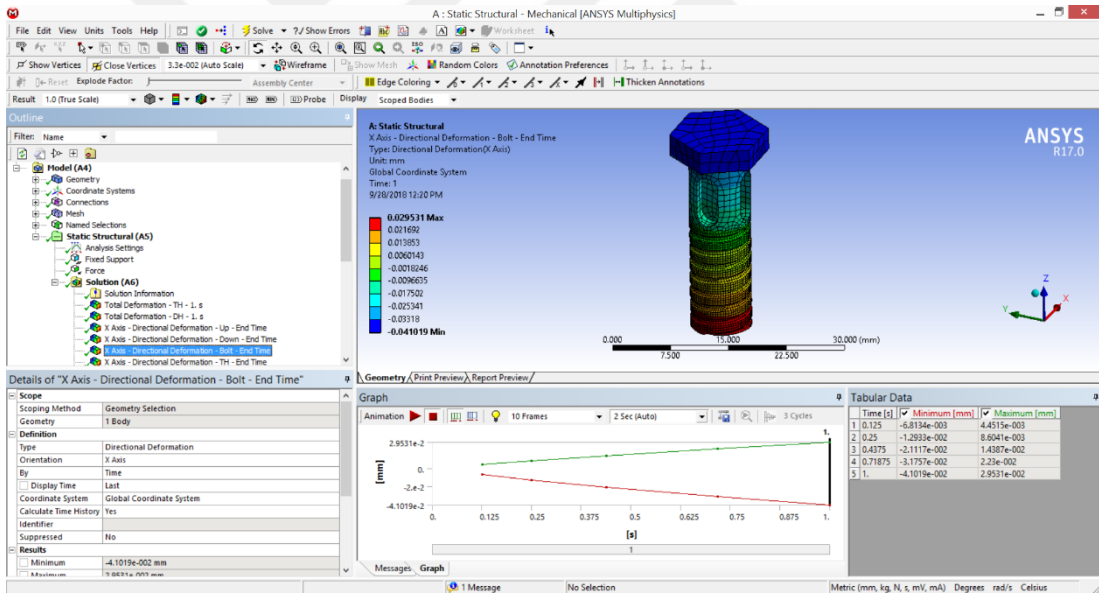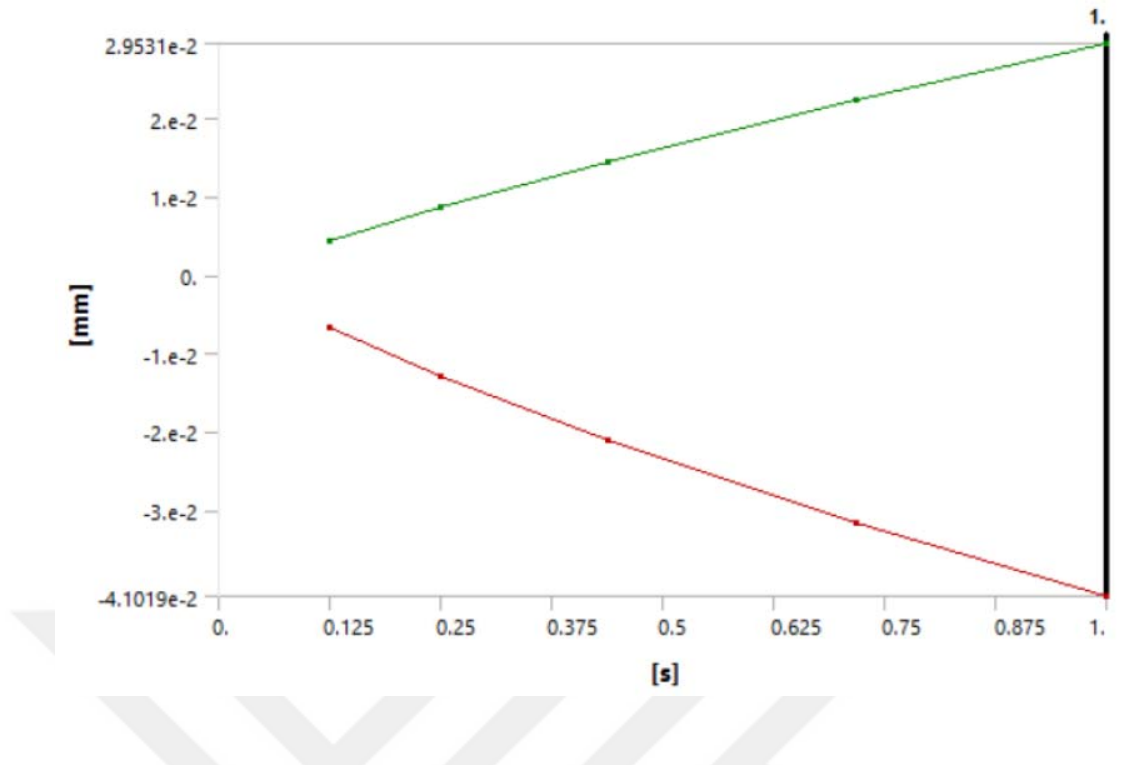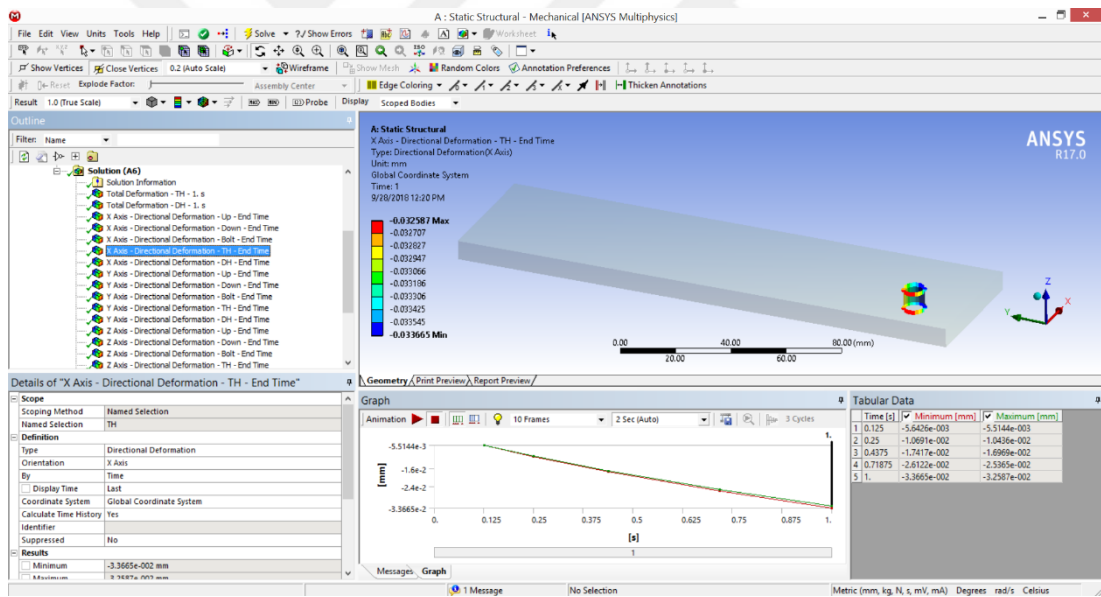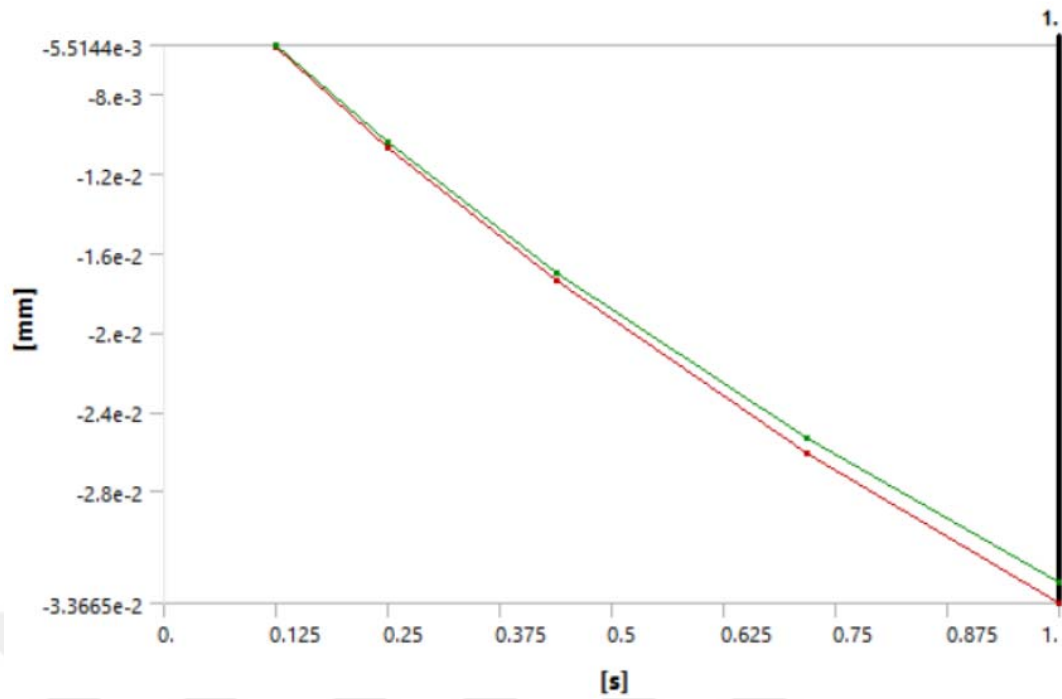**Figure 3.22:** Y Axis - Directional deformation of bottom laminate plate.
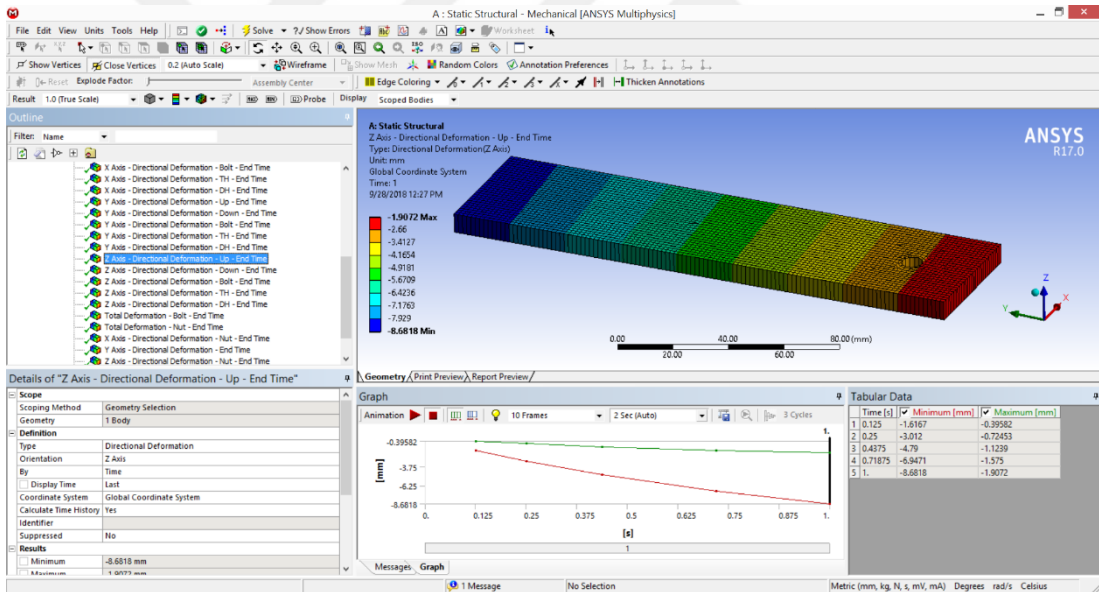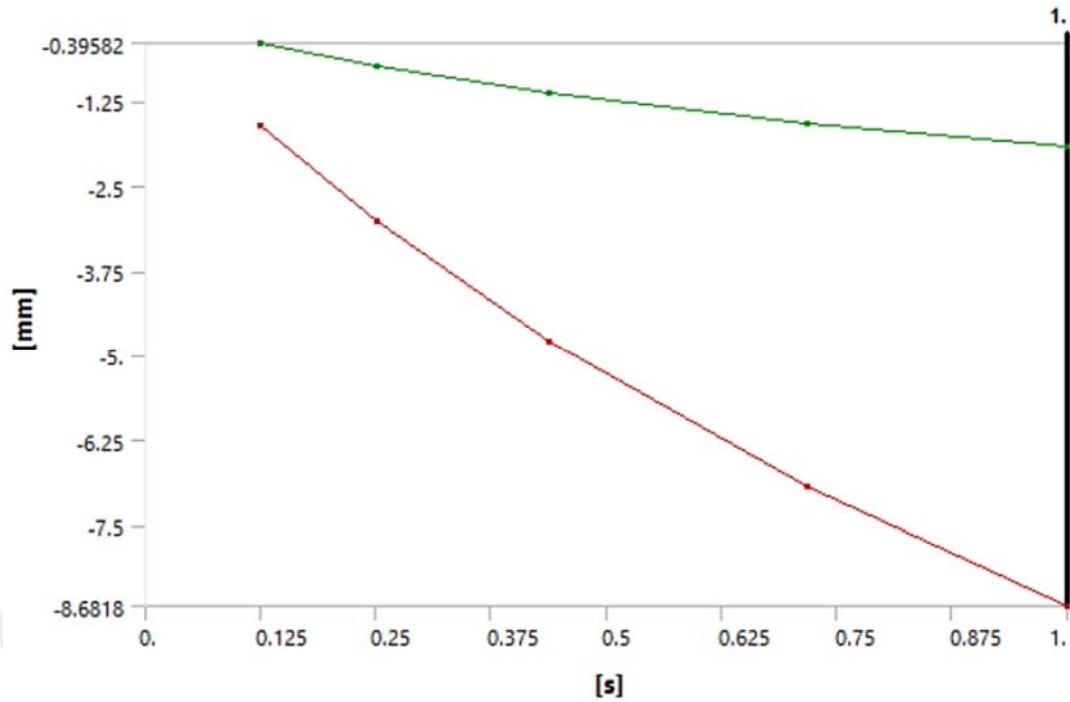
Figure 3.23: Z Axis - Directional deformation of upper laminate plate.
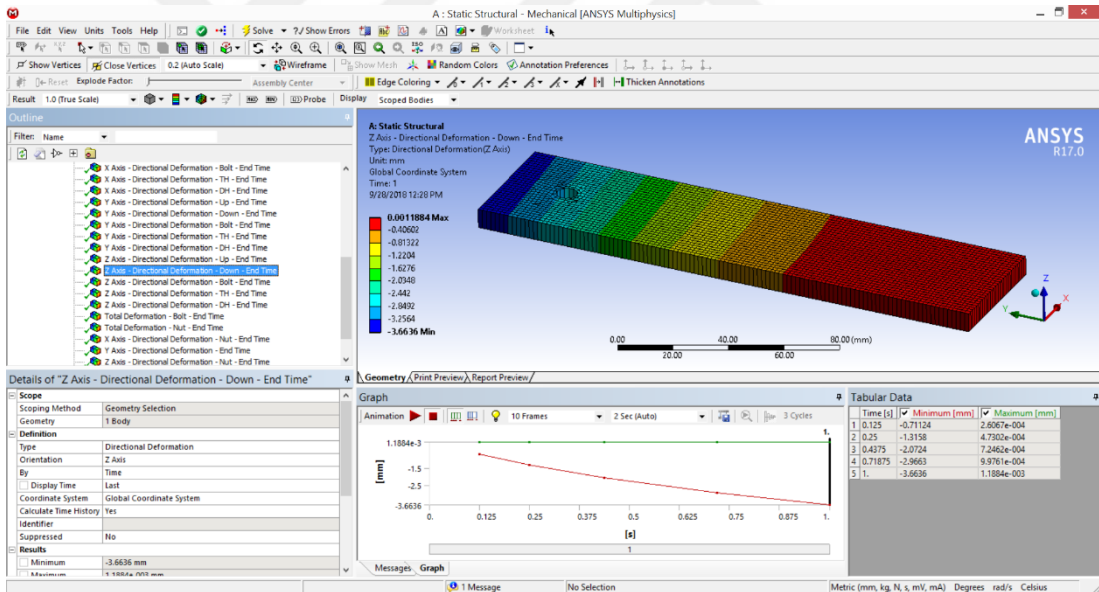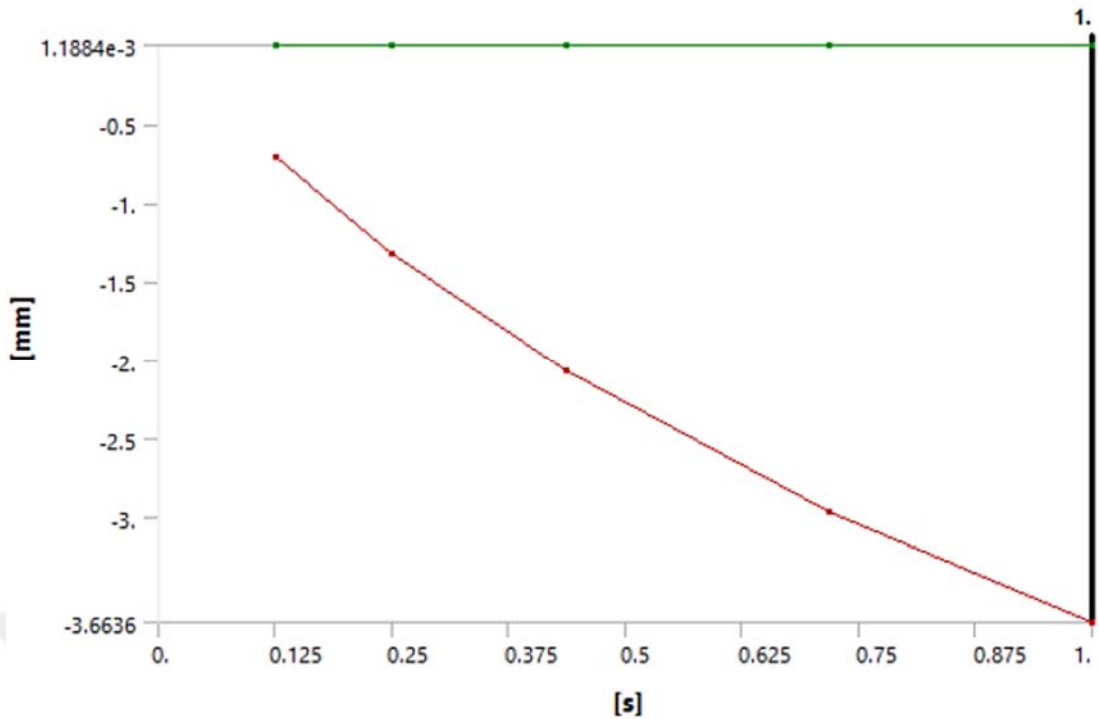
Figure 3.24: Z Axis - Directional deformation of bottom laminate plate.
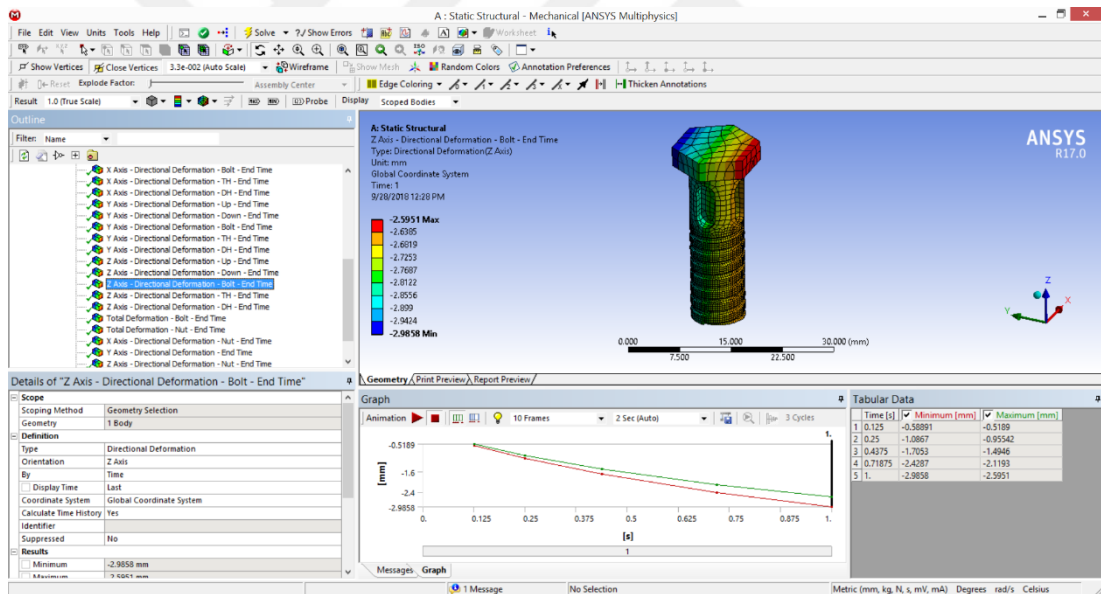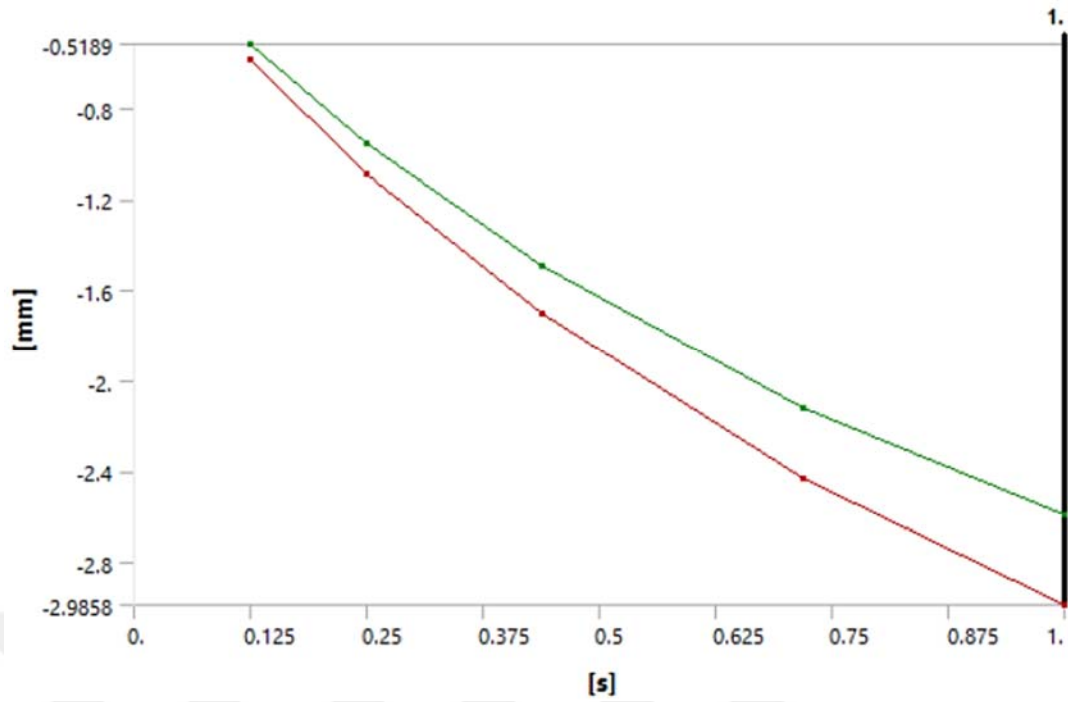
Figure 3.25: Z Axis - Directional deformation of the bolt.
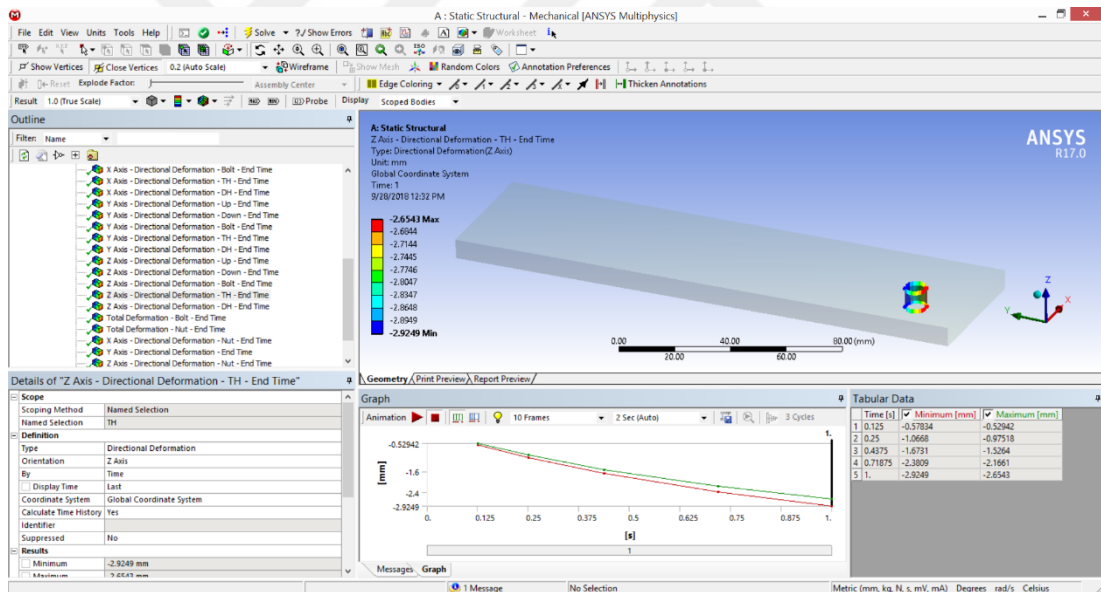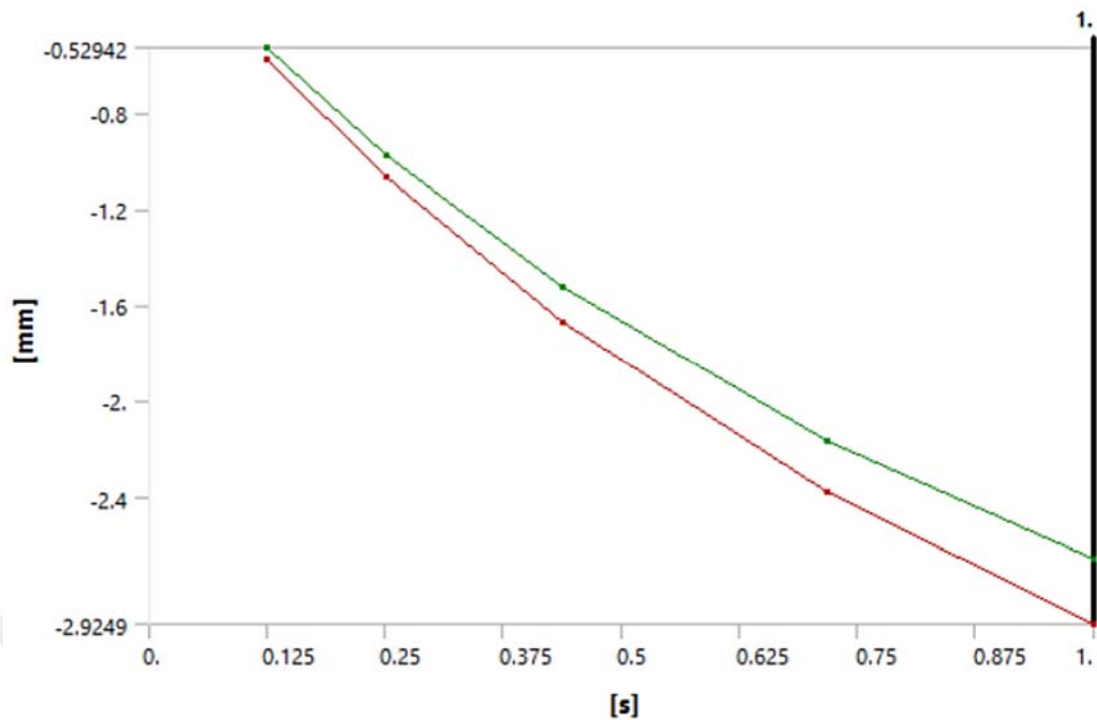
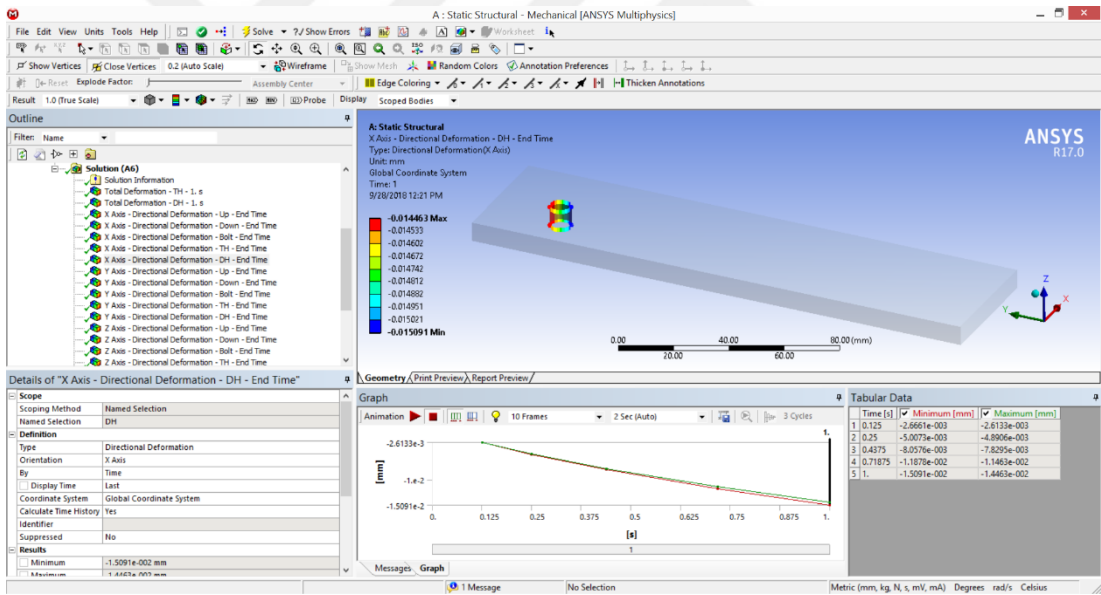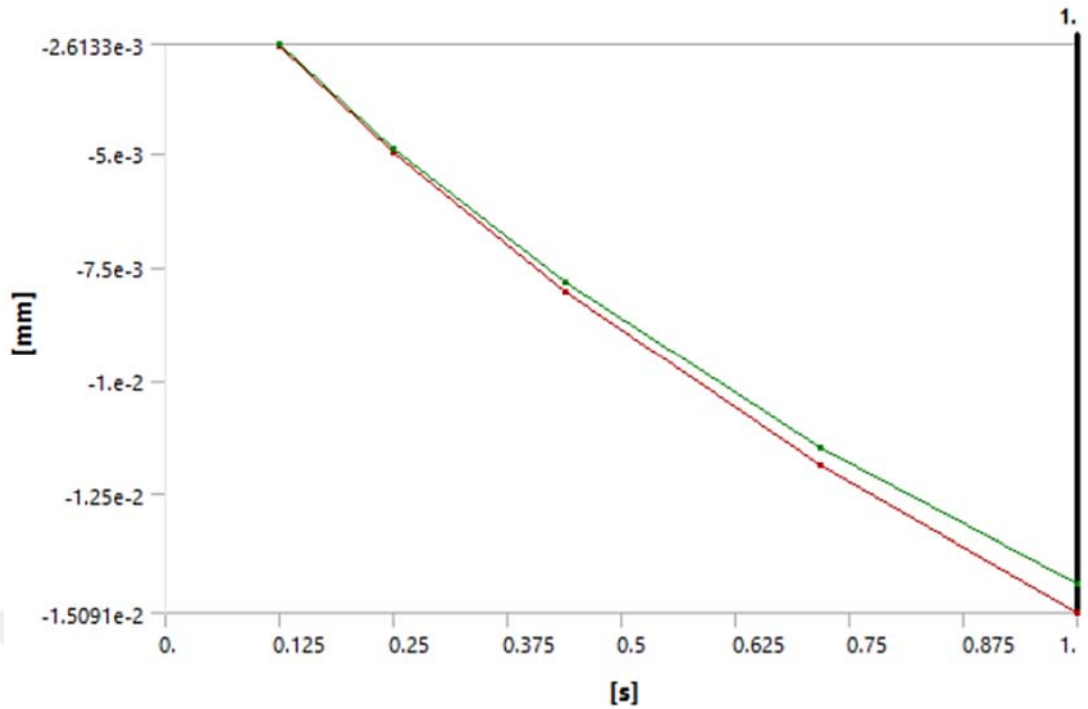**Figure 3.26:** Z Axis - Directional deformation of the hole in upper laminate plate.

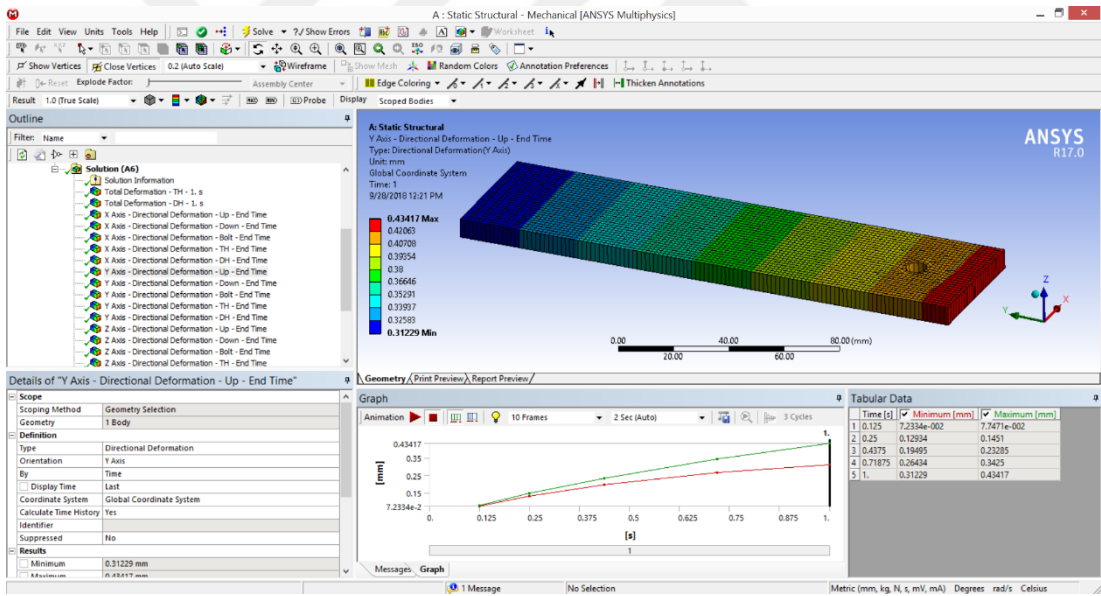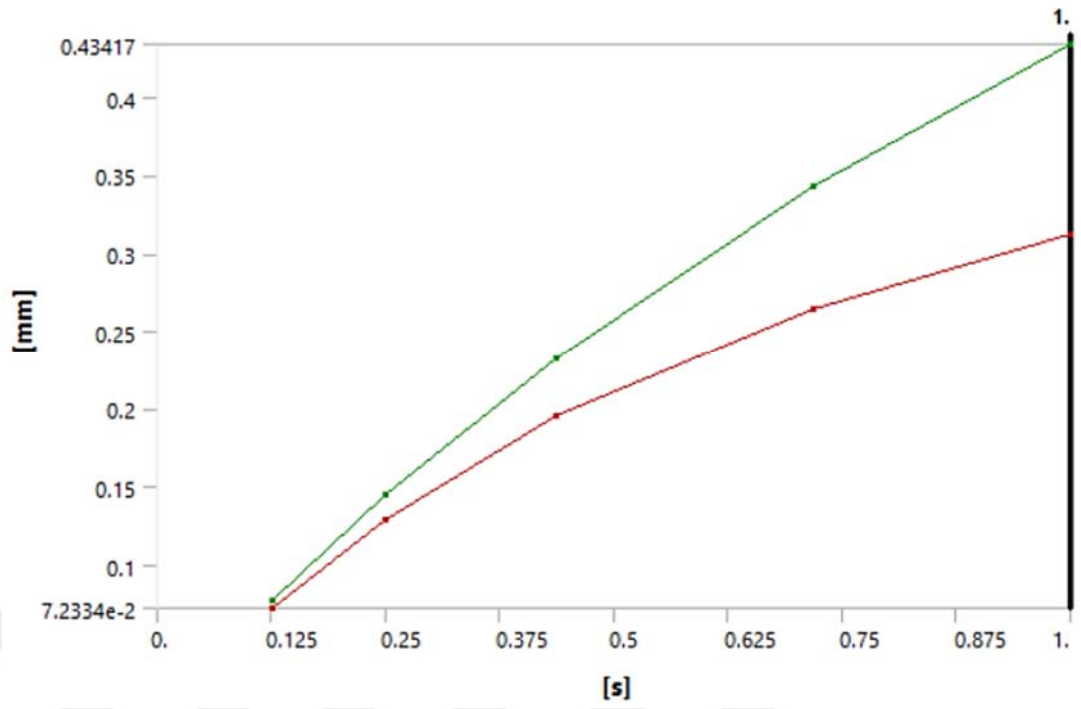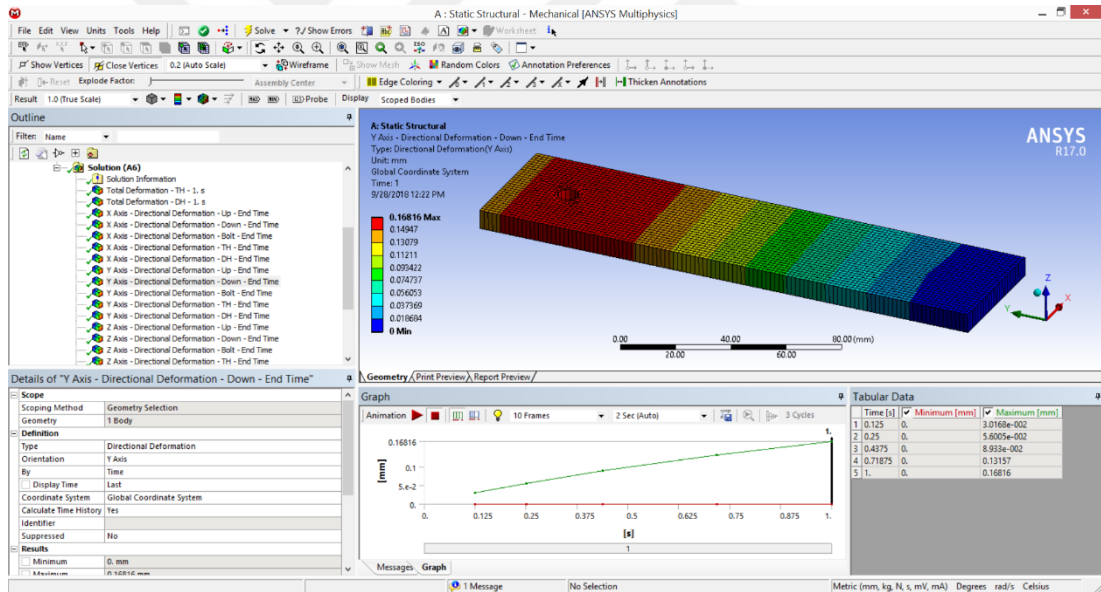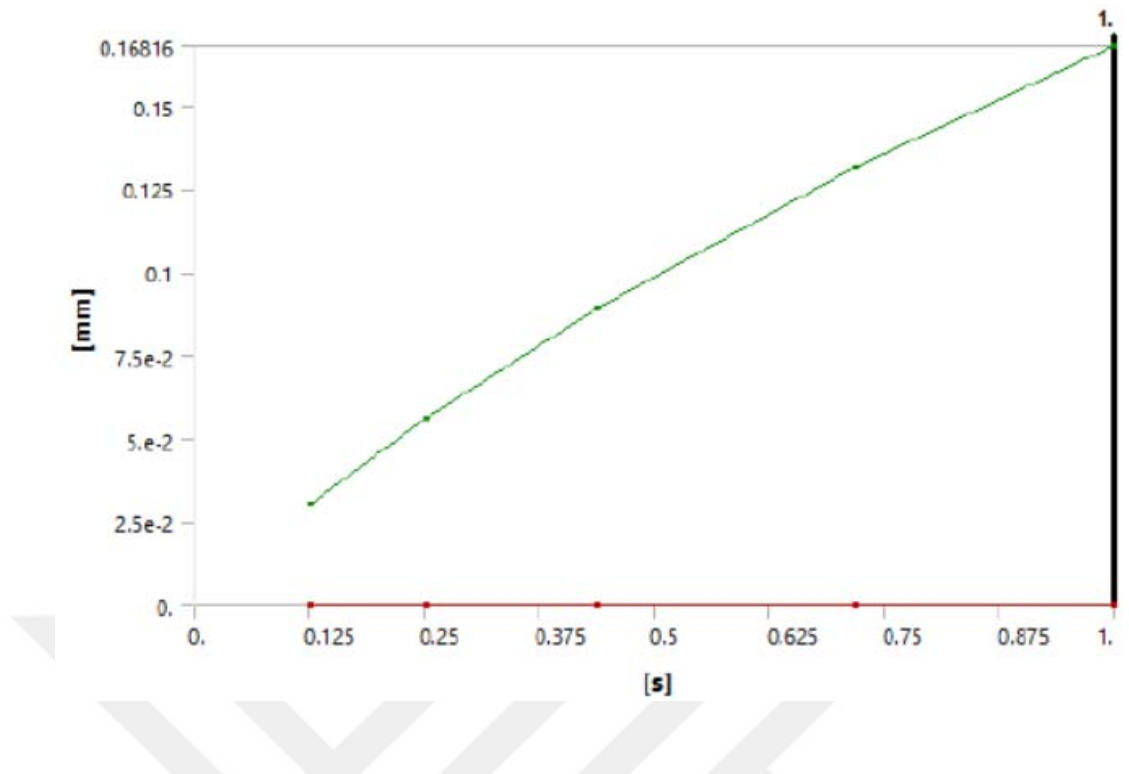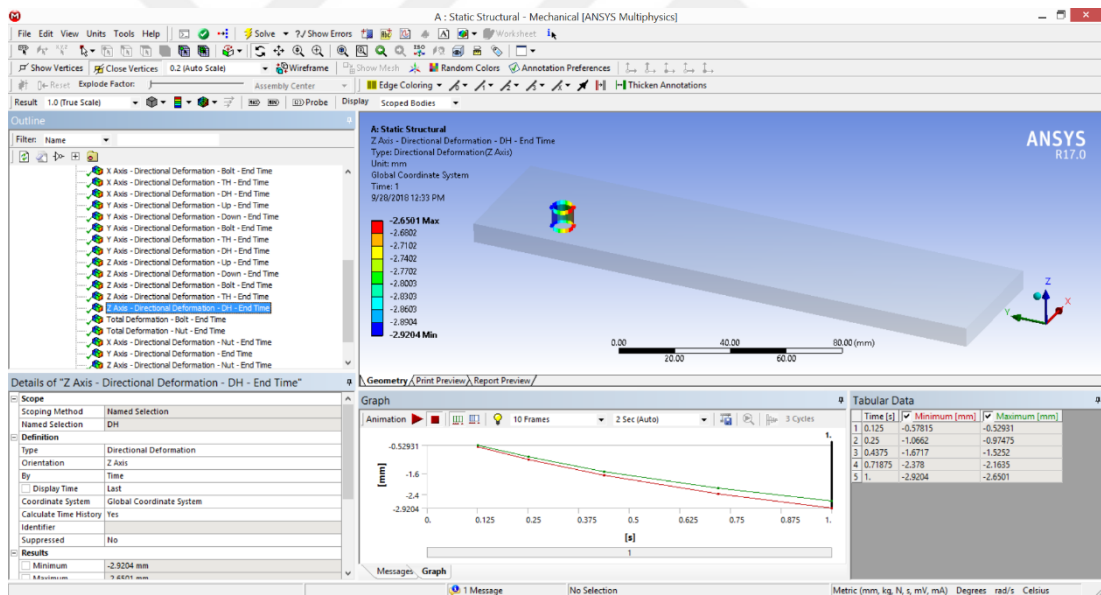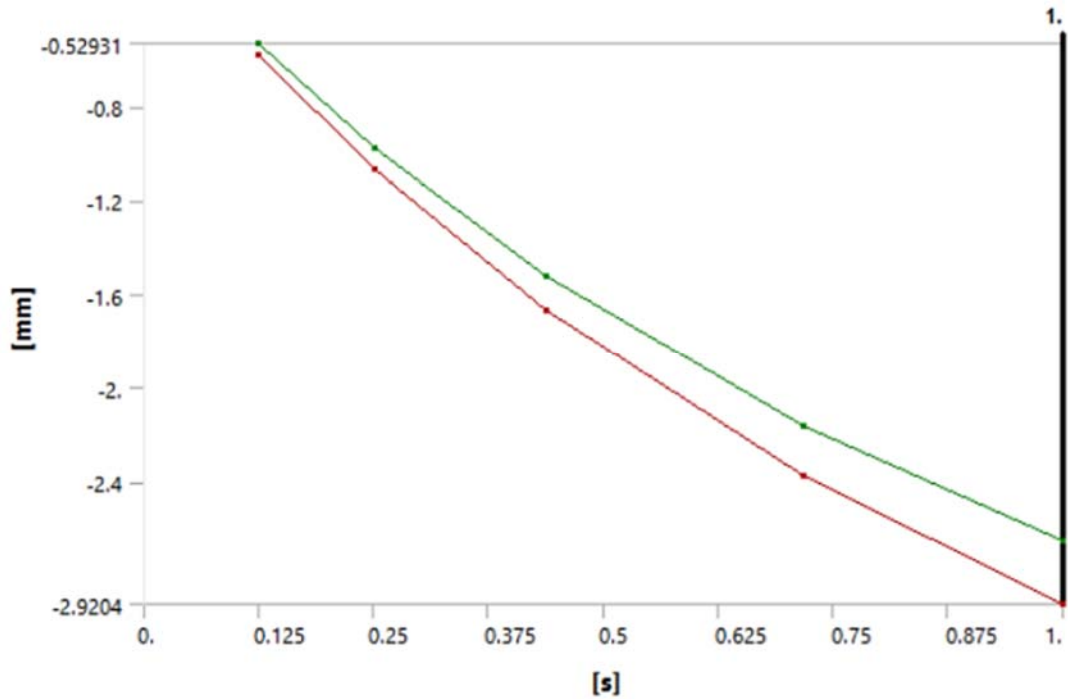**Figure 3.27:** Z Axis - Directional deformation of the hole in bottom laminate plate.

In the following the shear stress and normal stress effect on the first case study are presented. Tables 3.5, 3.6, 3.7 and 3.8 represent the shear stress based on bolt, nut, bottom and upper laminate, respectively.

Table 3.5: The bolt shear stress.

Time [s]	Minimum [MPa]	Maximum [MPa]
0.125	-1875.4	3406.2
0.25	-7733.9	13301
0.375	-9577.1	15562
0.5	-15025	26356
0.625	-18989	27484
0.75	-16850	34127
0.875	-19372	42292
1.	-21236	63653

Table 3.6: The nut shear stress.

Time [s]	Minimum [MPa]	Maximum [MPa]
0.125	-441.3	228.35
0.25	-12931	4024.2
0.375	-21154	5050.3
0.5	-37132	10862
0.625	-43461	12328
0.75	-48726	16057
0.875	-53831	13357
1.	-64660	14529

Table 3.7: The bottom laminate plate shear stress.

Time [s]	Minimum [MPa]	Maximum [MPa]
0.125	-2.0311e-015	1.3763e-015
0.25	-4.4121e-015	2.6351e-015
0.375	-6.8025e-015	4.0474e-015
0.5	-9.4196e-015	5.5458e-015
0.625	-1.1668e-014	7.0666e-015
0.75	-1.3997e-014	8.592e-015
0.875	-1.6572e-014	1.0263e-014
1.	-1.9104e-014	1.269e-014

Table 3.8: The upper laminate plate shear stress.

Time [s]	Minimum [mm]	Maximum [mm]
0.125	-5.4172e-002	-4.0311e-002
0.25	-9.4984e-002	-6.2017e-002
0.375	-0.11928	-8.7198e-002
0.5	-0.16065	-0.11654
0.625	-0.15444	-0.10376
0.75	-0.1855	-0.10279
0.875	-0.20834	-0.10435
1.	-0.31373	-0.20924

Tables 3.9, 3.10, 3.11 and 3.12 are represented the normal stress along X- axis based on bolt, nut, bottom and upper laminate, respectively.

Table 3.9: The bolt normal stress along X- axis.

Time [s]	Minimum [MPa]	Maximum [MPa]
0.125	-3803.8	3994.6
0.25	-45613	18717
0.375	-63191	25906
0.5	-81040	66933
0.625	-98868	47573
0.75	-1.1121e+005	41667
0.875	-1.2819e+005	47958
1.	-1.7835e+005	61927

Table 3.10: The nut normal stress along X- axis.

Time [s]	Minimum [MPa]	Maximum [MPa]
0.125	-1649.8	1446.9
0.25	-24609	6313.4
0.375	-34427	11160
0.5	-46896	15429
0.625	-44023	15690
0.75	-55636	17949
0.875	-61509	19871
1.	-77353	24546

Table 3.11: The upper laminate plate normal stress along X- axis.

Time [s]	Minimum [MPa]	Maximum [MPa]
0.125	-4.0904e-030	2.596e-030
0.25	-8.8166e-030	7.2677e-030
0.375	-1.9745e-029	1.8194e-029
0.5	-3.0184e-029	2.5776e-029
0.625	-3.3412e-029	3.2052e-029
0.75	-4.0568e-029	4.0279e-029
0.875	-4.0975e-029	4.6087e-029
1.	-4.7246e-029	5.1611e-029

Table 3.12: The upper bottom plate normal stress along X- axis.

Time [s]	Minimum [MPa]	Maximum [MPa]
0.125	-2.4842e-031	2.3246e-031
0.25	-5.3676e-031	4.4516e-031
0.375	-8.2436e-031	6.8365e-031
0.5	-1.1379e-030	9.3764e-031
0.625	-1.4081e-030	1.1948e-030
0.75	-1.6863e-030	1.4535e-030
0.875	-1.9928e-030	1.7375e-030
1.	-2.2902e-030	2.1514e-030

Tables 3.13, 3.14, 3.15 and 3.16 are represented the normal stress along Y- axis based on bolt, nut, bottom and upper laminate, respectively.

Table 3.13: The bolt normal stress along Y- axis.

Time [s]	Minimum [MPa]	Maximum [MPa]
0.125	-4320.9	4482.4
0.25	-23779	39181
0.375	-28191	50275
0.5	-40278	56116
0.625	-47740	58306
0.75	-53853	63237
0.875	-61490	67472
1.	-1.0395e+005	78312

Table 3.14: The nut normal stress along Y- axis.

Time [s]	Minimum [MPa]	Maximum [MPa]
0.125	-523.34	349.83
0.25	-27341	21171
0.375	-42102	28868
0.5	-74950	26726
0.625	-77058	32498
0.75	-88509	34595
0.875	-93335	37228
1.	-1.0558e+005	40380

Table 3.15: The upper laminate plate normal stress along Y- axis.

Time [s]	Minimum [MPa]	Maximum [MPa]
0.125	-416.	196.59
0.25	-320.07	1252.9
0.375	-745.52	2532.9
0.5	-1288.1	3606.6
0.625	-2093.9	4279.
0.75	-3912.7	4574.2
0.875	-5074.1	5461.7
1.	-2930.1	6651.5

Table 3.16: The bottom plate normal stress along Y- axis.

Time [s]	Minimum [MPa]	Maximum [MPa]
0.125	-19.619	8.1724
0.25	-41.527	15.64
0.375	-65.11	24.03
0.5	-90.191	32.898
0.625	-111.76	41.919
0.75	-133.89	50.941
0.875	-157.38	60.8
1.	-180.57	75.084

3.3.2 The Second Case Study

The second case study is based on the A. Olmedo, C. Santiuste and E. Barbero research [57]. In this paper the IM7/MTM-45-1 carbon epoxy composite is considered as the laminate material and 6Al–4V titanium alloy is considered for bolt and nut.

The main factors which are considered for analyzing in the proposed research can be regarded as, the estimation of secondary bending as a function of geometrical parameters, the properties of material, and the sequence of stacking. Based on the aforementioned research, the friction force that the joint can transmit based on the applying the maximum load. The down and upside laminate plates was modeled with 3911 elements and the bolt and nut with 27361 and 116442 elements. Figure 3.28, represents the geometry model of a single-lap composite bolted-joint, which is used for the proposed research.
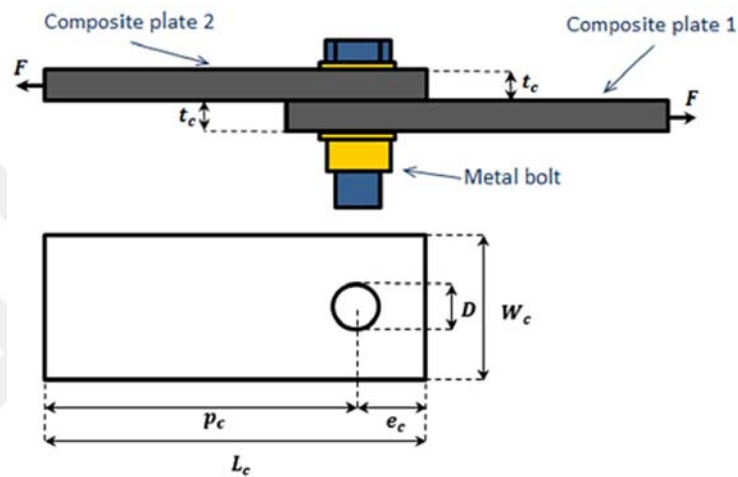
Figure 3.28: The geometry model of a single-lap composite bolted-joint based on [57].

The composite plates length and width were L_c = 140 mm and W_c = 30 mm respectively; and the distance between the hole center and the plate free end where load is applied was p_c = 135 mm. Both laminates had quasi-isotropic lay-up with stacking sequence [45/-45/0/90]$_{3S}$. Its ply had a thickness of 0.125 mm, yielding a laminate thickness of 3 mm. two different values of bolt torque where applied, 8 Nm and 1 Nm. Moreover, when the values of plate length be increased, it leads to a lower joint stiffness. On the contrary, when the values of plate width be increased, it leads to a higher joint stiffness. Based on the proposed research, if the bolt diameter is reduced, the joint stiffness increases only in the first region, where the stiffness is dominated by the friction forces.

Figure 3.29 represents the comparison between analytical model and experimental results based on load–displacement.
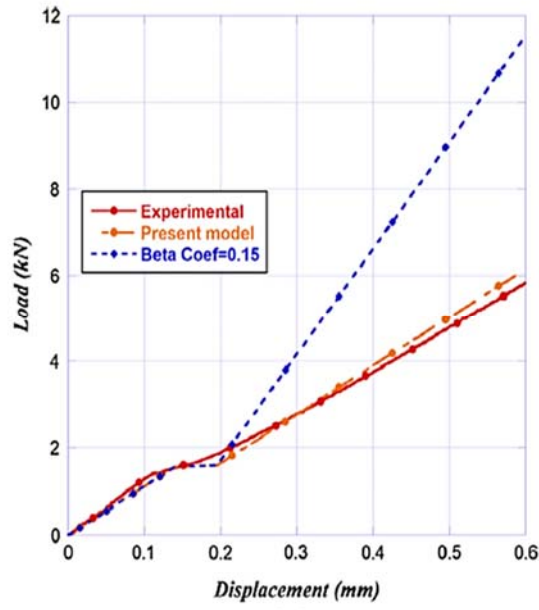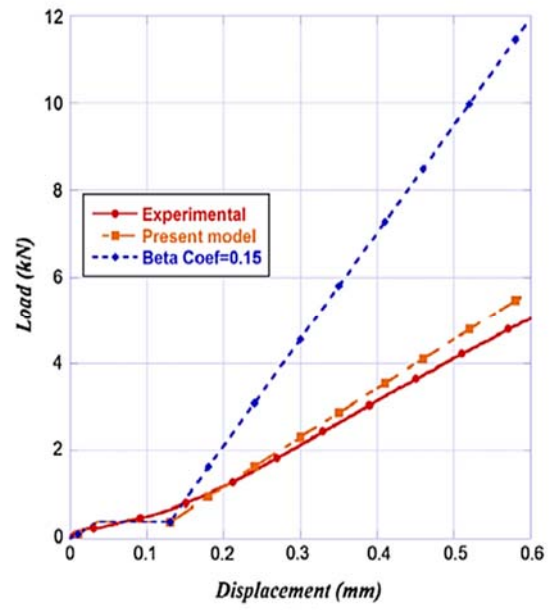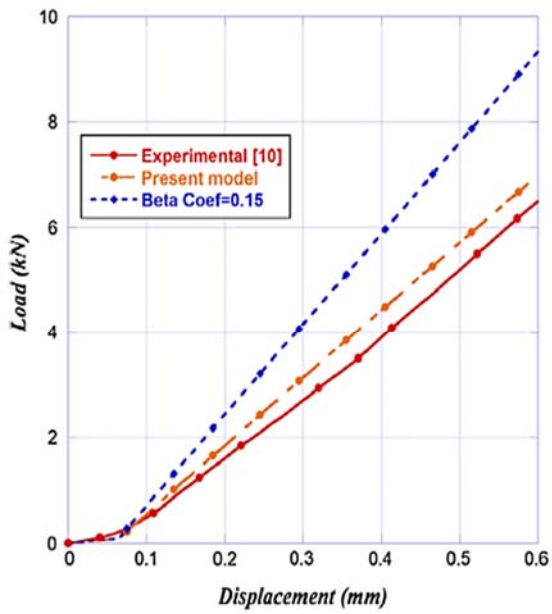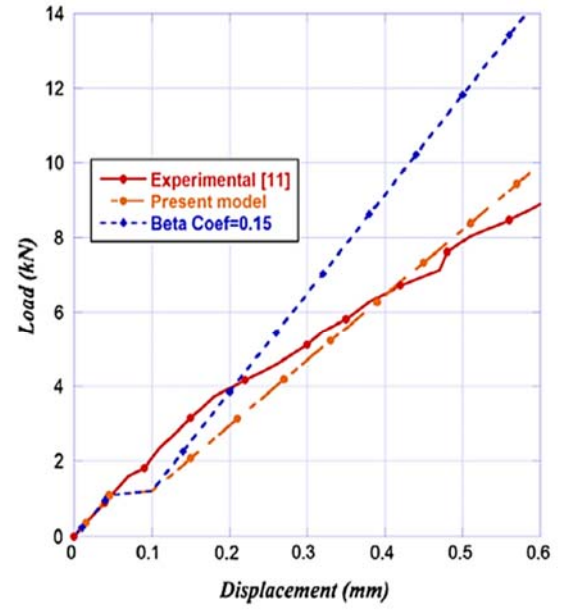
Figure 3.29. The comparison between analytical model and experimental results based on load–displacement [57].

The model which is presented in the proposed paper has also shown a direct relationship between the material elastic properties and the joint stiffness.

3.3.2.1 Simulation of the Second Case Study in ANSYS
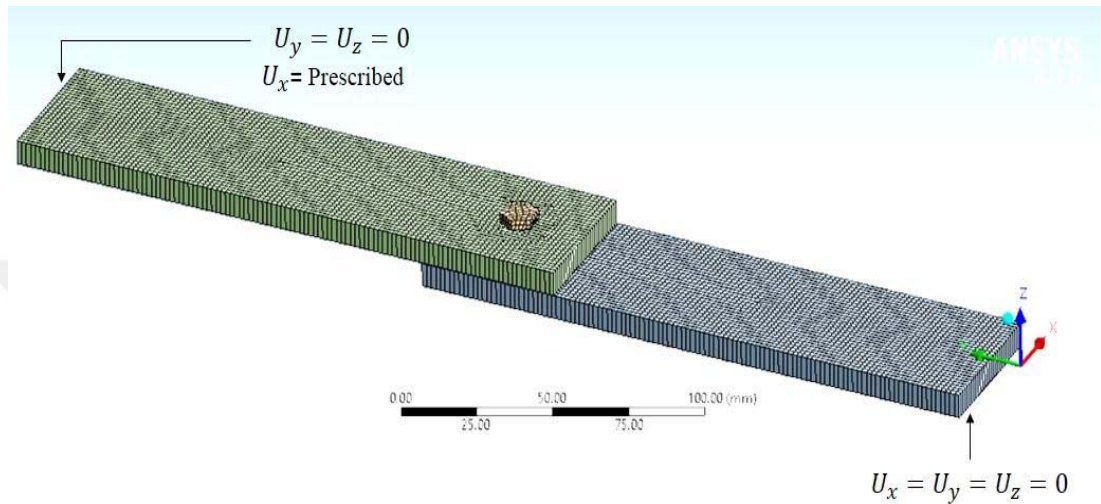
In the following the single-lap composite bolted-joint structure which is presented in [57], is redesigned and simulated in ANSYS. Table 3.17 represents the characteristics of the proposed single-lap, single-bolt joint, which is analyzed in ANSYS. According to the paper, the characteristic element size in the final mesh was 0.26 mm. Furthermore, Table 3.18 represents the minimum and maximum total and directional deformation values.

Table 3.17: Characteristics of the designed single-lap, single-bolt joint, which is analyzed in ANSYS software.

Assignment	Titanium 6Al-4V	Epoxy Carbon IM7 MTM-45-1		Titanium 6Al-4V	
Nonlinear Effects		Yes			
Thermal Strain Effects		Yes			
Bounding Box					
Length X	3.0004 mm	0. mm		17.001 mm	6.9754e-002 mm
Length Y	6.597 mm	140. mm		9.7099 mm	0.98837 mm
Length Z	7.4971 mm	30. mm		9.3191 mm	0.6617 mm
Properties					
Volume	48.884 mm³	12546 mm³		331.71 mm³	0. mm³
Mass	7.8214e-005 kg	1.8693e-002 kg		5.3074e-004 kg	
Centroid X	-4.4998 mm	2.6077e-008 mm	3. mm	-2.6023 mm	-7.1611 mm
Centroid Y	38.301 mm	103.58 mm	-26.974 mm	38.304 mm	37.589 mm
Centroid Z	-1.0567e-002 mm	6.1114e-010 mm	-6.1114e-010 mm	-2.4071e-004 mm	-2.2664 mm
Moment of Inertia Ip1	4.1765e-004 kg·mm²	31.732 kg·mm²		1.5247e-002 kg·mm²	
Moment of Inertia Ip2	4.1863e-004 kg·mm²	1.4079 kg·mm²		1.5247e-002 kg·mm²	
Moment of Inertia Ip3	7.1667e-004 kg·mm²	30.324 kg·mm²		1.8127e-003 kg·mm²	
Surface Area(approx.)		4181.9 mm²			9.7214e-004 mm²

Table 3.18: The minimum and maximum total and directional deformation values.

Object Name	Total Deformation - C2 - End Time	Total Deformation - End Time	Total Deformation - Bolt - End Time	Total Deformation - C1 - End Time	Strain Energy - End Time	Total Deformation - TH - End Time	Total Deformation - DH - End Time	X Axis - Directional Deformation - C2 - End Time	X Axis - Directional Deformation - C1 - End Time	X Axis - Directional Deformation - Bolt - End Time	X Axis - Directional Deformation - Nut - End Time
Minimum	0.73967 mm	0. mm	0.78444 mm	0. mm	1.8161e-023 mJ	0.82133 mm	0.83875 mm	0.50648 mm	-3.0682e-003 mm	0.7436 mm	0.74437 mm
Maximum	8.2676 mm		1.0713 mm	1.0948 mm	2.5426 mJ	0.99672 mm	0.94476 mm	3.3256 mm	1.0388 mm	0.9126 mm	0.91201 mm
Minimum Occurs On	C2	C1	Bolt	C1		C2	C1	C2	C1	Bolt	Nut
Maximum Occurs On	C2		Bolt	C1		C2	C1	C2	C1	Bolt	Nut

Figures 3.30 and 3.31 depict the total deformation of the hole in upper and bottom plates, respectively. Moreover, Figs. 3.32, 3.33, 3.34, 3.35 and 3.36 illustrate the X- directional deformation of upper and bottom laminate plates and the bolt, the hole in the upper and bottom laminate plates based on XY plane, respectively.
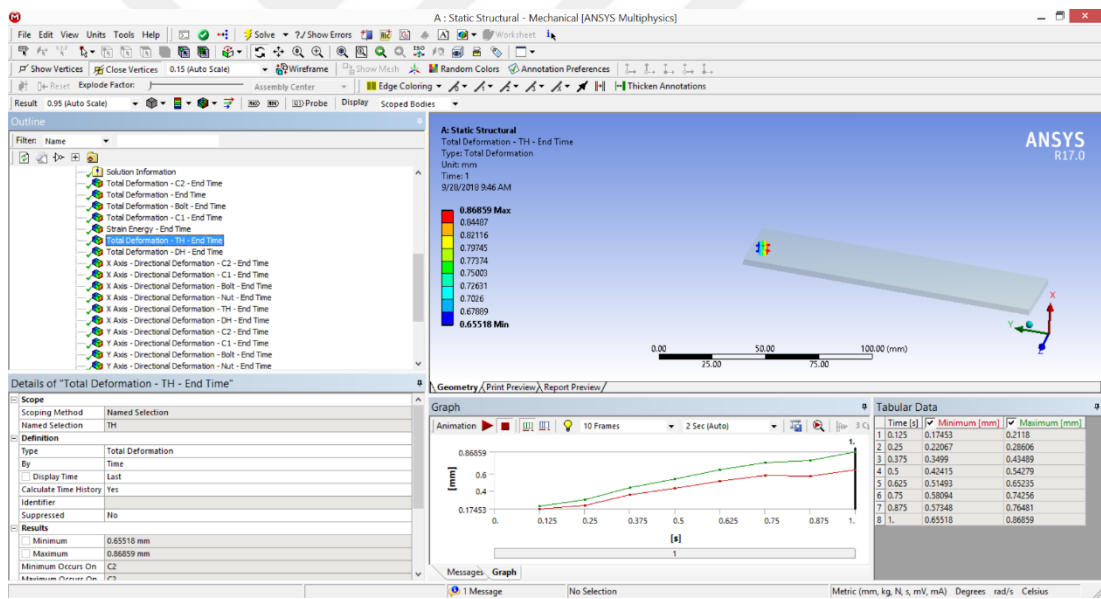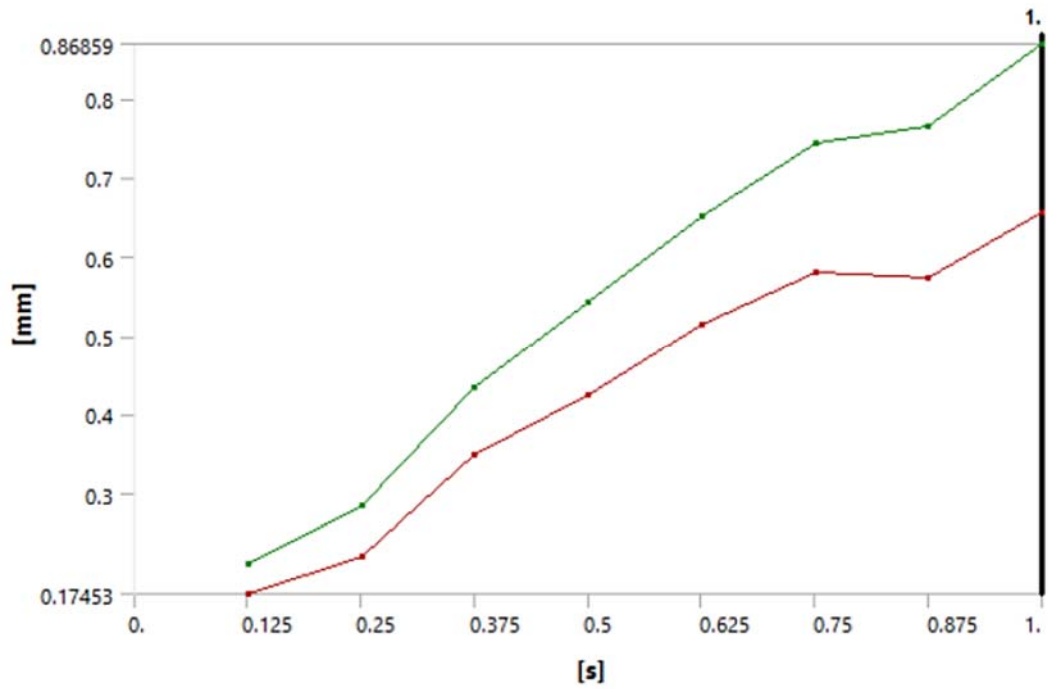
Figure 3.30: Total deformation of the hole in upper laminate plate.
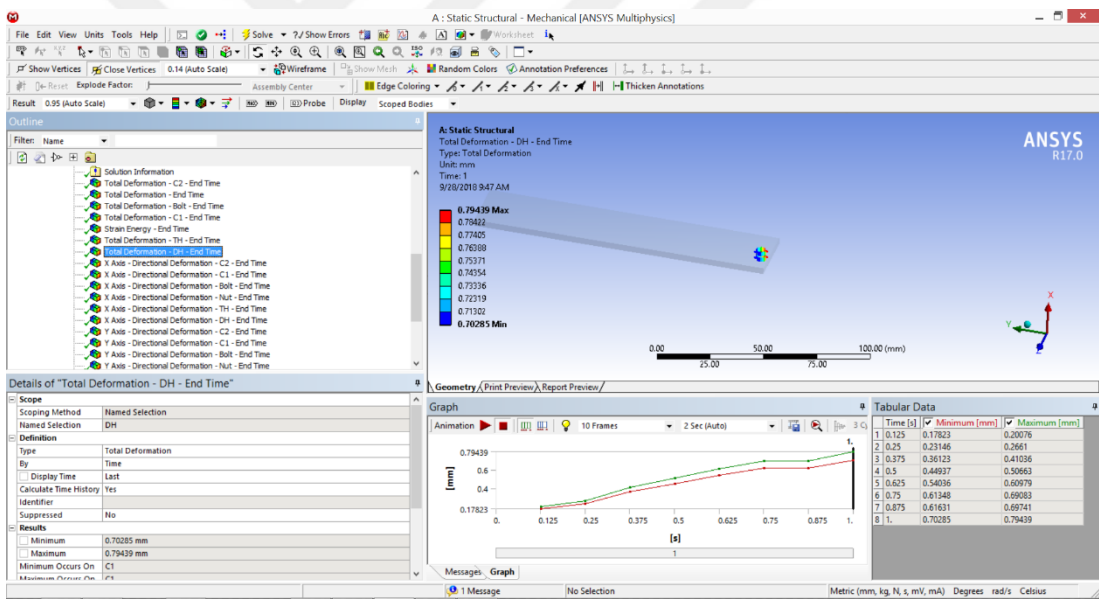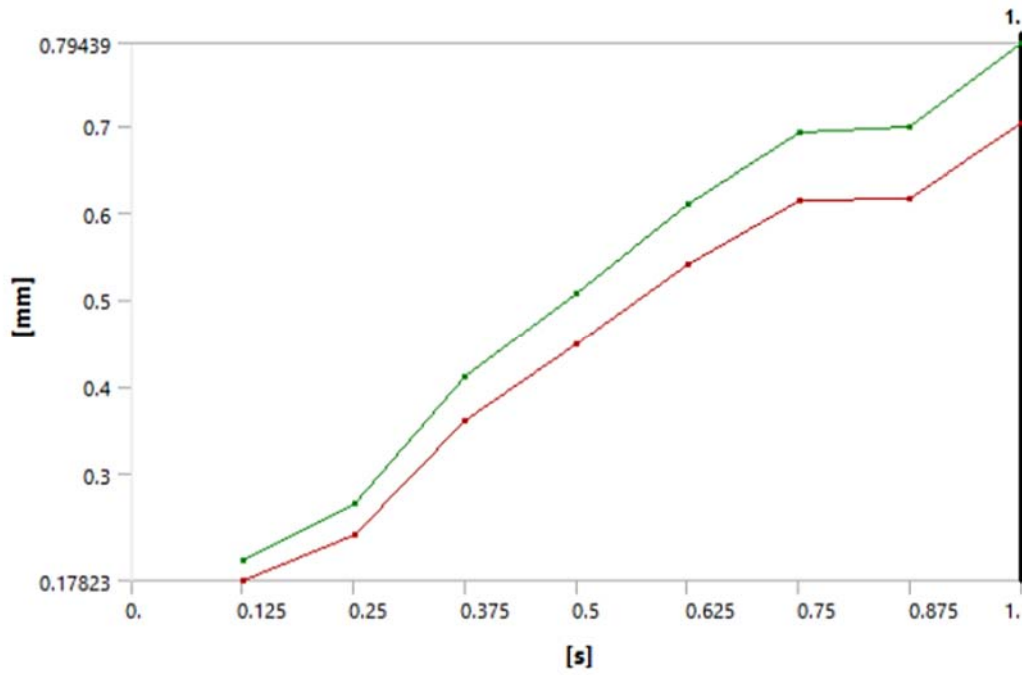
Figure 3.31: Total deformation of the hole in bottom laminate plate.

Figure 3.32: X Axis - Directional deformation of upper laminate plate.

Figure 3.33: X Axis - Directional deformation of bottom laminate plate.

Figure 3.34: X Axis - Directional deformation of the bolt.

Figure 3.35: X Axis - Directional deformation of the hole in the upper laminate plate.

Figure 3.36: X Axis - Directional deformation of the hole in the bottom laminate plate.

Figure 3.37: Y Axis - Directional deformation of upper laminate plate.
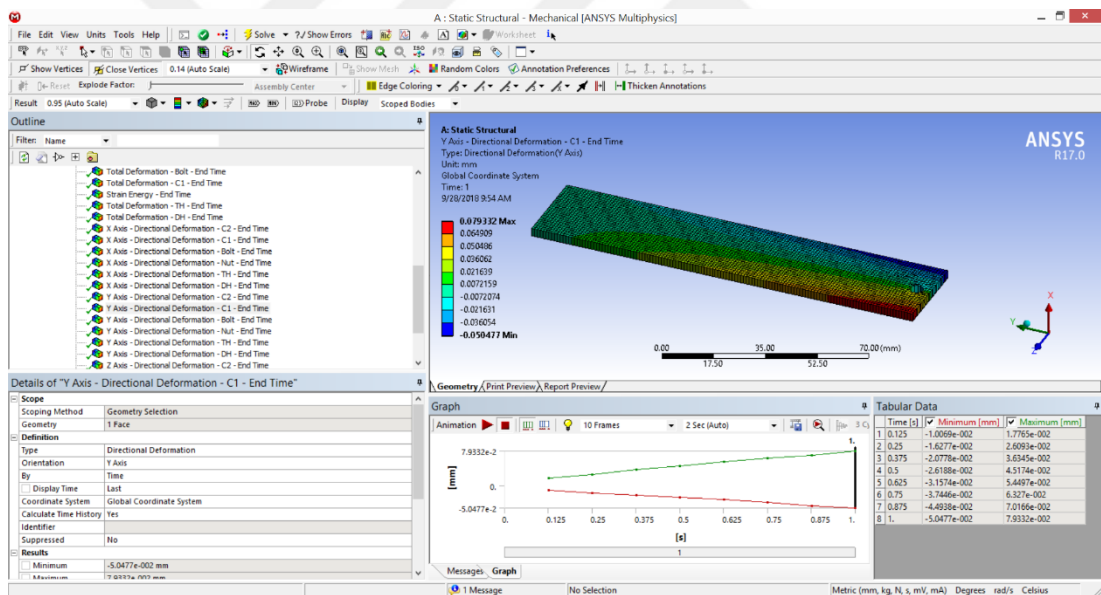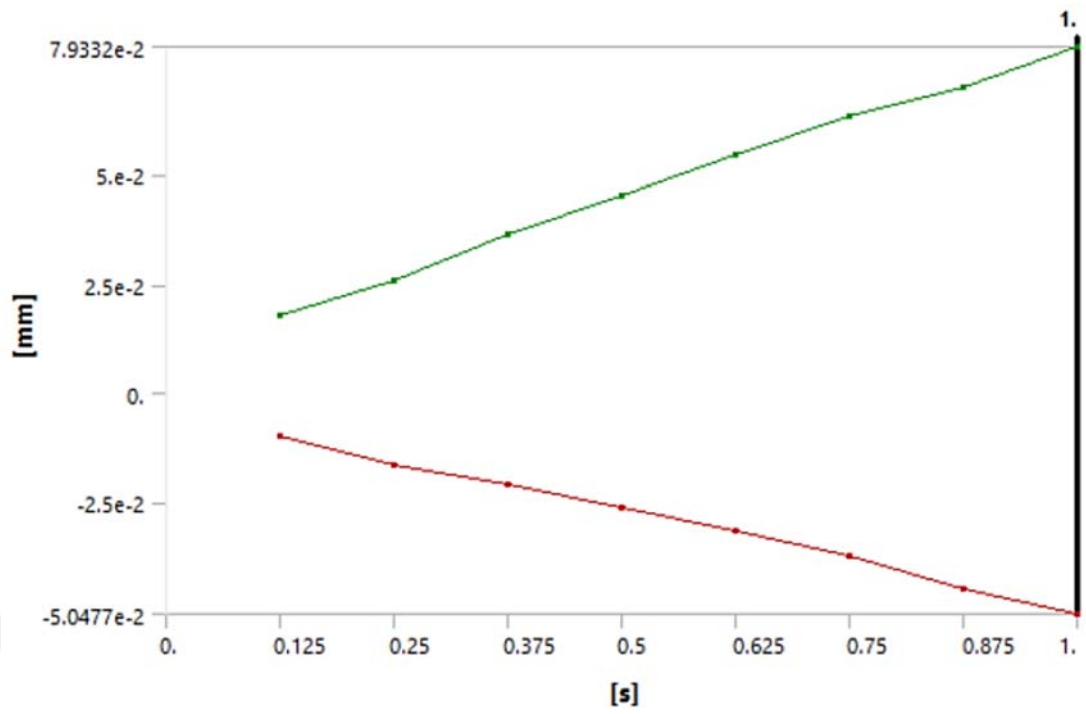
Figure 3.38: Y Axis - Directional deformation of bottom laminate plate.

Figures 3.37, 3.38 and 3.39 represent the Y-directional deformation of upper laminate plate bottom laminate plate and the bolt. Furthermore, Table 3.19 represents the minimum and maximum total and directional deformation values.

Table 19: The minimum and maximum total and directional deformation values.

Object Name	X Axis - Directional Deformation - TH - End Time	X Axis - Directional Deformation - DH - End Time	Y Axis - Directional Deformation - C2 - End Time	Y Axis - Directional Deformation - C1 - End Time	Y Axis - Directional Deformation - Bolt - End Time	Y Axis - Directional Deformation - Nut - End Time	Y Axis - Directional Deformation - TH - End Time	Y Axis - Directional Deformation - DH - End Time	Z Axis - Directional Deformation - C2 - End Time	Z Axis - Directional Deformation - C1 - End Time	Z Axis - Directional Deformation - Bolt - End Time
Minimum	0.77338 mm	0.77994 mm	-0.72349 mm	-4.7382e-002 mm	-0.2534 mm	-0.20151 mm	-4.9315e-002 mm	-2.0438e-002 mm	8.5839e-002 mm	0. mm	4.1035e-002 mm
Maximum	0.88293 mm	0.88095 mm	0.87268 mm	8.3598e-002 mm	0.31515 mm	9.7017e-002 mm	0.1985 mm	5.4707e-002 mm	7.5346 mm	0.35732 mm	0.56469 mm
Minimum Occurs On	C2	C1	C2	C1	Bolt	Nut	C2	C1	C2	C1	Bolt
Maximum Occurs On	C2	C1	C2	C1	Bolt	Nut	C2	C1	C2	C1	Bolt

Figure 3.39: Y Axis - Directional deformation of the bolt.

Figures 3.40, 3.41, 3.42, 3.43 and 3.44 depict Z Axis directional deformation of upper and bottom laminate plates, the bolt, the hole in upper and bottom laminate plates.
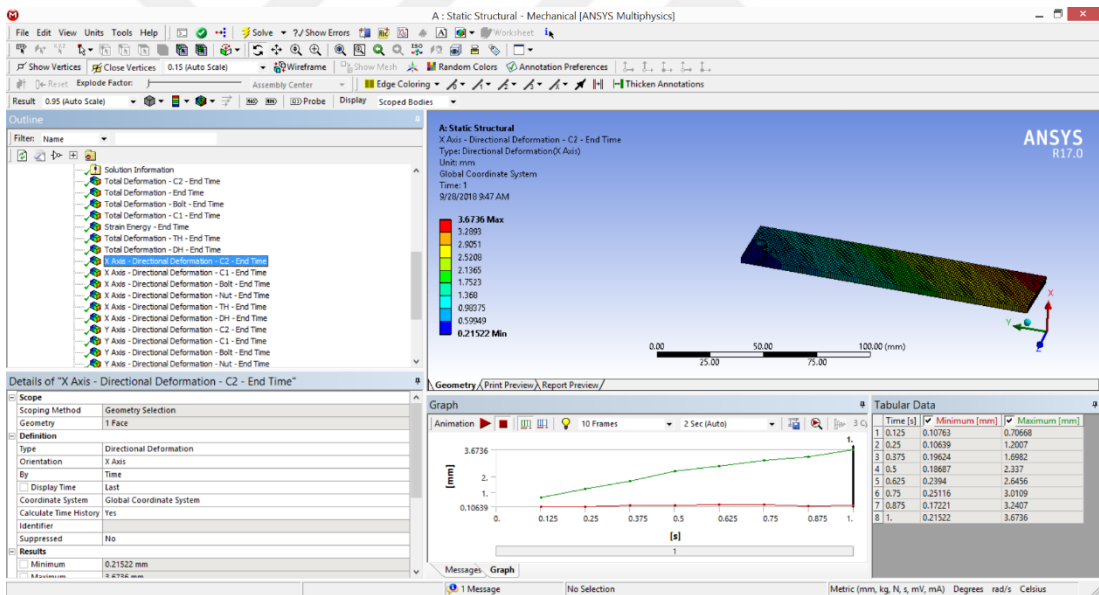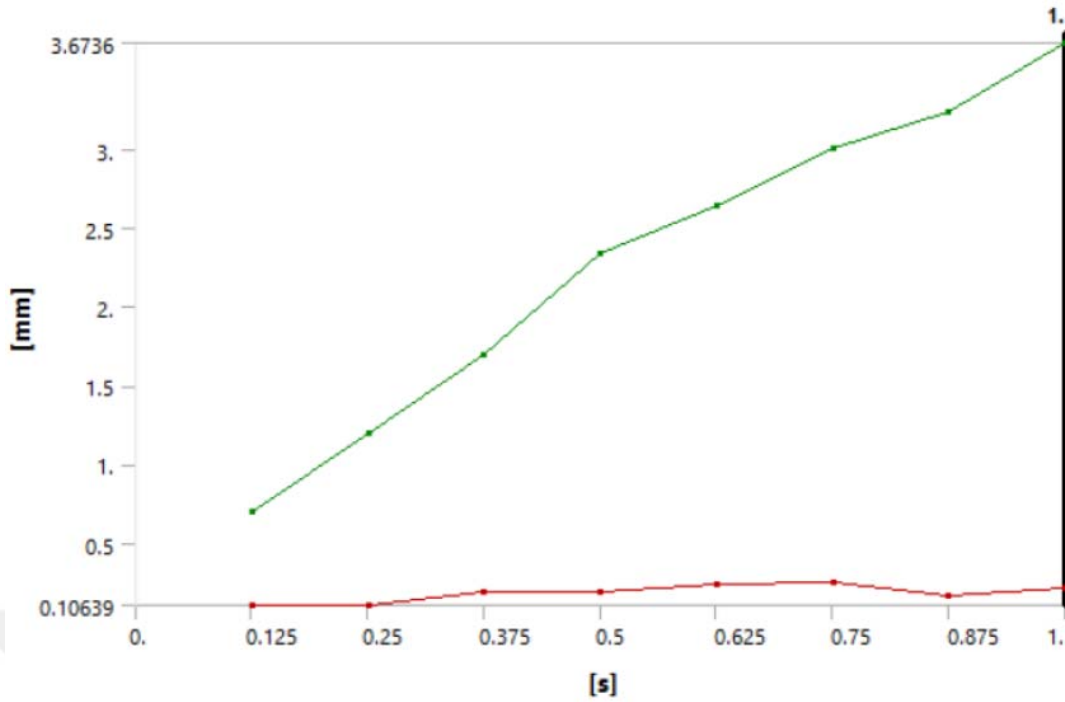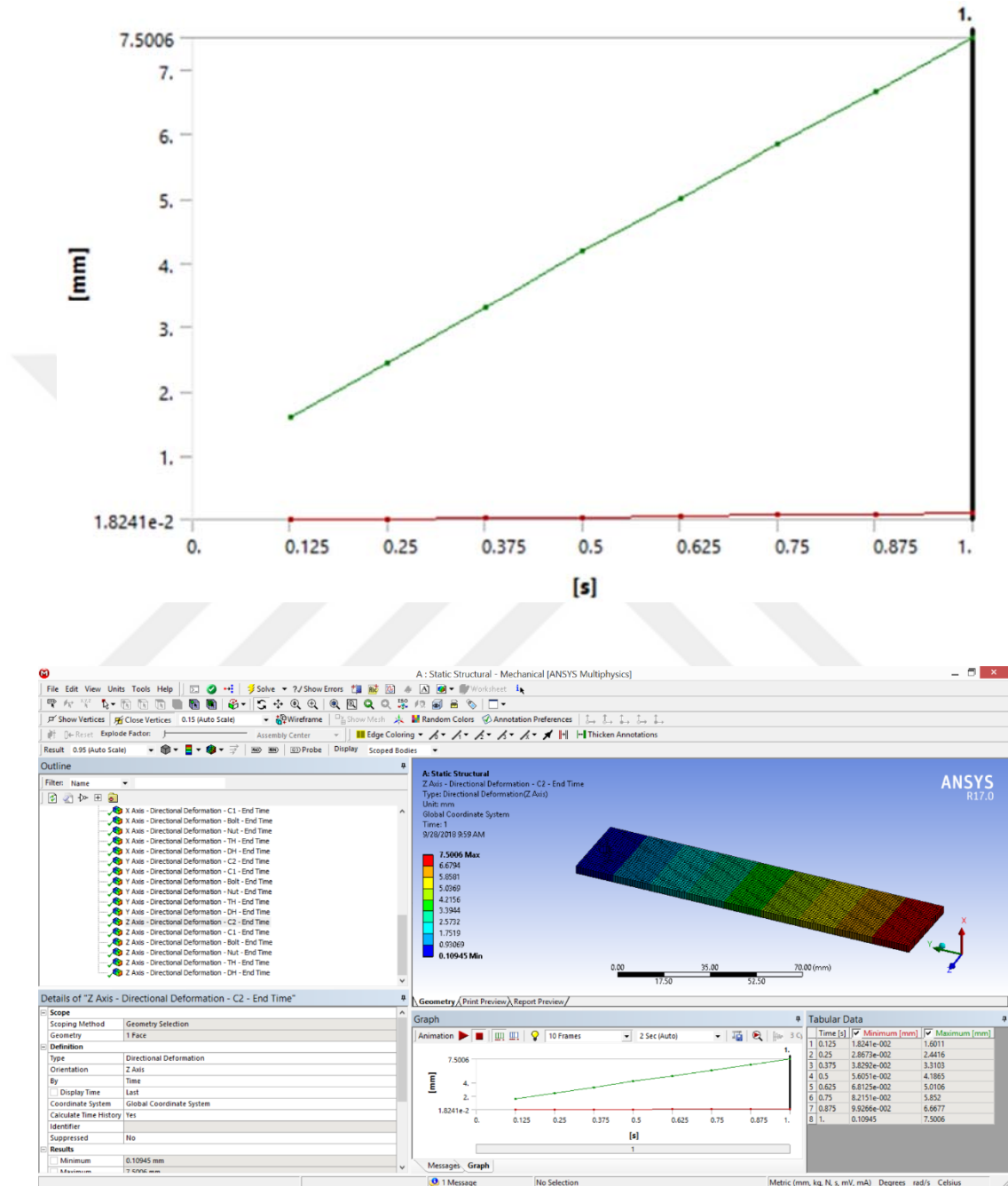

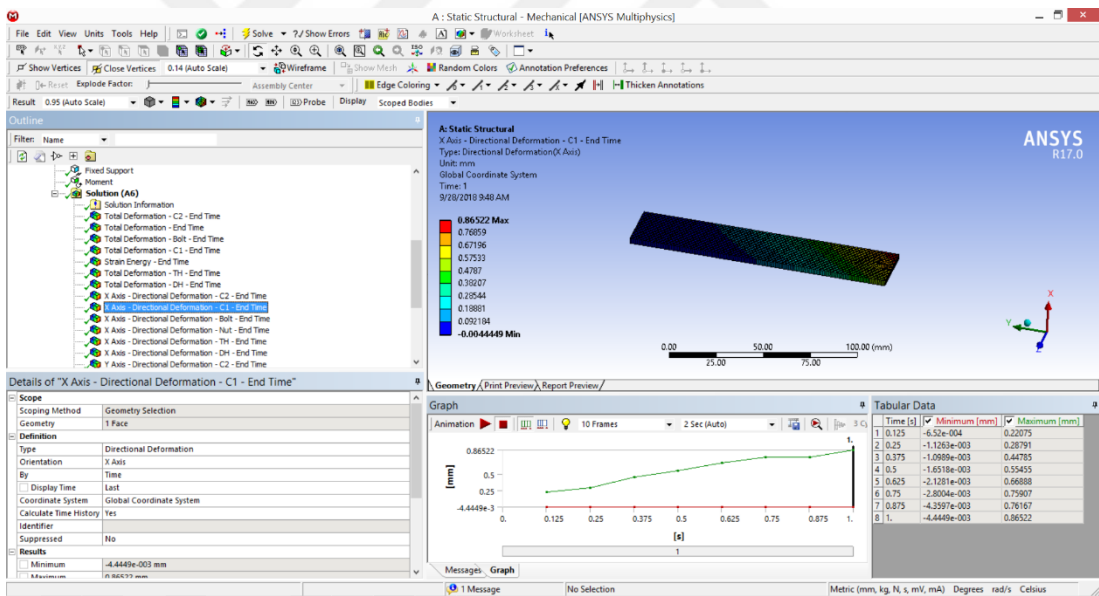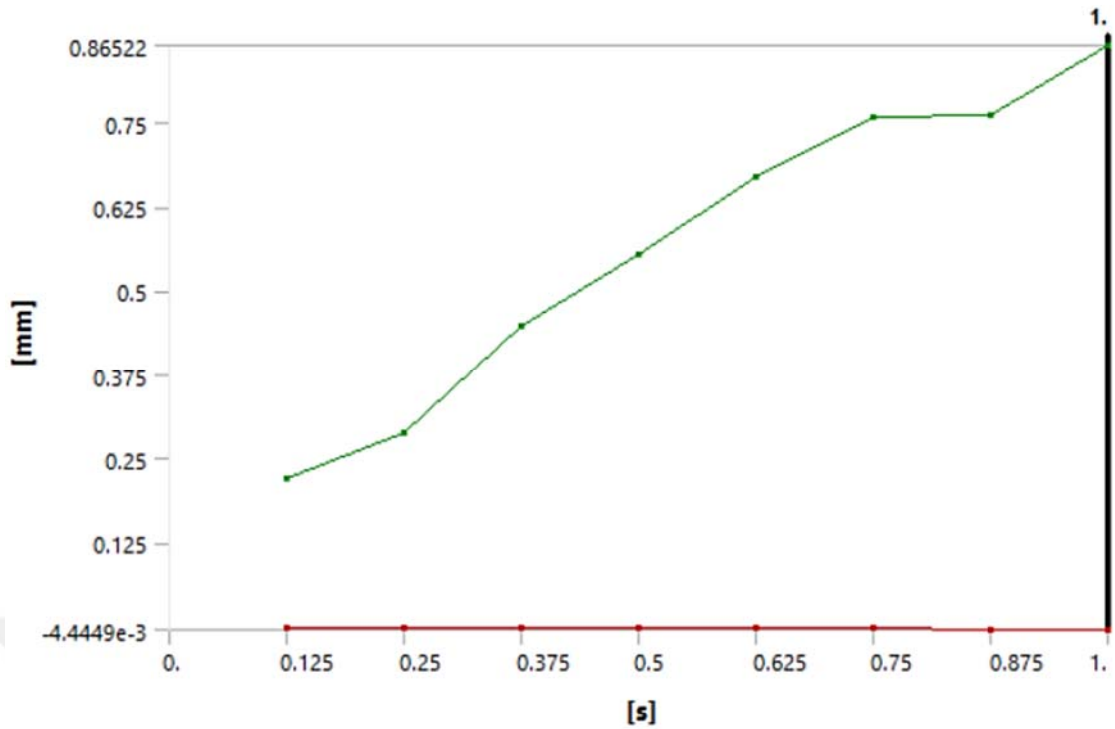**Figure 3.40:** Z Axis - Directional deformation of upper laminate plate.
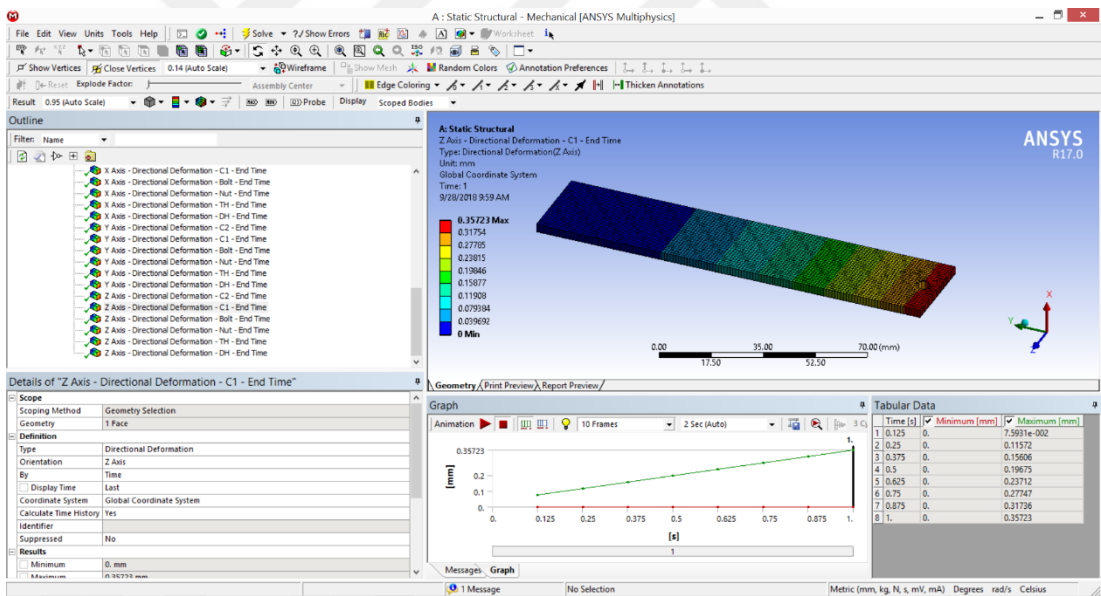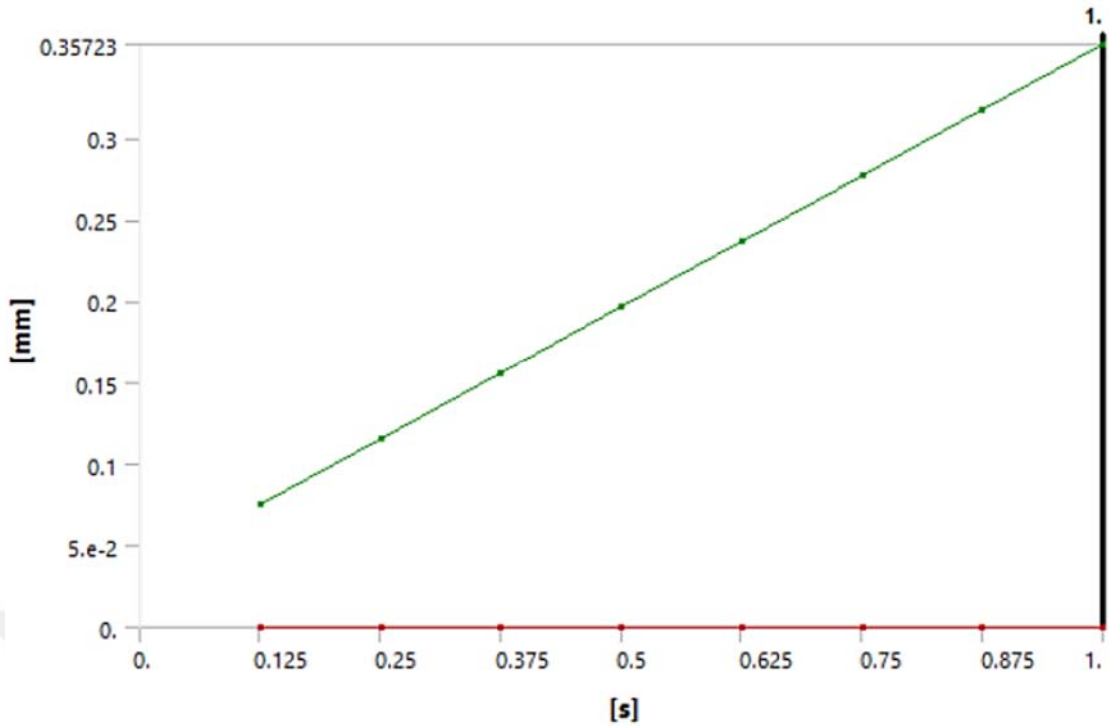
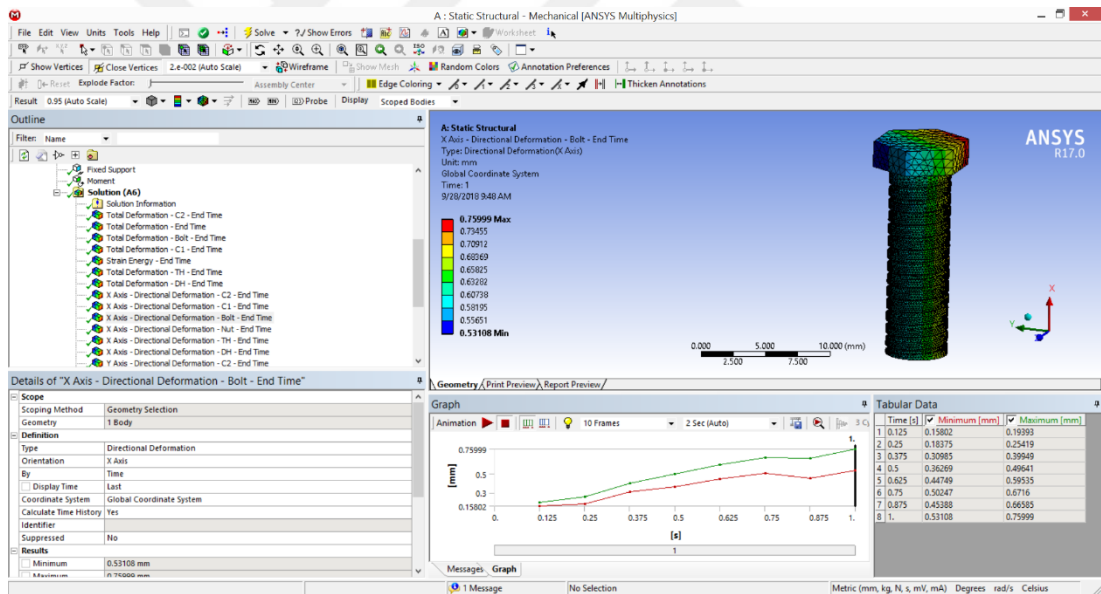**Figure 3.41:** Z Axis - Directional deformation of bottom laminate plate.
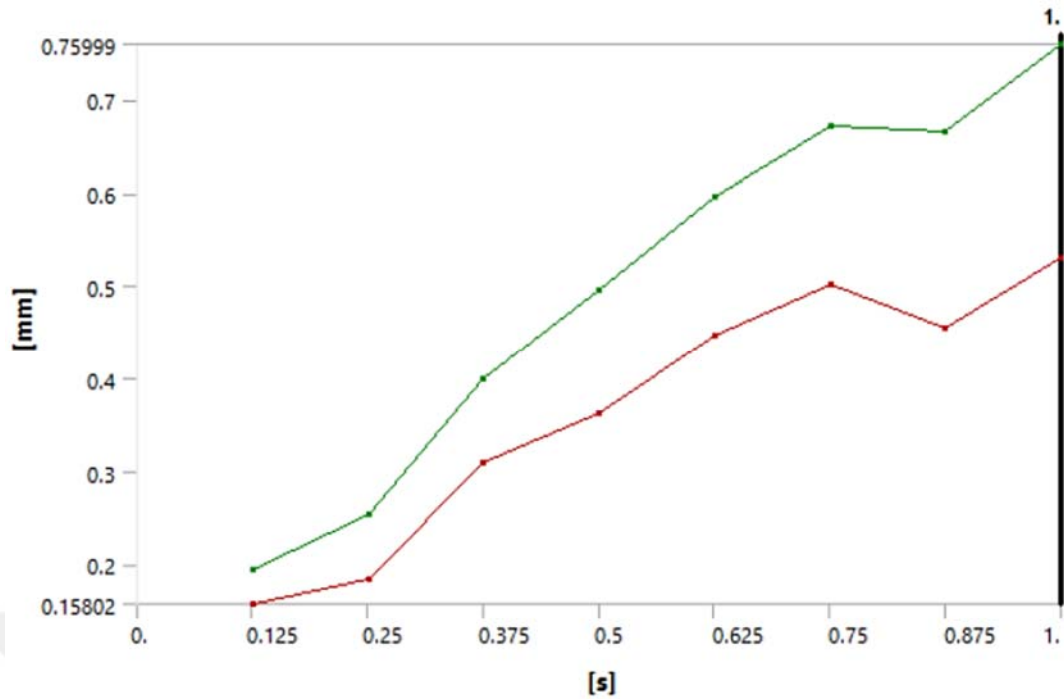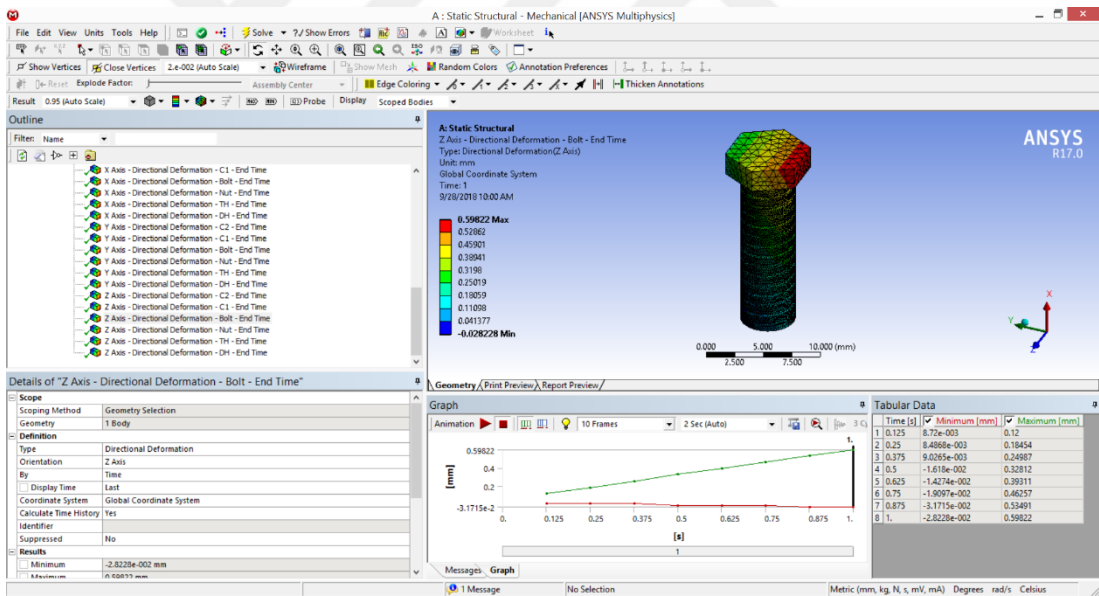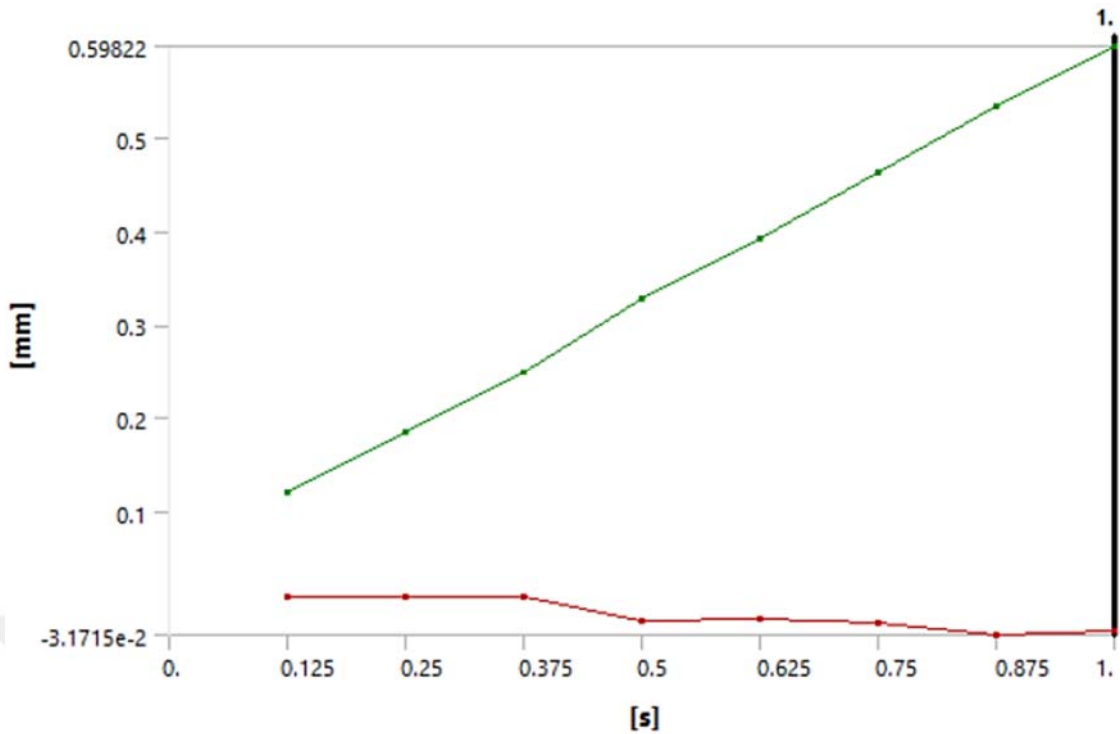
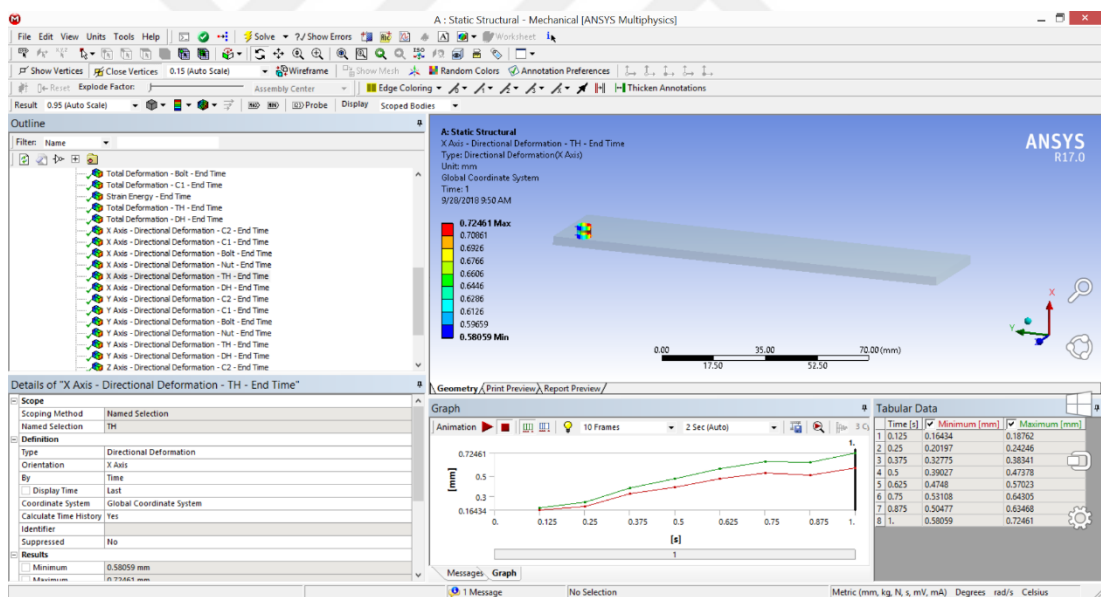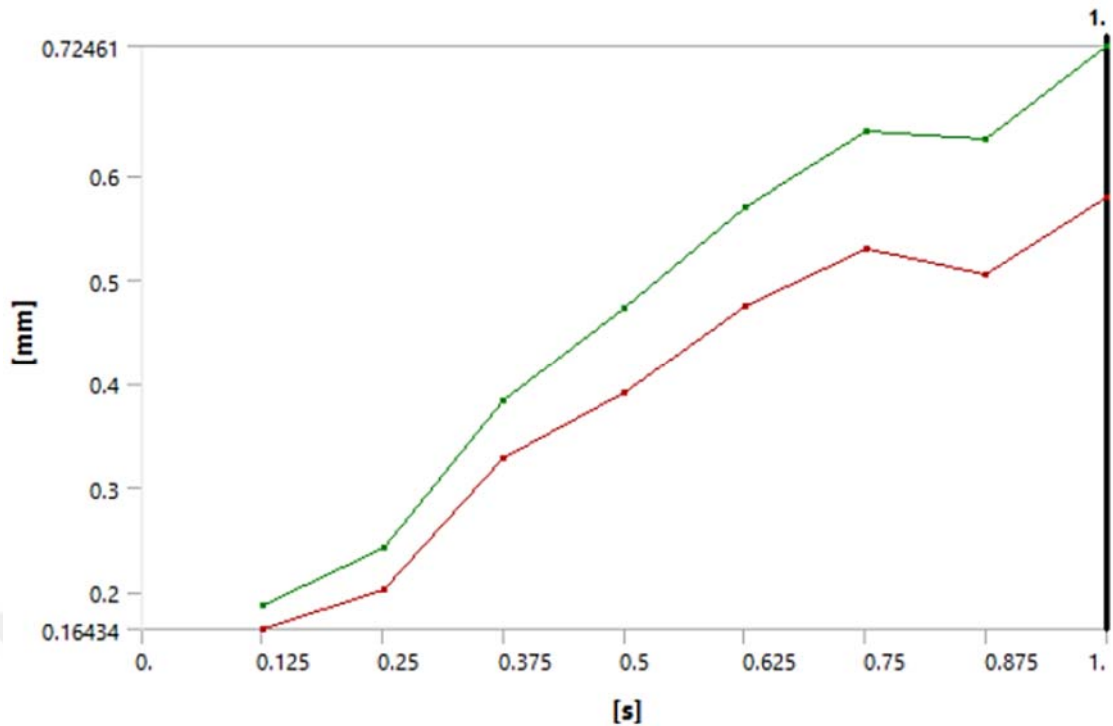**Figure 3.42:** Z Axis - Directional deformation of the bolt.
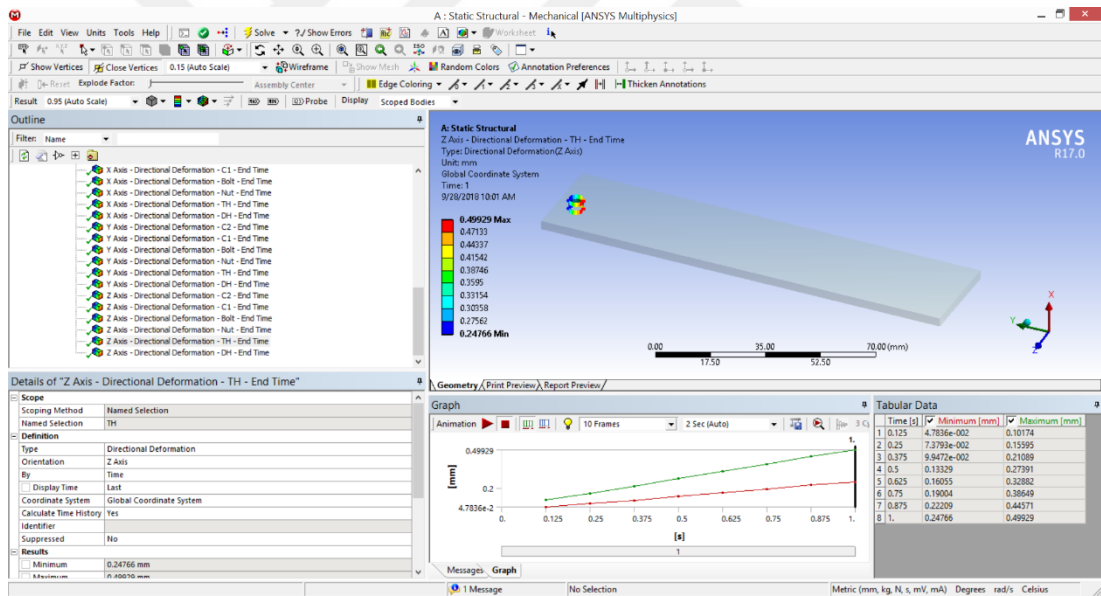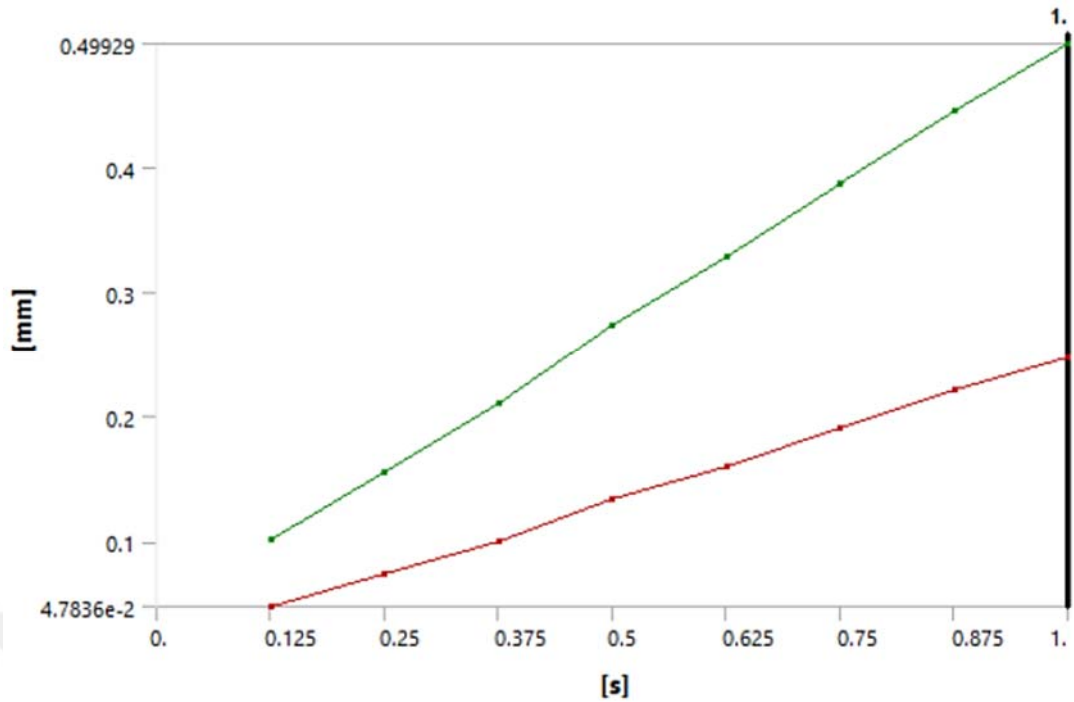
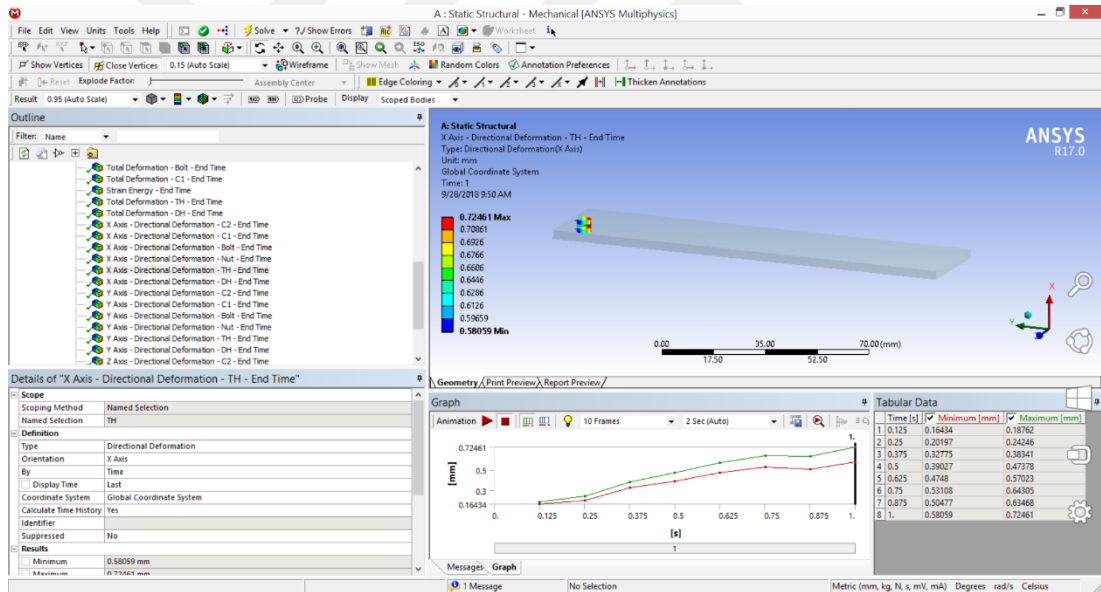**Figure 3.43:** Z Axis - Directional deformation of the hole in upper laminate plate.
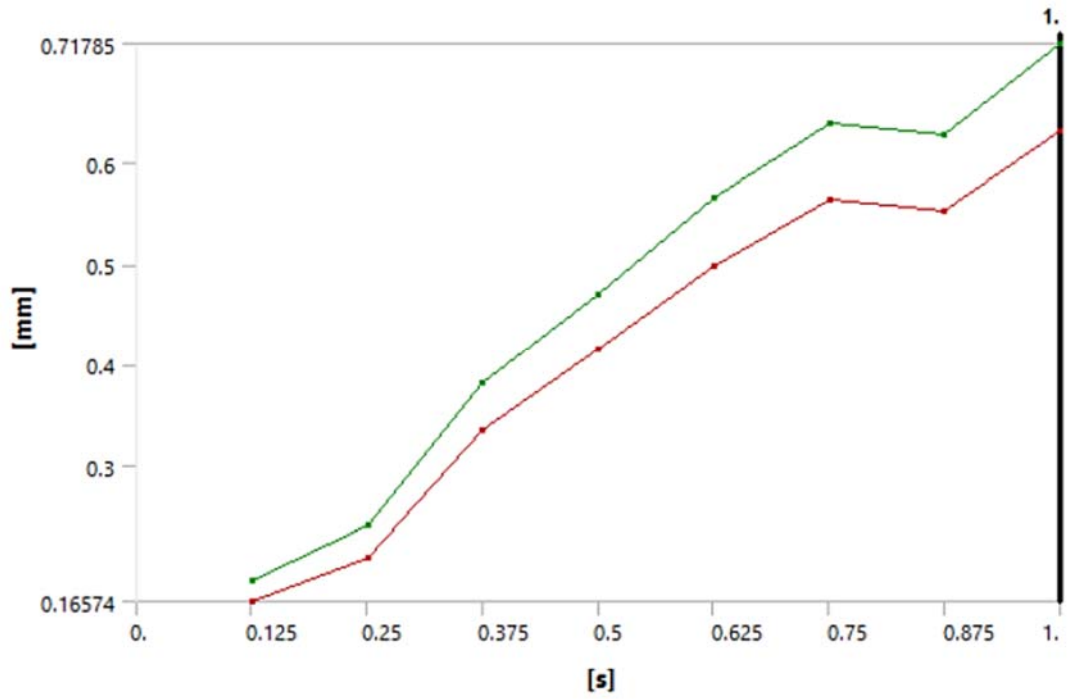
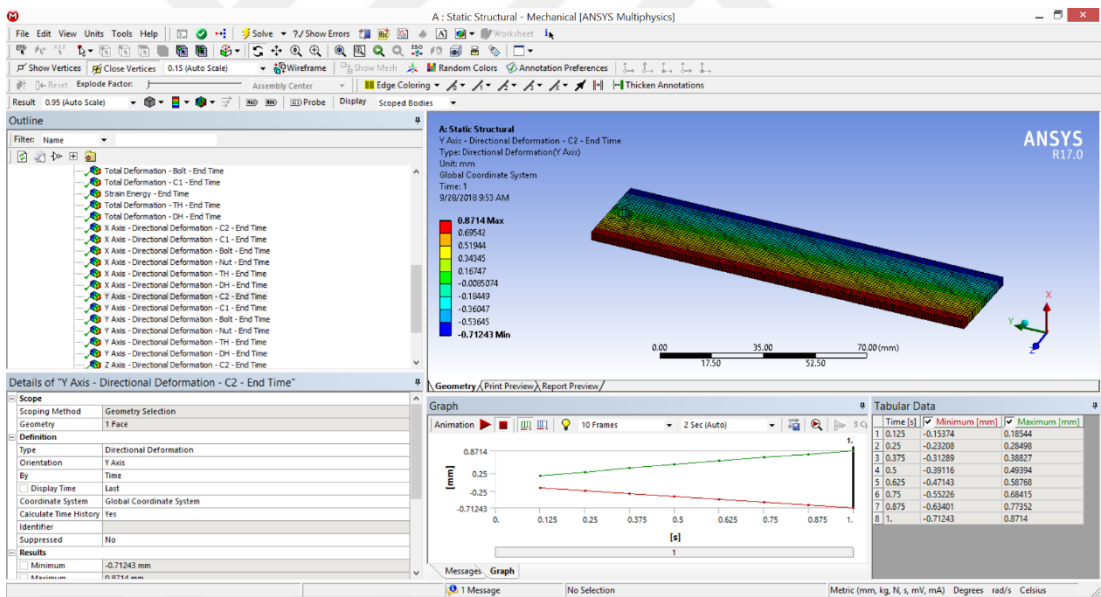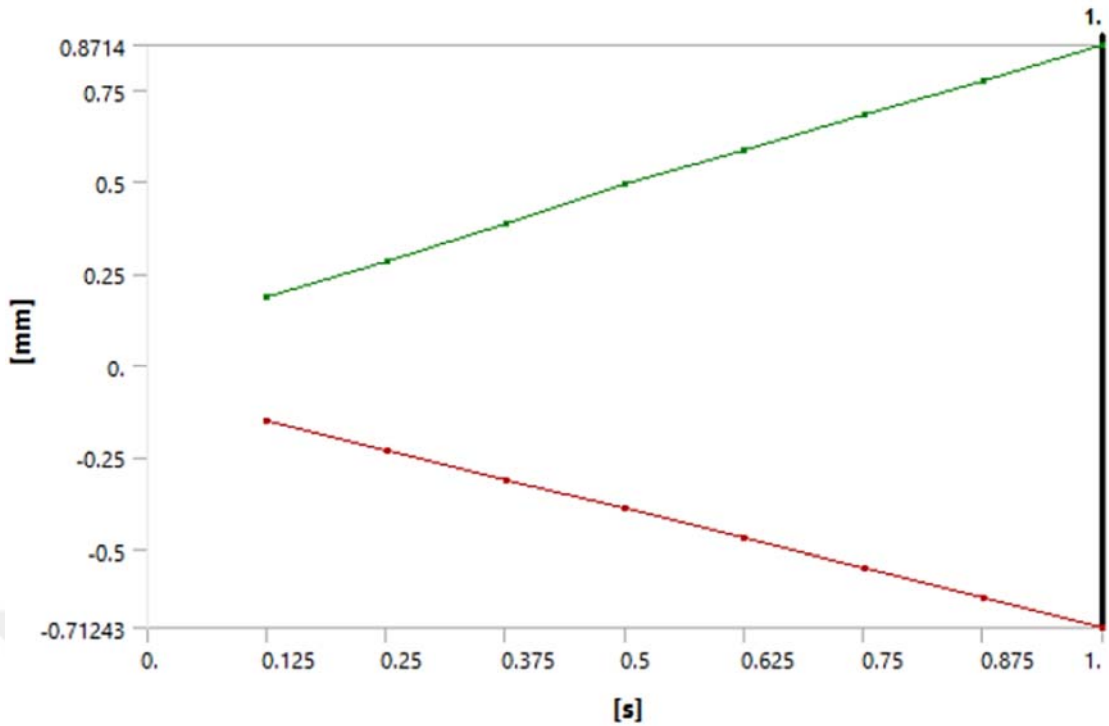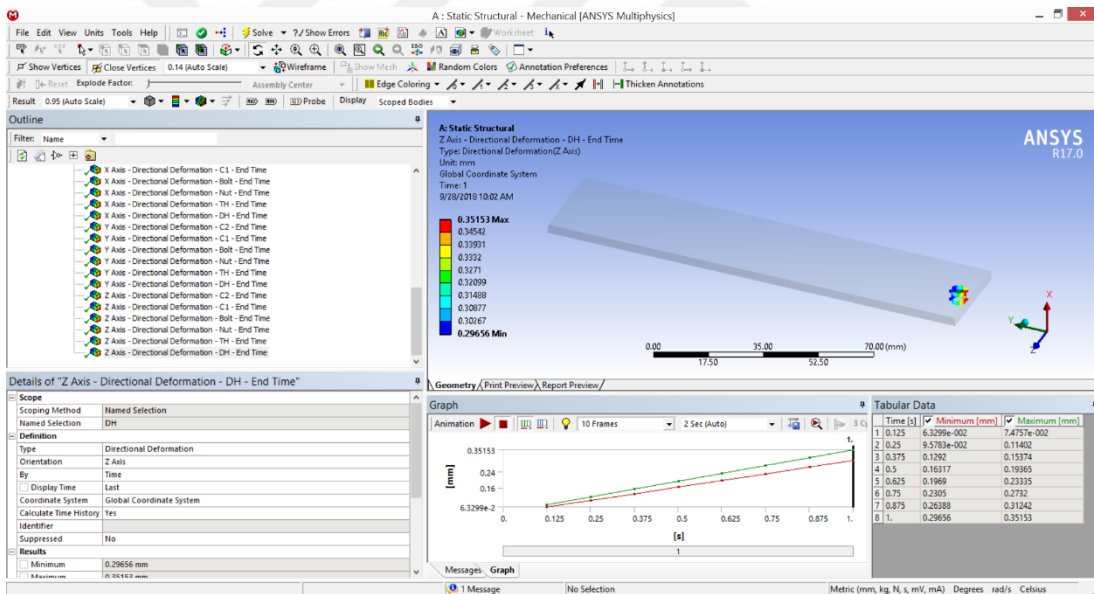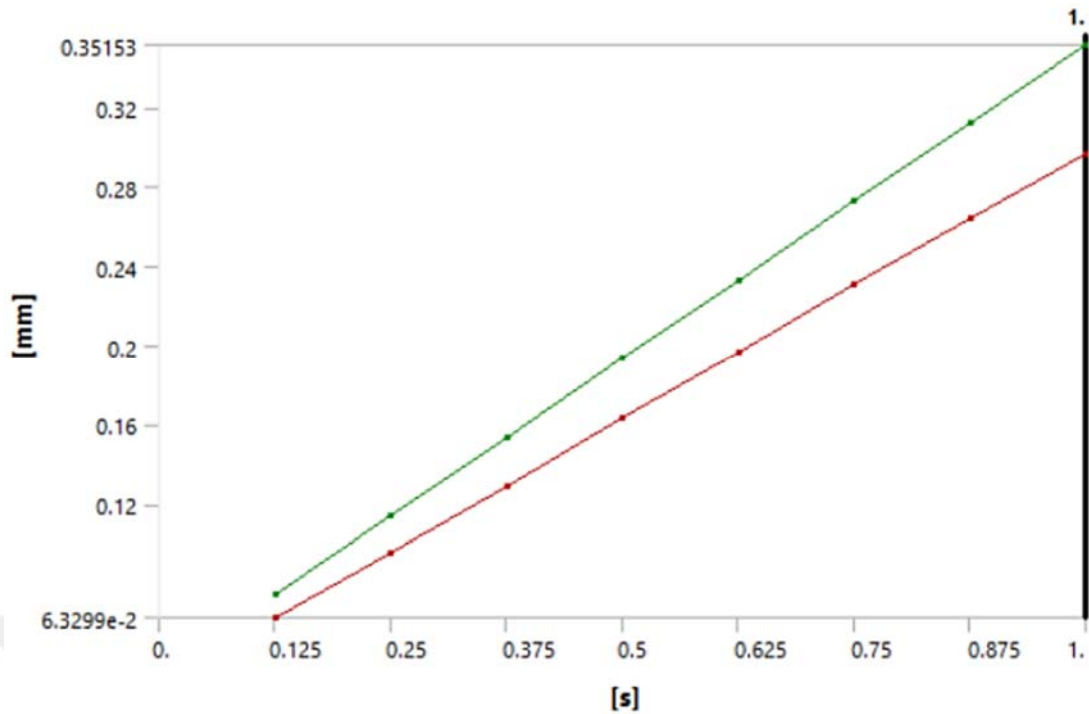**Figure 3.44:** Z Axis - Directional deformation of the hole in bottom laminate plate.

Tables 3.20, 3.21, 3.22 and 3.23 represent the shear stress based on bolt, nut, upper and bottom laminates, respectively.

Table 3.20: The bolt shear stress.

Time [s]	Minimum [MPa]	Maximum [MPa]
0.125	-2.7139e-002	7.1904e-003
0.25	-5.372e-002	1.4227e-002
0.4375	-9.2464e-002	2.4455e-002
0.71875	-0.14714	3.8943e-002
1.	-0.19743	5.2709e-002

Table 3.21: The nut shear stress.

Time [s]	Minimum [MPa]	Maximum [MPa]
0.125	-8.4721e-002	0.11914
0.25	-0.17087	0.24197
0.4375	-0.30862	0.42886
0.71875	-0.55872	0.73542
1.	-0.82153	1.0225

Table 3.22: The upper laminate plate shear stress.

Time [s]	Minimum [MPa]	Maximum [MPa]
0.125	-5.7358	3.4224
0.25	-11.476	6.8523
0.4375	-19.913	11.895
0.71875	-31.836	19.013
1.	-42.615	25.432

Table 3.23: The bottom laminate plate shear stress.

Time [s]	Minimum [MPa]	Maximum [MPa]
0.125	-3.8678	6.2147
0.25	-7.1571	12.411
0.4375	-11.668	21.597
0.71875	-18.927	35.051
1.	-26.056	48.044

Tables 3.24, 3.25, 3.26 and 3.27 are represented the normal stress along X- axis based on bolt, nut, bottom and upper laminate, respectively.

Table 3.24: The bolt normal stress along X- axis.

Time [s]	Minimum [MPa]	Maximum [MPa]
0.125	-8.4244e-002	1.635e-002
0.25	-0.16683	3.2527e-002
0.4375	-0.28945	5.6831e-002
0.71875	-0.47451	9.5624e-002
1.	-0.66039	0.13128

Table 3.25: The nut normal stress along X- axis.

Time [s]	Minimum [MPa]	Maximum [MPa]
0.125	-6.5861e-002	0.21557
0.25	-0.13387	0.43801
0.4375	-0.26027	0.80729
0.71875	-0.58449	1.5801
1.	-1.0384	2.5108

Table 3.26: The upper laminate plate normal stress along X- axis.

Time [s]	Minimum [MPa]	Maximum [MPa]
0.125	-5.477	3.2554
0.25	-10.96	6.5189
0.4375	-19.027	11.321
0.71875	-30.452	18.113
1.	-40.813	24.254

Table 3.27: The upper bottom plate normal stress along X- axis.

Time [s]	Minimum [MPa]	Maximum [MPa]
0.125	-3.2348	6.0417
0.25	-6.4597	12.07
0.4375	-11.248	21.02
0.71875	-18.305	34.163
1.	-25.38	46.899

Tables 3.28, 3.29, 3.30 and 3.31 are represented the normal stress along Y- axis based on bolt, nut, upper and bottom laminate, respectively.

Table 3.28: The bolt normal stress along Y- axis.

Time [s]	Minimum [MPa]	Maximum [MPa]
0.125	-4.7711e-002	1.8931e-002
0.25	-9.4095e-002	3.7706e-002
0.4375	-0.15972	6.4675e-002
0.71875	-0.24337	0.10331
1.	-0.32731	0.1337

Table 3.29: The nut normal stress along Y- axis.

Time [s]	Minimum [MPa]	Maximum [MPa]
0.125	-9.7955e-002	0.16963
0.25	-0.19646	0.34153
0.4375	-0.36021	0.60192
0.71875	-0.7139	1.0634
1.	-1.1839	1.5419

Table 3.30: The upper laminate plate normal stress along Y- axis.

Time [s]	Minimum [MPa]	Maximum [MPa]
0.125	-7.9543	4.3865
0.25	-15.912	8.7809
0.4375	-27.588	15.235
0.71875	-44.016	24.323
1.	-58.76	32.485

Table 3.31: The bottom plate normal stress along Y- axis.

Time [s]	Minimum [MPa]	Maximum [MPa]
0.125	-4.5337	9.2369
0.25	-9.0476	17.502
0.4375	-15.736	29.945
0.71875	-25.518	48.579
1.	-34.959	66.547

3.3.3 The Third Case Study

The third case study is based on the Alvaro Olmedo and Carlos Santiuste [58]. The laminate plate's material considered as carbon epoxy HTA 7/6376, the other plate's material is aluminum AA7475-T76 and titanium 6Al114VSTA applied as the bolt and nut material. Figure 3.45 represent the boundary conditions and geometrical description of the single-lap-joint, based on the proposed research.
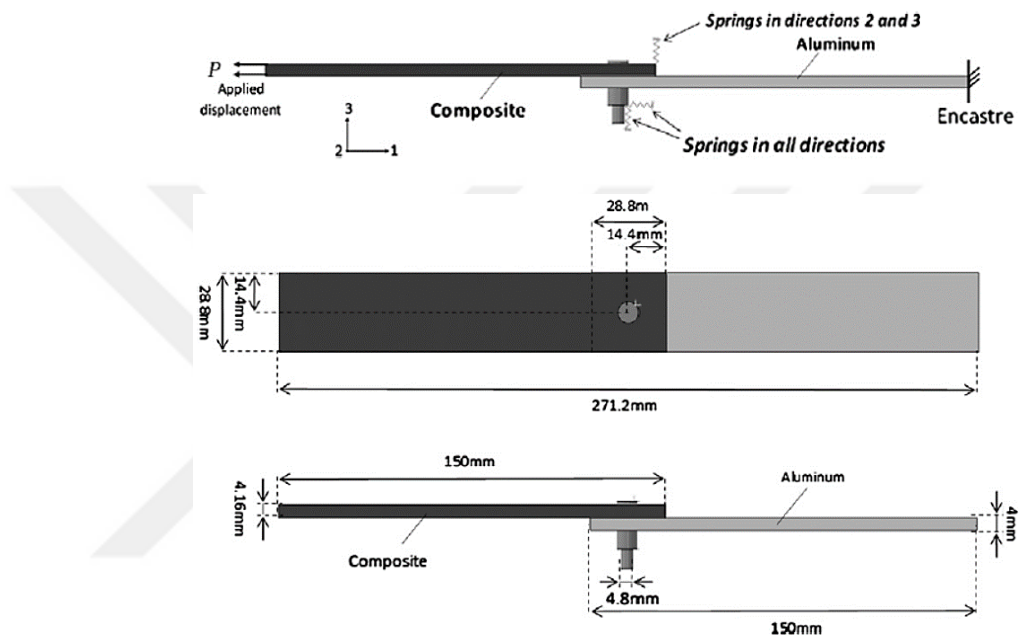
Figure 3.45: The boundary conditions and geometrical description of the single-lap-joint [58].

The composite lay-up was [(0/±45/90)2]s. Moreover, five contact interactions were defined between the three solids; the composite plate was in contact with aluminum plate, bolt head and bolt shank. Composite plate was modelled with 30,720 elements, aluminum plate with 5120 elements, and 6010 elements were used to model the bolt and the nut.

Based on the proposed research, the effect of tightening torque and the through-the thickness stress distribution are affected by the secondary bending phenomenon.

Figures 3.46 and 3.47 illustrate the load–displacement curves.
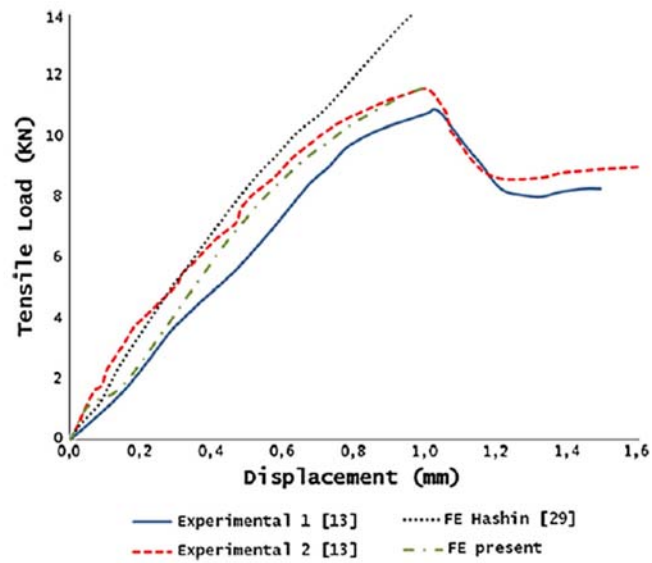
Figure 3.46: Load–displacement curves. Numerical predictions and experimental results [58].
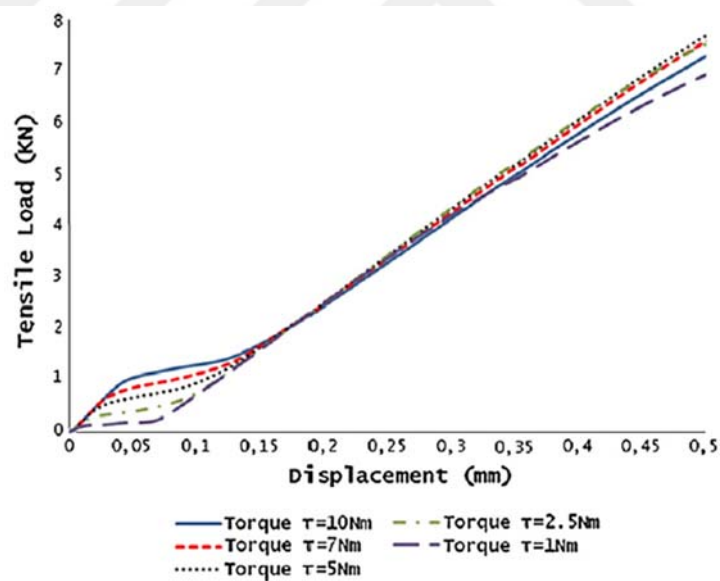
Figure 3.47: Load–displacement curves. Friction coefficient equal to 0.1. Influence of torque [58].

3.3.1.1 Simulation of the Third Case Study in ANSYS

The third case study is based on the research of Alvaro Olmedo, Carlos

Santiuste. In the proposed research new set of failure criteria to predict composite failure in single-lap bolted-joints is presented. Furthermore, the analyses of the stress field in single-lap bolted-joints have shown that secondary bending produce non-uniform stress distributions through the composite laminates' thickness in the vicinity of the bolt hole. Moreover, Table 3.32 represents the minimum and maximum total and directional deformation values.

Table 3.32: Characteristics of the designed single-lap, single-bolt joint, which is analyzed in ANSYS software.

|	Aluminum AA7475-T76	Titanium 6Al114VSTA	Epoxy Carbon HTA 7/6376	Titanium 6Al114VSTA
Assignment				
Nonlinear Effects		Yes		
Thermal Strain Effects		Yes		
Bounding Box				
Length X	151.37 mm	8. mm	151.37 mm	6.9282 mm
Length Y	37.089 mm	6.9282 mm	37.089 mm	8. mm
Length Z	4. mm	3.0009 mm	0. mm	22. mm
Properties				
Volume	17208 mm³	68.807 mm³	17208 mm³	435.65 mm³
Mass	4.8583e-002 kg	3.0473e-004 kg	3.0285e-002 kg	1.9294e-003 kg
Centroid X	105.77 mm	45.008 mm	-15.339 mm	45.007 mm
Centroid Y	-3.3807 mm	7.8763e-004 mm	3.3578 mm	8.8328e-005 mm
Centroid Z	-2. mm	-5.4998 mm	4. mm	-3.8664 mm
Moment of Inertia Ip1	3.4367 kg·mm²	1.7097e-003 kg·mm²	2.102 kg·mm²	9.1233e-002 kg·mm²
Moment of Inertia Ip2	90.795 kg·mm²	1.709e-003 kg·mm²	56.559 kg·mm²	9.1234e-002 kg·mm²
Moment of Inertia Ip3	94.102 kg·mm²	2.9581e-003 kg·mm²	58.661 kg·mm²	6.7879e-003 kg·mm²
Surface Area(approx.)			4301.9 mm²	

Table 3.33 represents the minimum and maximum total and directional deformation values. Figures 3.48 and 3.49 depict the total deformation of the hole in upper and bottom plates, respectively. Moreover, Figs. 3.50, 3.51, 3.52, 3.53 and 3.54 illustrate the X- directional deformation of upper and bottom laminate plates and the bolt, the hole in the upper and bottom laminate plates, respectively.

Table 3.33: The minimum and maximum total and directional deformation values.

Object Name	Total Deformation - Composite plate - End Time	Total Deformation - Aluminium plate - End Time	Total Deformation - Bolt - End Time	Total Deformation - TH - End Time	Total Deformation - DH - End Time	X Axis - Directional Deformation - Composite plate - End Time	X Axis - Directional Deformation - Aluminium plate - End Time	X Axis - Directional Deformation - Bolt - End Time	X Axis - Directional Deformation - Nut - End Time	Y Axis - Directional Deformation - Composite plate - End Time	Y Axis - Directional Deformation - Aluminium plate - End Time
Minimum	3.979 mm	0. mm	4.7701 mm	4.8341 mm	4.8464 mm	-0.55389 mm	-0.49015 mm	-0.66492 mm	-0.11266 mm	-2.1084 mm	-0.99723 mm
Maximum	14.534 mm	6.0581 mm	5.2954 mm	5.1397 mm	5.1631 mm	-0.18993 mm	7.9633e-002 mm	0.73127 mm	0.14881 mm	-0.71407 mm	9.1476e-004 mm
Minimum Occurs On	Composite plate	Aluminium plate	Bolt	Composite plate	Aluminium plate	Composite plate	Aluminium plate	Bolt	Nut	Composite plate	Aluminium plate
Maximum Occurs On	Composite plate	Aluminium plate	Bolt	Composite plate	Aluminium plate	Composite plate	Aluminium plate	Bolt	Nut	Composite plate	Aluminium plate

Figure 3.48: Total deformation of the hole in upper laminate plate.
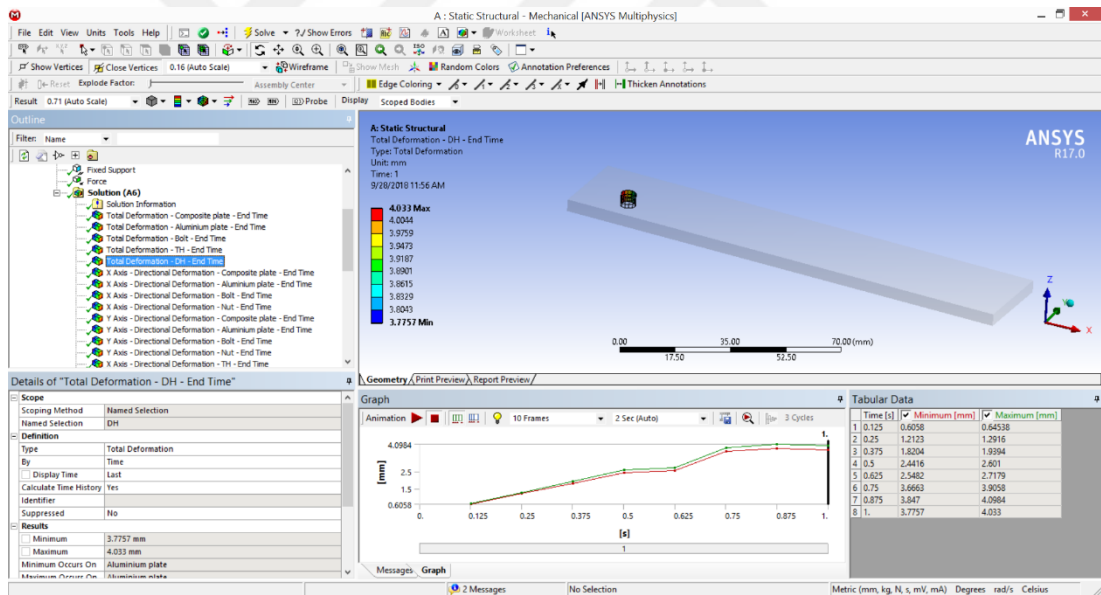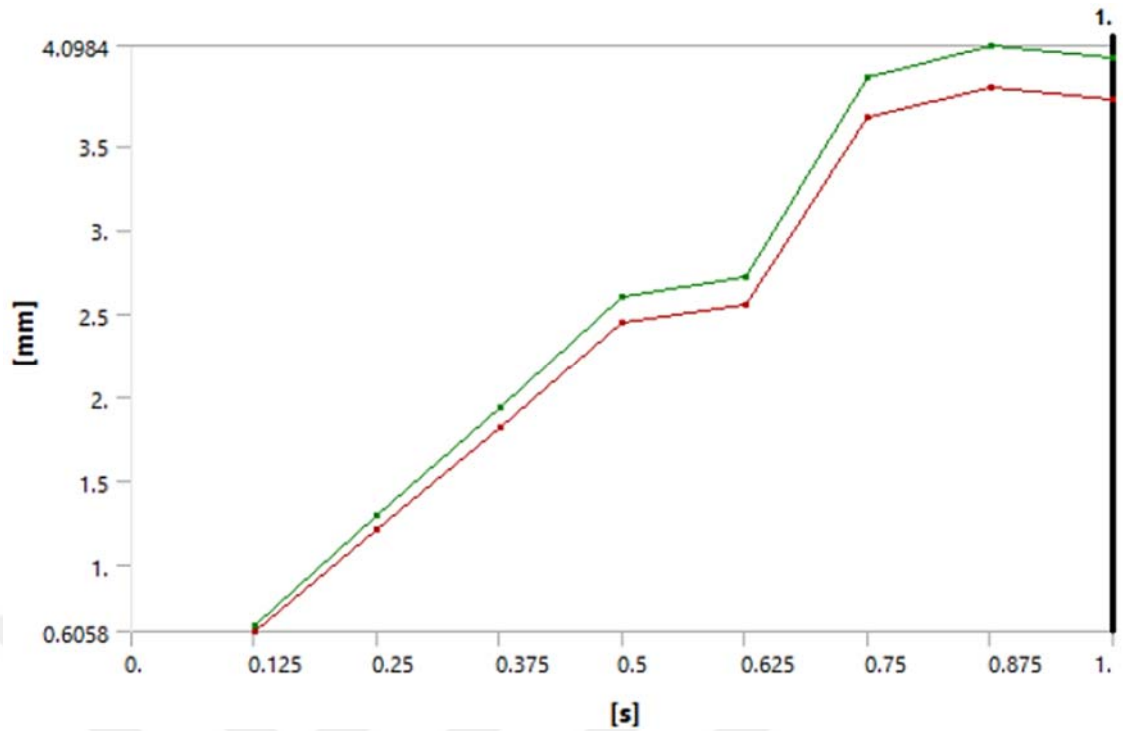
Figure 3.49: Total deformation of the hole in bottom laminate plate.

Figure 3.50: X Axis - Directional deformation of upper laminate plate.

Figure 3.51: X Axis - Directional deformation of bottom laminate plate.

Figure 3.52: X Axis - Directional deformation of the bolt.

Figure 3.53: X Axis - Directional deformation of the hole in the upper laminate plate.

Figure 3.54: X Axis - Directional deformation of the hole in the bottom laminate plate.

Figure 3.55: Y Axis - Directional deformation of upper laminate plate.
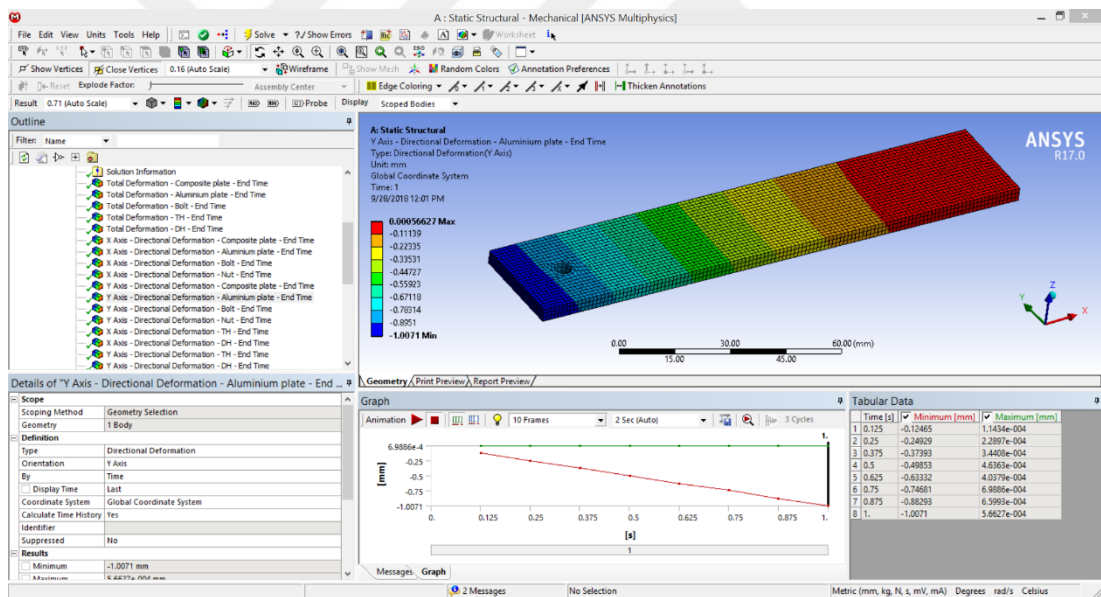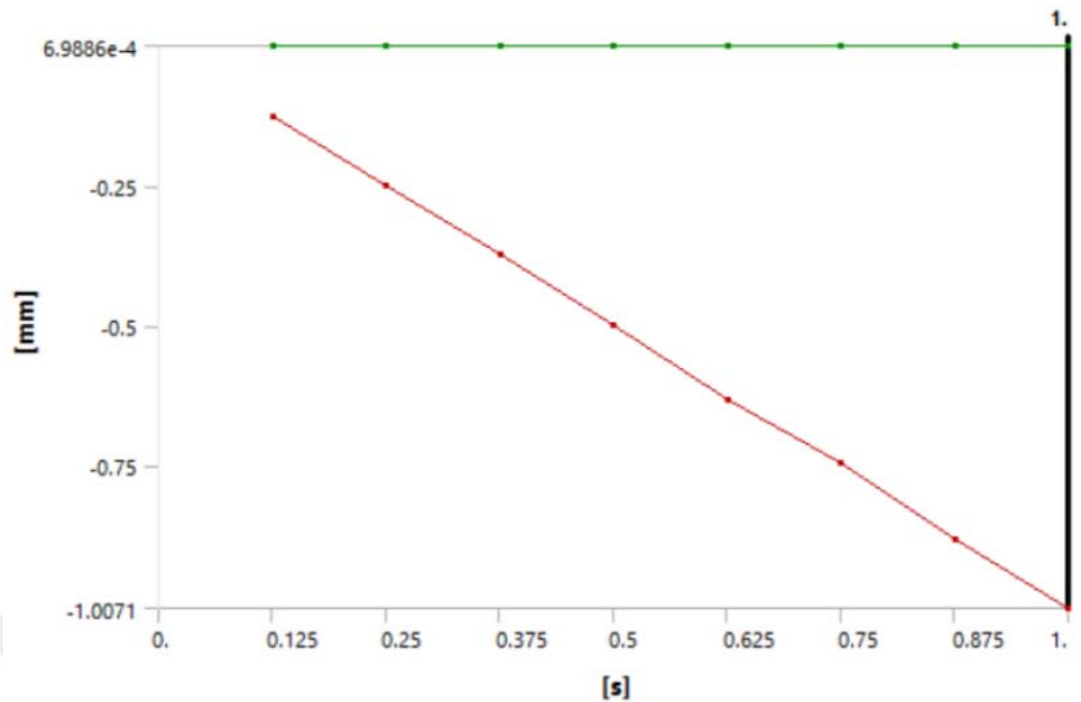
Figure 3.56: Y Axis - Directional deformation of bottom laminate plate.

Figures 3.55, 3.56 and 3.57 represent the Y-directional deformation of upper laminate plate bottom laminate plate and the bolt. Furthermore, Table 3.34 represents the minimum and maximum directional deformation values.
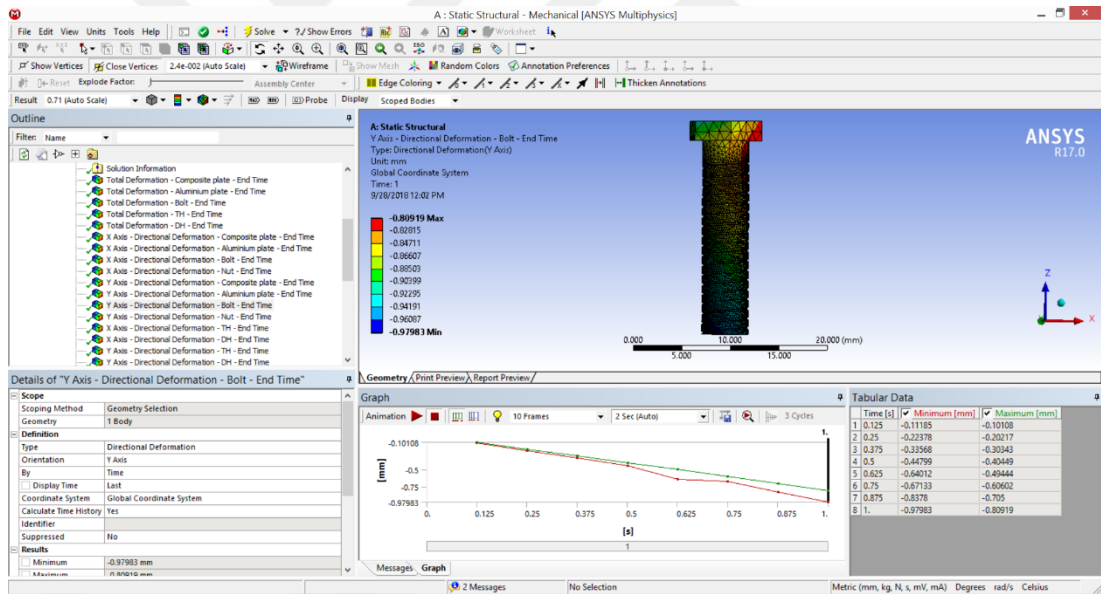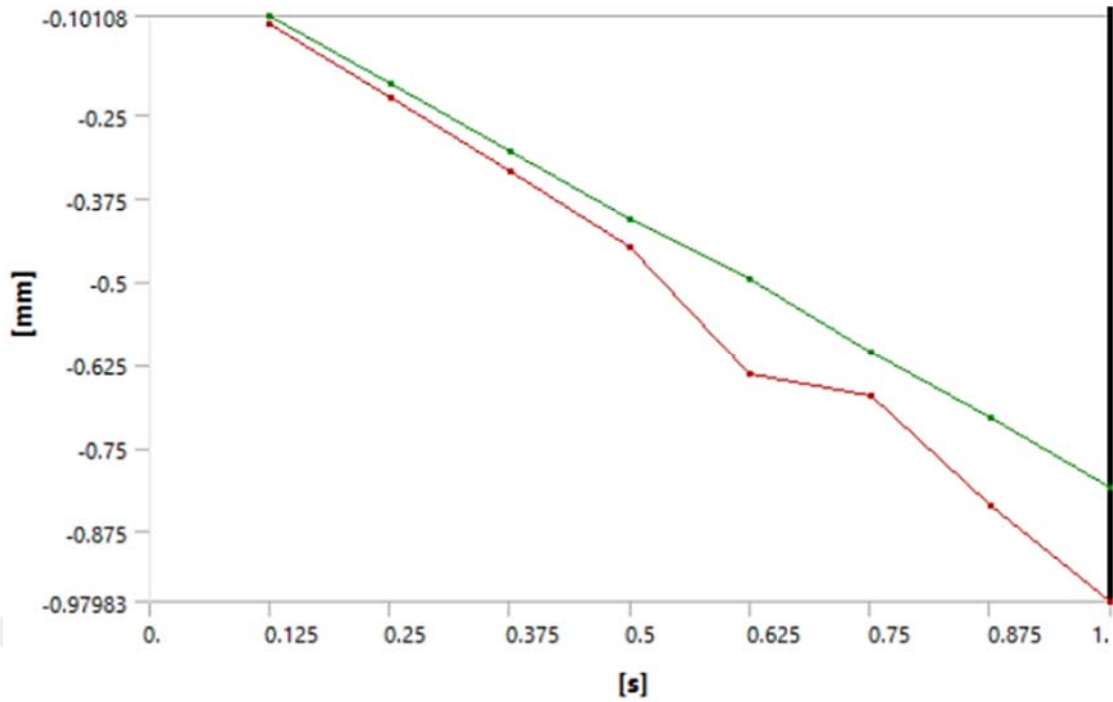
Figure 3.57: Y Axis - Directional deformation of the bolt.

Table 3.34: The minimum and maximum directional deformation values.

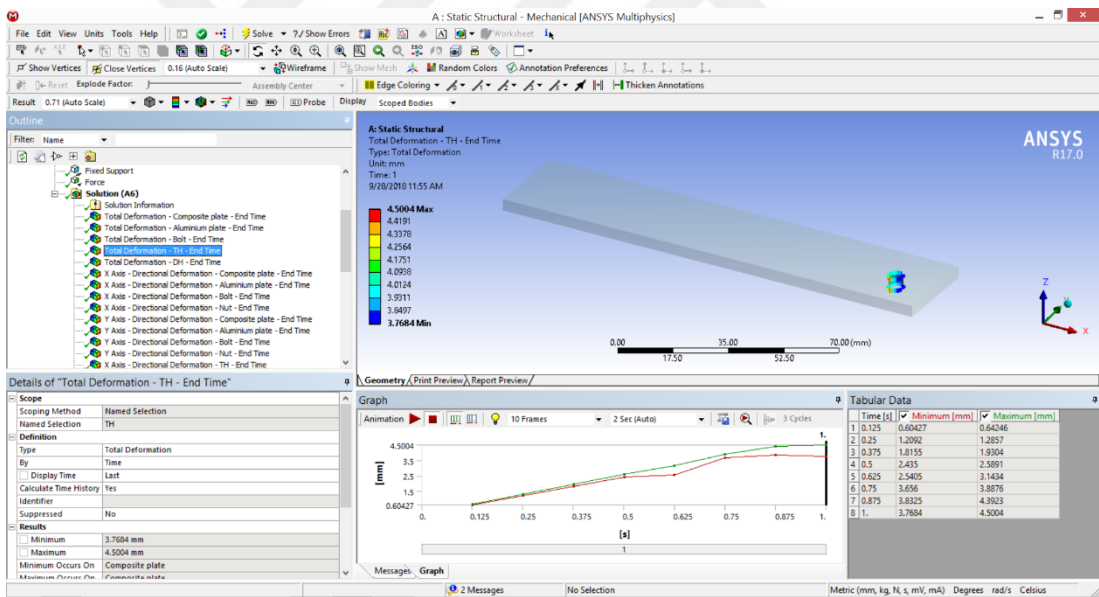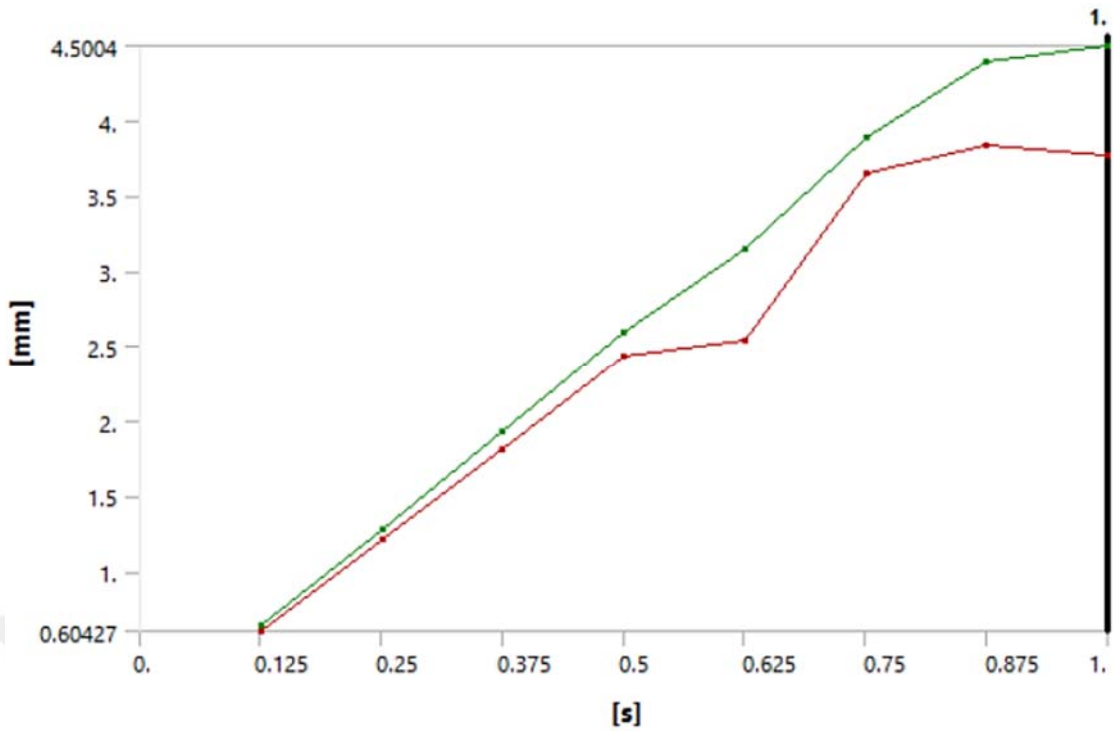| Object Name	Y Axis - Directional Deformation - Bolt - End Time	Y Axis - Directional Deformation - Nut - End Time	X Axis - Directional Deformation - TH - End Time	X Axis - Directional Deformation - DH - End Time	Y Axis - Directional Deformation - TH - End Time	Y Axis - Directional Deformation - DH - End Time	Z Axis - Directional Deformation - Composite plate - End Time	Z Axis - Directional Deformation - Aluminium plate - End Time	Z Axis - Directional Deformation - Bolt - End Time	Z Axis - Directional Deformation - Nut - End Time	Z Axis - Directional Deformation - TH - End Time
Minimum	-0.8948 mm	-0.8916 mm	-0.38817 mm	-0.38288 mm	-0.87027 mm	-0.87587 mm	-14.377 mm	-5.9718 mm	-5.1862 mm	-5.1961 mm	-5.0523 mm
Maximum	-0.80861 mm	-0.81634 mm	-0.34086 mm	-5.9077e-002 mm	-0.82641 mm	-0.83033 mm	-3.8878 mm	2.2256e-003 mm	-4.6778 mm	-4.6671 mm	-4.7495 mm
Minimum Occurs On	Bolt	Nut	Composite plate	Aluminium plate	Composite plate	Aluminium plate	Composite plate	Aluminium plate	Bolt	Nut	Composite plate
Maximum Occurs On	Bolt	Nut	Composite plate	Aluminium plate	Composite plate	Aluminium plate	Composite plate	Aluminium plate	Bolt	Nut	Composite plate

Moreover, Figs. 3.57, 3.58, 3.59, 3.60 and 3.61 depict Z Axis directional deformation of upper and bottom laminate plates, the bolt, the hole in upper and bottom laminate plates.
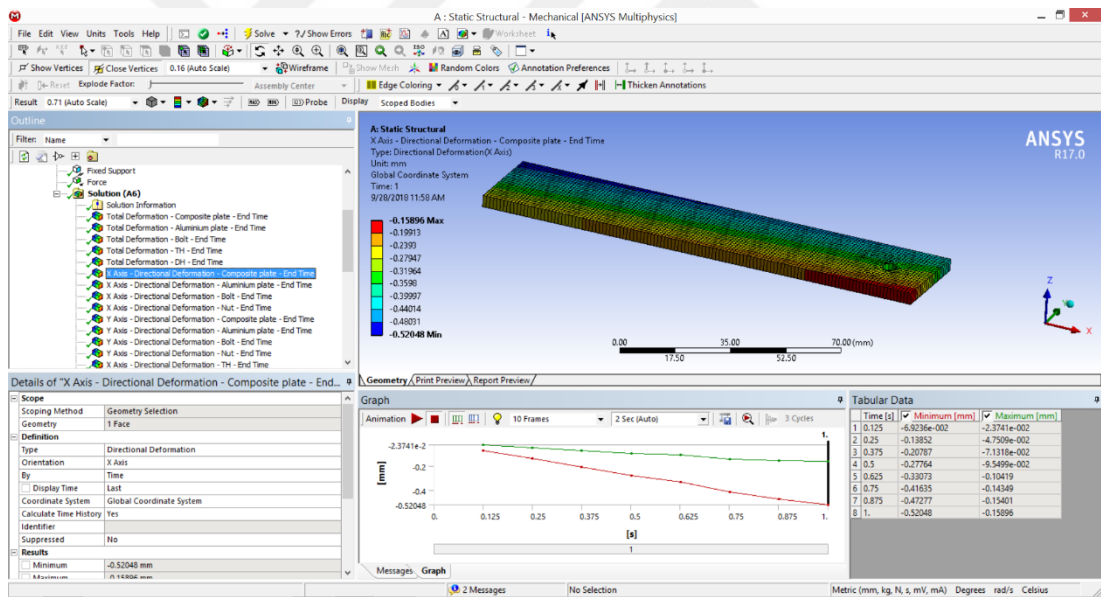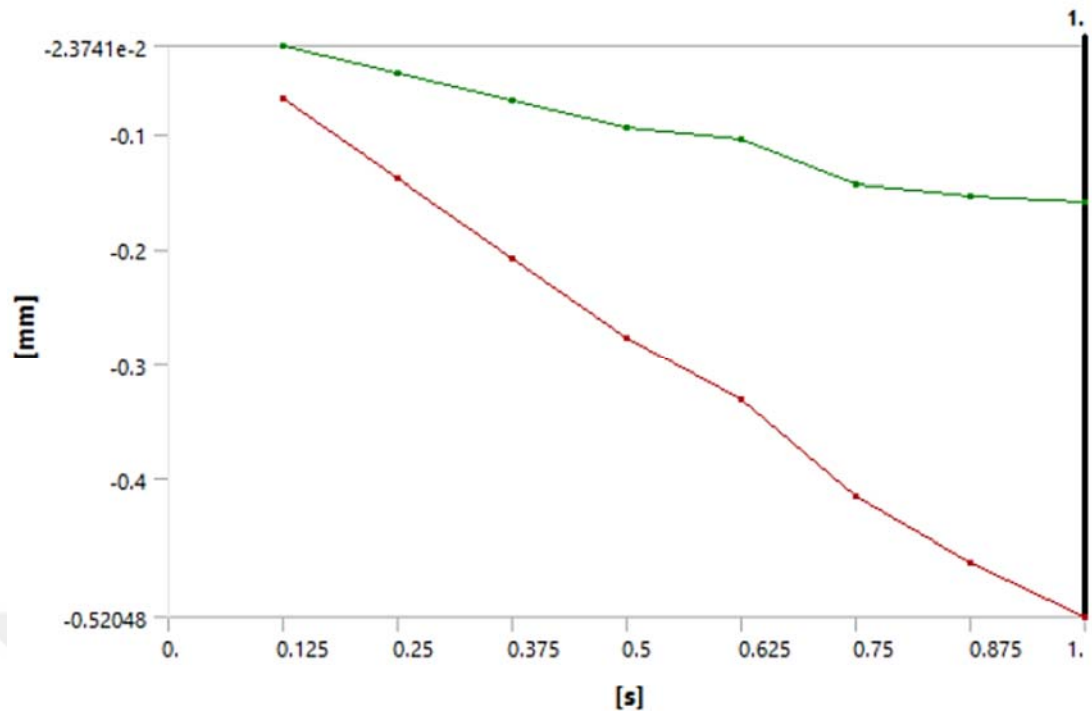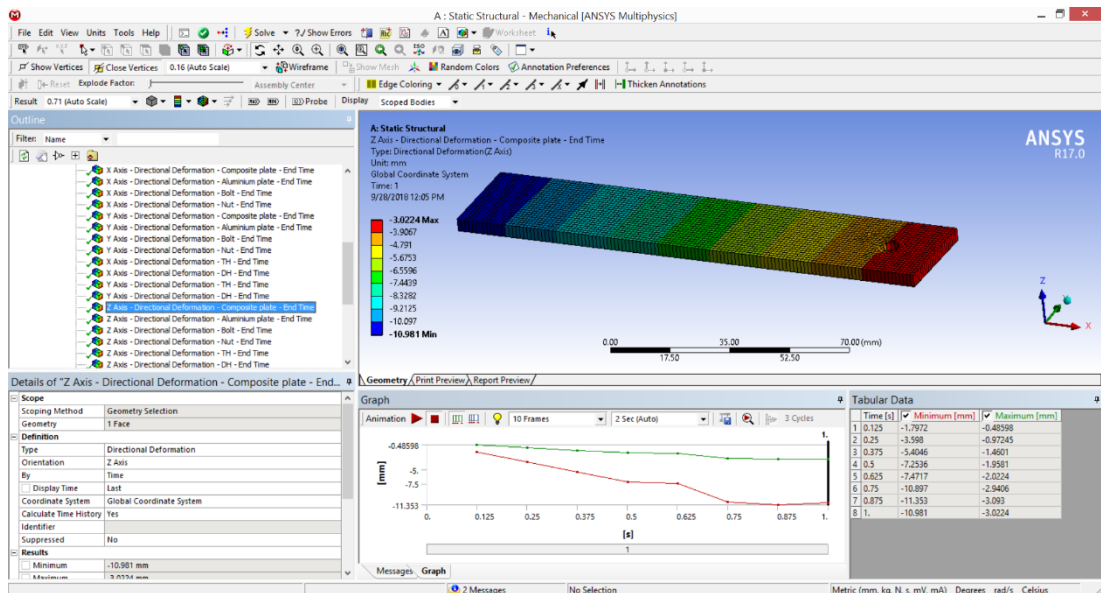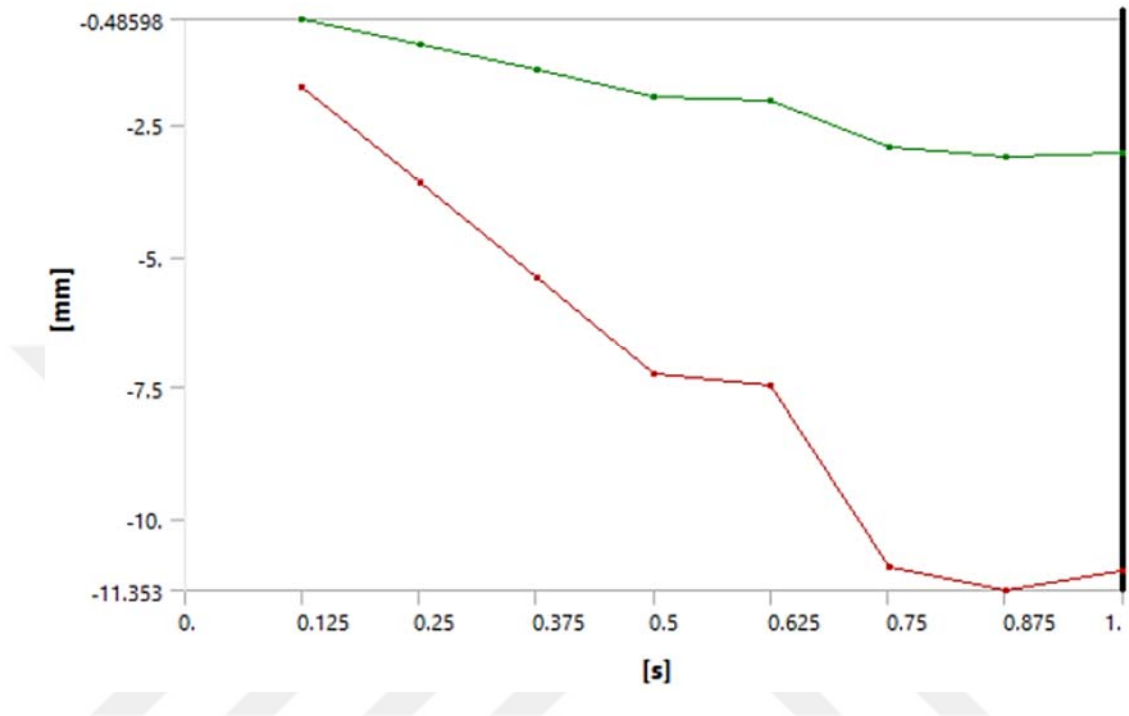

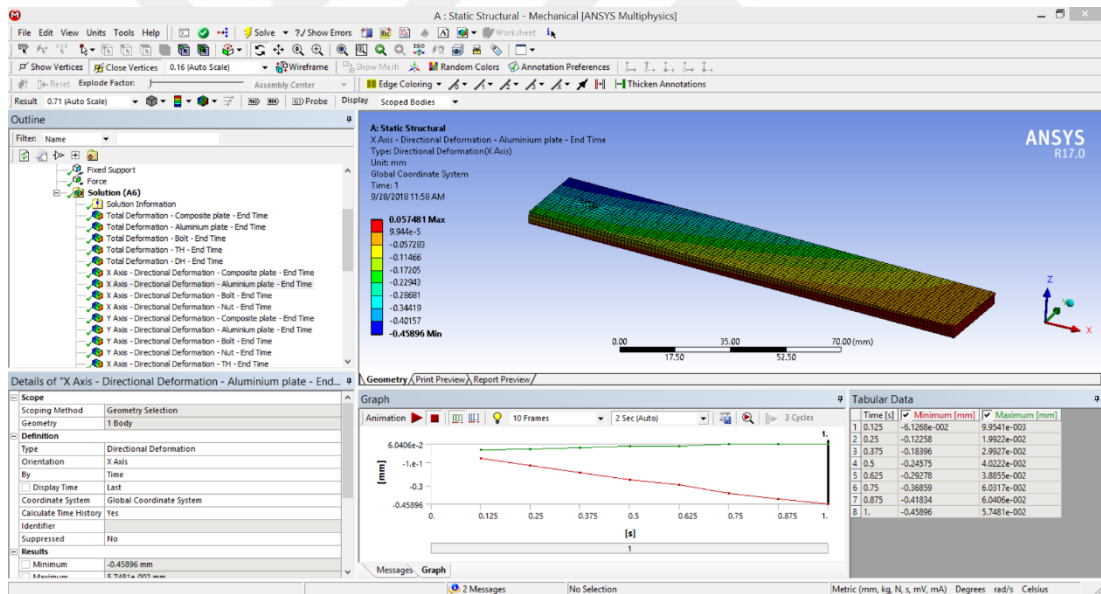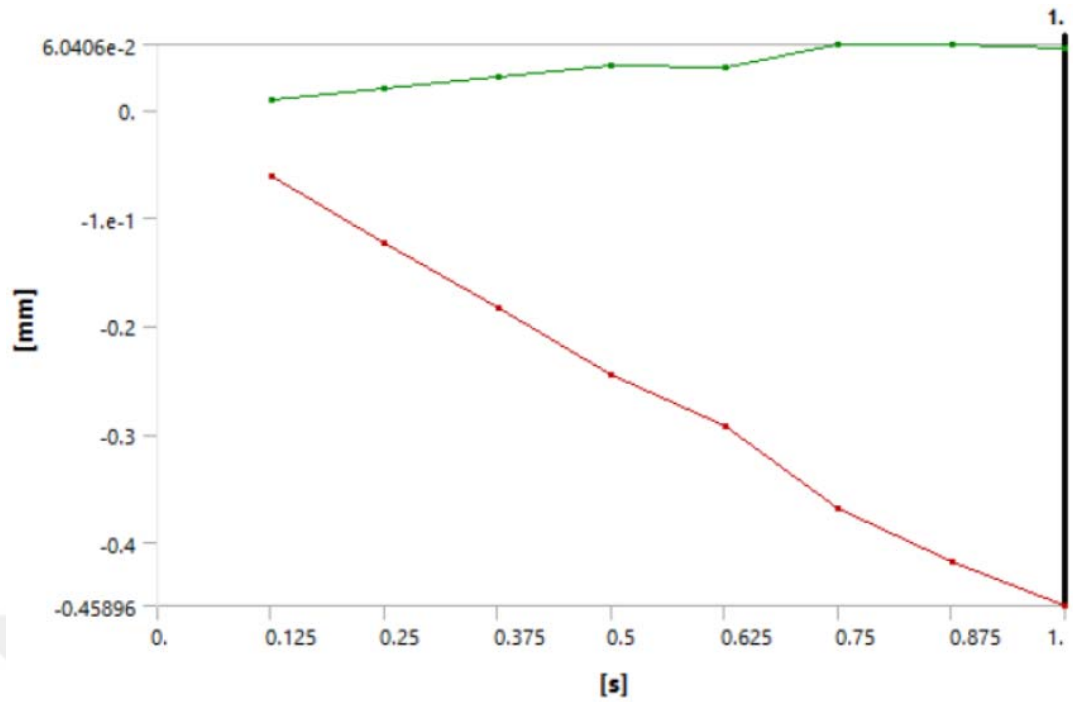**Figure 3.58:** Z Axis - Directional deformation of upper laminate plate.
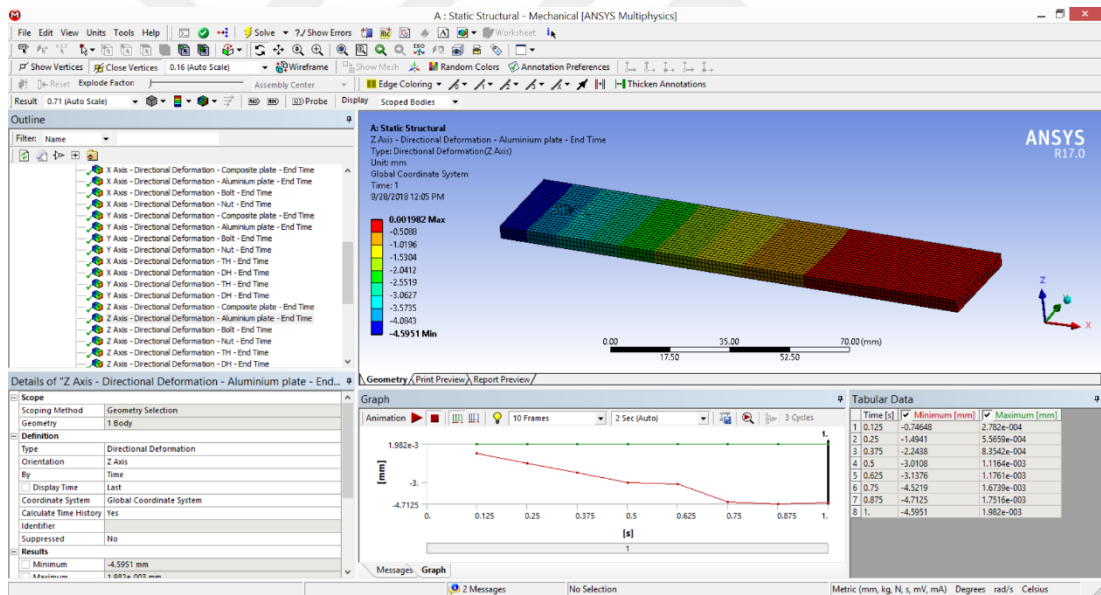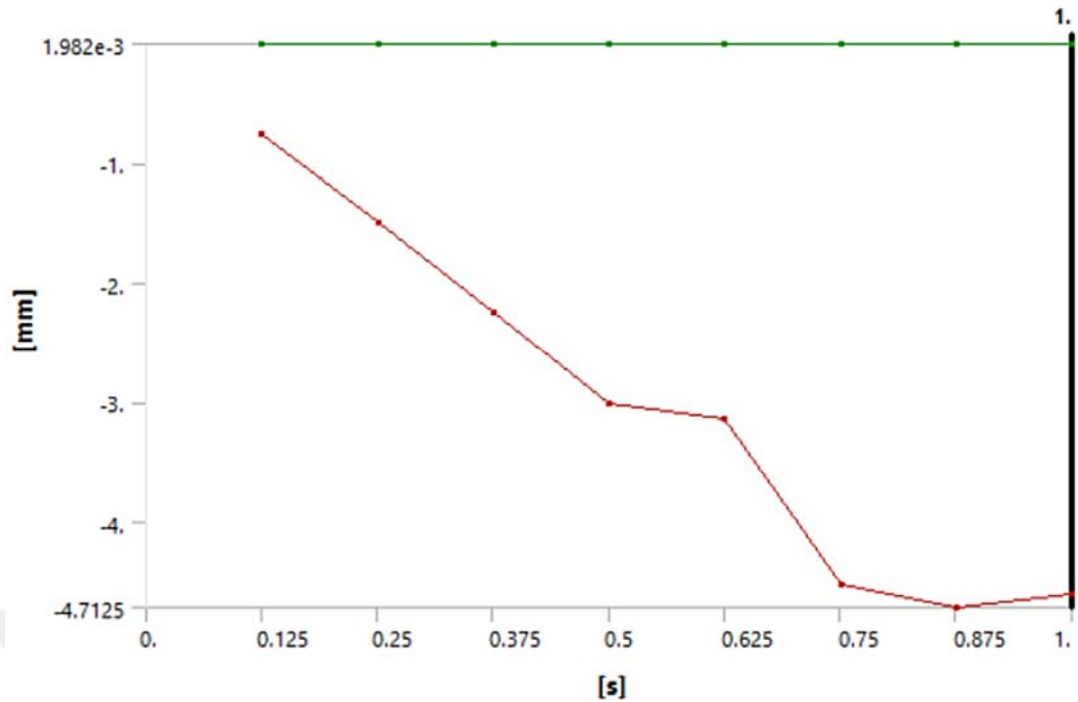
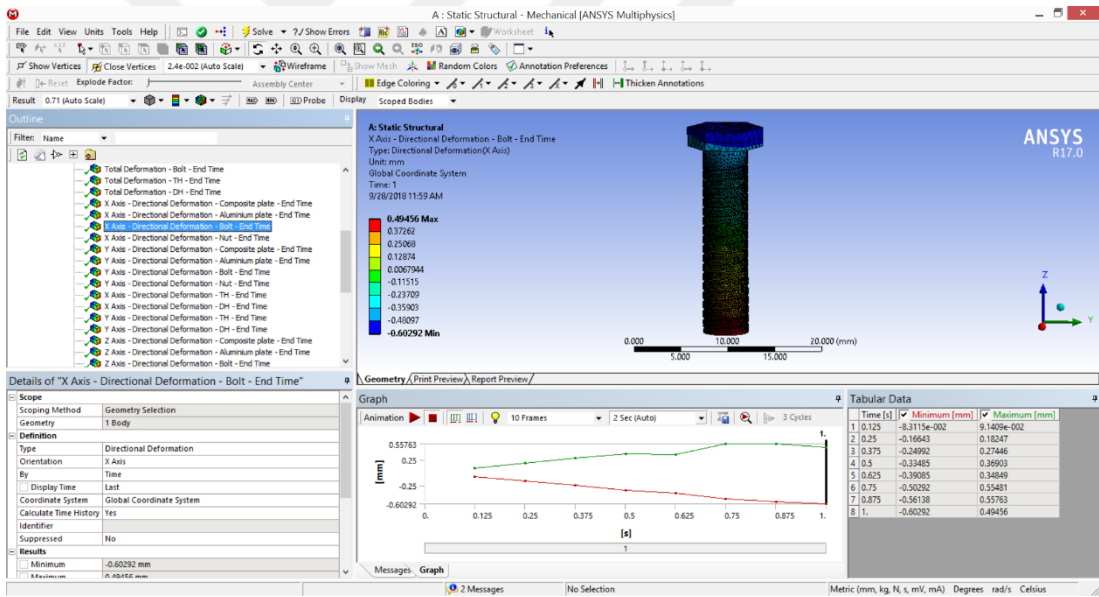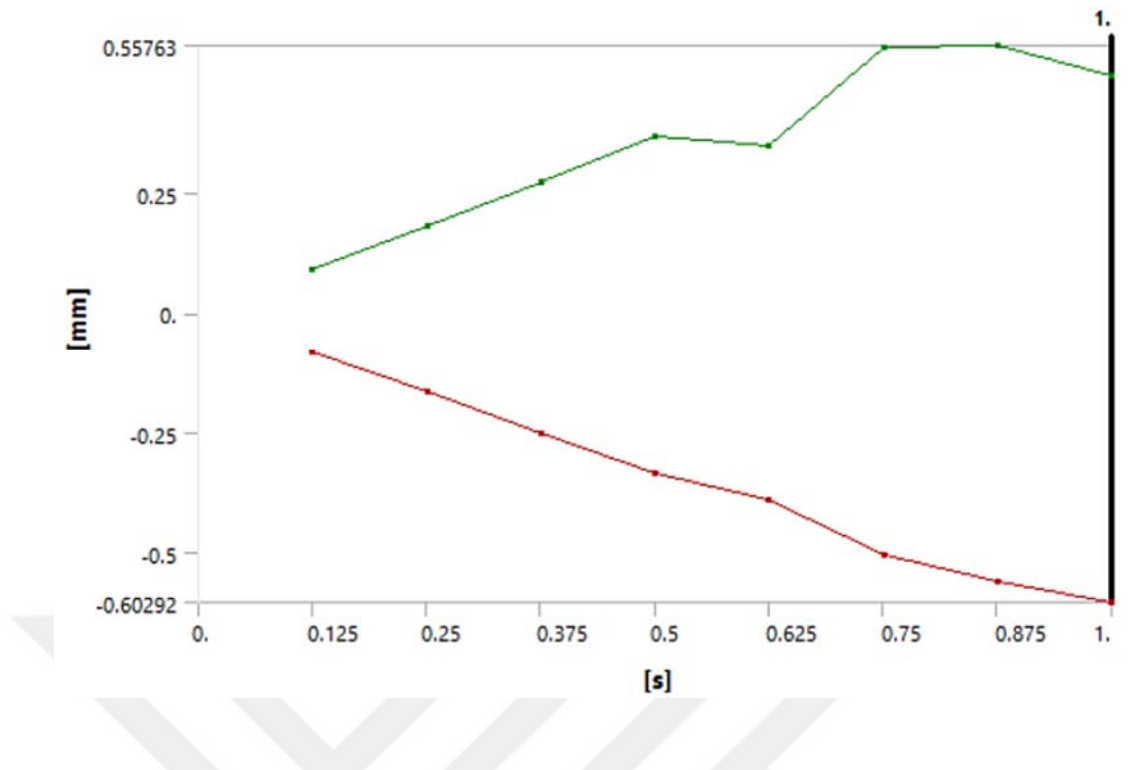**Figure 3.59:** Z Axis - Directional deformation of bottom laminate plate.

Figure 3.60: Z Axis - Directional deformation of the bolt.
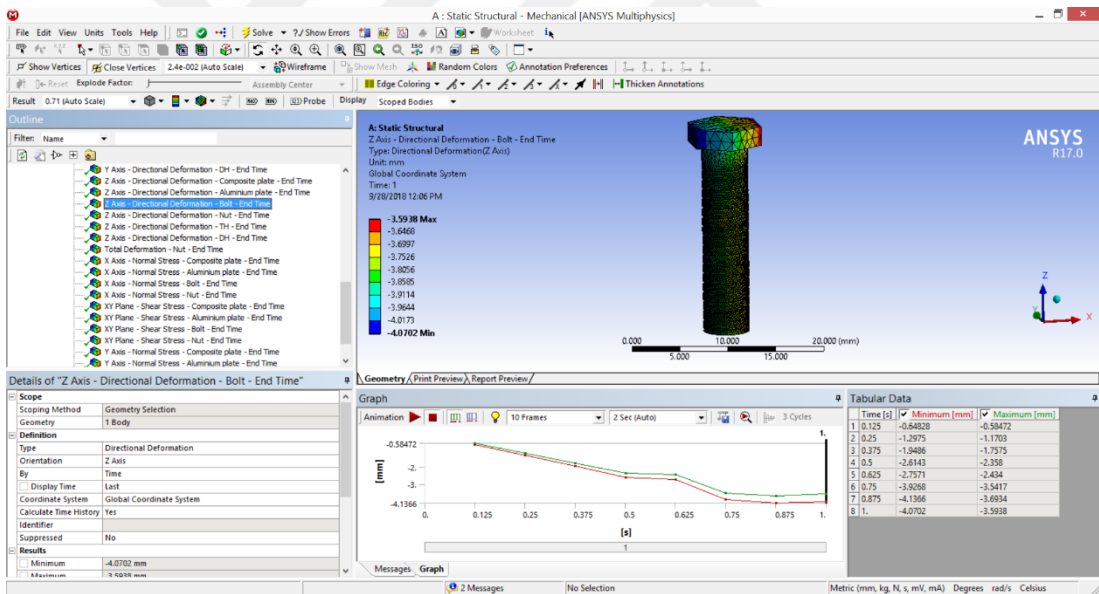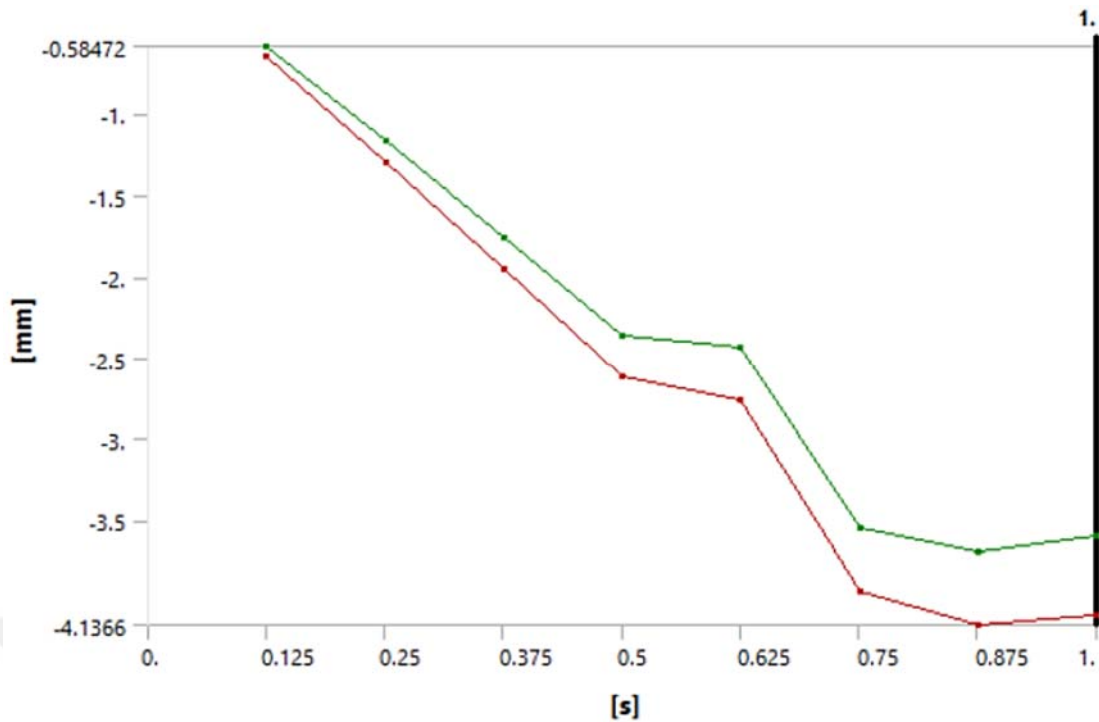
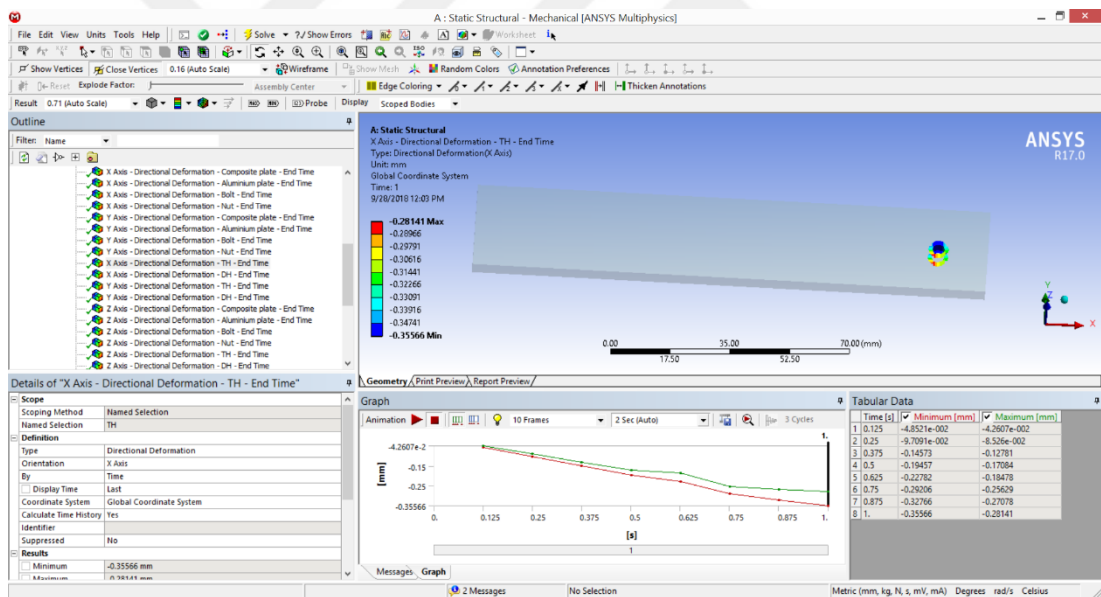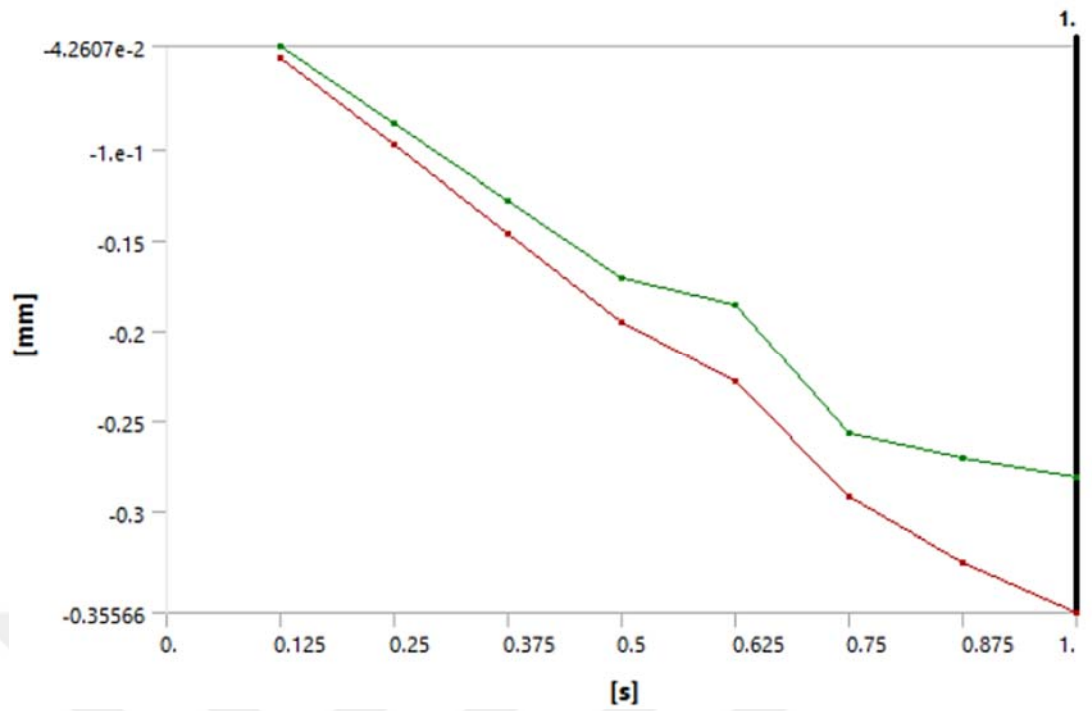**Figure 3.60:** Z Axis - Directional deformation of the bolt.
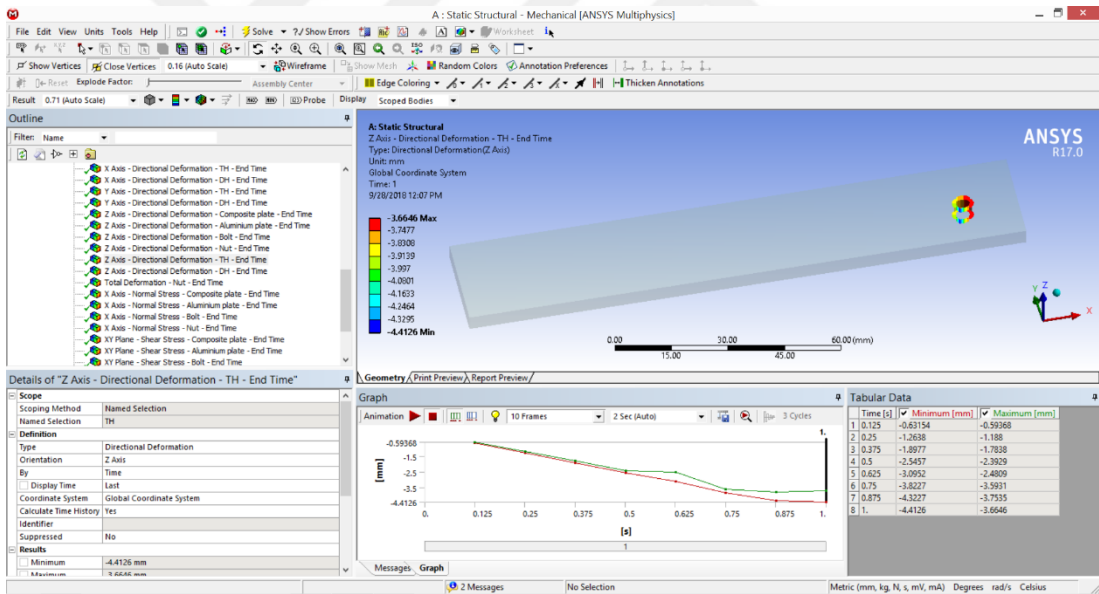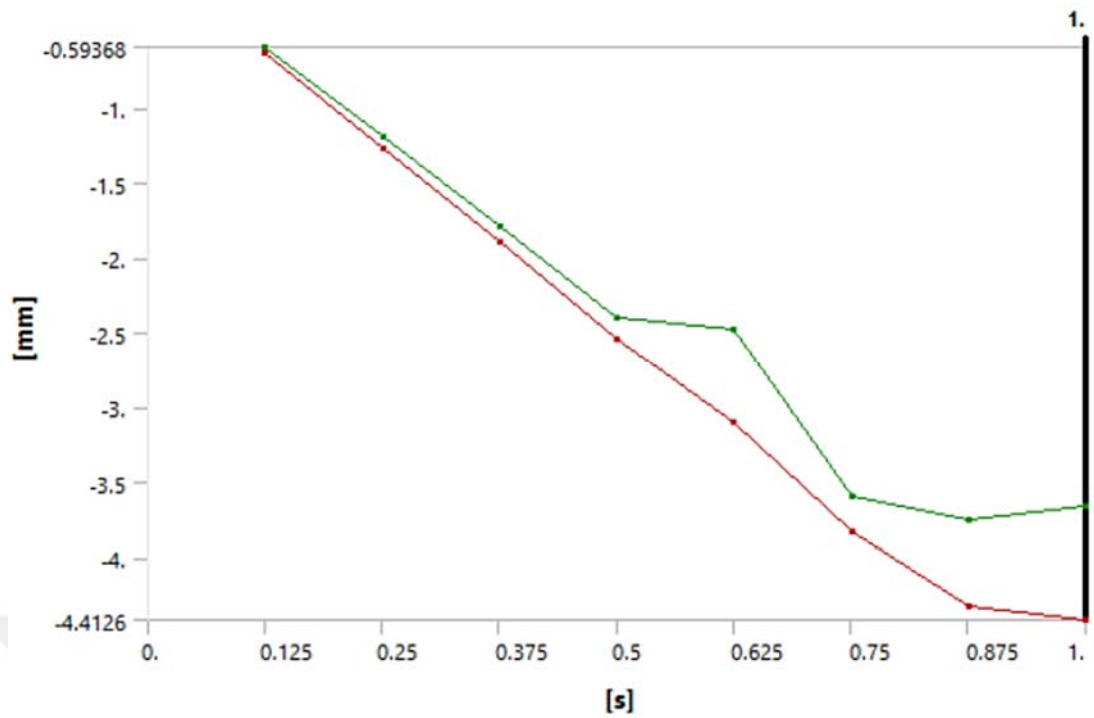
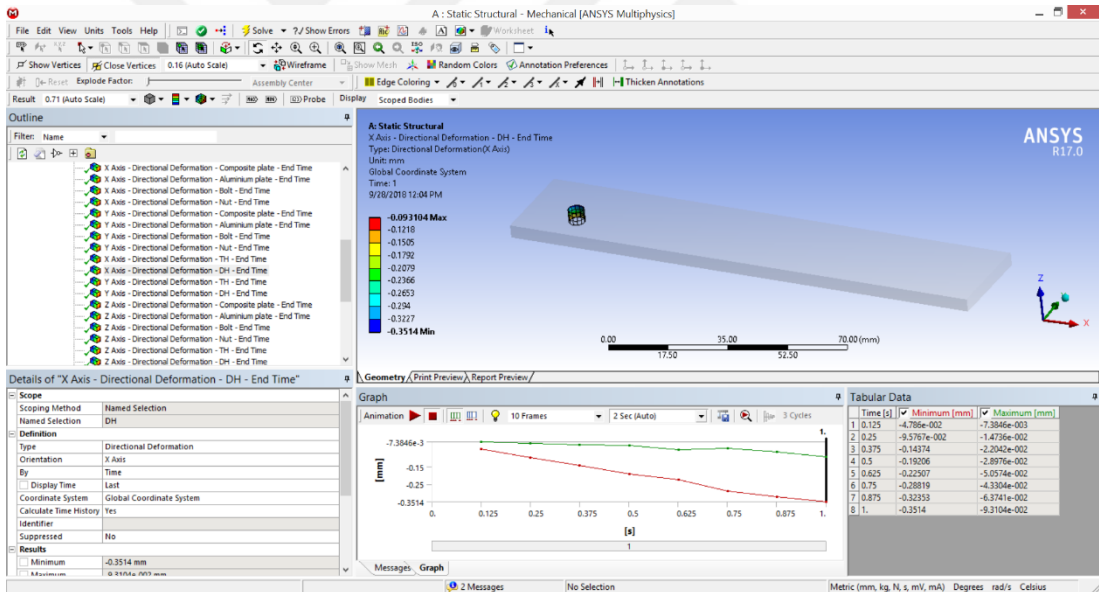**Figure 3.61:** Z Axis - Directional deformation of the hole in upper laminate plate.
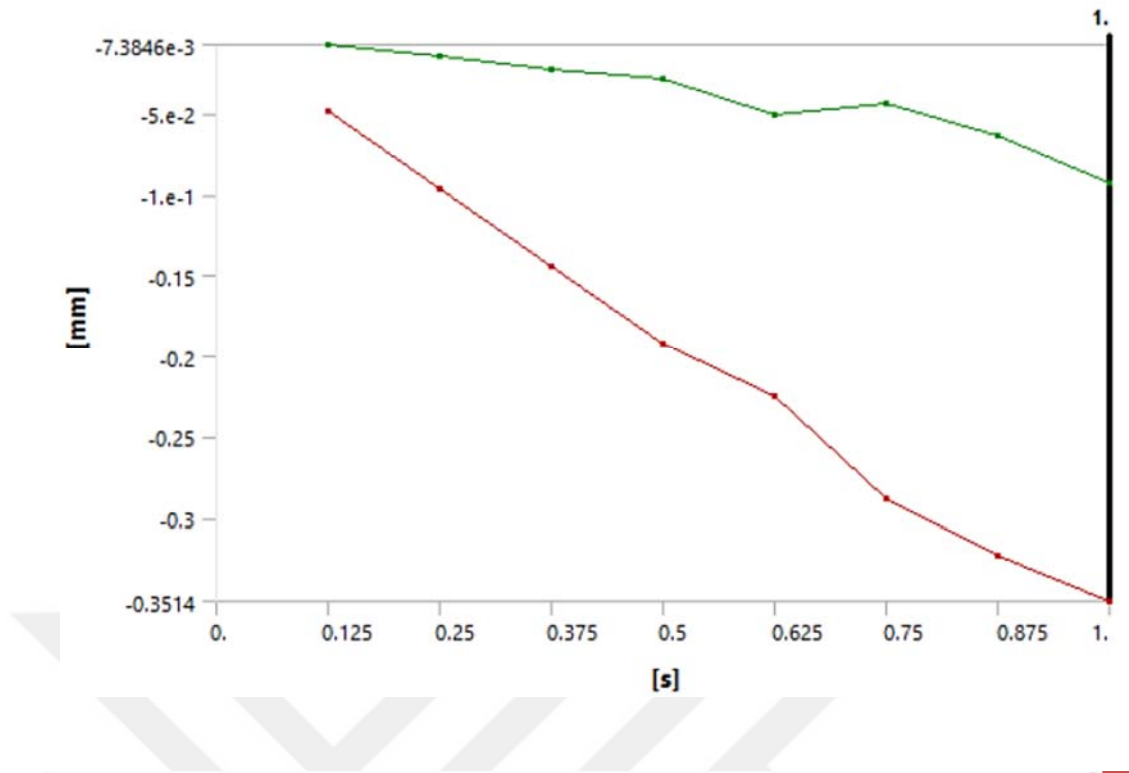
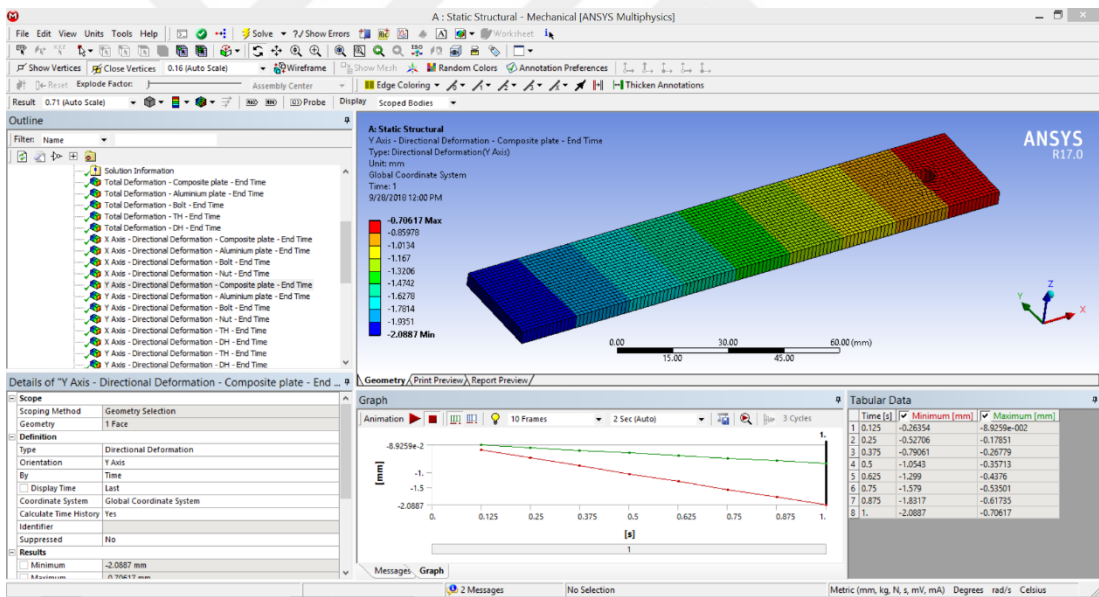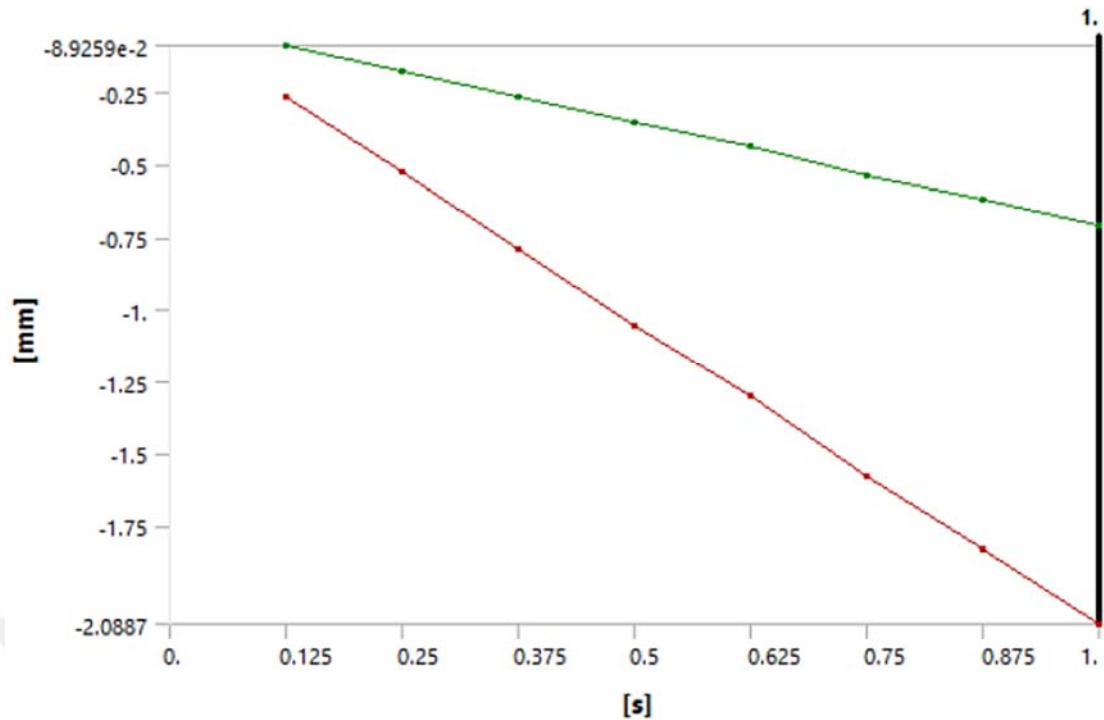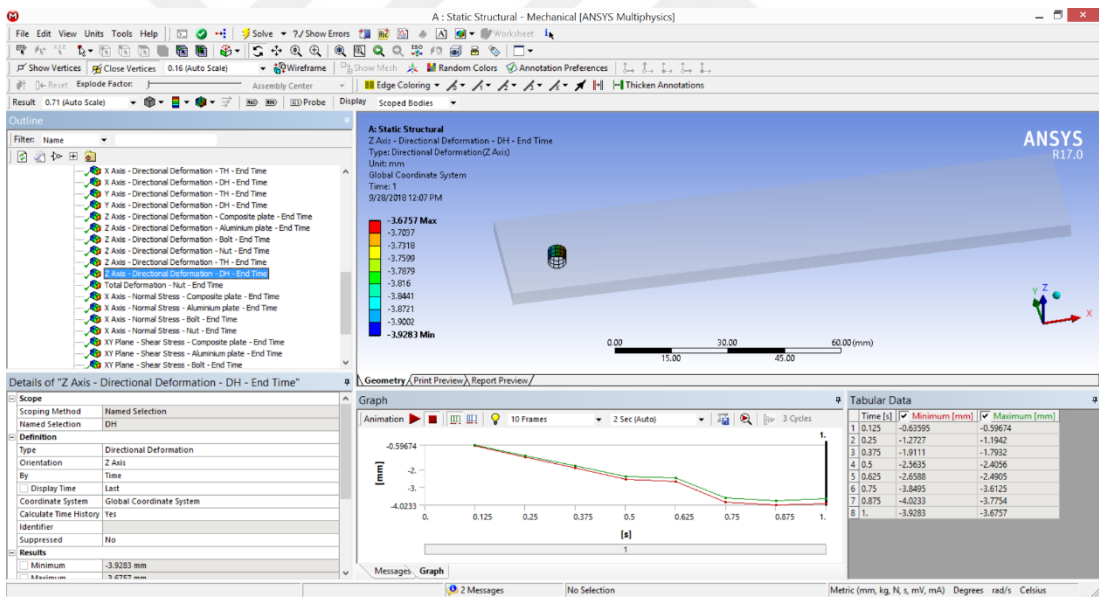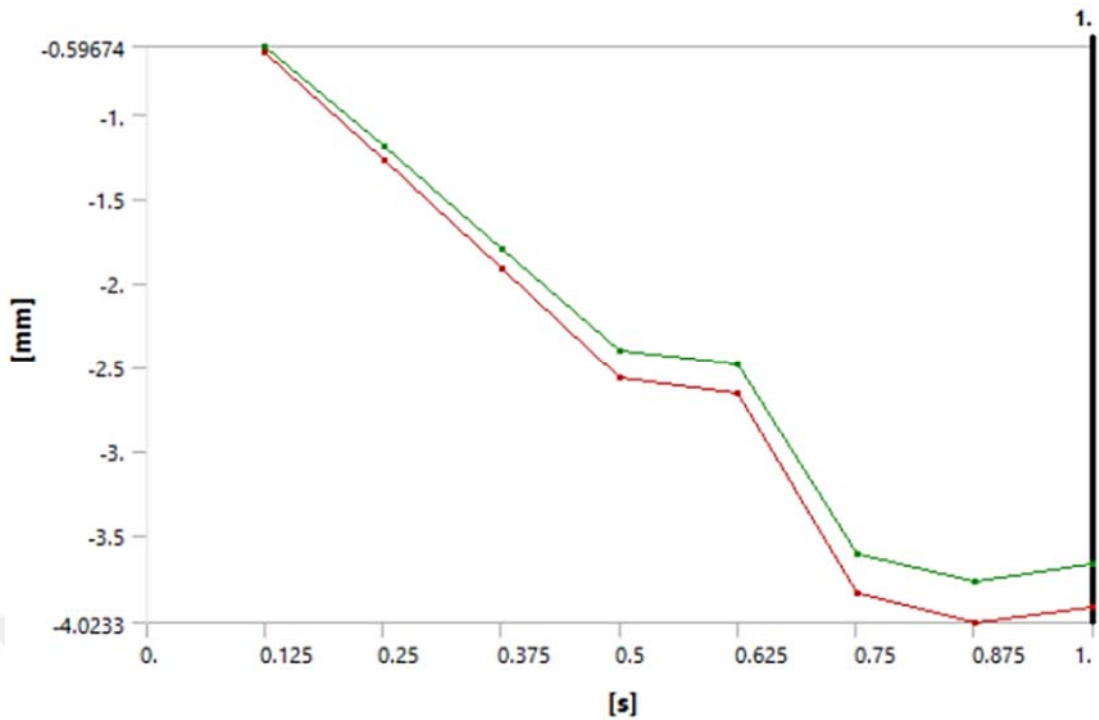**Figure 3.62:** Z Axis - Directional deformation of the hole in bottom laminate plate.

Tables 3.35, 3.36, 3.37 and 3.38 represent the shear stress based on bolt, nut, aluminum and laminate, respectively.

Table 3.35: The bolt shear stress.

Time [s]	Minimum [MPa]	Maximum [MPa]
0.125	-319.03	203.89
0.25	-1894.8	2295.5
0.375	-1912.	2302.5
0.5	-3881.	7872.6
0.625	-3604.5	8755.3
0.75	-5555.2	8823.
0.875	-3839.8	8784.9
1.	-3567.2	8797.3

Table 3.36: The nut shear stress.

Time [s]	Minimum [MPa]	Maximum [MPa]
0.125	-15.829	14.079
0.25	-1365.5	990.68
0.375	-1413.8	1009.4
0.5	-2594.8	1994.
0.625	-6719.5	4167.5
0.75	-8686.8	4620.3
0.875	-8422.4	4499.5
1.	-8432.	4969.8

Table 3.37: The aluminum plate shear stress.

Time [s]	Minimum [MPa]	Maximum [MPa]
0.125	-74.864	89.443
0.25	-151.06	179.04
0.375	-227.43	267.27
0.5	-303.09	360.48
0.625	-499.05	471.05
0.75	-454.72	537.34
0.875	-509.86	564.75
1.	-631.14	666.14

Table 3.38: The laminate plate shear stress.

Time [s]	Minimum [MPa]	Maximum [MPa]
0.125	-13.156	15.365
0.25	-26.224	30.88
0.375	-39.114	46.43
0.5	-52.045	62.226
0.625	-265.36	214.42
0.75	-77.471	93.649
0.875	-220.47	190.35
1.	-315.33	276.31

Table 3.39: The bolt normal stress along x- axis.

Time [s]	Minimum [MPa]	Maximum [MPa]
0.125	-1113.3	774.76
0.25	-3100.2	3828.3
0.375	-3576.8	3890.
0.5	-7084.2	21919
0.625	-7656.2	24189
0.75	-8352.5	24315
0.875	-7650.5	19027
1.	-7233.5	17821

Table 3.40: The nut normal stress along X- axis.

Time [s]	Minimum [MPa]	Maximum [MPa]
0.125	-37.668	61.432
0.25	-16982	14193
0.375	-18258	14495
0.5	-23521	14720
0.625	-22619	19465
0.75	-22856	22899
0.875	-22802	22695
1.	-22628	22564

Table 3.41: Aluminum plate normal stress along X- axis.

Time [s]	Minimum [MPa]	Maximum [MPa]
0.125	-265.61	259.53
0.25	-522.61	520.31
0.375	-786.45	782.34
0.5	-1092.6	1053.4
0.625	-1141.5	1858.3
0.75	-1643.2	1585.4
0.875	-1763.3	1609.6
1.	-1797.9	1484.6

Table 3.42: The laminate plate normal stress along X- axis.

Time [s]	Minimum [MPa]	Maximum [MPa]
0.125	-41.221	58.904
0.25	-83.242	118.54
0.375	-125.9	177.96
0.5	-170.03	236.57
0.625	-208.86	407.06
0.75	-258.5	367.62
0.875	-301.32	381.12
1.	-330.86	516.57

Table 3.43: The bolt normal stress along Y- axis.

Time [s]	Minimum [MPa]	Maximum [MPa]
0.125	-348.89	241.5
0.25	-2179.7	1619.2
0.375	-2195.6	1822.5
0.5	-3196.7	11056
0.625	-6167.4	12100
0.75	-3936.5	12152
0.875	-6655.8	9563.6
1.	-8105.8	11277

Table 3.44: The nut normal stress along Y- axis.

Time [s]	Minimum [MPa]	Maximum [MPa]
0.125	-52.23	75.487
0.25	-6441.7	2657.1
0.375	-6861.7	2658.4
0.5	-7166.2	4073.5
0.625	-7612.2	6239.5
0.75	-7734.4	7291.8
0.875	-7793.5	7170.7
1.	-11208	9130.3

Table 3.45: The upper laminate plate normal stress along Y- axis.

Time [s]	Minimum [MPa]	Maximum [MPa]
0.125	-97.592	76.543
0.25	-192.84	153.54
0.375	-289.63	231.03
0.5	-484.96	311.24
0.625	-666.12	461.88
0.75	-777.11	468.9
0.875	-906.09	504.13
1.	-792.22	479.42

Table 3.46: The bottom plate normal stress along Y- axis.

Time [s]	Minimum [MPa]	Maximum [MPa]
0.125	-8.4027	5.618
0.25	-16.871	11.189
0.375	-25.427	16.58
0.5	-33.7	22.899
0.625	-386.12	472.11
0.75	-52.26	34.044
0.875	-406.22	373.77
1.	-426.78	555.11

3.4 Conclusion

The researches about single-lap bolted-joints are reviewed in this chapter and three of them that they have better results in terms of deformation based on clearance and thickness are considered to be simulated in ANSYS. The proposed three ones are designed in SOLIDWORKS and then imported to ANSYS. In ANSYS software the total deformation and directional deformations of the bolt, nut and the plates based on different materials are analyzed. Moreover, the shear stress and normal stress in X and Y axes are analyzed. According to the aforementioned analyses the performance of the single-lap bolted-joint, which is constructed based on T800 carbon epoxy and Titanium 6AI-4V alloy is better than the other two ones in term of total deformation and generally in term of directional deformation, shear stress and normal stress. The other main parameter that is considered as the main factor to design the proposed single-lap bolted-joint as a better one is having a low weight.

CHAPTER 4

ANALYSIS OF A CONCEPT DESIGN OF A SINGLE COMPOSITE LAP-JOINT

4.1 Introduction

In this chapter a new design due to the pros and cons of other single composite lap-joints which are analyzed in chapter three is presented. The proposed single composite lap-joint is designed in SOLIDWORKS and then imported in ANSYS software. The obtained result corroborates the high efficient performance of the designed single composite lap-joint under 5kN pressure compare to the other ones, which are presented in chapter 3.

4.2 Concept Design

Based on the structure of the single composite lap-joint, two aluminum plates are set in top and bottom of the designed single composite lap-joint. Figures 4.1 and 4.2 illustrate the proposed single composite lap-joint, which is designed for this project. Moreover, Figure 3 depicts the single-lap, single bolt joint and its geometric dimensions.
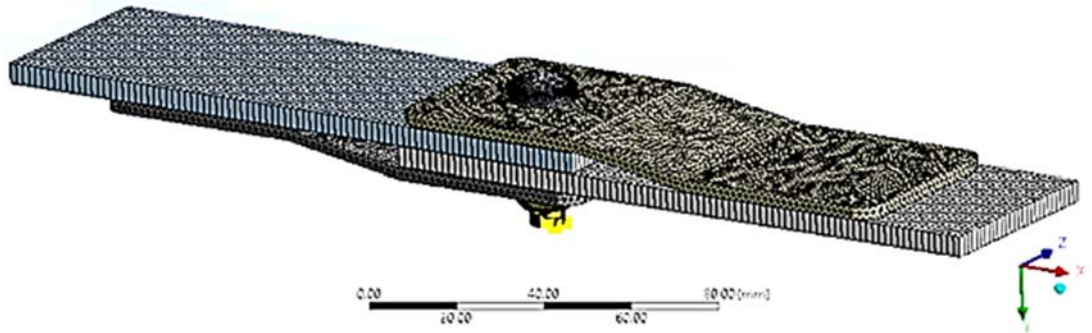
Figure 4.1: The designed single composite lap-joint.

$U_y = U_z = 0$
$U_x =$ Prescribed

$U_x = U_y = U_z = 0$
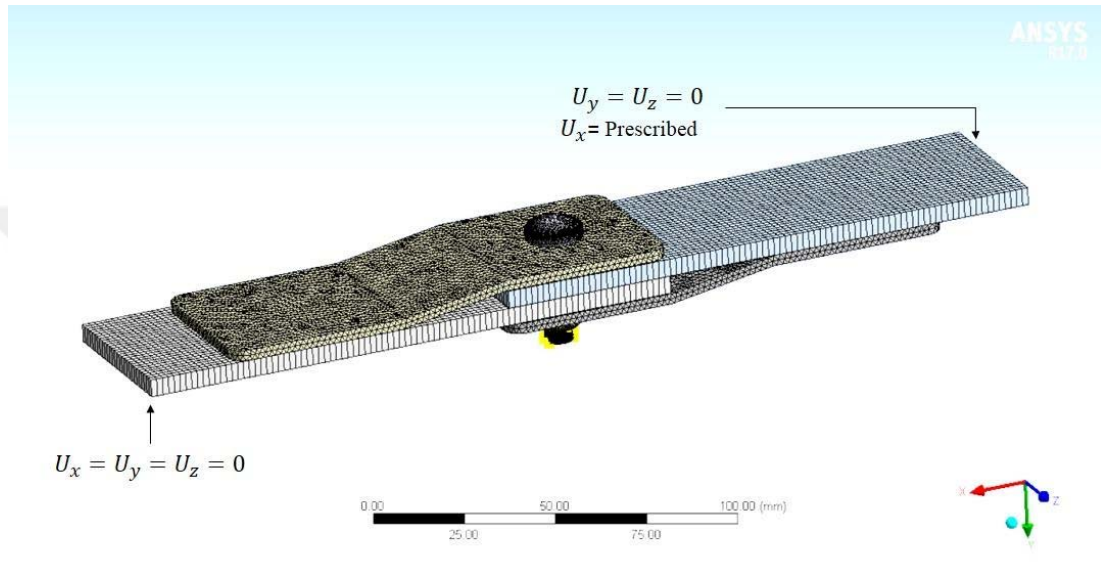
Figure 4.2: Boundary condition for our design

Upper laminate plate

Bolt

Upper Aluminum plate

Bottom Aluminum plate

Nut

Bottom laminate plate
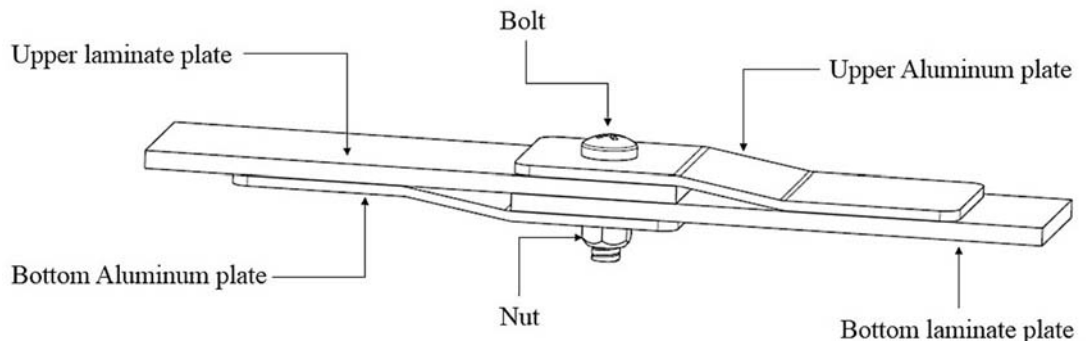
Figure 4.3: The different parts of designed single composite lap-joint.
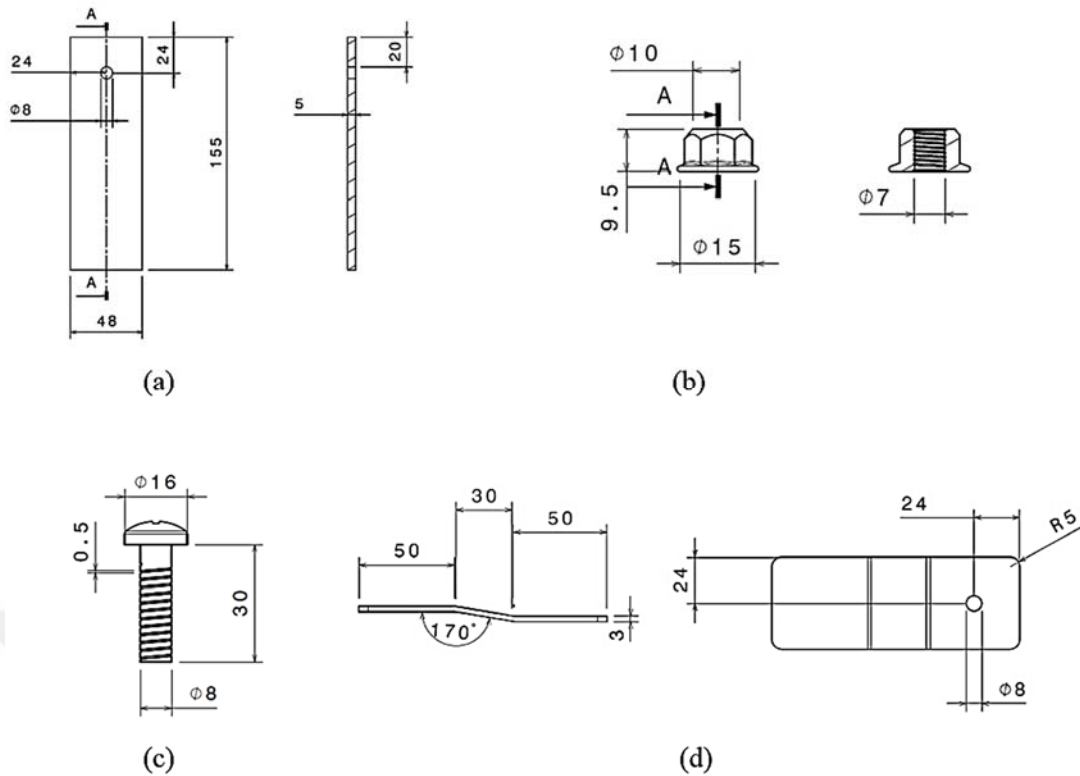
Figure 4.4: The sizes of different parts of the designed single composite lap-joint.

Table 4.1 represents the characteristics of the designed single-lap, single-bolt joint, which is obtained based on ANSYS software. The laminates were made of T800 carbon-epoxy composites with lay-ups of $[45/0/-45/0/90/0/45/0/-45/0]_{s2}$. The thickness of each lamina was 0.125 mm, yielding a total laminate thickness of 5 mm. Furthermore, the bolt and nut material are considered as Titanium 6AI-4V. Tables 4.2 and 4.3 illustrate the minimum and maximum total and directional deformation values. In order to ensure hexahedral meshes on the outer layer of the bolt shank, the bolt has been subdivided into an internal cube and surrounding part. Moreover, the meshes far from the hole boundary is not as refined as those near the hole, which improve the computational efficiency. The free face mesh type in Ansys software is considered as Quad/Tri. The boundary condition of our design for the simulation is like the first case study which is presented in chapter 3. The down and upside laminate plates was modeled with 2515 elements and the aluminum plates with 30710 elements. Moreover, the bolt and nut are modeled with 83010 and 117680 elements.

Table 4.1: The characteristics of the designed single-lap, single-bolt joint.

Assignment	T800 Carbon Epoxy	Aluminum Alloy			Titanium 6Al-4V		
Nonlinear Effects			Yes				
Thermal Strain Effects			Yes				
Bounding Box							
Length X	155. mm	130. mm	155. mm	8. mm	17.9 mm	22.146 mm	1.604 mm
Length Y	0. mm	8.2 mm	0. mm		9.4 mm	35.946 mm	0.13704 mm
Length Z		48. mm		8. mm	17.9 mm	22.146 mm	1.2315 mm
Properties							
Volume	36949 mm³	18254 mm³	0. mm³		1123.7 mm³	2364.5 mm³	0. mm³
Mass	5.5054e-002 kg	5.0564e-002 kg			1.7979e-003 kg	3.7832e-003 kg	
Centroid X	65.739 mm	-41.981 mm	53.229 mm	-29.471 mm	11.879 mm		14.722 mm
Centroid Y	-2.9338 mm	-6.9714 mm	1.1039 mm		9.3105 mm	-2.6078 mm	16.737 mm
Centroid Z		155. mm			155. mm		152.23 mm
Moment of Inertia Ip1	10.641 kg·mm²	71.84 kg·mm²			4.3148e-002 kg·mm²	6.036e-002 kg·mm²	
Moment of Inertia Ip2	109.9 kg·mm²	81.486 kg·mm²			4.3147e-002 kg·mm²	0.47055 kg·mm²	
Moment of Inertia Ip3	120.54 kg·mm²	9.8007 kg·mm²			5.9112e-002 kg·mm²	0.4705 kg·mm²	
Surface Area(approx.)	7389.7 mm²						1.7472e-003 mm²

Table 4.2: The minimum and maximum total and directional deformation values.

Object Name	Total Deformation - Bolt - End Time	Total Deformation - Nut - End Time	Total Deformation - UP - End Time	Total Deformation - DP - End Time	Total Deformation - DLP - End Time	Total Deformation - ULP - End Time	X Axis - Directional Deformation - Bolt - End Time	X Axis - Directional Deformation - Nut - End Time	X Axis - Directional Deformation - DP - End Time	X Axis - Directional Deformation - UP - End Time	X Axis - Directional Deformation - DLP - End Time
Minimum	3.5024 mm	3.4121 mm	0. mm	2.3687 mm	2.8564e-003 mm	2.2516 mm	-0.70084 mm	0.31232 mm	-0.18624 mm	-0.56466 mm	-0.17078 mm
Maximum	4.3357 mm	4.3163 mm	5.4075 mm	9.3638 mm	5.5279 mm	10.583 mm	1.0117 mm	0.92322 mm	0.47202 mm	0.1232 mm	0.118 mm
Minimum Occurs On	Bolt	Nut	UP	DP	DLP	ULP	Bolt	Nut	DP	UP	DLP
Maximum Occurs On	Bolt	Nut	UP	DP	DLP	ULP	Bolt	Nut	DP	UP	DLP
Minimum Value Over Time											
Minimum	0.44028 mm	0.42958 mm	0. mm	0.29304 mm	3.5086e-004 mm	0.28005 mm	-0.70084 mm	4.1659e-002 mm	-0.18624 mm	-0.56466 mm	-0.17078 mm
Maximum	3.5024 mm	3.4121 mm	0. mm	2.3687 mm	2.8564e-003 mm	2.2516 mm	-8.9474e-002 mm	0.31232 mm	-2.3215e-002 mm	-7.0286e-002 mm	-2.1739e-002 mm
Maximum Value Over Time											
Minimum	0.54959 mm	0.5464 mm	0.69161 mm	1.2127 mm	0.6933 mm	1.3776 mm	0.13208 mm	0.10777 mm	6.3353e-002 mm	1.539e-002 mm	1.4736e-002 mm
Maximum	4.3357 mm	4.3163 mm	5.4075 mm	9.3638 mm	5.5279 mm	10.583 mm	1.0117 mm	0.92322 mm	0.47202 mm	0.1232 mm	0.118 mm

Table 4.3: The minimum and maximum total and directional deformation values.

Object Name	Z Axis - Directional Deformation - DLP - End Time	Z Axis - Directional Deformation - ULP - End Time	Total Deformation - DH - End Time	Total Deformation - UH - End Time
Minimum	-0.61599 mm	-1.1728 mm	3.6702 mm	3.67 mm
Maximum	7.6656e-002 mm	-0.36497 mm	4.1317 mm	4.1299 mm
Minimum Occurs On	DLP	ULP	DLP	ULP
Maximum Occurs On	DLP	ULP	DLP	ULP
Minimum Value Over Time				
Minimum	-0.61599 mm	-1.1728 mm	0.45927 mm	0.45928 mm
Maximum	-7.7816e-002 mm	-0.14956 mm	3.6702 mm	3.67 mm
Maximum Value Over Time				
Minimum	9.5587e-003 mm	-0.36497 mm	0.51411 mm	0.51407 mm
Maximum	7.6656e-002 mm	-4.595e-002 mm	4.1317 mm	4.1299 mm

In all results in this chapter the forces are implemented on the system from zero to 5 KN for a one second period. Figures 4.4-4.11 depict the total deformation of the bolt, nut, upper and bottom Aluminum plates, upper and bottom laminate plates, respectively.
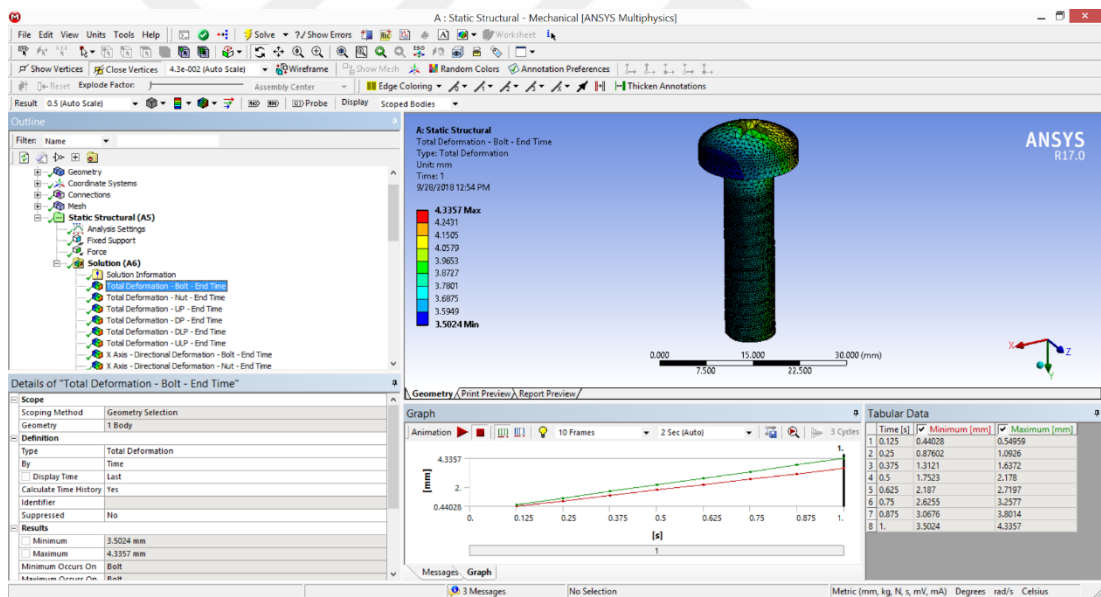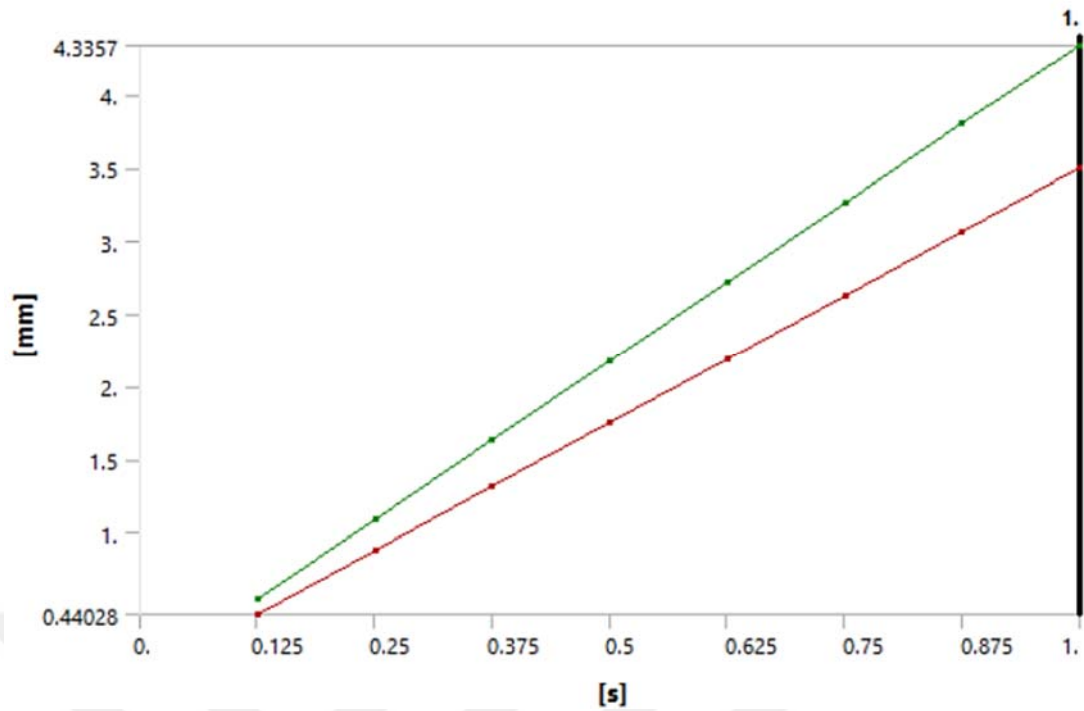
Figure 4.5: Total deformation of the bolt.

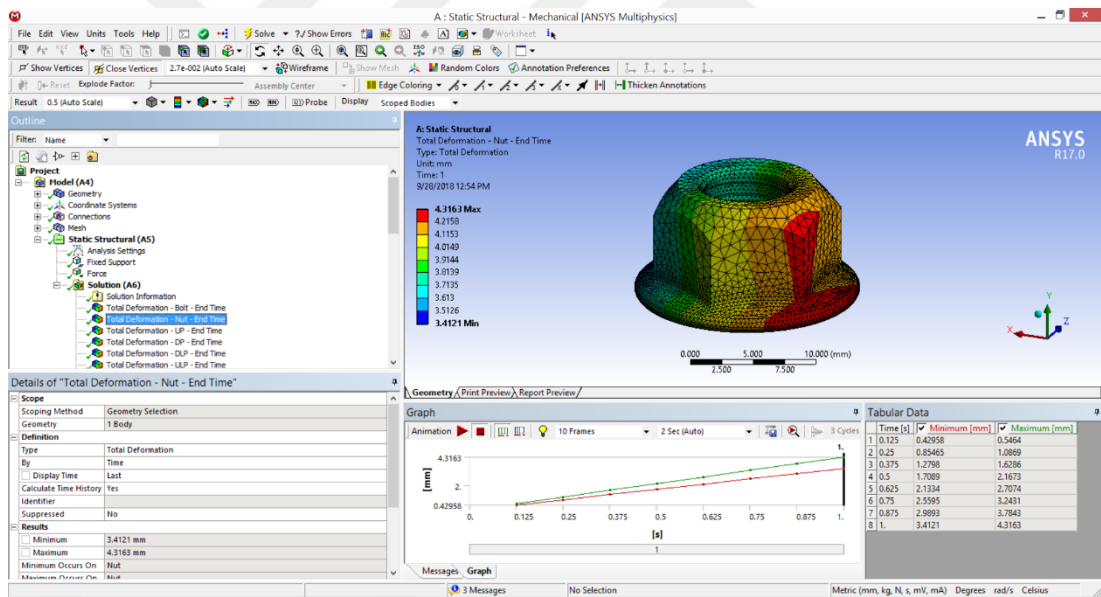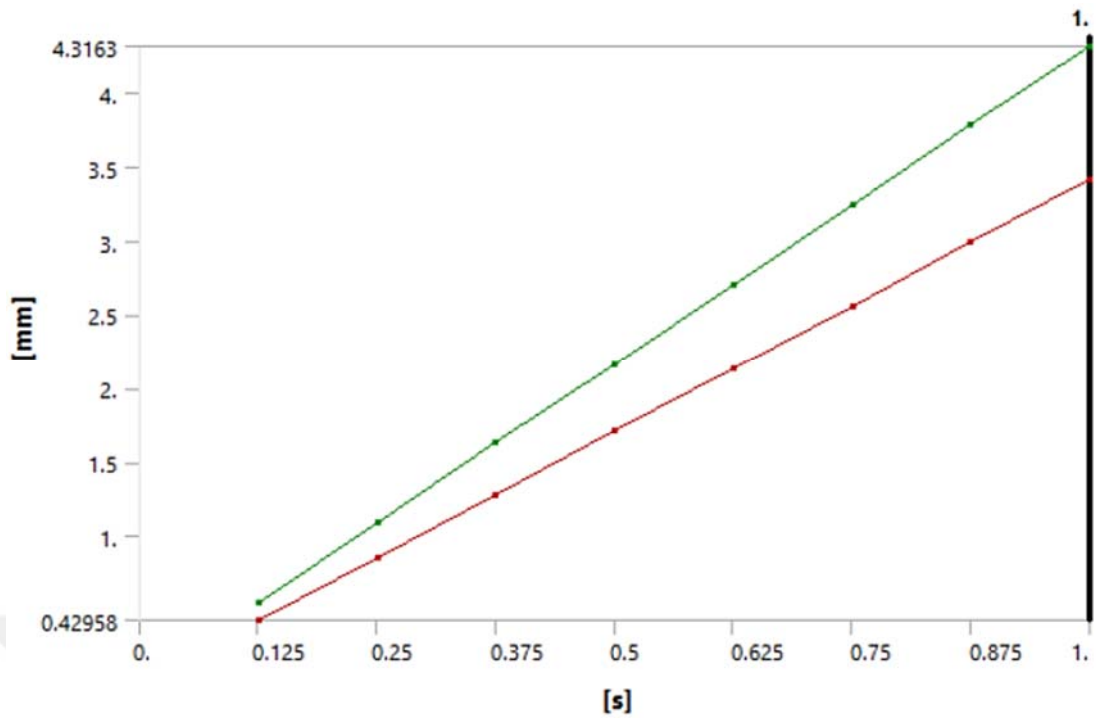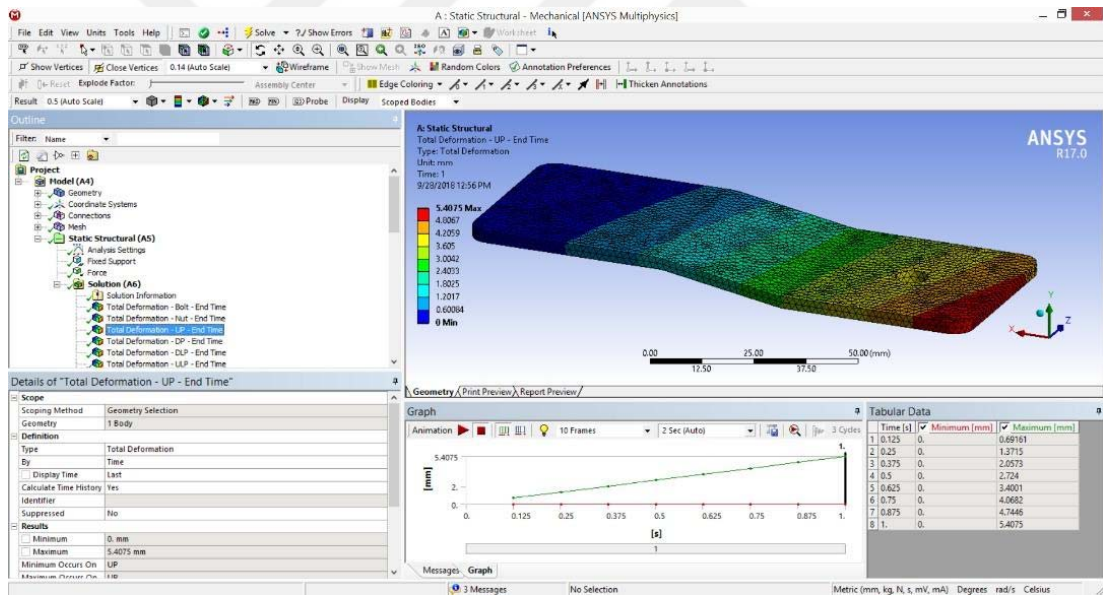**Figure 4.6:** Total deformation of the nut.

Figure 4.7: Total deformation of the hole in upper Aluminum plate.
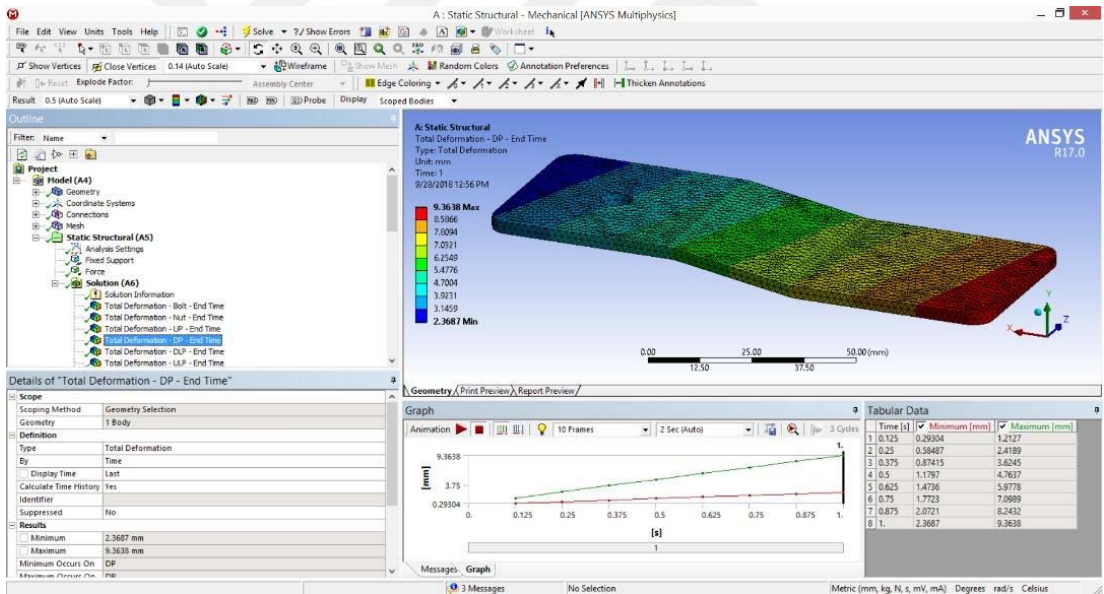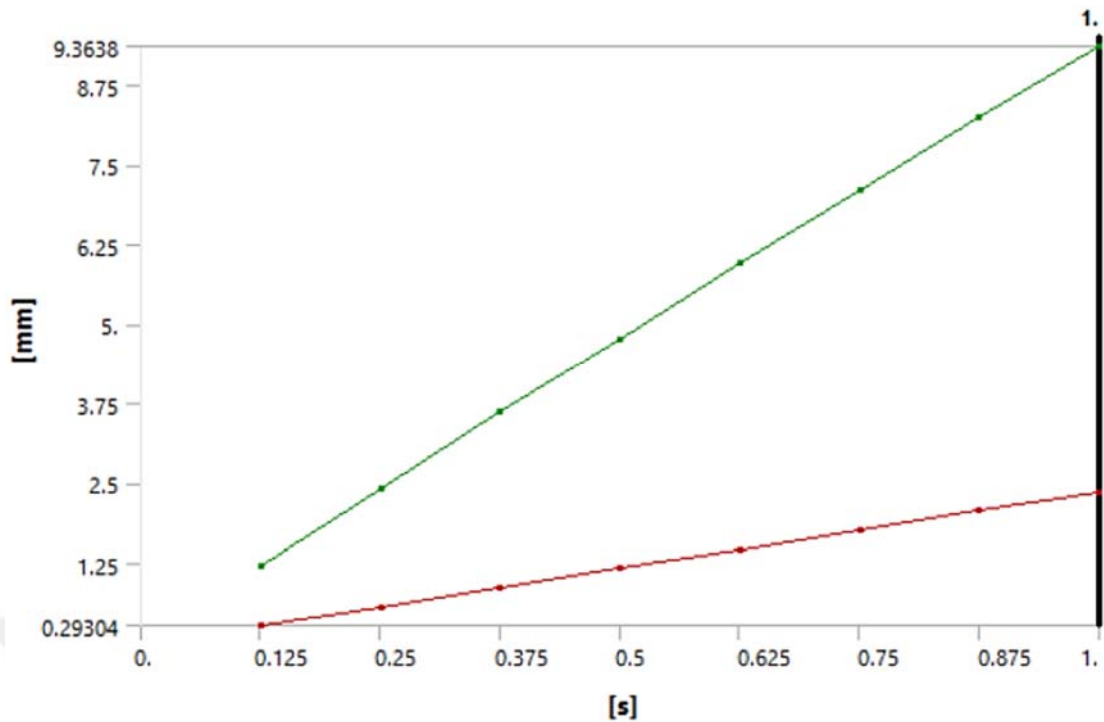
Figure 4.8: Total deformation of the hole in bottom Aluminum plate.
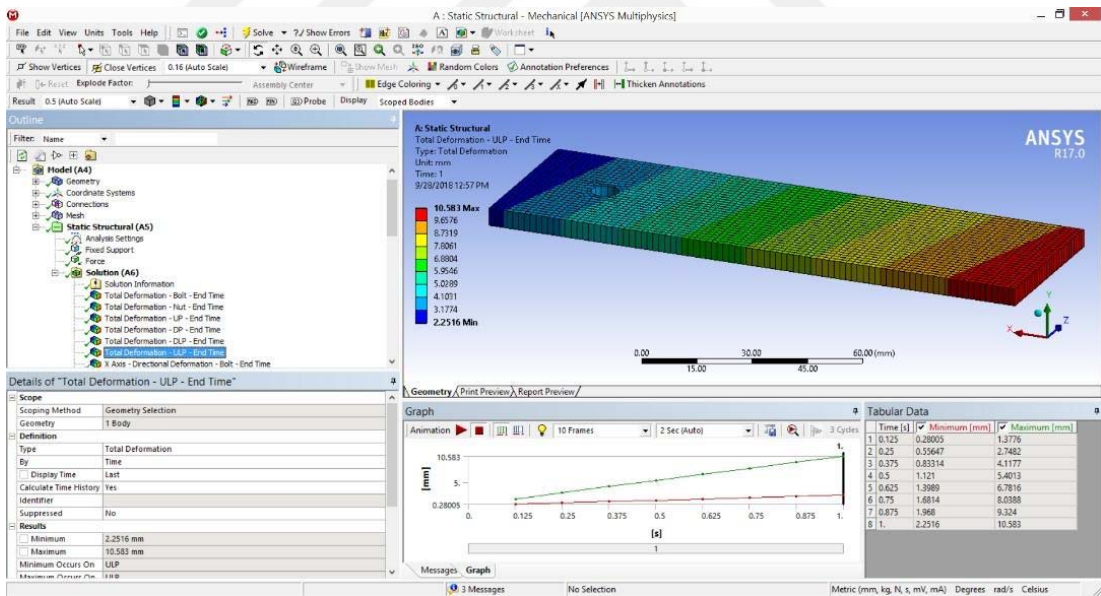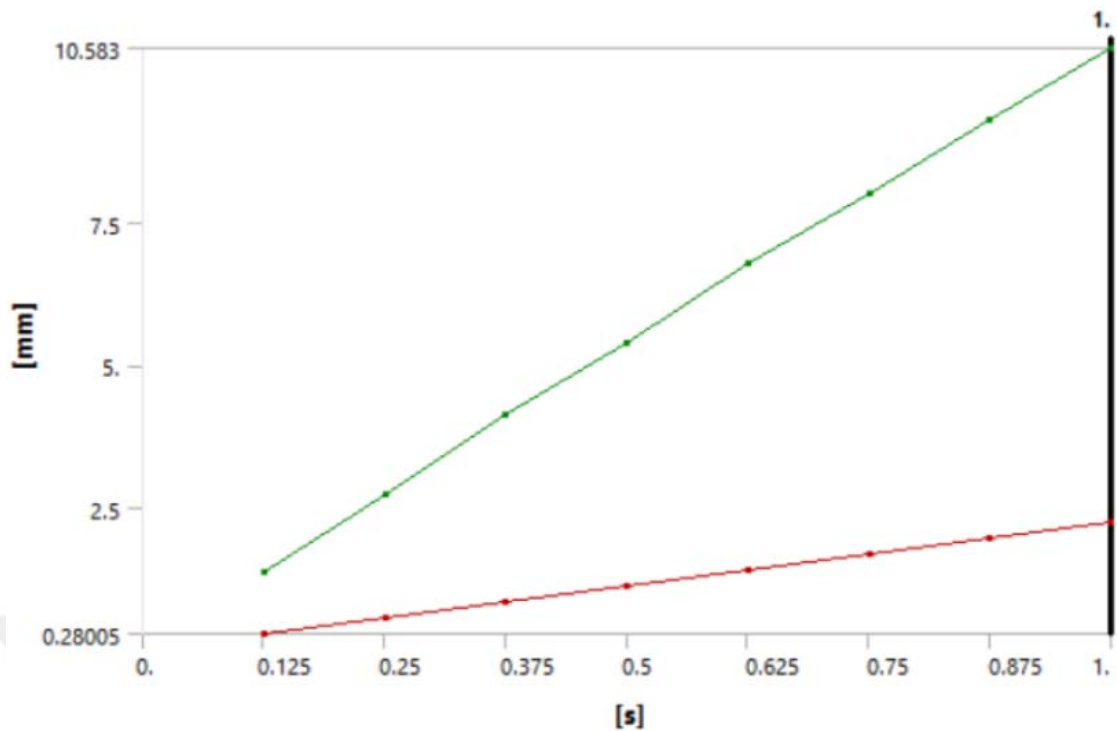
Figure 4.9: Total deformation of the upper laminate plate.
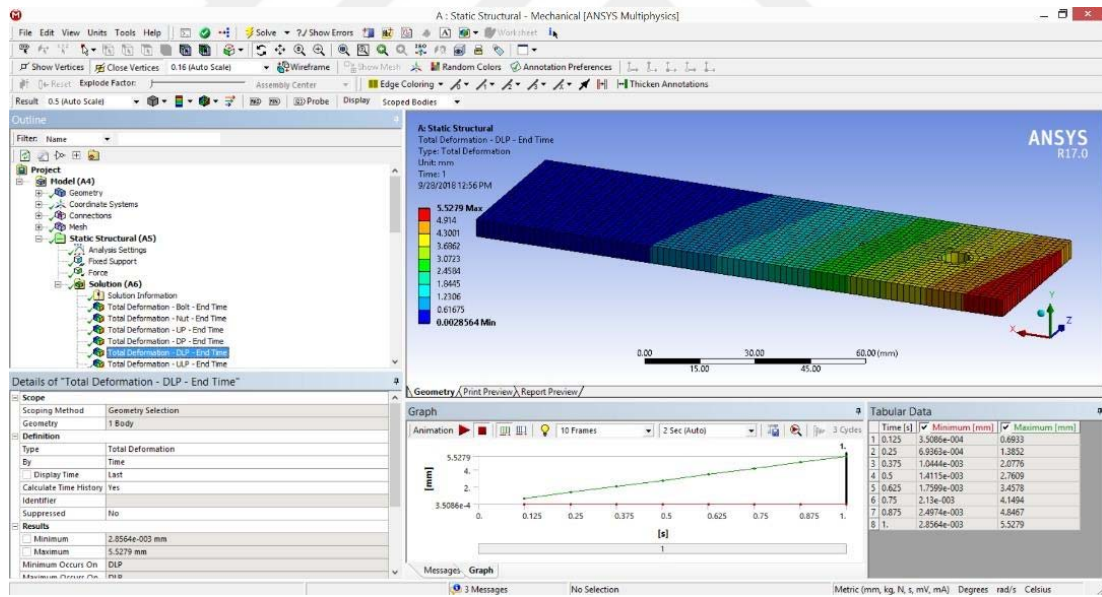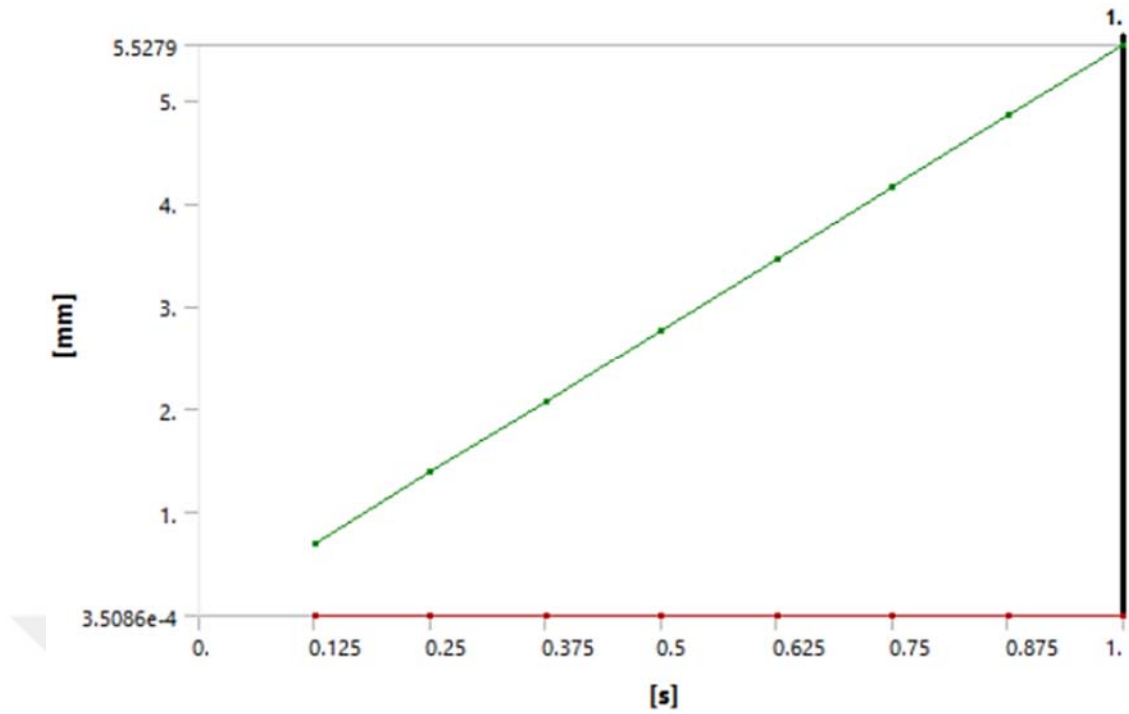
Figure 4.10: Total deformation of the bottom laminate plate.
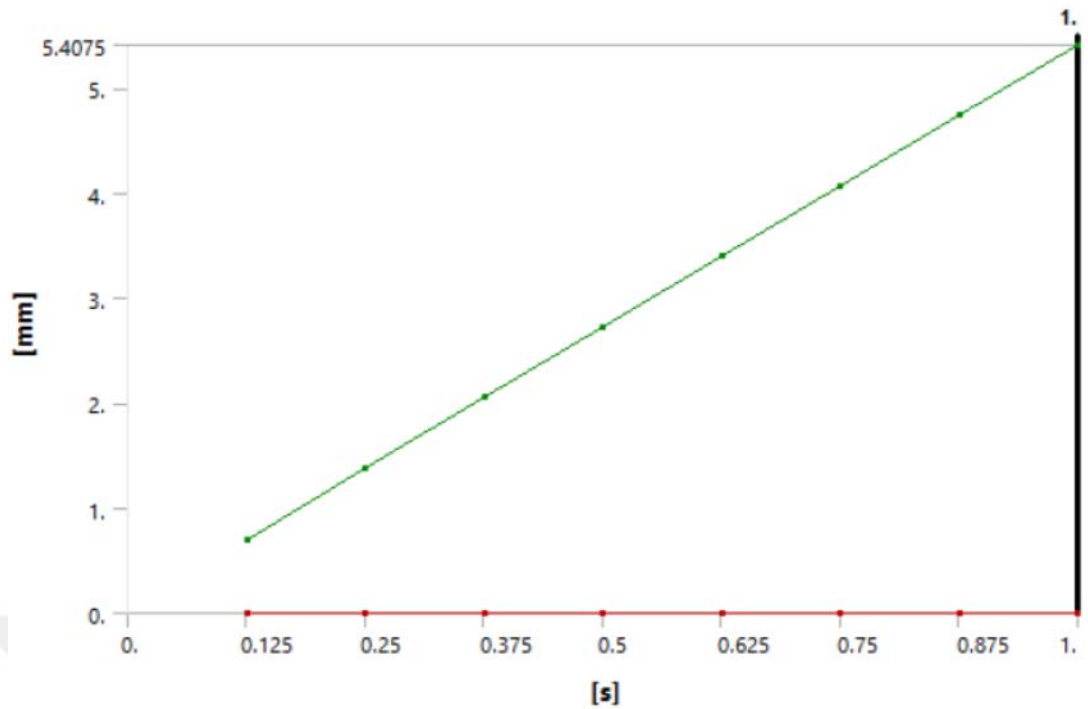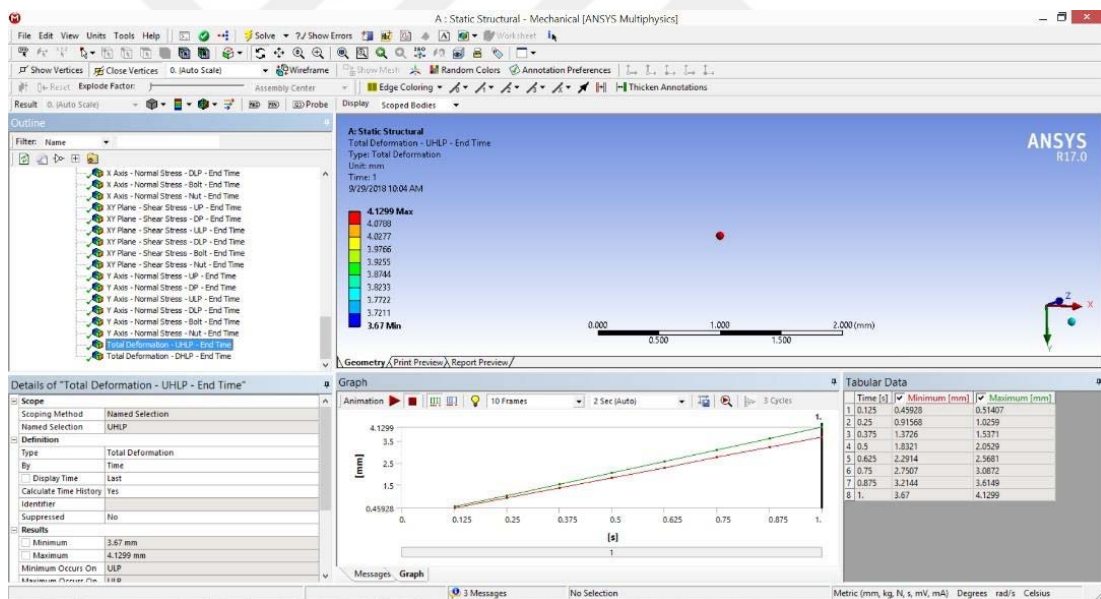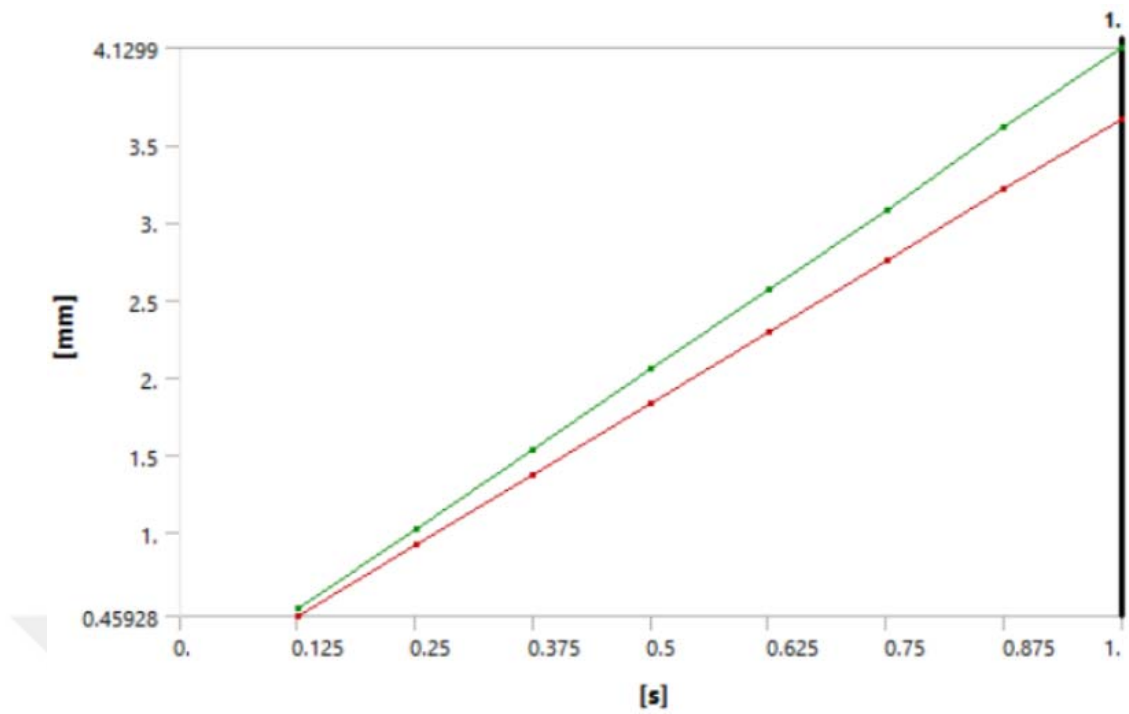
Figure 4.11: Total deformation of the hole in upper laminate plate.
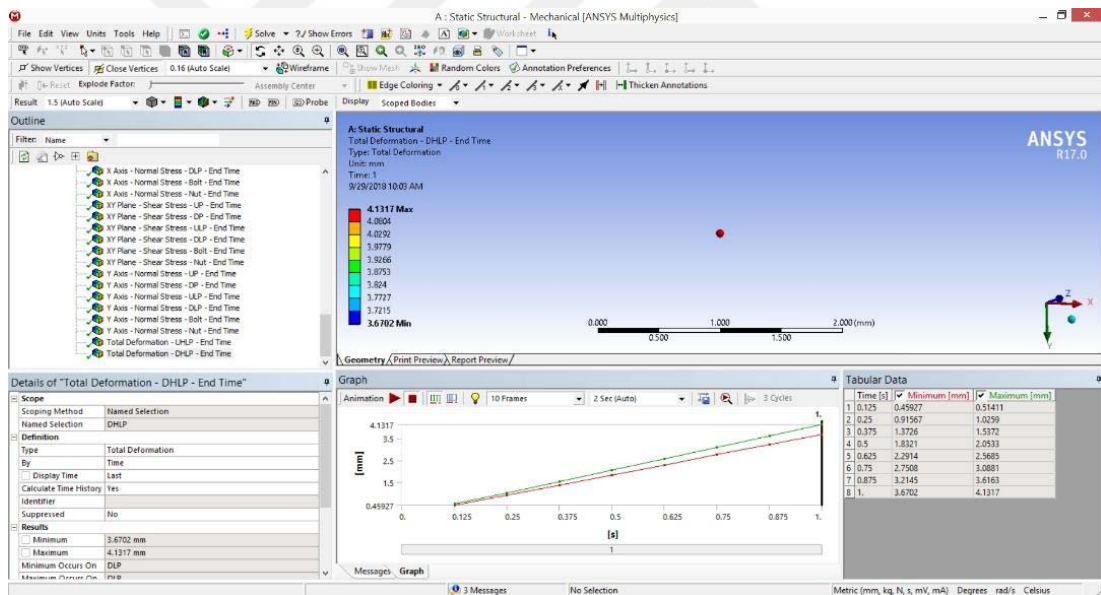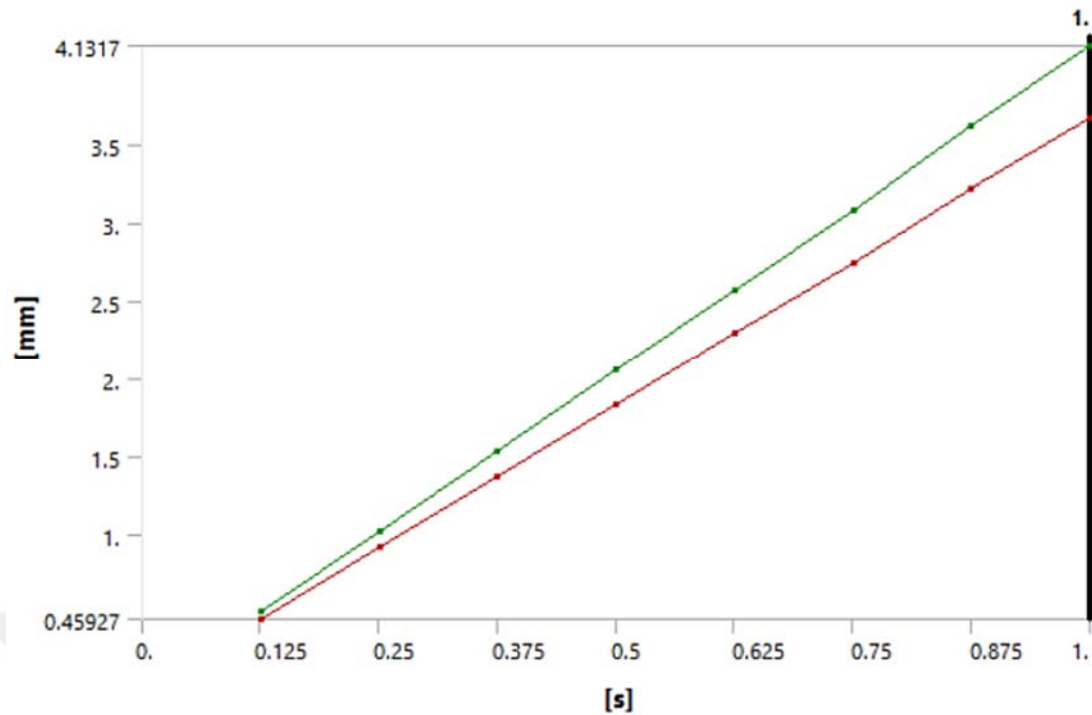
Figure 4.12: Total deformation of the hole in bottom laminate plate.

Figures 4.12-4.17 illustrates the directional deformation of the bolt, nut, upper and bottom Aluminum plates, upper and bottom laminate plates in X axis, respectively.
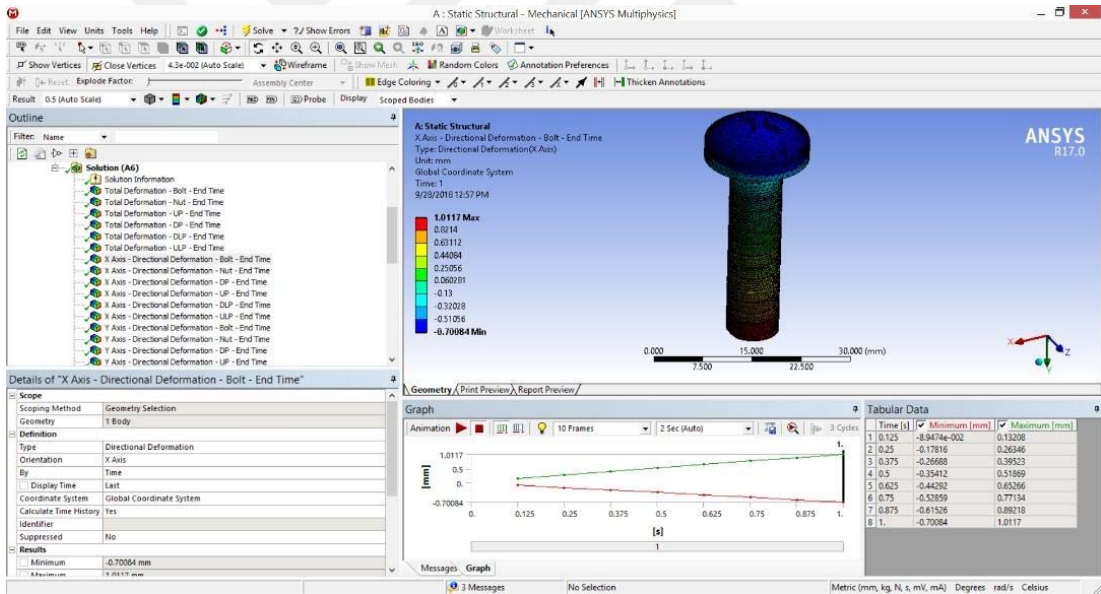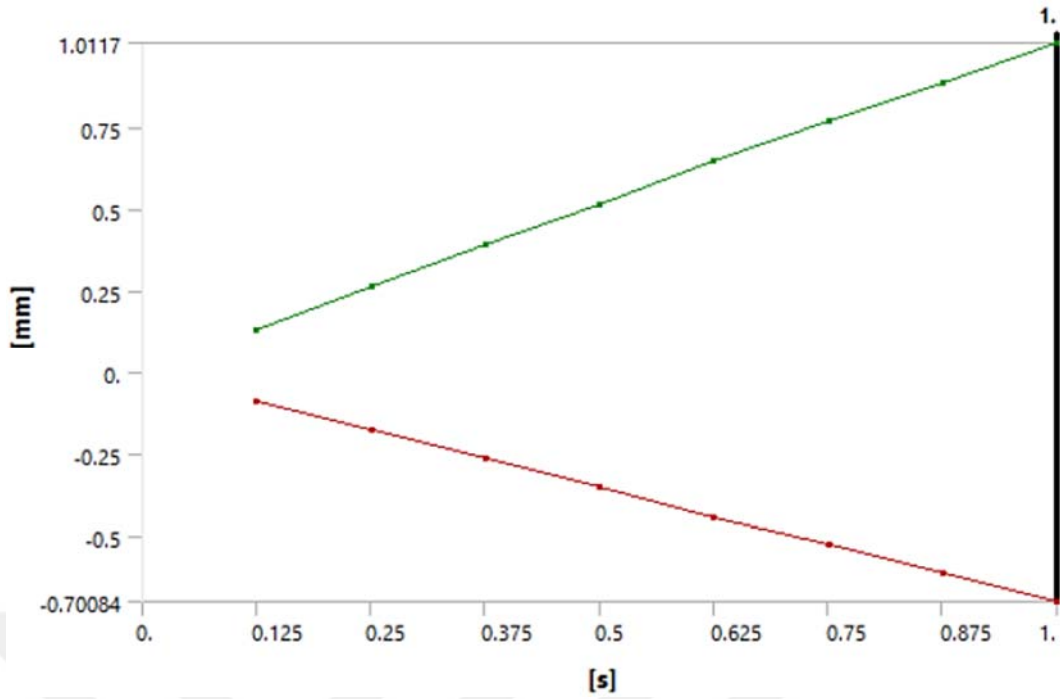
Figure 4.13: X Axis - Directional deformation of the bolt.
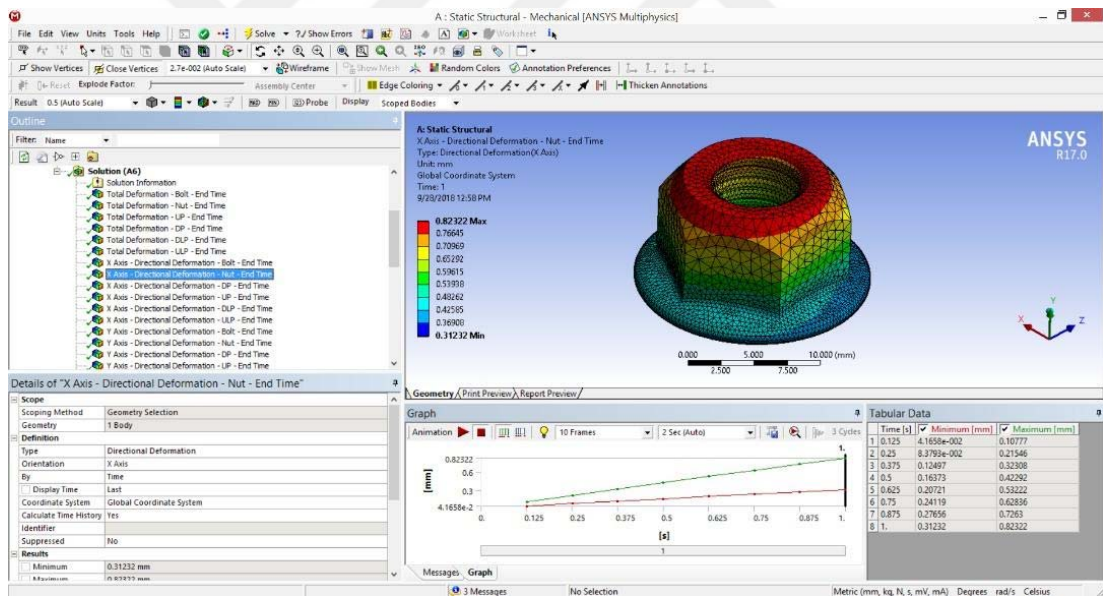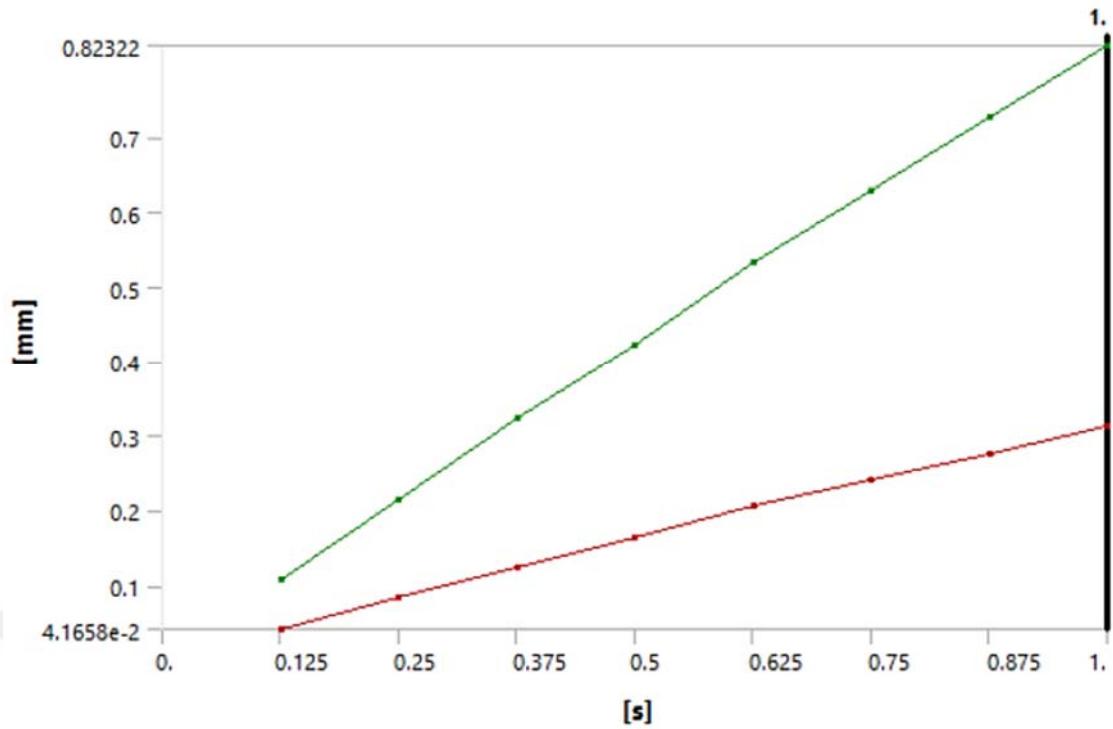
Figure 4.14: X Axis - Directional deformation of the nut.

Figure 4.15: X Axis - Directional deformation of upper Aluminum plate.
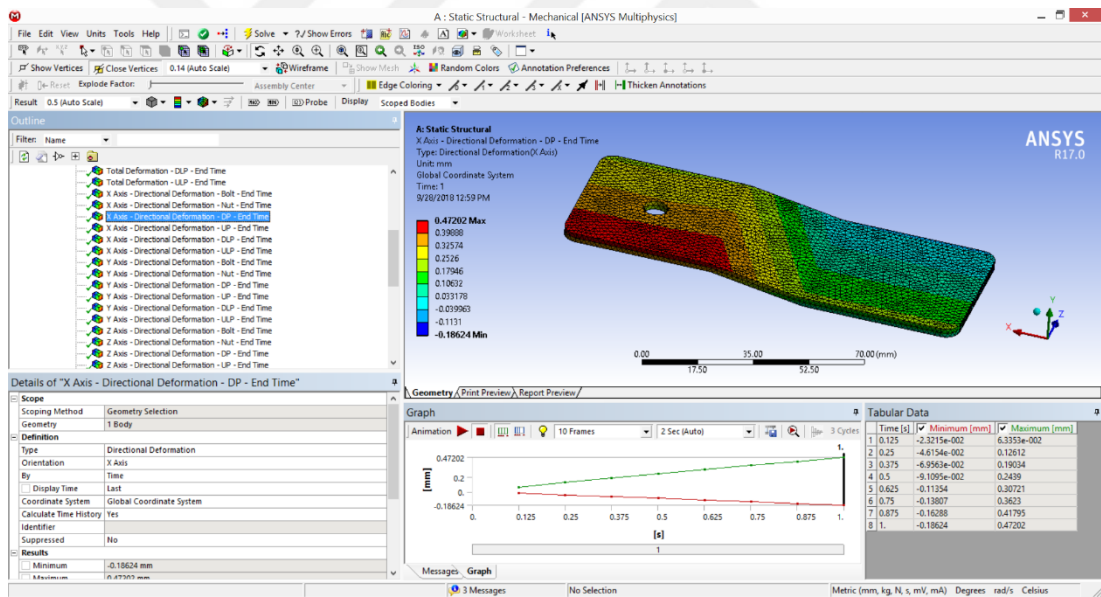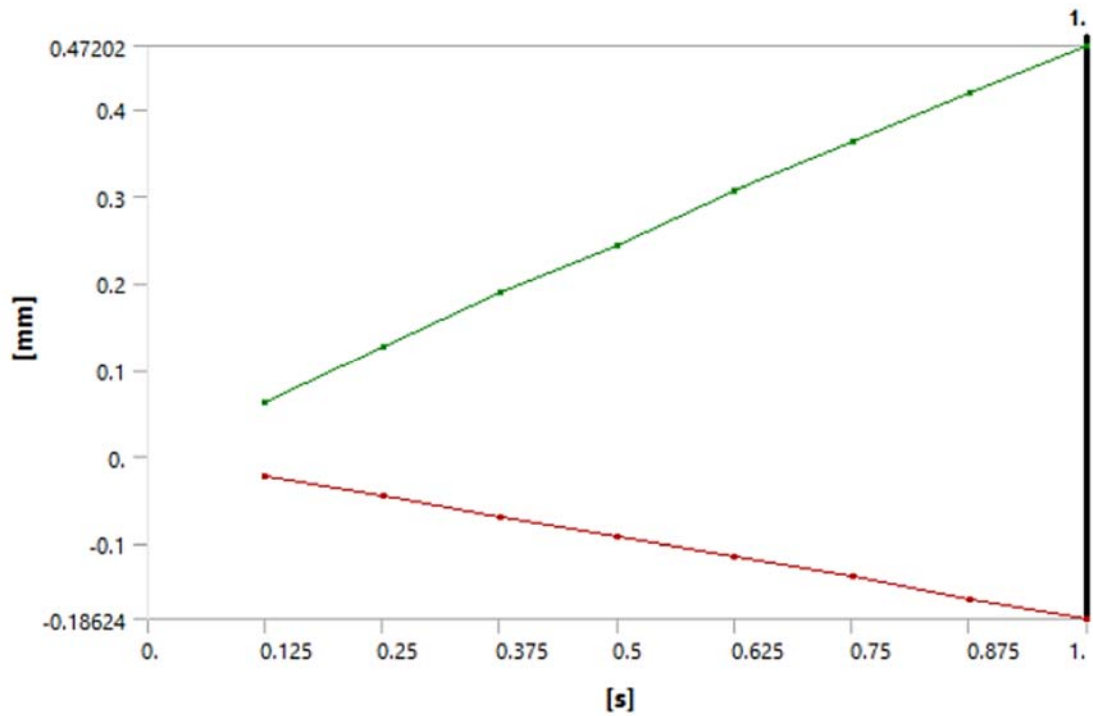
Figure 4.16: X Axis - Directional deformation of bottom Aluminum plate.
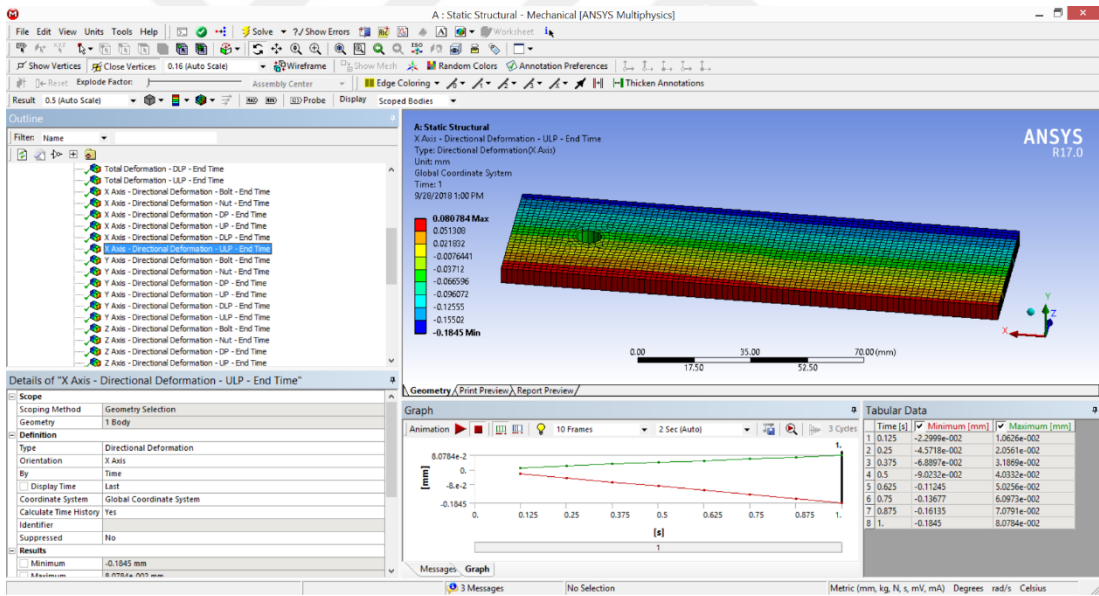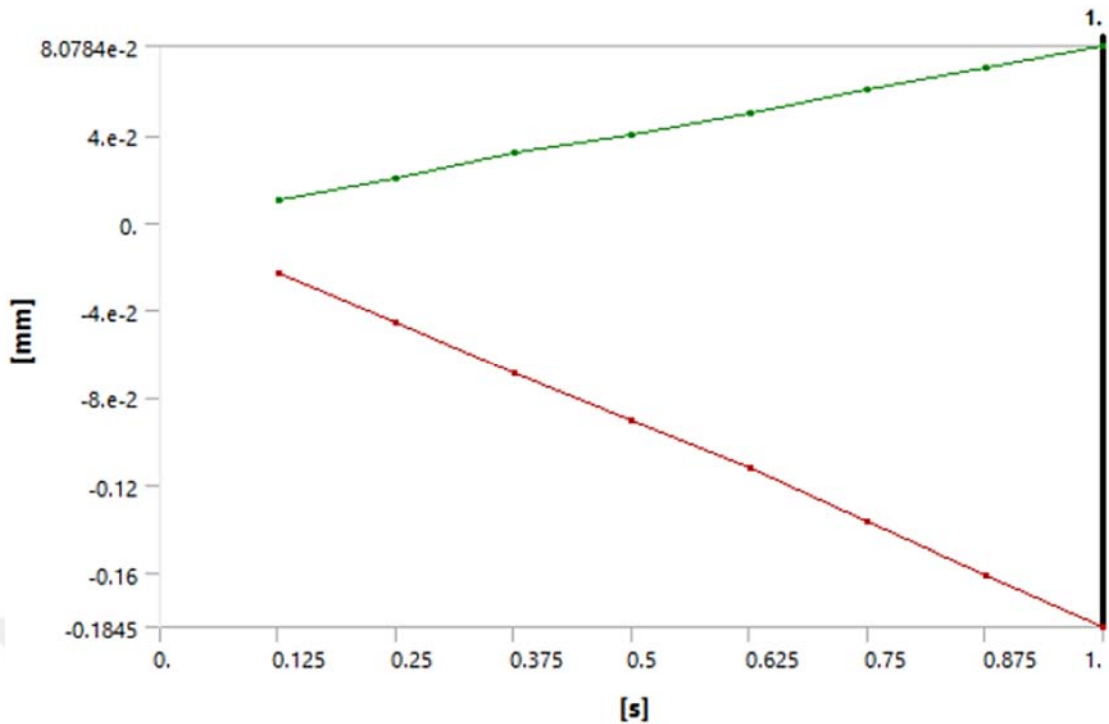
Figure 4.17: X Axis - Directional deformation of upper laminate plate.
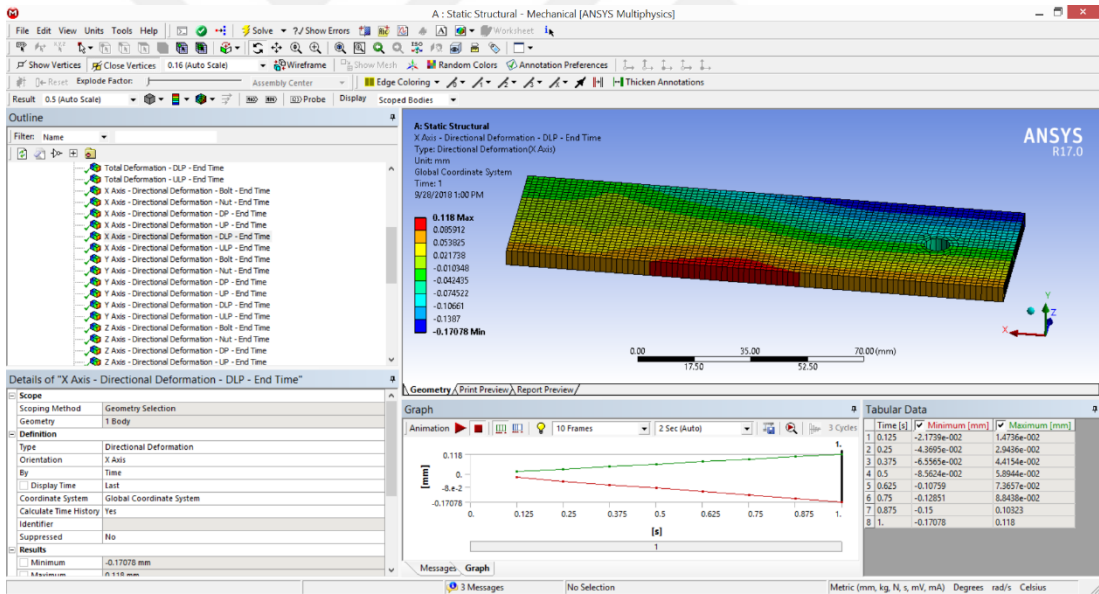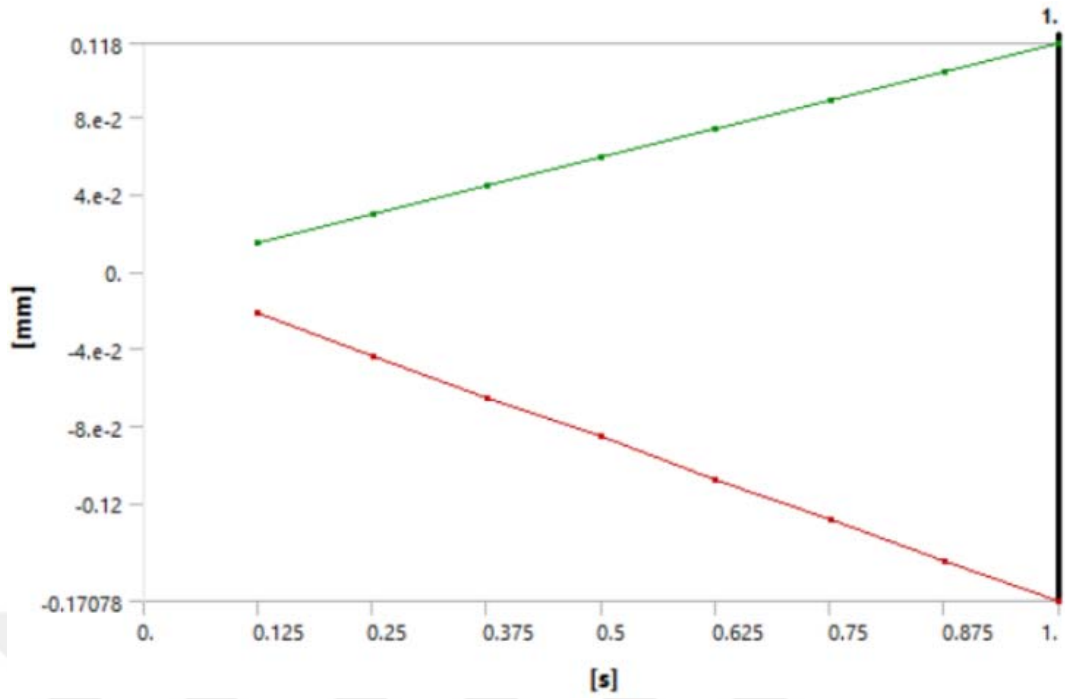
Figure 4.18: X Axis - Directional deformation of bottom laminate plate.

Figures 4.18-4.23 depict the directional deformation of the bolt, nut, upper and bottom Aluminum plates, upper and bottom laminate plates in Y axis, respectively.
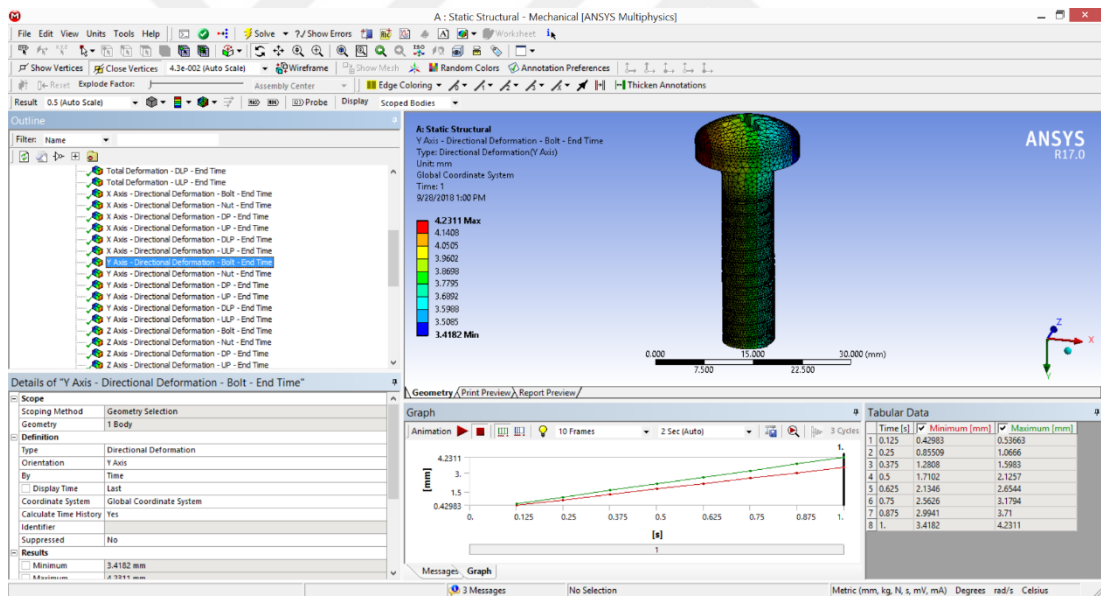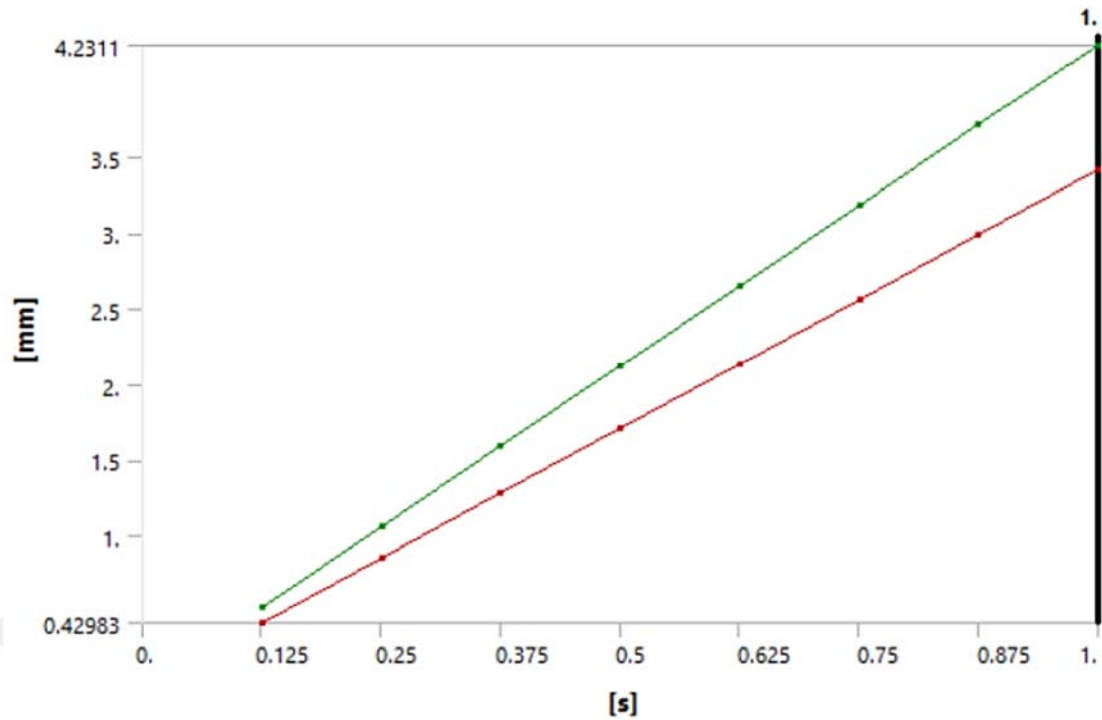
Figure 4.19: Y Axis - Directional deformation of the bolt.
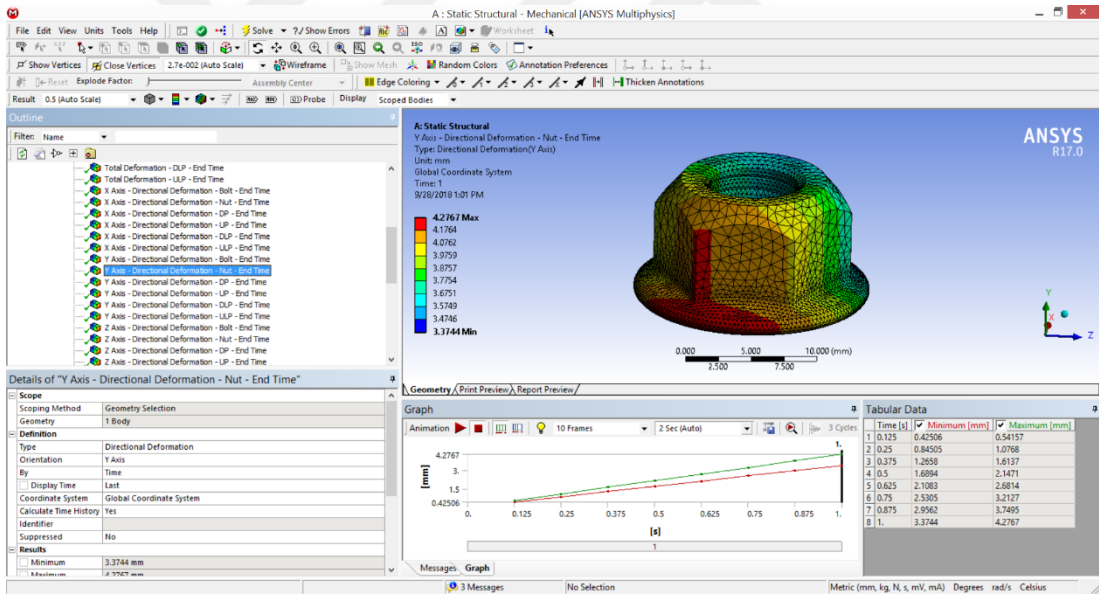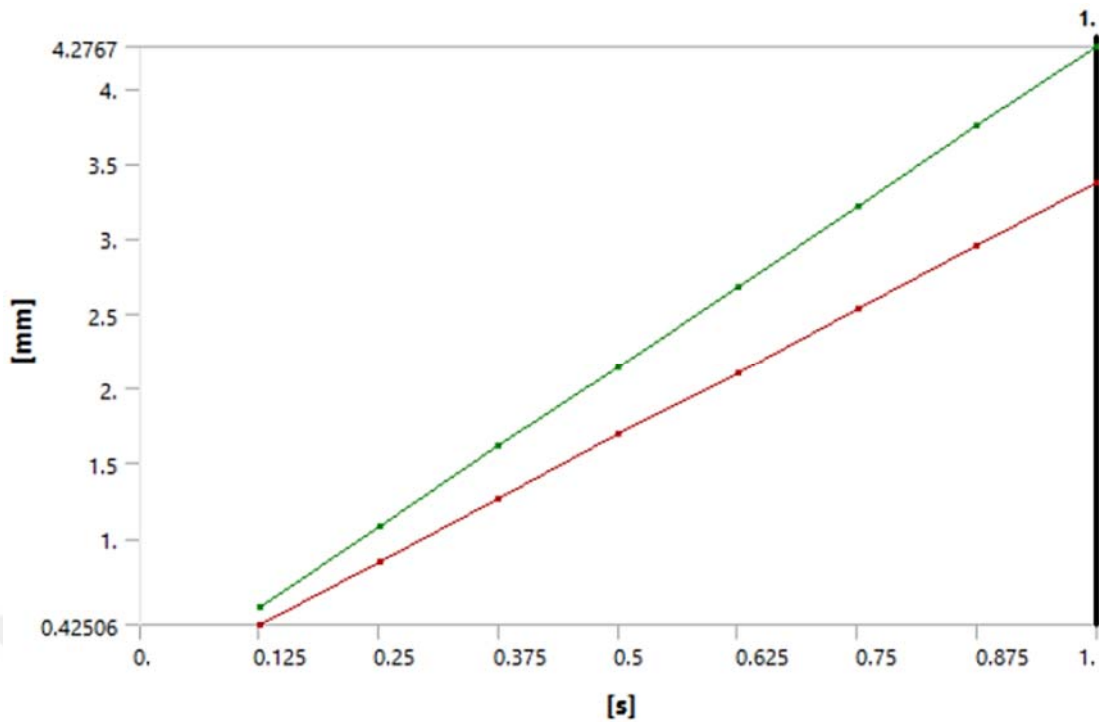
Figure 4.20: Y Axis - Directional deformation of nut.
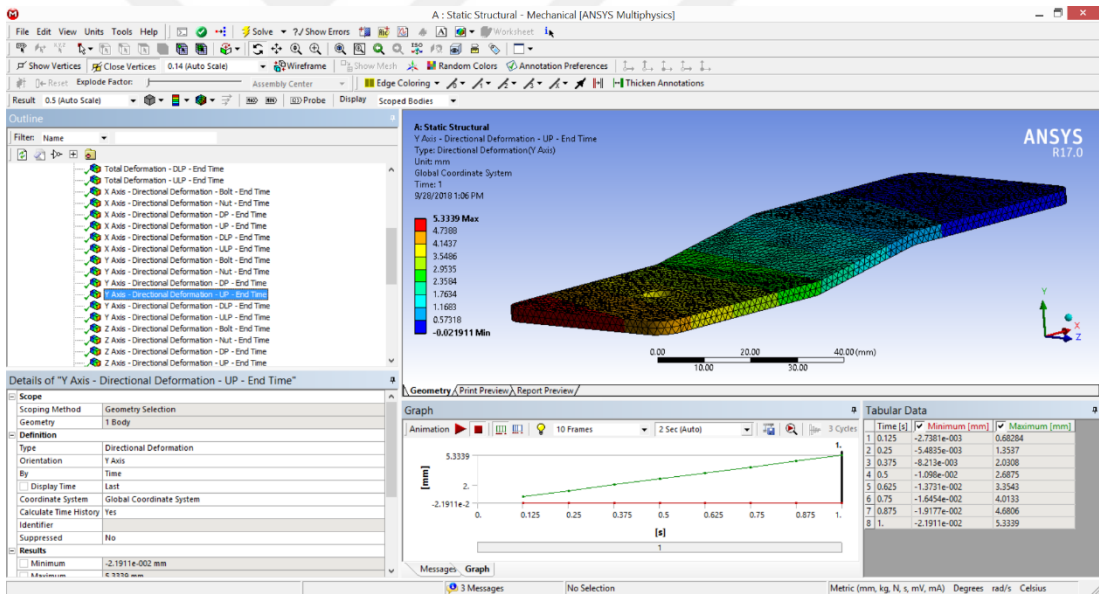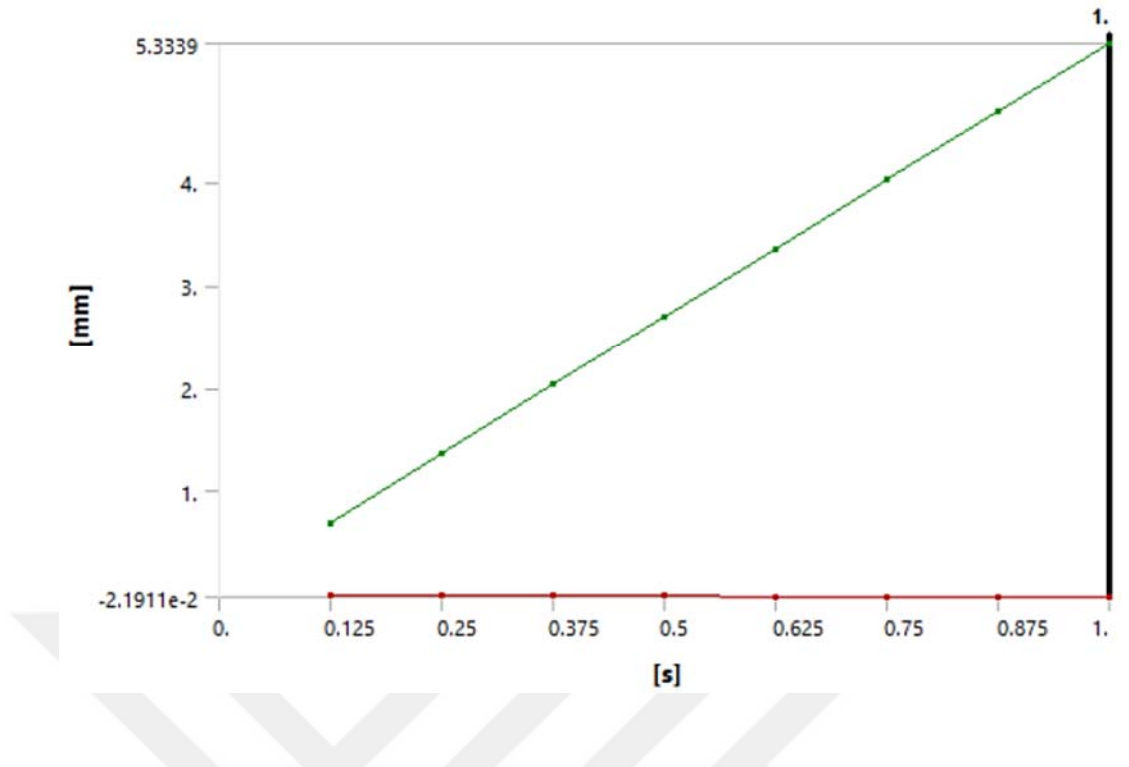
Figure 4.21: Y Axis - Directional deformation upper Aluminum plate.
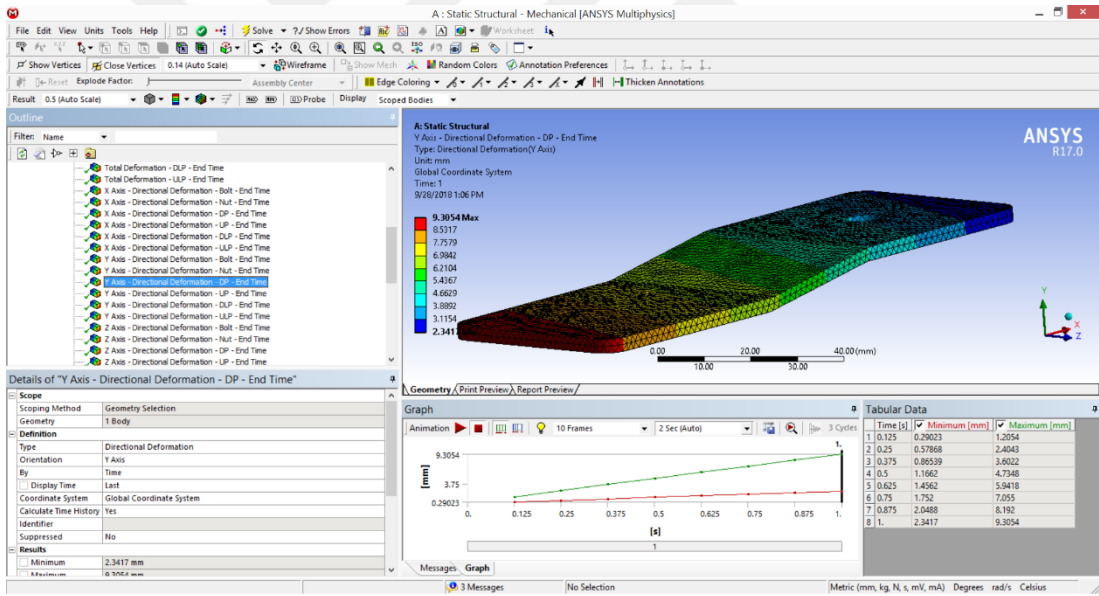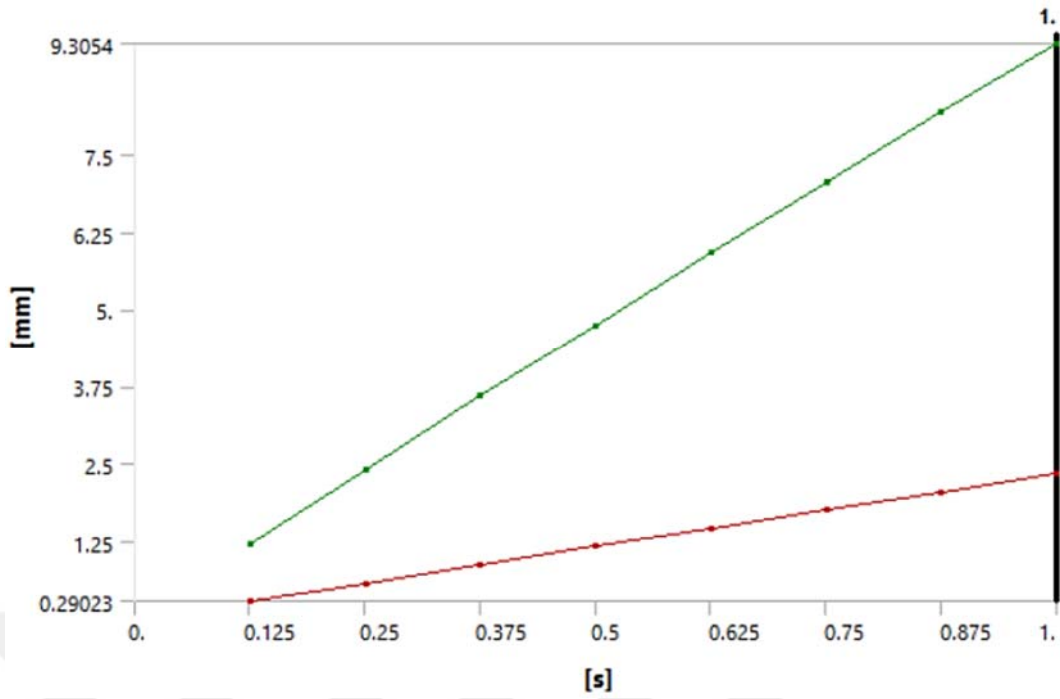
Figure 4.22: Y Axis - Directional deformation bottom Aluminum plate.
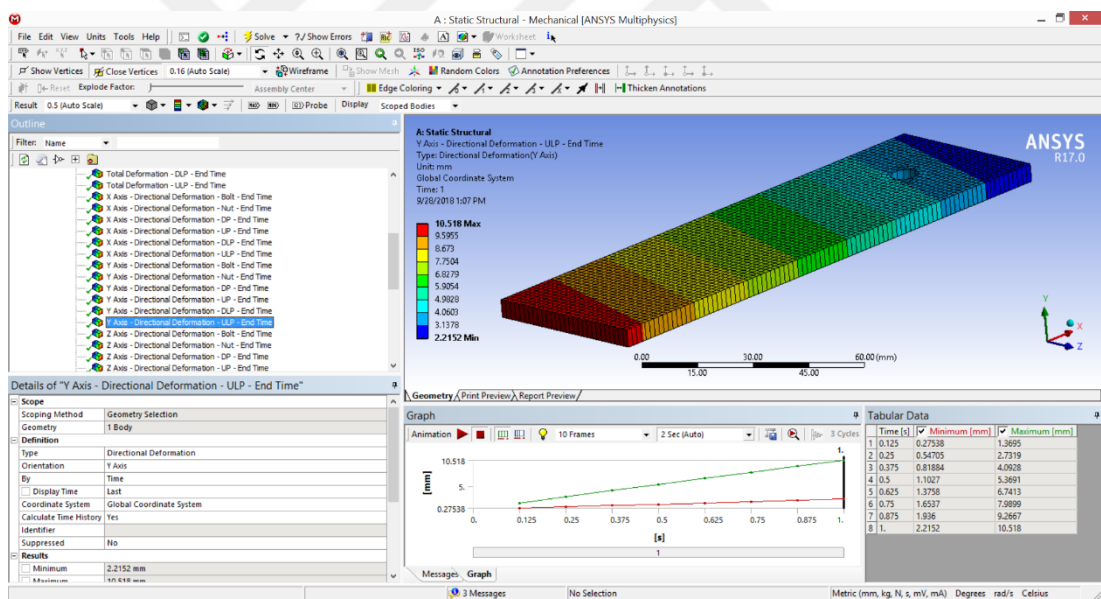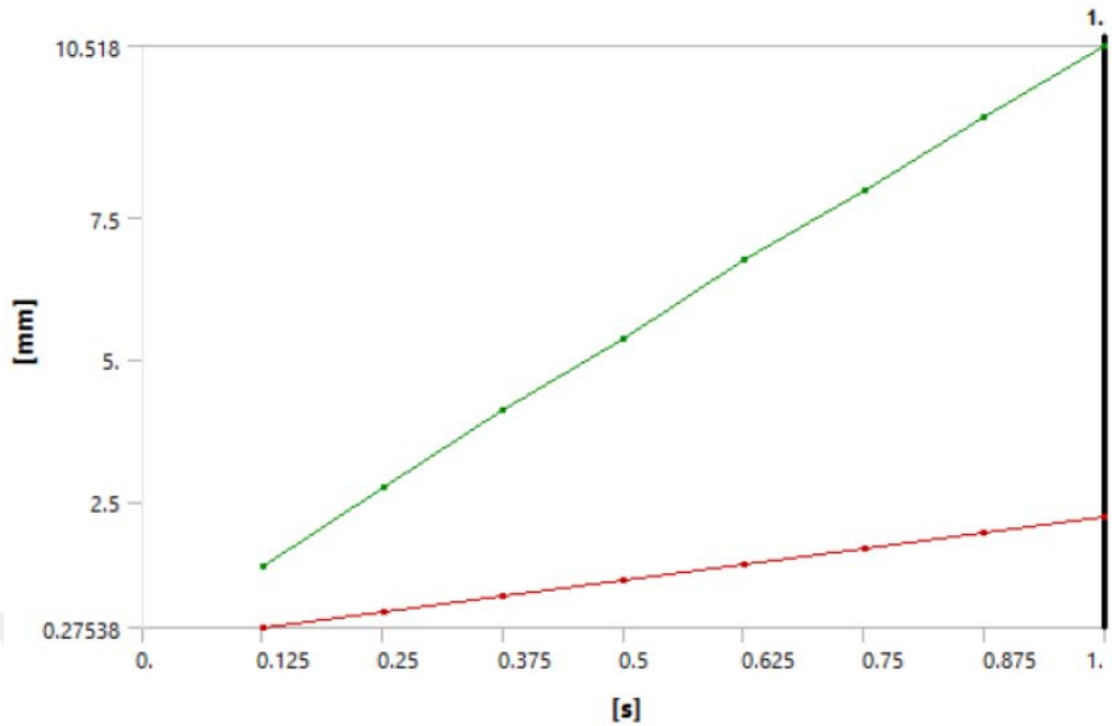
Figure 4.23: Y Axis - Directional deformation of upper laminate plate.
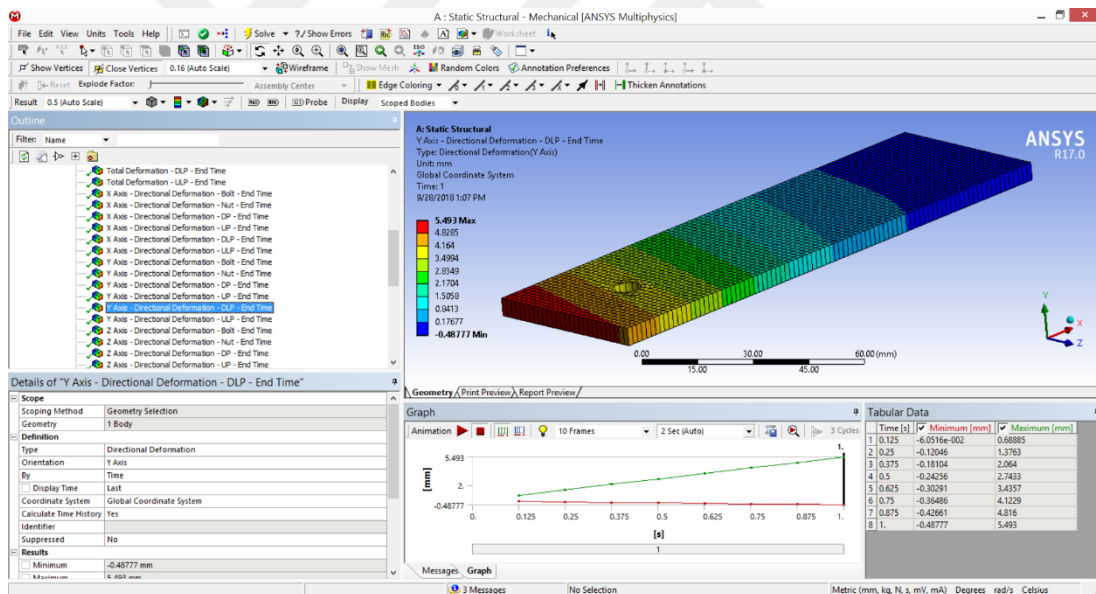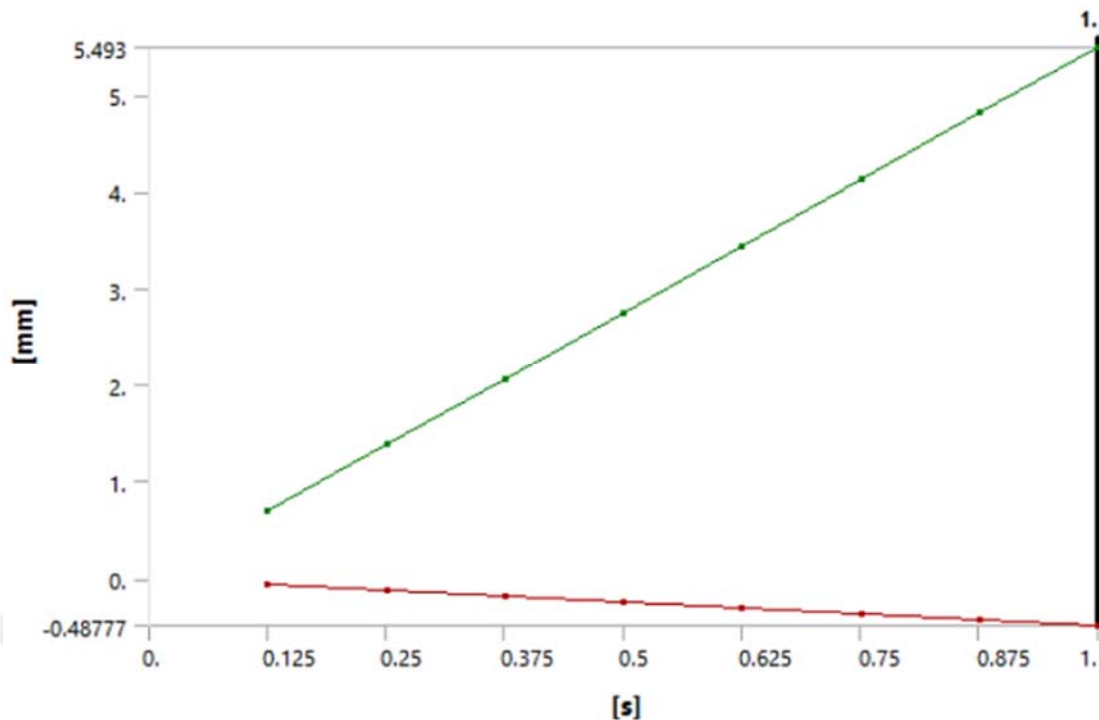
Figure 4.24: Y Axis - Directional deformation of bottom laminate plate.

Figures 4.24-4.29 represents the directional deformation of the bolt, nut, upper and bottom Aluminum plates, upper and bottom laminate plates in Y axis, respectively.
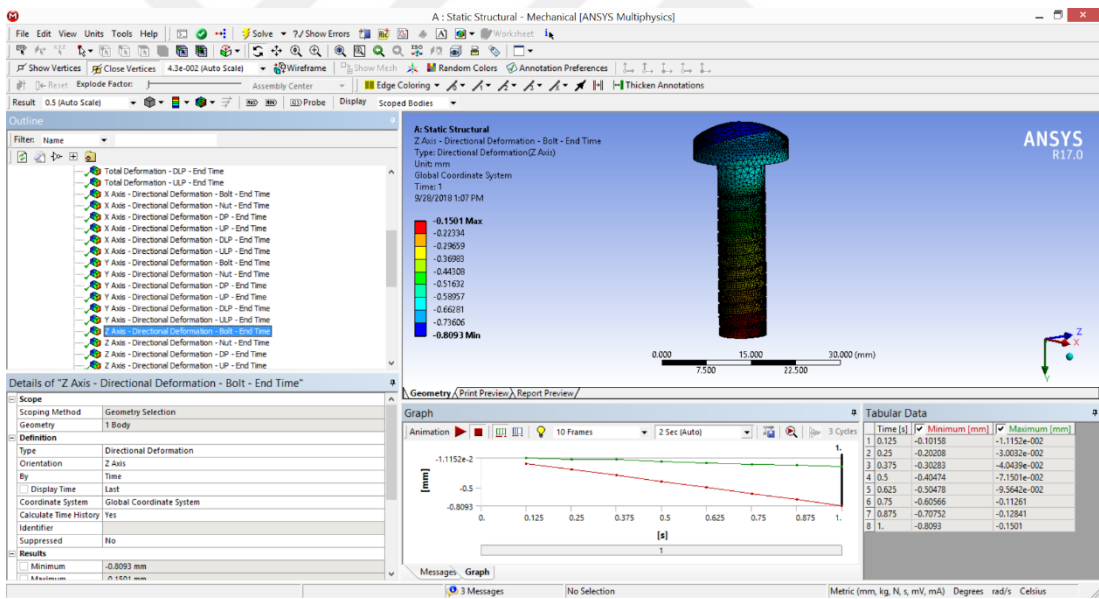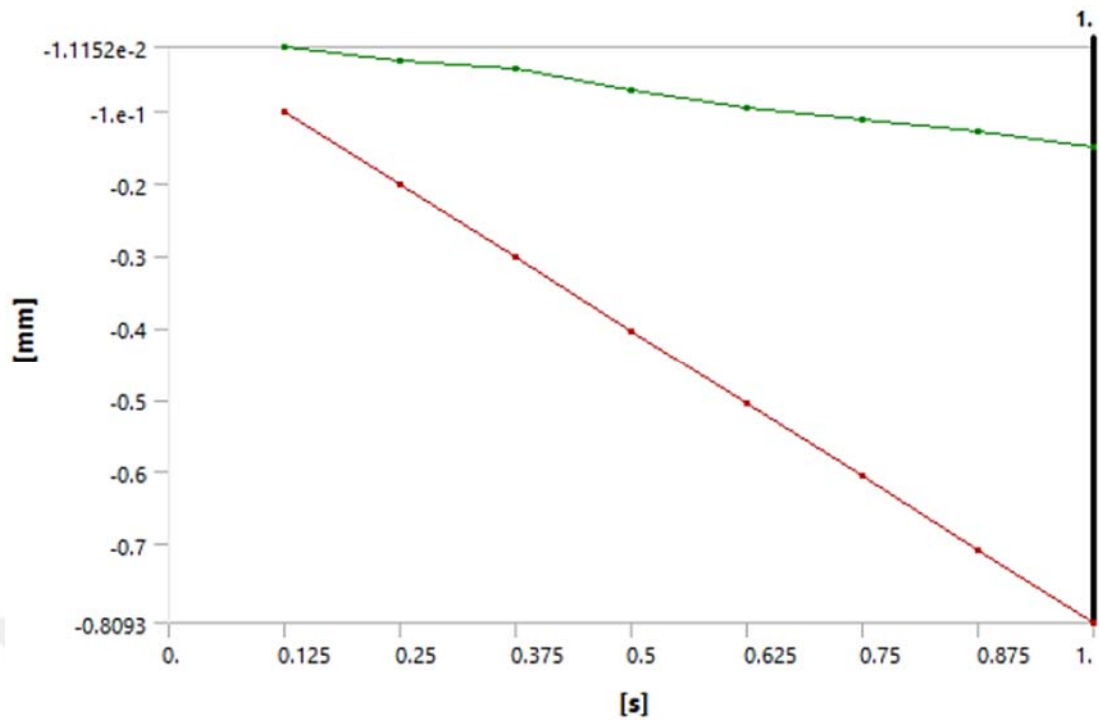
Figure 4.25: Z Axis - Directional deformation of the bolt.
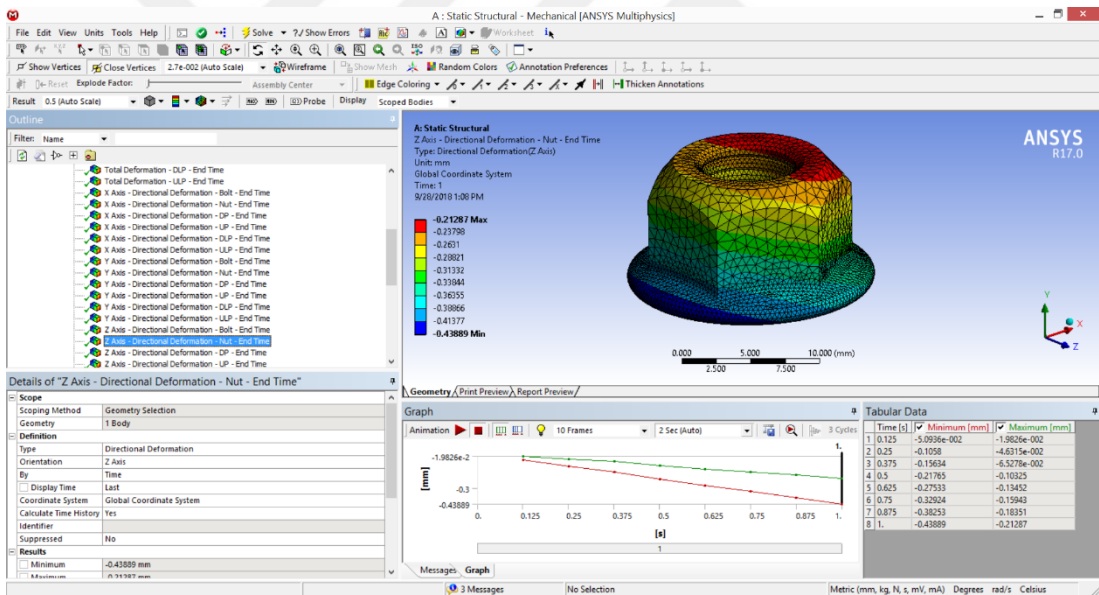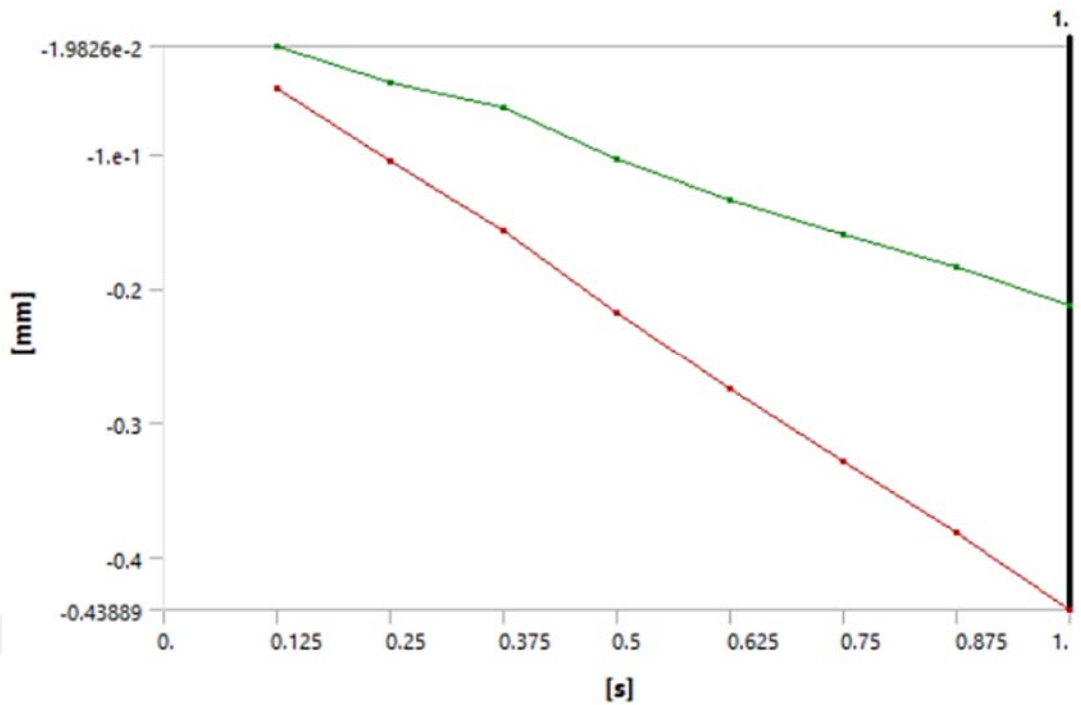
Figure 4.26: Z Axis - Directional deformation of the nut.
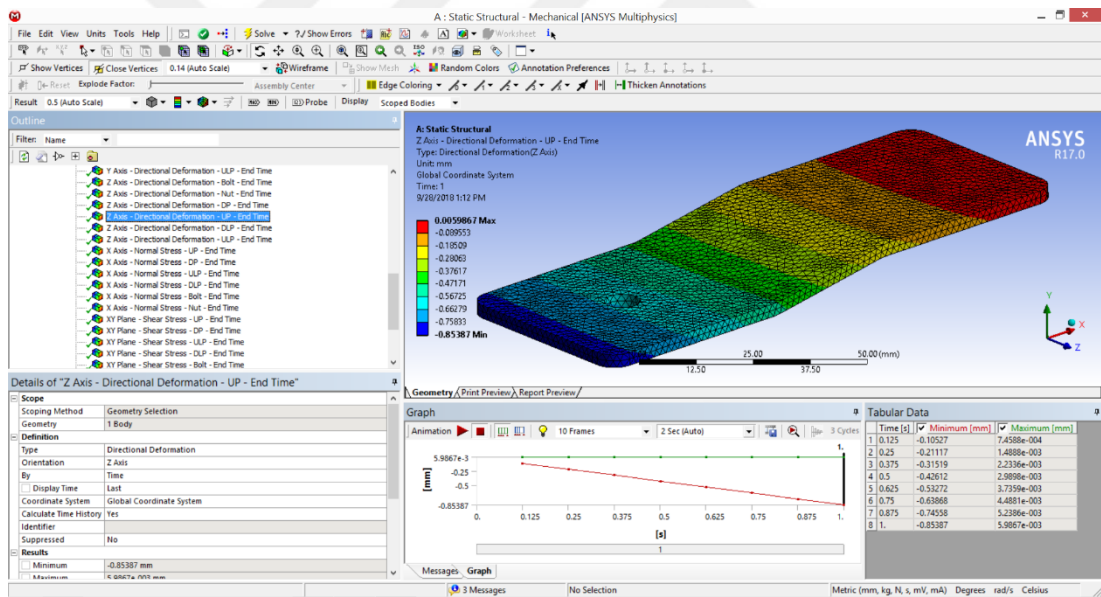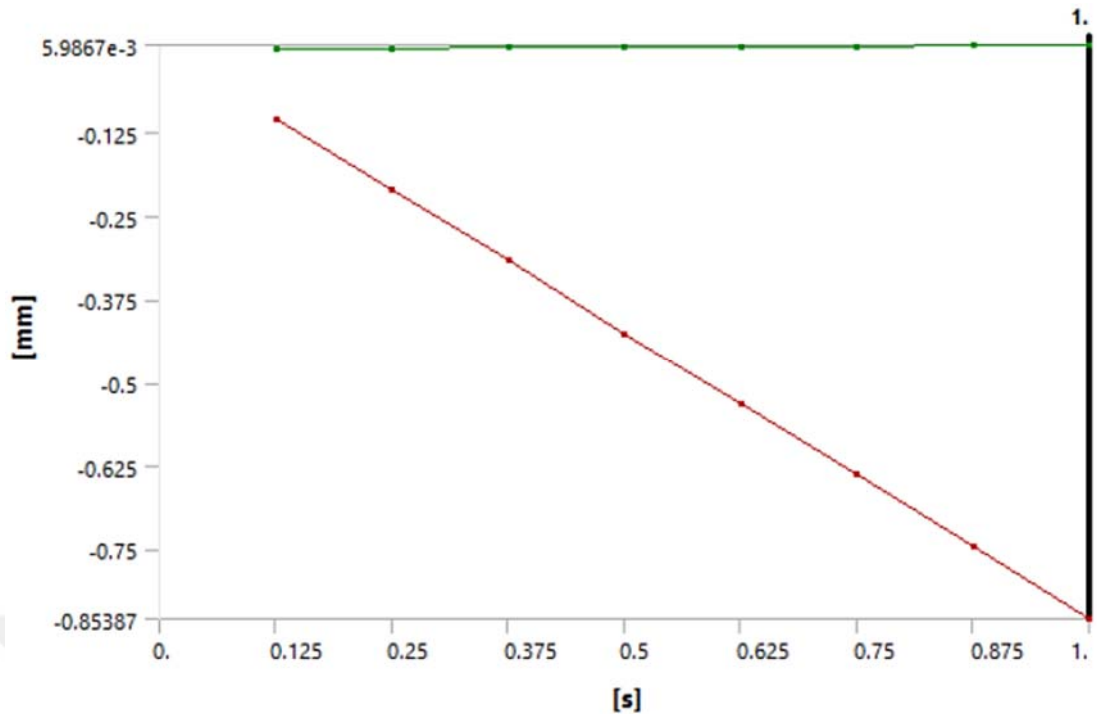
Figure 4.27: Z Axis - Directional deformation upper Aluminum plate.
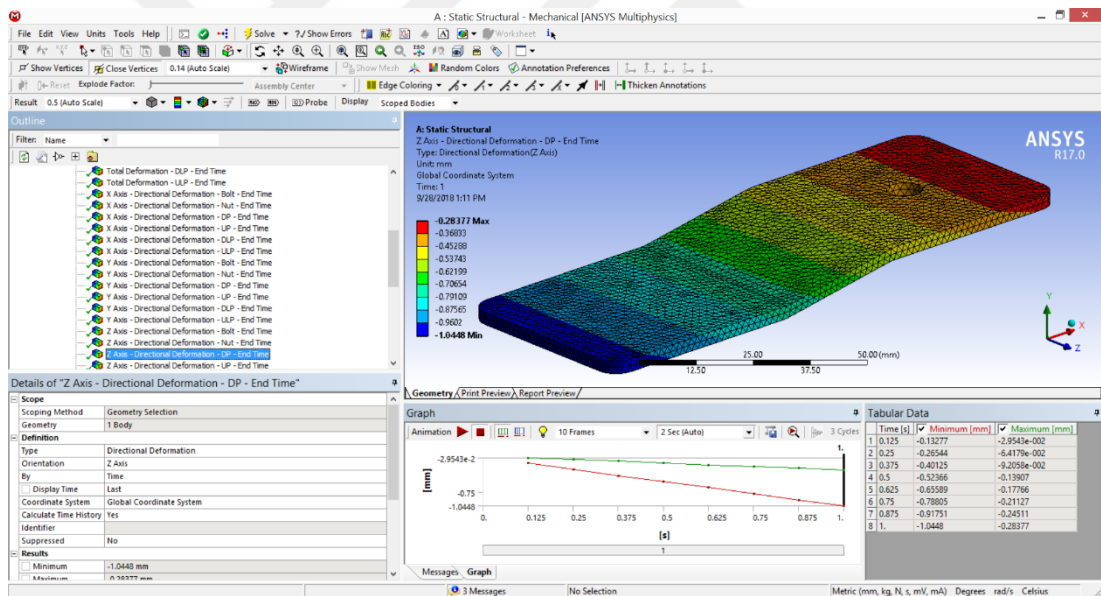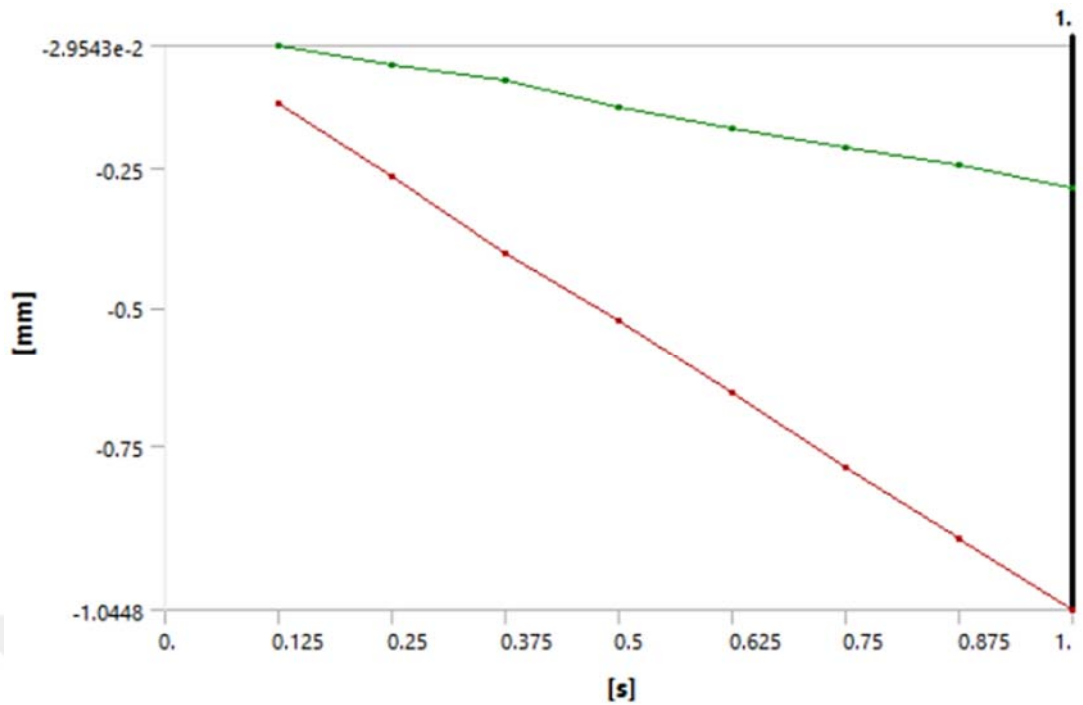
Figure 4.28: Z Axis - Directional deformation bottom Aluminum plate.
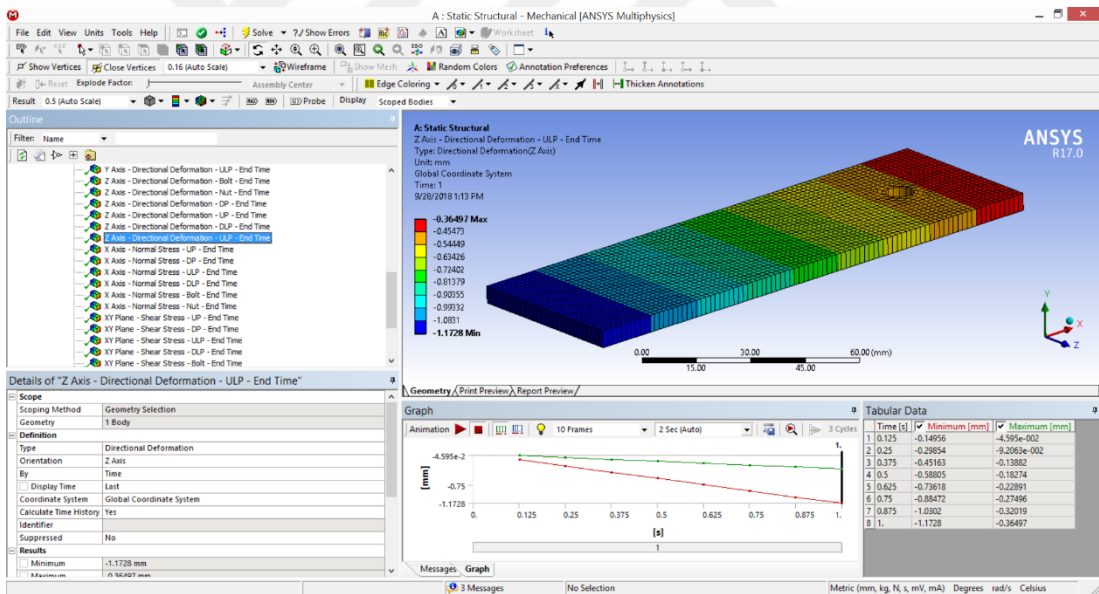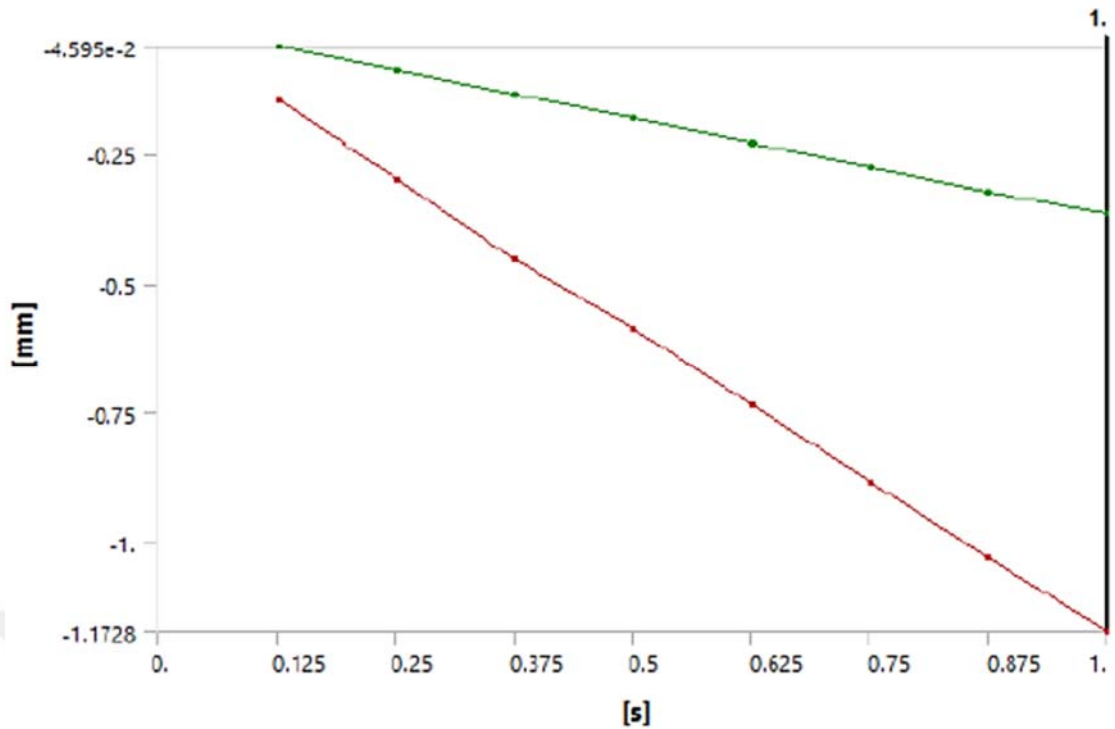
Figure 4.29: Z Axis - Directional deformation of upper laminate plate.

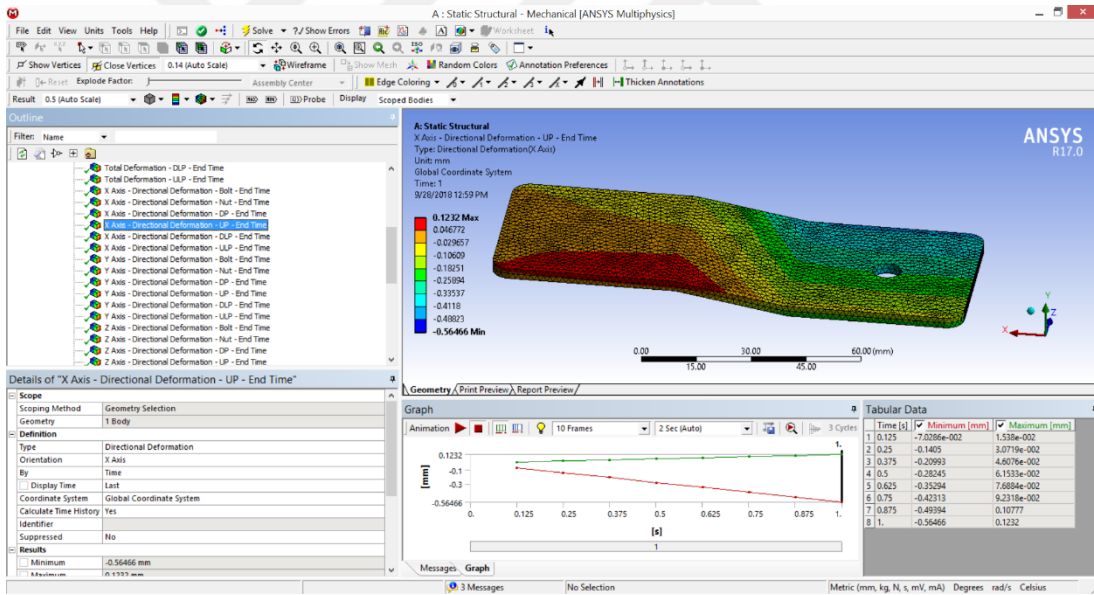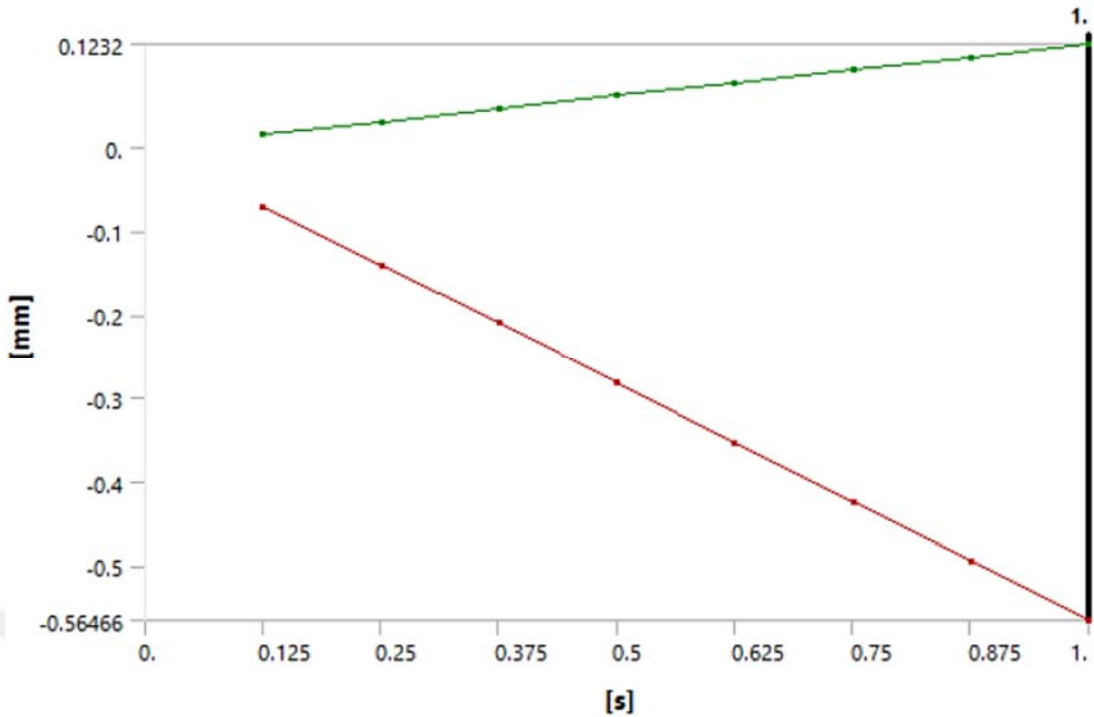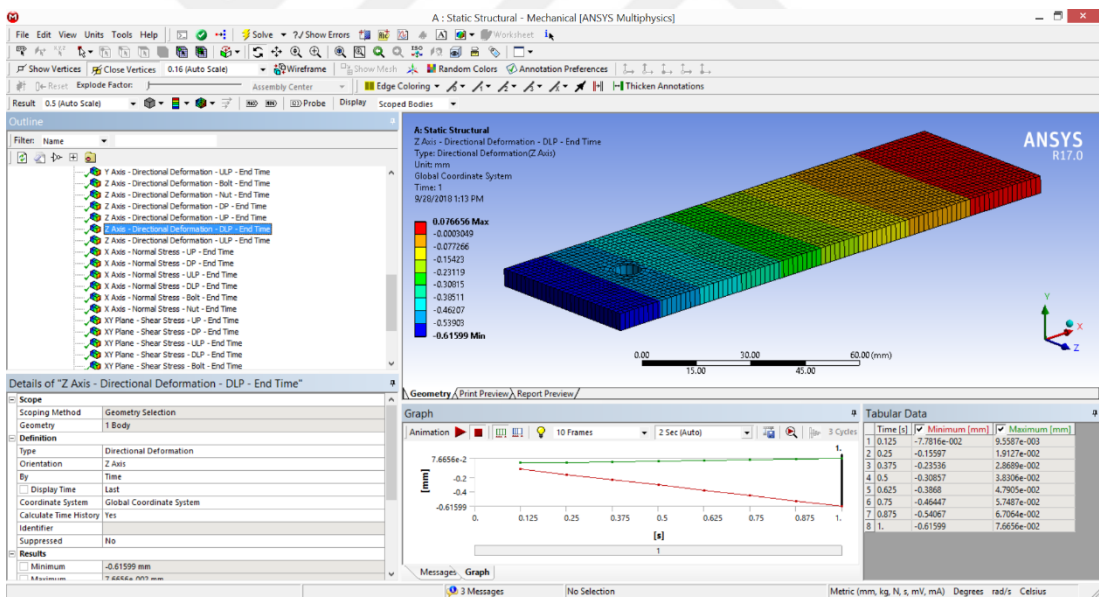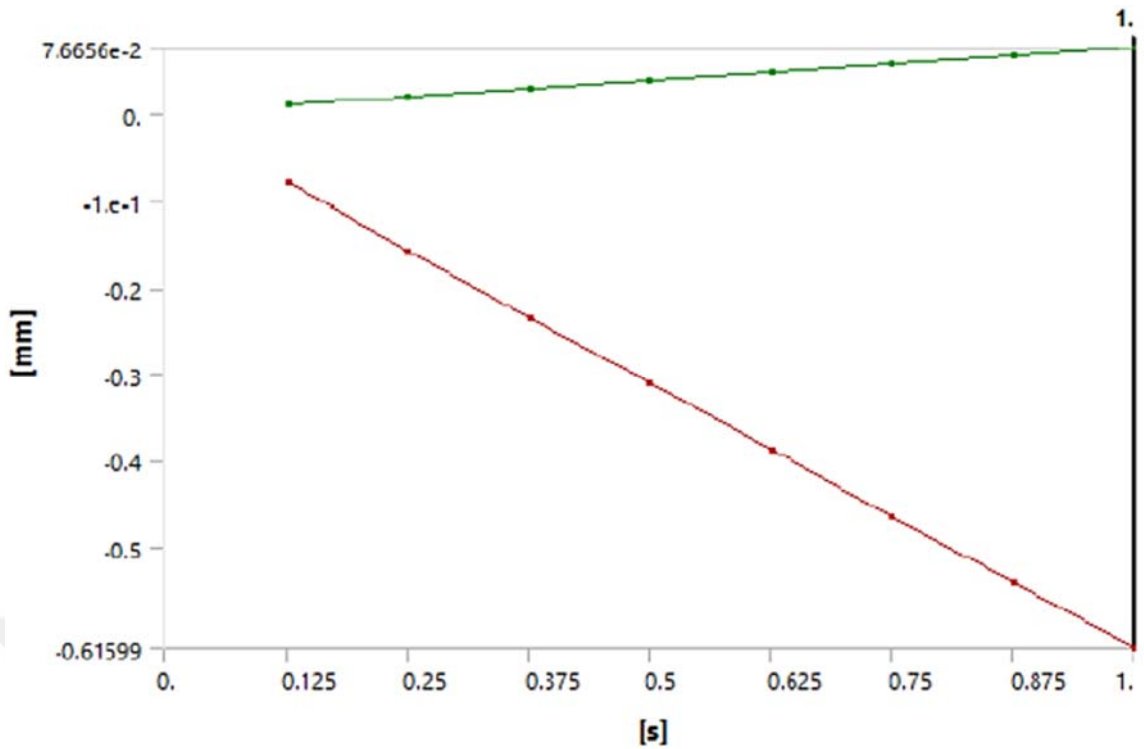**Figure 4.30:** Z Axis - Directional deformation of bottom laminate plate.

Tables 4.4, 4.5, 4.6, 4.7 and 4.8 represent the shear stress based on bolt, nut, bottom and upper laminate, and bottom and upper aluminum, respectively.

Table 4.4: The bolt shear stress.

Time [s]	Minimum [MPa]	Maximum [MPa]
0.125	-71.554	70.402
0.25	-3675.1	1872.6
0.375	-3668.4	1893.7
0.5	-3668.9	1911.
0.625	-3670.8	1929.8
0.75	-3672.2	1946.8
0.875	-3673.8	1963.9
1.	-2524.9	2081.4

Table 4.5: The nut shear stress.

Time [s]	Minimum [MPa]	Maximum [MPa]
0.125	-44.67	50.47
0.25	-2332.6	1489.4
0.375	-2351.4	1519.9
0.5	-2367.2	1543.9
0.625	-2385.8	1568.8
0.75	-2401.9	1594.1
0.875	-2418.1	1620.
1.	-4548.	4767.1

Table 4.6: The bottom laminate plate shear stress.

Time [s]	Minimum [MPa]	Maximum [MPa]
0.125	-1.5602e-015	9.5758e-016
0.25	-3.122e-015	1.8977e-015
0.375	-4.6836e-015	2.7989e-015
0.5	-6.2586e-015	3.8806e-015
0.625	-7.8284e-015	4.8362e-015
0.75	-9.3965e-015	5.7598e-015
0.875	-1.0964e-014	6.758e-015
1.	-1.2534e-014	7.7755e-015

Table 4.7: The upper laminate plate shear stress.

Time [s]	Minimum [MPa]	Maximum [MPa]
0.125	-7.3571e-016	7.3137e-016
0.25	-2.2213e-015	2.6794e-015
0.375	-3.1021e-015	2.7901e-015
0.5	-2.8349e-015	2.9153e-015
0.625	-5.0756e-015	6.1941e-015
0.75	-4.1276e-015	6.7766e-015
0.875	-4.7139e-015	8.2907e-015
1.	-5.3189e-015	8.6036e-015

Table 4.8: The upper Aluminum plate shear stress.

Time [s]	Minimum [MPa]	Maximum [MPa]
0.125	-7.3571e-016	7.3137e-016
0.25	-2.2213e-015	2.6794e-015
0.375	-3.1021e-015	2.7901e-015
0.5	-2.8349e-015	2.9153e-015
0.625	-5.0756e-015	6.1941e-015
0.75	-4.1276e-015	6.7766e-015
0.875	-4.7139e-015	8.2907e-015
1.	-5.3189e-015	8.6036e-015

Table 4.9: The bottom Aluminum plate shear stress.

Time [s]	Minimum [MPa]	Maximum [MPa]
0.125	-3.6773	4.5128
0.25	-15.398	30.961
0.375	-16.238	32.018
0.5	-17.224	31.647
0.625	-18.527	31.19
0.75	-22.094	30.832
0.875	-25.82	30.469
1.	-29.917	31.378

Tables 4.10, 4.11, 4.12, 4.13, 4.14 and 4.15 represent the normal stress along X- axis based on bolt, nut, bottom and upper laminate, and bottom and upper aluminum, respectively.

Table 4.10: The bolt normal stress along X- axis.

Time [s]	Minimum [MPa]	Maximum [MPa]
0.125	-54.557	89.74
0.25	-3261.9	2052.5
0.375	-3263.1	2035.1
0.5	-3264.6	2038.2
0.625	-3268.5	2040.9
0.75	-3269.2	3390.4
0.875	-3269.7	3958.2
1.	-7530.4	7592.2

Table 4.11: The nut normal stress along X- axis.

Time [s]	Minimum [MPa]	Maximum [MPa]
0.125	-226.3	216.25
0.25	-5679.1	3732.1
0.375	-5688.4	3738.1
0.5	-5710.7	3747.6
0.625	-5737.6	3760.3
0.75	-5759.6	3770.5
0.875	-5782.2	3780.8
1.	-14939	7933.1

Table 4.12: The upper laminate plate normal stress along X- axis.

Time [s]	Minimum [MPa]	Maximum [MPa]
0.125	-7.2529	12.185
0.25	-23.61	20.419
0.375	-23.207	32.632
0.5	-26.687	63.069
0.625	-54.274	71.424
0.75	-60.072	134.5
0.875	-74.475	180.7
1.	-85.901	186.13

Table 4.13: The bottom laminate plate normal stress along X- axis.

Time [s]	Minimum [MPa]	Maximum [MPa]
0.125	-13.124	18.313
0.25	-26.405	37.015
0.375	-40.009	55.232
0.5	-51.994	72.871
0.625	-65.568	92.092
0.75	-78.652	109.12
0.875	-99.472	126.88
1.	-103.5	144.26

Table 4.14: The upper aluminum plate normal stress along X- axis.

Time [s]	Minimum [MPa]	Maximum [MPa]
0.125	-209.14	114.81
0.25	-417.58	230.53
0.375	-626.57	345.19
0.5	-837.41	459.6
0.625	-1046.4	575.17
0.75	-1256.9	688.2
0.875	-1467.2	801.49
1.	-1676.8	915.83

Table 4.15: The bottom aluminum plate normal stress along X- axis.

Time [s]	Minimum [MPa]	Maximum [MPa]
0.125	-21.161	9.6485
0.25	-46.093	58.635
0.375	-63.453	59.477
0.5	-84.313	56.183
0.625	-106.07	54.47
0.75	-125.87	65.611
0.875	-147.06	77.86
1.	-167.64	89.972

Tables 4.16, 4.17, 4.18, 4.19, 4.20 and 4.21 represent the normal stress along Y- axis based on bolt, nut, bottom and upper laminate, and bottom and upper aluminum, respectively.

Table 4.16: The bolt normal stress along Y- axis.

Time [s]	Minimum [MPa]	Maximum [MPa]
0.125	-109.05	107.87
0.25	-1515.5	2805.8
0.375	-1598.2	2790.
0.5	-1649.2	2555.8
0.625	-1702.9	3643.2
0.75	-1915.9	3594.9
0.875	-2552.3	4272.2
1.	-3171.8	4030.5

Table 4.17: The nut normal stress along Y- axis.

Time [s]	Minimum [MPa]	Maximum [MPa]
0.125	-83.489	74.683
0.25	-1251.3	2813.6
0.375	-1251.5	2869.9
0.5	-1246.9	2901.1
0.625	-1242.5	2936.2
0.75	-1238.9	2967.6
0.875	-1235.5	2999.4
1.	-3637.2	6594.5

Table 4.18: The upper laminate plate normal stress along Y- axis.

Time [s]	Minimum [MPa]	Maximum [MPa]
0.125	-1.0695e-031	1.022e-031
0.25	-2.8241e-031	2.0016e-031
0.375	-3.1065e-031	3.1313e-031
0.5	-4.0185e-031	3.8717e-031
0.625	-5.9723e-031	4.8471e-031
0.75	-6.6857e-031	5.678e-031
0.875	-8.3334e-031	6.5349e-031
1.	-8.452e-031	7.3856e-031

Table 4.19: The bottom plate normal stress along Y- axis.

Time [s]	Minimum [MPa]	Maximum [MPa]
0.125	-1.2474e-031	1.8523e-031
0.25	-2.4809e-031	3.7065e-031
0.375	-3.7273e-031	5.5605e-031
0.5	-4.9847e-031	7.4307e-031
0.625	-6.2201e-031	9.2946e-031
0.75	-7.4879e-031	1.1157e-030
0.875	-8.7496e-031	1.3018e-030
1.	-9.9964e-031	1.4882e-030

Table 4.20: The upper aluminum plate normal stress along Y- axis.

Time [s]	Minimum [MPa]	Maximum [MPa]
0.125	-73.185	55.308
0.25	-146.11	110.93
0.375	-219.22	166.17
0.5	-292.91	221.41
0.625	-365.97	276.99
0.75	-439.54	331.68
0.875	-512.98	386.46
1.	-586.19	441.6

Table 4.21: The bottom aluminum plate normal stress along Y- axis.

Time [s]	Minimum [MPa]	Maximum [MPa]
0.125	-4.1654	3.6715
0.25	-10.881	20.248
0.375	-13.211	19.973
0.5	-18.497	17.337
0.625	-23.52	19.064
0.75	-30.193	23.917
0.875	-38.705	29.135
1.	-44.989	33.668

4.4 Conclusion

In this chapter a new design for a single composite lap-joint is presented. Based on the simulation results which are obtained from the represented single composite lap-joint in chapter 3, it has been considered to add two external plate to support the composite plates, which has had better response in terms of total and directional deformation compare to the aforementioned single composite lap-joints. The T800 carbon-epoxy, aluminum alloy and Titanium 6AI-4V are considered as laminate plates, holder plates and bolt and nut, respectively. Based on the simulation process which is done in ANSYS software, the total and directional deformations of the designed single composite lap-joint 5000 N is better than the other ones, which are presented in chapter 3.

CHAPTER 5

CONCLUSION

5.1 Introduction

In this chapter firstly, a short review about previous chapters and a sum up about the results, which are obtained based on the analysis that are done in chapters 3 and 4 are described. Finally, some suggestions as ongoing works are presented. Moreover, some of our suggestion about the ongoing works which can do in this area are presented.

5.2 Chapters Review

In chapters one and two a bibliography about the composite materials and some of the features of them are described. Then, in chapter 3, three researches which were done based on different kinds of single composite lap-joints are presented. In the proposed research IM7/MTM-45-1, T800 and HTA 7/6376 carbon epoxy were considered as the main material for constructing the laminate plates. Moreover, 40CrNiMo alloy, Titanium 6AI-4V and Titanium 6Al114VSTA were set as the materials of the bolts and nuts. According to the deformation analysis that was done in ANSYS software the performance of T800 carbon epoxy and Titanium 6AI-4V alloy under load is better than the other two ones in term of total deformation and generally in term of directional deformation. Based on the proposed points a new design for a single-lap bolted-joint was presented in chapter 4. The materials which are set for the proposed structure are T800 carbon epoxy for laminate plates, Titanium 6AI-4V alloy for bolt and nut and Aluminum alloy for two holder plates. The results of analysis in ANSYS in terms of total and directional deformation verified the high

performance of the proposed structure in terms of robustness under load against the deformation.

5.3 Ongoing Works

As ongoing works based on the structure of this thesis two suggestions are provided that are explained in the following:

❖ One of the best way that can reduce the single composite lap-joints constructing expenses is doing simulation in different software like ANSYS or ABAQUS, but the process of simulating always is so time consuming and sometimes the results are not so good and the material or the structure need to change. In order to accelerate the process of simulating and obtaining better results, using the machine learning methods to find the general shape and the best material can be considered as a novel method.

❖ Moreover, the process of this thesis was based on finding a better structure which can tolerate more load and have a robust behavior against the deformation. As future works, the structure which is presented as a concept design in chapter 4 and the materials which are set on them can be constructed and analyzed and then the experimental results can be compared with the simulation ones.

REFERENCES

1. Bogdanovich, A.E. and R.L.J.A.M.R. Sierakowski, *Composite Materials and Structures: Science, Technology and Applications-A Compendium of Books, Review Papers, and Other Sources of Information.* 1999. **52**(12): p. 351-366

2. Bhatt, A.T., P.P. Gohil, and V. Chaudhary. *Primary Manufacturing Processes for Fiber Reinforced Composites: History, Development & Future Research Trends.* in *IOP Conference Series: Materials Science and Engineering.* 2018. IOP Publishing.

3. *Glass Fiber Market - Global Industry Analysis, Size, Share, Growth, Trends, and Forecast 2016 - 2024.* May 2016; Available from: https://www.transparencymarketresearch.com/glass-fibers-market.html.

4. Pickering, K.L., et al., *A review of recent developments in natural fibre composites and their mechanical performance.* 2016. **83**: p. 98-112.

5. Cyriac, A.J., *Metal matrix composites: History, status, factors and future.* 2011, Oklahoma State University.

6. Ireman, T.J.C.s., *Three-dimensional stress analysis of bolted single-lap composite joints. Composite Structures.* 1998. **43**(3): p. 195-216.

7. Vicari, A., *Carbon Fiber Composites Market Update.* October 25, 2014.

8. Beardmore, P., C.J.C.s. Johnson, and Technology, *The potential for composites in structural automotive applications. Composite Science and Technology.* 1986. **26**(4): p. 251-281.

9. Bayne, S.C., et al., *A characterization of first-generation flowable composites. American Dental Association.* 1998. **129**(5): p. 567-577.

10. Williams, E.L.J.U.o.B., *Composite Materials and Helicopter Rotor Blades. Mechanics of Composite Materials.* 2008.

11. Jones, R.M., *Mechanics of composite materials.* 2014: CRC press.

12. Krenkel, W.J.I.J.o.a.c.t., *Carbon fiber reinforced CMC for high‑performance structures. Ceramics International.* 2004. **1**(2): p. 188-200.

13. Ltd, I.M., *High Strength and Light Weight of Carbon Fiber Driving Strong Demand Growth in Aircraft and Automotive Manufacturing, IHS Markit Says.* Dec. 20, 2016.

14. John, J., S.A. Gangadhar, and I.J.T.J.o.p.d. Shah, *Flexural strength of heat-polymerized polymethyl methacrylate denture resin reinforced with glass, aramid, or nylon fibers. Prosthetic Dentistry.* 2001. **86**(4): p. 424-427.

15. Taj, S., M.A. Munawar, and S.J.P.-P.A.o.S. Khan, *Natural fiber-reinforced polymer composites. Natural Fibers.* 2007. **44**(2): p. 129.

16. Naga, S.M., et al., *Synthesis and characterization of laminated Si/SiC composites. Advanced Research.* 2013. **4**(1): p. 75-82.

17. Yajima, S., J. Hayashi, and M.J.C.L. Omori, *Continuous silicon carbide fiber of high tensile strength. Fundamental and Solid Reaction.* 1975. **4**(9): p. 931-934.

18. Mehta, P., et al., *Nonlinear transmission properties of hydrogenated amorphous silicon core optical fibers.* 2010. **18**(16): p. 16826-16831.

19. Lassila, L., et al., *Mechanical properties of fiber reinforced restorative composite with two distinguished fiber length distribution. Mechanical Behavior of Biomedical Materials.* 2016. **60**: p. 331-338.

20. Altenbach, H., J. Altenbach, and W. Kissing, *Classification of Composite Materials*, in *Mechanics of Composite Structural Elements.* 2018, Springer. p. 3-18.

21. Ireman, T., T. Ranvik, and I.J.C.S. Eriksson, *On damage development in mechanically fastened composite laminates. Composite Structures.* 2000. **49**(2): p. 151-171.

22. Otani, L.B., et al., *Elastic Moduli characterization of composites using the Impulse Excitation.* 2014.

23. Bert, C.W., D.M.J.J.o.S. Egle, and Rockets, *Dynamics of composite, sandwich, and stiffened shell-type structures. Spacecraft and Rockets.* 1969. **6**(12): p. 1345-1361.

24. Herakovich, C.T., *Fibrous Composite Materials*, in *A Concise Introduction to Elastic Solids. The Mechanics of Elastic Materials and Structures.* 2017, Springer. p. 101-119.

25. Gutowski, T.G.P., *Advanced composites manufacturing.* 1997: John Wiley & Sons.

26. Mouritz, A.P., et al., *Review of advanced composite structures for naval ships and submarines.* 2001. **53**(1): p. 21-42.

27. Thomas, S., et al., *Composite Materials.* 2000: p. 1-44.

28. Cardon, A., et al., *Durability analysis of polymer matrix composites for structural applications. Computers & Structures.* 2000. **76**(1-3): p. 35-41.

29. Hollaway, L., *Polymer composites for civil and structural engineering.* 2012: Springer Science & Business Media.

30. Chen, H., et al., *Polymerization contraction stress in light-cured packable composite resins. Dental Materials (DENT MATER).* 2001. **17**(3): p. 253-259.

31. L, D.N., *Effective Properties of Randomly Oriented Kenaf Short Fiber Reinforced Epoxy Composite.* 2015, UTAH STATE UNIVERSITY.

32. Group, W.R. *Ultralight Cellular Materials* 20-Jan-2014; Available from: http://www.virginia.edu/ms/research/wadley/celluar-materials.html.

33. McCarthy, M., et al., *Bolt-hole clearance effects and strength criteria in single-bolt, single-lap, composite bolted joints. Composite Science and Technology.* 2002. **62**(10-11): p. 1415-1431.

34. Agarwal, B.D., L.J. Broutman, and K. Chandrashekhara, *Analysis and performance of fiber composites.* 2017: John Wiley & Sons.

35. Coelho, A.M.G., J.T.J.M. Mottram, and Design, *A review of the behaviour and analysis of bolted connections and joints in pultruded fibre reinforced polymers. Materials & Design.* 2015. **74**: p. 86-107.

36. Jackson, R.D. and M.J.T.J.o.t.A.D.A. Morgan, *THE NEW POSTERIOR RESINS AND: A SIMPLIFIED PLACEMENT TECHNIQUE.* 2000. **131**(3): p. 375-383.

37. McCarthy, M., C.J.P. McCarthy, rubber, and composites, *Finite element analysis of effects of clearance on single shear composite bolted joints. Macromolecular Engineering.* 2003. **32**(2): p. 65-70.

38. Armentani, E., et al., *Numerical FEM Evaluation for the Structural Behaviour of a Hybrid (bonded/bolted) Single-lap Composite Joint. Procedia Structural Integrity.* 2018. **8**: p. 137-153.

39. Kallaur, M., *Sheet molding compound.* 1981, Google Patents.

40. Lecomte, J., et al., *An analytical model for the prediction of load distribution in*

multi-bolt composite joints including hole-location errors. Composite Structures. 2014. **117**: p. 354-361.

41. Shalin, R.E.e., *Polymer matrix composites*. Vol. 4. 2012: Springer Science & Business Media. *Technology & Engineering.*

42. Yuanxin, D., et al., *Analysis of bolt-to-laminate interface friction in bolted composite joint with interference-fit. Materials Research Innovations.* 2015. **19**(sup6): p. S6-42-S6-45.

43. Chawla, K.K.J.M.S. and Technology, *Metal matrix composites. Material Science and Technology.* 2006.

44. Ainsworth, J.H. and R.E. Shepler, *Ceramic-metal composites*. 1987, Google Patents.

45. Labella, R., et al., *Polymerization shrinkage and elasticity of flowable composites and filled adhesives. Dental Materials.* 1999. **15**(2): p. 128-137.

46. Ishikawa, T. and T.-W.J.J.o.c.m. Chou, *Elastic behavior of woven hybrid composites. Composite Materials.* 1982. **16**(1): p. 2-19.

47. Mishra, S., et al., *Studies on mechanical performance of biofibre/glass reinforced polyester hybrid composites. Composites Science and Technology.* 2003. **63**(10): p. 1377-1385.

48. Johnson, T. *Composites In Aerospace* April 02, 2017 Available from: https://www.thoughtco.com/composites-in-aerospace-820418.

49. Botelho, E.C., et al., *A review on the development and properties of continuous fiber/epoxy/aluminum hybrid composites for aircraft structures.* 2006. **9**(3): p. 247-256.

50. Karataş, M.A. and H.J.D.T. Gökkaya, *A review on machinability of carbon fiber reinforced polymer (CFRP) and glass fiber reinforced polymer (GFRP) composite materials. Defence Technology.* 2018.

51. Hale, J., *Boeing 787 from the Ground Up (COMPOSITES IN THE AIRFRAME AND PRIMARY STRUCTURE).* 2008.

52. Manhart, J., et al., *Mechanical properties and wear behavior of light-cured packable composite resins. Dental Materials.* 2000. **16**(1): p. 33-40.

53. Bodjona, K., L.J.J.o.r.p. Lessard, and composites, *Hybrid bonded-fastened joints and their application in composite structures: A general review. Reinforced*

Plastics and Composites. 2016. **35**(9): p. 764-781.

54. Hart-Smith, L., *Design and analysis of bolted and riveted joints in fibrous composite structures*, in *Recent advances in structural joints and repairs for composite materials*. 2003, Springer. p. 211-254.

55. Ekh, J., J. Schön, and L.G.J.C.P.B.E. Melin, *Secondary bending in multi fastener, composite-to-aluminium single shear lap joints. Composites Part B Engineering.* 2005. **36**(3): p. 195-208.

56. Liu, F., et al., *An interpretation of the load distributions in highly torqued single-lap composite bolted joints with bolt-hole clearances. Composites Part B Engineering.* 2018. **138**: p. 194-205.

57. Olmedo, A., C. Santiuste, and E.J.C.s. Barbero, *An analytical model for the secondary bending prediction in single-lap composite bolted-joints. Composite Structures.* 2014. **111**: p. 354-361.

58. Olmedo, Á. and C.J.C.S. Santiuste, *On the prediction of bolted single-lap composite joints. Composite Structures.* 2012. **94**(6): p. 2110-2117.

59. Bodjona, K. and L.J.C.S. Lessard, *Load sharing in single-lap bonded/bolted composite joints. Part II: Global sensitivity analysis. Composite Structures.* 2015. **129**: p. 276-283.

60. Gray, P., R. O'higgins, and C.J.C.s. McCarthy, *Effect of thickness and laminate taper on the stiffness, strength and secondary bending of single-lap, single-bolt countersunk composite joints. Composite Structures.* 2014. **107**: p. 315-324.

61. Kelly, G. and S.J.C.P.B.E. Hallström, *Bearing strength of carbon fibre/epoxy laminates: effects of bolt-hole clearance. Composites Part B Engineering.* 2004. **35**(4): p. 331-343.

62. McCarthy, C. and M.J.C.S. McCarthy, *Three-dimensional finite element analysis of single-bolt, single-lap composite bolted joints: Part II—effects of bolt-hole clearance. Composite Structures.* 2005. **71**(2): p. 159-175.

63. Ekh, J., J.J.C.S. Schön, and Technology, *Effect of secondary bending on strength prediction of composite, single shear lap joints. Composites Science and Technology.* 2005. **65**(6): p. 953-965.